3,4,3',4'-TETRACHLOROBIPHENYL-INDUCED GASTROPATHY IN THE RHESUS MONKEY (*Macaca mulatta*)

by

Gregory M. Becker

A THESIS

Presented to the Department of Pathology
and the Graduate Division of the University of Oregon
Health Sciences Center School of Medicine
in partial fulfillment of
the requirements for the degree of

Doctor of Philosophy
February 1981

ABSTRACT

Polychlorinated biphenyls (PCBs) are known to induce a hyperplastic lesion in the gastric mucosa of rhesus monkeys. The manner in which proliferation is altered, the detailed morphologic characteristics, and the secretory products of this lesion were not known. These properties were investigated in this study.

Rhesus monkeys, (Macaca mulatta) were fed diets containing 1 or 3 mg/kg (ppm) of 3,4,3',4'-tetrachloro-biphenyl, a particularly toxic PCB isomer, or a control diet. The experimental animals developed skin lesions characteristic of PCB poisoning and became moribund after 7 to 14 weeks of toxic feeding. They were pulse labeled with ^{3}H-thymidine and sacrificed. Tissues were prepared for autoradiography, light microscopy, and transmission and scanning electron microscopy.

The experimental animals had gastric lesions characteristic of PCB-poisoning in which the mucosa was thickened in the body region and formed cystic, dilated gastric glands which penetrated the muscularis mucosae. The specialized cells of the gastric glands, the zymogenic, the parietal, and the enteroendocrine cells were replaced with or converted into mucus-secreting cells, which stained strongly for acidic sulphomucins; in the controls only

weakly staining surface epithelial and mucous neck cells were seen. Autoradiographs of control tissue revealed that gastric epithelial cell proliferation was limited to the isthmus and neck regions of the glands throughout the stomachs. In the experimental animals, proliferation also occurred in these regions, but in addition ^{3}H-thymidine labelled cells were seen in the bases of the glands. In some experimental sections, labeled cells were seen abnormally high in the glands. The relative numbers of labeled epithelial cells were greatest in the body regions of both the experimental and control stomachs, but there were no differences between the two groups.

Transmission electron microscopic examination of this lesion revealed that the mucus-secreting epithelial cells lining the gastric glands showed signs of cell injury such as irregular apical membranes, apical regions of the cells apparently discharged into the lumina of the glands, dilated rough endoplasmic reticulum, and autophagic vacuoles. Exaggerated interdigitations of the plasmalemma with neighboring cells and large, depleted Golgi apparati were also noted. Many of the surface epithelial cells appeared unaffected, but cytoplasmic irregularities were also seen.

Scanning electron microscopy of the surface of the gastric mucosa revealed outward bulging and irregular configurations of the epithelial cells: an indication of hyperplasia or excessive cell loss.

In 2 of 3 of the experimental animals, tissue pepsin levels were very low. Parietal cells were rare in the experimental stomachs. Thus the normal secretory functions of the stomach were replaced by mucus production. Fasting and postprandial gastrin levels were not significantly altered through the course of the experimental feeding: an indication that gastrin was not involved with the abnormal proliferation and differentiation seen in this lesion.

The author believes that the thickened mucosa in this lesion develops by a failure of the newly formed, downward migrating cells to differentiate and lose their proliferative capacity. These cells continue to proliferate in the bases of the gastric glands, where this abnormal cell production results in a downward growth of the gastric glands through weak-points in the muscularis mucosae, forming submucosal glands and cysts. 3,4,3',4'-tetrachloro-biphenyl may also be injurious to the cells, as the relatively undifferentiated cells in this lesion showed abnormalities not seen in control undifferentiated cells.

APPROVED:

[redacted]

(Professor in Charge of Thesis)

[redacted]

(Chairman, Graduate Council)

ACKNOWLEDGEMENTS

I would like to express particular gratitude to my thesis advisor, Dr. Wilbur P. McNulty, who provided the guidance, support, facilities and encouragement that made this study possible. His clear scientific thinking will serve as a model for me to follow throughout my career.

I would also like to thank the entire staff at the Oregon Regional Primate Research Center who have all been very helpful to me throughout this study. I am especially thankful to Dr. John Senner for assisting me with computer programming and statistics, Mr. Vaughn Wells for his expert animal care and assistance, Dr. Henner Fahrenbach and Mr. Michael Webb for training me in electron microscopy, Mr. Helmy Hawash for assisting me with autopsies, Ms. Verna Russell and Mr. David Tacha for instruction in histological techniques, Ms. Isabel McDonald and her library staff for providing me with the many references I required for this study, Ms. Janina Ely for editing this manuscript, Mr. Joel Ito and Ms. Jeannette Cissman for help with the artwork, Mr. Harry Wohlsein and Ms. Linda Lauterbach for photographic assistance and advice, and Mr. Wayne Borum and Mr. Robert Coffin for advice and assistance with the use of the Primate Center's computing facilities for the preparation of this manuscript.

This work was supported by a National Institutes of Health Grant to my advisor, Dr. Wilbur P. McNulty.

TABLE OF CONTENTS

LIST OF FIGURES

Figure no. Page no.

Figure no. Page no.

Figure no. Page no.

Figure no. Page no.

I. INTRODUCTION

A. General background

3,4,3′,4′-Tetrachlorobiphenyl is one highly toxic isomer (116) of the six possible symmetrical tetrachlorobiphenyls, all of which are members of the larger class of chlorobiphenyls. Mixtures of chlorobiphenyls are referred to collectively as polychlorinated biphenyls and are commonly abbreviated as PCBs (75). The structure of 3,4,3′,4′-tetrachlorobiphenyl and the structures of three closely related, approximately isosteric, and more toxic polychlorinated polycyclic compounds, 2,3,6,7-tetrachlorobiphenylene, 2,3,7,8-tetrachlorodibenzofuran, and 2,3,7,8-tetrachlorodibenzodioxin, are shown in figure 1. There are 209 possible chlorobiphenyls that differ from one another in the number and position of chlorine substitutions on the two benzene rings. Although individual chlorobiphenyls are crystalline solids at room temperature, commercial PCB preparations, which are mixtures of numerous chlorobiphenyls, are viscous liquids or sticky resins at room temperature owing to the mutual depression of the melting points of the individual chlorobiphenyls (75). PCB mixtures exhibit high chemical and thermal stability, excellent dielectric properties and low vapor pressures. These properties have resulted in the extensive use of PCBs in electrical capacitors and transformers, vacuum pumps,

lubricants, carbonless reproducing paper, hydraulic systems, and adhesives, and as wax extenders, and pesticide extenders, and vehicles for inks (75).

Unfortunately, however, PCBs are highly toxic to a variety of animals, including humans (35, 46, 87). The high thermal and chemical stability of PCBs, which contributes to their industrial usefulness, also contributes to their persistence in the environment, moreover these compounds accumulate in food chains (138). Because of these factors, PCBs have become the subject of intensive investigation since 1967.

Although the mechanism of toxicity of PCBs is as yet unknown, PCBs have been shown to induce numerous pathologic changes. Perhaps the most striking pathologic change is the hyperplasia of the gastric mucosa of rhesus monkeys maintained on diets containing PCBs (7, 13). In this gastropathy, there is an apparently abnormal pattern of proliferation and differentiation of the gastric epithelium that results in an extension of the gastric epithelium into the submucosa, which then forms cysts. This study will report my detailed investigation of this lesion. Before proceeding, I shall first review the scope of PCB-induced disease in all animals, in order to convey the uniqueness of the pathologic changes that occur in monkeys.

B. Polychlorinated-Biphenyl-Induced Pathological Lesions

Generally, in lower animals the major pathological changes have been limited to the liver, whereas in monkeys skin and gastric lesions, but not liver lesions, have been observed.

1. Fish

In rainbow trout, changes in the ultrastructure of the nuclei of liver cells predominate (55). These changes, seen at PCB (Aroclor 1254) dietary levels of of 10 and 100 mg/kg (or parts per million, abbreviated ppm), but not at 1 ppm, included irregular nuclear outlines, separation of nucleolar components, and nuclear pseudoinclusions. Other liver changes observed at these dietary levels were the formation of concentric membrane arrays from rough endoplasmic reticulum and proliferation of the membranes surrounding lipid droplets. In channel catfish exposed to 1000 mg of Aroclor 1254 / kg of body weight in a single intragastric injection, liver changes were also observed. These included increases in tubular smooth endoplasmic reticulum, formation of stacks of smooth endoplasmic reticulum continuous with the rough endoplasmic reticulum, and concentric membrane arrays. However, nuclear changes such as seen in rainbow trout were not observed (89).

2. Birds

Polychlorinated biphenyl intoxication produces accumulations of fluids in the subcutaneous tissues, in abdominal and thoracic cavities, and in the pericardial sac. These effects, referred to collectively as chick edema disease (87), have been observed in accidental poisonings of fowl (87) and in experimental feedings of PCBs at dietary levels of 200 or more ppm (46). Atrophy of the thymus, loss of adipose tissue, and reduced spleen (19, 169) were additional pathologic findings. Liver changes included fatty liver and centrolobular necrosis (58, 169). Dilatation of kidney tubules was also reported (169). Decreased egg shell thickness and poor hatching rates of chicken eggs were observed after chickens ingested food containing 10 or more ppm of PCBs (87).

3. Nonprimate mammals

The major pathologic changes induced by PCBs in nonprimate mammals are in the liver (86). In rats, mice, and rabbits these changes include adenofibrosis and hepatomas (88), megahepatocytosis (94), apparent carcinomas (76, 88), proliferation of smooth endoplasmic reticulum (23, 29, 70, 82) and fatty liver (70, 91). Also observed in the liver was the formation of concentric membrane arrays, which were thought to arise from alterations in the endoplasmic reticulum (125).

These morphological changes in the liver, observed at

dietary levels of 100 ppm or more for many months, were accompanied by such biochemical changes as increases in cytochrome P-450 (23, 70, 166) and cytochrome P-448 (168), and increases in various drug-metabolizing enzyme activities coupled to the microsomal mixed-function oxidase system (10, 18, 23, 107, 166, 168). The majority of biochemical studies were performed at dietary levels of at least 100 ppm, or total doses of 100 mg of PCBs / kg of body weight by intraperitoneal injections.

A hyperplastic lesion of the gastric mucosa similar to that about to be described in monkeys has to date been observed in only one nonprimate species; the domestic swine (59), but not in sheep, mink, rats, mice, and rabbits. In swine fed PCBs at a dietary level of 100 ppm for 11 days deep ulcerative lesions with inflammation and edema of the gastric wall developed. In certain areas, hyperplasia of the mucosal epithelium with downward growth through the muscularis mucosae into the submucosa, excessive mucus-secretion resulting in cyst formation, and extensive involvement of eosinophils and neutrophils were observed.

4. Primates

The constellation of pathologic signs induced by PCBs in primates, including humans, is quite different from that observed in lower animals. In rhesus monkeys acneiform

lesions develop in the skin at dietary levels of PCBs of 2.5 ppm within 1 to 2 months (2). These lesions are sebaceous glands in which the normal sebum-producing epithelium has undergone squamous metaplasia to keratin-producing epithelial cells (14). The resulting accumulation of keratin forms cysts within the sebaceous glands. Similar skin lesions were observed in industrial workers exposed to PCBs as early as 1936 and numerous times since then (35, 117).

These skin lesions were also seen on the human victims of accidental PCB poisonings, most notably in the "yusho," PCB-contaminated rice oil incident in Japan in 1968 (69). More than 1200 persons ingested the contaminated oil (96). Total PCB intake per person was estimated at between 0.5 and 2 g (96). In addition to acneiform lesions, these human victims exhibited hyperpigmentation of the skin and nails, and swelling of hair follicles and upper eyelids (85).

Rhesus macaques develop skin changes similar to those seen in humans. In addition, the following also develop: alopecia, periorbital edema and erythema, anemia, hypoproteinemia, bone marrow atrophy (2), thymic involution (116), hyperplasia of the biliary ducts (McNulty, unpublished data), and hyperplasia of the gastric mucosa with extension of the gastric epithelium into the submucosa with cyst formation (2, 3, 7, 13, 14). This PCB-induced gastric lesion has only been observed in rhesus monkeys and swine, but not in any of the 1200 human "yusho" victims of

accidental PCB poisoning in Japan. As of May 1974, 24 of these human victims had died and 5 were examined post mortem (85). Although a gastric ulcer was seen in one victim, no gastric hyperplasia as seen in PCB-fed rhesus monkeys was described. In these human victims, the only consistent histopathologic changes attributable to PCB poisoning were hyperkeratosis of the hair follicles, hyperpigmentation, and in three of the five patients, proliferation of the ductal epithelium of the esophageal glands.

As in lower animals, PCBs induce liver changes in primates, however in primates the changes are not pathologic. Induction of the liver drug metabolizing enzyme activities aryl hyrdocarbon hydroxylase (123) and N-demethylase (3, 123), and the protein cytochrome P-450 (6, 123), as well as an increase in smooth endoplasmic reticulum (2, 124) and increased numbers of lysosomes and vacuoles (124) have been observed.

Acneiform lesions have been produced in rhesus monkeys by commercial mixtures of PCBs fed at dietary levels as low as 2.5 ppm for 1 to 2 months (2, 115), levels that might be encountered in the environment or in contaminated foods (93, 138, 162). Since these skin lesions are similar to those seen in humans accidentally poisoned by PCBs, rhesus monkeys appear to be the best available experimental animal for studies on PCB toxicity. This is particularly true with regard to the possible long-term effects on the general human population, which continues to be exposed to low

dietary levels of PCBs in its diet, despite the discontinuation of production and use of PCBs in the U.S.A. and elsewhere.

The acneiform lesions in man and monkey appear to have as common features the loss of control of growth and differentiation of constantly renewed epithelial cell populations. In acneiform lesions, the normal epithelial cells in the sebaceous glands fail to produce sebum and instead produce keratin (14). Similarly, the epithelial cells of the Meibomian glands in the eyelids of monkeys fed 3,4,3',4'-tetrachlorobiphenyl are converted from sebum-producing to keratin-producing cells (116). The resulting keratin accumulates within the ducts of the glands, and causes swelling of the eyelids. An additional location of abnormal keratin production is in the nailbeds of monkeys fed PCBs. Normally the nailbed consists of stratified squamous epithelial cells that do not produce keratin. When PCBs are are ingested, keratin is produced and accumulates, and the nail becomes raised, and falls off (116).

In the gastric lesions of monkeys fed PCBs there is also an apparent lack of formation of specialized epithelial cell types: the enzyme-secreting zymogenic (chief) cells and the HCl-secreting parietal (oxyntic) cells. Instead of these specialized cells, less differentiated cells resembling mucous neck cells are formed (13). The normal regulation of the rate of cell renewal is also apparently disrupted: as the gastric glands penetrate the muscularis

mucosae and form cysts lined with relatively undifferentiated cell types, and the overall thickness of the gastric mucosa increases (7, 13, 116). This chemically induced change in both proliferation and differentiation of gastric epithelial cells is the primary focus of my study. At this point, a detailed discussion of the normal stomach and gastric mucosa is warranted.

C. Normal Stomach and Gastric Mucosa

1. Gross anatomy of the stomach

The stomach of the rhesus macaque is similar to that of man, although proportionately somewhat larger (17). It can be divided into five regions (figure 2): the cardia; where the esophagus joins the stomach; the fundus; the body; the antrum and the pylorus, where the stomach joins the duodenum (17). The outermost surface of the stomach, a serosal membrane, is a continuation of the peritoneum. Three thick muscular layers lie just beneath this serosa: the longitudinal outer, the circular middle, and the inner oblique layer (17, 153). The next layer beneath the inner oblique muscle layer is the submucosa, which consists of loose connective tissue. Just beneath the submucosa is the lamina muscularis mucosae, and then a layer of areolar and reticular connective tissue, the lamina propria. The innermost layer of the stomach wall is the gastric

epithelium.

2. Gastric glands

The lamina propria and the gastric epithelium together constitute the gastric mucosa (137). The gastric epithelium indents into the lamina propria to form gastric pits or foveolae, which branch and extend further toward the muscularis mucosae and form tubular gastric glands, whose lumina are continuous with the lumen of the stomach. Short, tortuously branched, tubuloalveolar, primarily mucus-secreting glands occupy the cardiac region in humans (95) and in monkeys. The glands of the fundus and the body regions are straighter and somewhat longer than cardiac glands, and are lined principally by four main epithelial cell types: surface epithelial cells, mucous neck cells, zymogenic (chief) cells and HCl-secreting parietal (oxyntic) cells (36, 67, 68, 77, 141, 158). Both zymogenic and parietal cells are considerably more numerous in the glands of the fundus and body region than they are in the cardiac glands, where they may be very sparse or absent (95).

In many mammalian species the gastric glands of the fundus and those of the body region are nearly identical, and are usually referred to in the literature as fundic glands. However, in macaques, the glands in the fundus contain very few if any parietal cells, while glands in the body region contain abundant parietal cells (84, 164). Therefore it is misleading to refer to the glands of the

body of the stomach as fundic glands, and henceforth in this study the term gastric glands will be applied to glands in the body region of the stomach, which normally contain abundant numbers of all major cell types.

Pyloric glands are found in the pyloric antrum and in the pyloric canal (42). These glands are shorter and more highly branched than those of the body of the stomach, and they empty into gastric foveolae, which are longer and wider than those of the body region (42). Mucous neck cells predominate in these glands (42), but the cells of the gastric endocrine system, called enteroendocrine cells, are particularly numerous in these glands in the pyloric and the antral regions of the stomach (54, 98, 154).

3. Gastric epithelial cell types

With its many highly specialized cell types, the stomach is a complex organ. Many excellent reviews of the structure and function of cells in the gastric epithelium in numerous mammals, including man, have been written (36, 54, 67, 68, 77, 98, 109 141, 154 158). Although the ultrastructure and function of gastric epithelial cells in the rhesus macaque have not been extensively studied, recently my colleagues and I (13) have shown that the histologic and ultrastructural characteristics of these cells in rhesus monkeys closely resemble those in other mammals, particularly man (141).

a. Surface epithelial cells

Surface epithelial cells (SECs) are tall cylindrical cells covering the luminal surface of the stomach in an uninterrupted layer. They extend into the gastric foveolae. Their nuclei are located in the bases of the cells. From a Golgi apparatus located supranuclearly, secretory granules migrate toward the apical, luminal end of the cells, where the granules coalesce to form a mass of larger secretory granules (141, 171). These secretory granules contain carbohydrate-rich substances whose compositions differ among species (150, 156). In an extensive comparative study by Sheahan and Jervis (150), the surface epithelial cells of rhesus monkeys were shown to contain both acidic and neutral mucins. The more numerous acidic mucins proved to be primarily nonsulfated sialomucins, but sulfomucins were seen in the surface epithelial cells of the cardiac region. These mucins were differentiated from one another by a sequence of staining with periodic acid-Schiff's reagent (PAS) followed by staining with alcian blue (AB). This sequence stains neutral mucosubstances bright red owing to the PAS stain and acidic mucosubstances blue, owing to the alcian blue stain. On additional sections sulfated acidic mucosubstances (sulfomucins) were differentiated from nonsulfated acidic mucosubstances (sialomucins) by a sequence of staining with high-iron diamine (HID), which stains sulfomucins black, and alcian blue, which stains the sialomucins blue (150, 155).

Recent data suggest that the role of these mucosubstances is to form a protective gel-like layer over the surfaces of surface epithelial cells, i.e., to provide a microenvironment into which HCO_3^- ions are actively secreted (1). This microenvironment acts as a barrier which protects the surface epithelial cells from the proteolytic digestive enzymes secreted by the zymogenic cells and the acid secreted by the parietal cells (1). Data from studies using various stimulating agents such as prostaglandins and carbachol, and metabolic inhibitors such as CN^- ions and dinitrophenol, suggest that HCO_3^- is actively secreted by the gastric mucosa, and quite possibly by the surface epithelial cells themselves (1).

b. Mucous neck cells

Mucous neck cells (MNCs) are located in the neck region of gastric glands, below the gastric foveola. Although they also secrete mucus, as do SECs, they are considerably shorter, and their secretory granules are more dispersed throughout the cytoplasm and are not as densely packed in the apical regions (141, 171). Like SEC nuclei, the nuclei of MNCs are located at the bases of the cells (141, 171). In the rhesus monkey, MNCs contain PAS-positive neutral mucosubstances, AB-positive nonsulfated acidic mucosubstances (sialomucins), and HID-positive acidic mucosubstances (sulfomucins) (150). An immunofluorescence study in dog and cat gastric mucosa revealed that these cells

contain, and presumably also secrete, pepsinogens (103). Some MNCs, because they contain fewer secretory granules, sparser endoplasmic reticulum, and a less dense cytoplasm, are called undifferentiated cells (141, 171).

c. Parietal cells

Parietal (oxyntic) cells are large, eosinophilic, and ovoid cells highly specialized for the secretion of HCl acid. They contain numerous mitochondria with prominent cristae arranged as parallel surfaces (67, 77, 141, 142, 158). In the resting, fasting state, parietal cells contain numerous tubulovesicles, but in the stimulated state the tubulovesicles apparently undergo reorganization to form an extensive intracellular canalicular system with numerous microvilli (41, 48, 139, 149, 178). These canaliculi have been shown to be the cellular site of HCl secretion (41). Human parietal cells have also been shown by immunocytochemical techniques to be the site of synthesis of human intrinsic factor, a glycoprotein necessary for the absorption of cobalamin (vitamin B12) in the ileus (102).

d. Zymogenic cells

The zymogenic (chief) cells are pyramidal cells in the lower region of the gastric glands. Their nuclei are basally located; large, electron-lucent, secretory vacuoles containing zymogen fill the apical region (13, 67, 77, 104, 141). As in other zymogenic cells, such as those in the

pancreas and salivary glands, in these cells the cytoplasm is filled with closely packed layers of rough (ribosome-studded) endoplasmic reticulum and a supranuclear, well-developed Golgi apparatus. These cells produce pepsinogens (immunohistochemical evidence), as do mucous neck cells, but unlike the later, they do not produce mucus. Pepsinogens are the inactive precursors of acidic proteases called pepsins (144). They become activated to pepsins when they are secreted into the acidic environment of the stomach lumen (144). Pepsinogens are the principal enzymes secreted by zymogenic cells.

e. Enteroendocrine cells

These cells are unique among gastric epithelial cells in that they are generally thought to originate from the neural crest or the neuroectoderm; however some investigators believe they are derived from endodermal cells, as are the other cells of the gastric epithelium (54). They are called enteroendocrine cells because most of them can synthesize gastrointestinal polypeptide hormones (enterohormones) (54). As many as 16 cell types have been described. Six to eight of these types occur in the stomach (54, 154). Some types and their secretory products have been clearly identified. The EC (enterochromaffin) cells produce 5-hydroxytryptamine (serotonin) and are also called argentaffin cells because they take up and reduce silver stains (154). The G cells produce gastrin (26, 54, 99, 154)

and other polypeptides (98). They are argyrophilic; i.e., they take up silver stains, which can subsequently be stained with a reducing agent, such as hydroquinone (26), but lack the ability to reduce silver stains by themselves. The D cells produce somatostatin (54, 97). The A cells produce glucagon (154). The ECL (enterochromaffin-like) cells in some animals produce histamine (56, 154).

These enterohormones act to modify gastric acid and zymogen secretion and gastric motility. Specifically, gastrin stimulates HCl secretion by parietal cells (71, 72, 140, 161) and pepsin secretion by zymogenic cells (71). It promotes proliferation of the gastric epithelium, i.e., increases the number of surface epithelial cells (30) and parietal cells formed (30, 61, 120, 174, 175). Histamine acts to stimulate HCl (71, 140) and pepsin secretion (71). Somatostatin inhibits a large variety of secretory activities (97, 147), as well as gastric and gut motility (97, 147). In the stomach, somatostatin apparently acts locally to inhibit acid and pepsin secretion in response to food (147). Serotonin and other substances such as kallikreins, prostaglandins, and motilin, which are thought to be produced by EC cells, are important in regulating gut motility (154).

f. Fibrillovesicluar cell

A relatively undifferentiated cell type with microvilli, a terminal web, and fibril bundles continuous

with the cores of the microvilli has been described in dogs and in man (57, 79). Called fibrillovesicular cells by Hammond and LaDeur (57), they are quite similar to the brush cells observed by Luciano et al. in the fundus of the hind stomach of llamas (109). They propose that these cells are a type of receptor cell. No one has observed these cells in rhesus monkeys (13).

4. Organization of the gastric glands

Wattel and Geuze (171) have conveniently divided the gastric gland of the body of the stomach into four regions whose boundaries are set by the extent of distribution of the various epithelial cell types. The gastric foveola, or gastric pit, includes the region of the gland between the free surface of the gastric mucosa and the uppermost parietal cells.

The isthmus includes the region between the uppermost parietal cell and the uppermost mucous neck cell. The boundaries of the neck region are set by the range of the mucous neck cells. The deepest region is the base region, which is the rest of the gastric gland between the neck region and the muscularis mucosae. Thus, the foveola is lined only with surface epithelial cells, the isthmus with surface epithelial and parietal cells, the neck region with mucous neck, parietal, and immature zymogenic cells, and the base region with zymogenic and parietal cells. Enteroendocrine cells occur throughout the gland except in

the foveolae.

5. Cell renewal in gastric epithelium

a. Location of the proliferative zone

As in all the other epithelial tissues, cells are constantly lost and replaced. In the gastric epithelium cells are primarily lost from the free surface, where surface epithelial cells are constantly being extruded into the lumen of the stomach and are replaced by dividing cells in a proliferative region of the glands located beneath the surface (38, 105, 159). In the gastric glands of the pylorus and antrum the proliferative zone is in the isthmus region, at the bottom of the foveola, above the beginning of the pyloric glands proper (66, 81, 163). In the gastric glands in the body region of the stomach, replacement of gastric epithelial cells occurs in the isthmus and neck zones of the glands (31, 64, 65, 74, 81, 83, 106, 118, 134, 141, 159, 171, 172). Cell renewal in the cardiac glands of the stomach has only been studied in the hamster (81); in these animals it occurs in the isthmus zone.

b. Types of dividing cells

The principal method of determining which cells in a tissue are undergoing proliferation is to pulse-label the tissue with ^{3}H-thymidine. Cells in the DNA-synthesizing phase (S-phase) at the time that ^{3}H-thymidine is introduced

incorporate the radiolabeled thymidine into DNA, which remains labeled during tissue processing. Autoradiographs produced from sections of the tissue show black silver grains over the nuclei of those cells which were in S-phase. A vast amount of data on ^{3}H-thymidine autoradiography, reviewed by Cleaver (34) has substantiated the validity of this method for identifying cells in S-phase, and hence cells committed to divide. Using this method in a variety of laboratory animals and man, investigators have identified the proliferative cells in gastric glands as relatively undifferentiated surface epithelial cells in the isthmus zone and mucous neck cells in the neck zone (31, 64, 65, 74, 81, 83, 106, 118, 134, 141, 158, 171, 172). Wattel and Geuze quantified the types of the labeled cells in their autoradiographs of rat fundic glands and found that 85% were in the isthmus and 15% were in the neck (170). When they prepared autoradiographs of thin sections and examined these by electron microscopy, they found that about half of the labeled surface epithelial and mucous neck cells contained a moderate amount of secretory granules, and the other half contained only a few granules. In numerous ultrastructural studies, proliferative cells in the gastric glands have been shown to have a high nucleus: cytoplasm ratio, sparsely distributed endoplasmic reticulum, abundant free ribosomes, and various numbers of electron-dense secretory granules (36, 64, 79, 83, 141, 171).

c. Migration and maturation of newly formed cells

The gastric epithelium, like other renewing cell populations, is in a dynamic steady-state in which mature cells are continuously being lost from the total population of cells, whose size remains constant because new cells are formed at a rate equal to that of cell loss (105). This formation occurs in the proliferative zone, which includes the isthmus and mucous neck zones.

Hattori (64) determined by scanning electron microscopy of fractured fundic glands of hamsters and by autoradiography of these glands, that the proliferative zone is tightly enclosed in a stromal sheath of fibroblasts and collagen fibers. Cells outside the sheath do not incorporate ^{3}H-thymidine, and therefore are not proliferative. Hattori believes that the proliferative capacity of the cells is maintained by their position within the sheath, and is lost when the cells migrate outside the sheath, where relatively undifferentiated cells become mature surface epithelial cells if they migrate upward, and mature parietal and zymogenic cells if they migrate downward.

The majority of newly formed cells migrate upward in a first-formed, first-migrated, pipeline fashion to become surface epithelial cells. In hamsters, this migration from the proliferative zone to the surface of the gastric mucosa occurs in 4 to 7 days (65). After the cells arrive at the surface, they are eventually extruded into the lumen of the

stomach (64, 65, 81).

The formation of parietal, mucous neck, and zymogenic cells is somewhat more complicated. In numerous studies it has been shown that parietal cells are produced by maturation of relatively undifferentiated, immature cells in the mucous neck zone and migrate downward in the gastric glands (81, 134, 171). One study suggests that immature parietal cells may themselves have some limited proliferative capacity (31).

Mucous neck cells, as described above, are themselves proliferative cells, but they may also migrate downward (65,83) and then become zymogenic cells (65).

Zymogenic cells have been shown in several studies to undergo division (31, 65, 121, 172); however, the majority of zymogenic cells appear to arise from maturing mucous neck cells migrating downward (65).

Hattori and Fujita (65) studied the migration of ^{3}H-thymidine labeled cells as a function of time, and they concluded that the downward migration is more complicated than the simple first-formed, first-migrated, pipeline system seen in the upward migration of surface epithelial cells. They have proposed that newly formed cells migrating downward pass from one compartment to another, and that all the cells within a compartment have a certain random probability of migrating downward to the next compartment. This model, which they call a <u>stochastic flow system</u>, is consistent with their observation that only 6 to 7% of newly

formed cells reach the lower end of the glands at the same time: all the others remain at higher positions. They further propose that random lateral migrations of cells within the glands disturb the downward migration of newly formed cells. Nevertheless, cells farthest from the proliferative zone are on the average older, and those closest to the generative zone are youngest.

The life spans of the parietal and zymogenic cells have not been definitively determined. Parietal cells in rodents have been estimated to have a halflife of 23 days (134), but in another study their life span and that of zymogenic cells were estimated at 200 $\pm$ 100 days (65).

The cell cycle of cells capable of division is represented below on a clock face.

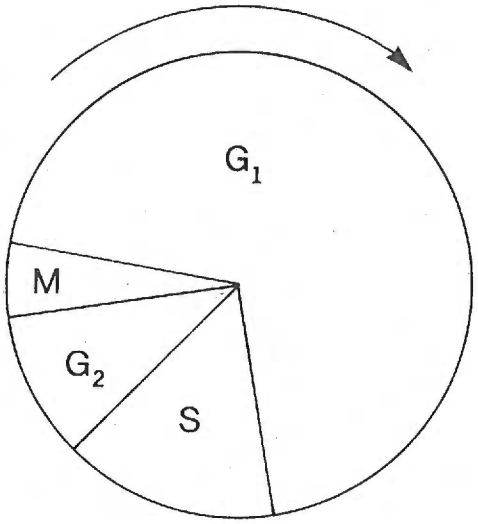

Figure 3. Phases of the cell cycle.

Cells progress from mitosis (M) to the first gap phase, (G_1), and then into the DNA-synthesizing S-phase (S) in which the DNA content of the chromosomes is replicated in preparation for the next mitosis. From S-phase the cells progress into the second gap phase, (G_2), prior to entering the next mitosis (73).

Cells in mitosis can be directly observed in ordinary sections; cells in S-phase can be distinguished autoradiographically after exposure to a short pulse of ^{3}H-thymidine,

followed by immediate fixation, and then standard embedding, sectioning, and autoradiographic procedures.

In order to better understand diseases of proliferation, investigators have directed intense interest and considerable effort toward the elucidation of the kinetics of cell proliferation, including the determination of cell cycle times and the durations of the individual phases of cell cycles in normal and diseased tissues. Many tecniques have been developed for determing these parameters in a given cell population.

A common and particularly useful method is the labeled mitosis wave method of Quastler and Sherman (133), which can yield estimates of the duration of all phases of the cell cycle, and therefore also the total cell cycle time. This method involves pulse labeling the cells with ^{3}H-thymidine and then sampling the cell population at intervals after the pulse to determine the fraction of cells in mitosis that appear labeled in autoradiographs. Cells that were in the S-phase at the time of the pulse label progress through the cell cycle; those which were at the end of the S-phase enter mitosis after passing through G_2 phase. These cells in mitosis will then be labeled with ^{3}H-thymidine. Only a small fraction of cells in mitosis will be labeled. After a little more time has passed, the cells that were in the middle of the S-phase at the time of the pulse labeling enter mitosis and are labeled. The fraction of labeled mitosis then reaches 1.0 and does not show a decline until

an interval of time equal to the S-phase plus the G_1 phase has passed. Thus a "wave of mitosis" has been formed as a function of time after the pulse labeling. The next wave does not appear until the cells have passed through an interval of time equal to one cell cycle time plus G_1. Because of the intercell variation in cell cycle times, the labeled waves appear more like sine waves than the somewhat truncated square waves predicted by theory (34).

The labeled mitosis wave method works well for cells in tissue culture. It works less well for biopsy samples because one has to obtain biopsy specimens at hourly or shorter intervals for at least as long as the anticipated duration of one and a half cell cycles; The inevitable surgical stress on the animal would very likely alter the cell cycle time (25, 50). Alternatively, one can use a large number of relatively homogenous animals and kill one or more at intervals.

Many investigators are particularly interested in determining the duration of the S-phase, Ts, since once it is known the cell cycle time, Tc, can be estimated by:

$$Tc = Ts/LI$$

In the formula above, LI , the labeling index, is the fraction of cells labeled after a short pulse of ^{3}H-thymidine (34). This relationship is only valid for cell populations in which all the cells are in the proliferative cycle, and

none have left to become mature, specialized cells no longer capable of division (34).

Since the wave of mitosis method of Quastler and Sherman (133) is an experimentally difficult way in which to determine Ts (one has to obtain multiple samples from an animal), other methods have been developed. In the continuous labeling method (34), cells in culture are continuously exposed to medium containing ^{3}H-thymdine or ^{3}H-thymidine is continuously infused into the animals. This method has been successfully applied to the study of cell proliferation in diseased and normal human gastric biopsy samples (63). Gastric mucosal samples were incubated in medium containing ^{3}H-thymidine for 30, 120, and 210 minutes. The labeling index, LI, which increases with time, was determined for the successive samples and plotted as a function of time of incubation in the medium. The slope of the regression line (Rs) of LI on time is related to Ts :

$$Ts = LIo/Rs$$

In the above formula, LIo is the intercept of the regression line with the Y axis at t = 0. This method has the disadvantage that biopsy and incubation may themselves alter the rate of proliferation. There is also the problem of the lack of penetration of medium with its nutrients, ^{3}H-thymidine, and oxygen into the biopsy specimen. Attempts have been made to improve the depth of label penetration

through hyperbaric oxygenation of specimens incubated with ^{3}H-thymidine in vitro (119).

The problem of label penetration can be minimized by continuous infusion of ^{3}H-thymidine into the animals and biopsy of the tissue at intervals to determine the Rs value. But this in vivo method requires large amounts of ^{3}H-thymidine and subjects the animals to the stress of multiple biopsies.

Another technique for determining Ts is a double-labeling technique (100) in which an animal is given an injection of ^{14}C-thymidine and an interval of time (t: usually 1 hour) is allowed to pass. Then the animal is given a second injection, but this time of ^{3}H-thymidine. Forty minutes later the animal is killed and the tissue is removed. In a steady-state population the following relationship holds true:

$$(F \text{ of } {}^{14}C)/(F \text{ of } {}^{3}H) = Ts/t$$

In the above formula, (F of ^{14}C) is the frequency of ^{14}C-labeled cells, with or without ^{3}H-labeling and (F of ^{3}H) is the frequency of cells labeled with ^{3}H only.

Although this technique would seems to be quite simple and to present the fewest experimental problems, with it one cannot easily distinguish cells labeled with both ^{14}C and ^{3}H from cells labeled with only ^{3}H (63). A technique for determining the mean generation time of a proliferating cell

population, Tg, has been described; it does not require that the Ts or LI value be determined (33). ^{3}H-thymidine is injected into an animal and biopsy samples are obtained at intervals on the order of days or multiples of the expected Tg. The biopsy specimens all undergo simultaneous autoradiography, and the median grain count of the labeled nuclei is determined. The median grain count over each cell halves with each cell division, and hence declines exponentially with time. The Tg can be estimated through construction of a least-squares fit of a straight line to a plot of the logarithm of the median grain count versus time. The mean grain count can also be used. The Tg value is equal to the cell cycle time, Tc, in a population in which all the cells are proliferating, or in which those maturating and ceasing proliferation leave the proliferative zone and can be distinguished from those retaining their proliferative properties, as is the case in gastric glands.

Thus, a variety of techniques exist for estimating rates of cell proliferation, each with its own advantages and disadvantages. Unfortunately, the most precise methods, such as the labeled mitosis wave method, require stressful procedures when applied to whole animals, and less stressful procedures such as the double-labeling method, are less precise.

D. Previous Studies on Polychlorinated-Biphenyl-Induced Gastropathy in Rhesus Monkeys

The first report of hypertrophic gastric lesions in the stomachs of monkeys fed a polychlorinated polyphenyl compound was published in 1967. Allen and Carstens (5) described this lesion in rhesus monkeys fed a toxic fat that was subsequently found to contain 1,2,3,7,8,9-hexachloro-dibenzo-p-dioxin (28). Later, in 1973, Allen and Norback (7) described a hyperplasia and dysplasia of the gastric mucosa of monkeys fed diets containing 25 to 300 ppm of PCBs and a diet containing 5000 ppm of polychloroinated tri-phenyls for 3 months (see also Allen, 1975, ref. 2). They observed an edematous thickening of the stomach wall with hypertrophy of both the pyloric and fundic regions of the stomach. (The term fundic is often misused; perhaps the body of the stomach was intended.) Furthermore, they observed greatly elongated hyperplastic glands containing mucus-secreting cells but no normal secretory cells. The ducts of the glands were large and cystic owing to an accumulation of mucus. The gastric epithelium invaded the submucosa and formed submucosal cysts. Serial sections of the submucosal cysts showed that the proliferating epithelial cells were stratified. They also described penetration of the basal lamina and invasion of the surrounding connective tissue of the submucosa. Dysplastic changes such as irregular hyperchromic nuclei and pleo-morphic cells were observed in areas where the mucosa was

stratified. They noted that inflammatory cells were common in the submucosa.

Identical gastric lesions were recently observed in rhesus monkeys housed in buildings whose concrete floors had been treated with concrete sealers containing PCBs (112). These animals demonstrated the same clinical pattern of PCB intoxication observed in other studies (2, 7, 8, 13).

Although a similar gastric lesion occurred in monkeys fed a diesel lubricating fluid (111) that may have contained polychlorinated polyphenyls, and also occurred in monkeys infested with nematodes (20), this lesion has been so consistently observed in monkeys intoxicated with PCBs (2, 7, 13, 112, 116) that these agents can also be considered causative agents of this change in the gastric mucosa (13).

Since Allen and his colleagues conducted only light microscopic studies on the advanced lesion in chronically ill PCB-intoxicated monkeys, McNulty, Bell and I studied early morphological changes at the cellular level to better understand how the advanced lesion develops (13). Monkeys were placed on diets containing 0, 3, 10, 30, or 100 ppm of PCBs. Gastric biopsy specimens were obtained during laparotomies at the start of the experiment, on day 12, and at monthly intervals for as long as 6 months, or until the animals became moribund. These specimens were studied by light and electron microscopy. Among the principal changes was an arrest of the differentiation of the proliferative cells of the isthmus and neck zones into parietal and

zymogenic cells. Mature parietal and zymogenic cells were found only in the bases of the gastric glands, where the oldest epithelial cells are normally found. These remaining mature, differentiated cells showed signs of injury such as dilatation of the rough endoplasmic reticulum in zymogenic cells, irregular luminal membranes in the apices of these cells, and an increase in the size and number of autophagic vesicles in both parietal and zymogenic cells.

E. Studies with Pure Polychlorinated Biphenyl Isomers and Related Compounds

Earlier experiments were all conducted with commercial PCBs, which are actually mixtures of the many possible congeners, all differing in the number and location of chlorine atoms; the identities of the compounds actually responsible for the toxic effects were not determined. Recently, McNulty, Cory, and I (116) studied the clinical toxicity and pathologic findings in rhesus monkeys chronically fed low levels of two pure, symmetrical tetrachlorobiphenyls, 3,4,3',4'-tetrachlorobiphenyl (3,4-TCB), which is subtituted in the para and meta positions, but unsubstituted in the ortho position, and 2,5,2',5'-tetrachlorobiphenyl (2,5-TCB), which is substituted in the ortho position, but unsubstituted in the para postion. We found that diets containing 0.3 to 3 ppm of the 3,4-TCB isomer caused the same toxic effects and pathologic lesions, including the gastric lesion, seen after poisoning of

monkeys with commercial PCBs, but the animals fed the 2,5-TCB isomer remained entirely normal. The pure tetrachlorobiphenyl isomers used in this study were checked for possible contamination by the more highly toxic tetra- and penta-chlorodibenzodioxins and chlorodibenzofurans by selected ion monitoring gas chromatography and mass spectrometry (37). The 3,4-TCB was found to be free of contamination by the tetrachloro compounds at a detection level of 1 ppm, and free of the pentachloro compounds at a detection level of 5 ppm. That level of contamination by toxic dibenzodioxins and dibenzofurans was probably too low to contribute to any of the toxic effects we observed. These findings are consistent with the hypothesis that an absence of chlorination in the ortho position correlates with toxicity in rhesus monkeys, as it does in other animals (19, 177).

In our study (116) we noted the relationship between the pattern of hepatic drug metabolizing enzyme activities induced by pure chlorobiphenyl isomers and the relative toxicities of these compounds. Several experiments with rats, mice, and chicken embryos (51, 129, 176) showed that chlorobiphenyl isomers chlorinated symmetrically in both the meta and para positions, but not in the ortho position, induce the formation of cytochrome P-448 and arylhydrocarbon hydroxylase activity (AHH), which is a 3-methylcholanthrene pattern of induction, and yet isomers chlorinated in both the para and ortho positions induce the formation of

cytochrome P-450 and aminopyrine N-demethylase activity, which is a phenobarbital pattern of induction. These conclusions are consistent with recent data on rhesus monkeys obtained by Nielsen-Smith and McNulty (123); monkeys given single doses of 1 mg of 3,4-TCB / kg of body weight showed a 3-methycholanthrene pattern of induction. Moreover, monkeys given 25 mg / kg of body weight of 2,5-TCB, which is chlorinated in the ortho and meta positions, showed a phenobarbital pattern of induction.

The highly toxic compound 2,3,7,8-tetrachloro-dibenzo-p-dioxin (TCDD) also induces the 3-methylcholanthrene pattern of enzyme activity, but with a 30,000 times greater potency (128). Furthermore, in the rhesus macaque TCDD produces a clinical pattern of toxicity very similar to poisoning with PCBs, except that TCDD produces these effects at a dietary level of only 0.5 parts per billion (ppb), an indication of a potency approximately 1000 times greater than that of the most toxic chlorobiphenyl isomers (4). Poland et al. (131) identified a binding receptor in rat and mouse hepatic cytosols that reversibly binds H-TCDD with high affinity. Certain chlorobiphenyl isomers also bind to this receptor, and their binding affinities closely correspond to their abilities to induce a 3-methycholanthrene pattern of enzyme activity (129). Poland et al. further report that both 3,4-TCB and 2,3,6,7-tetrachlorobiphenylene, a more rigidly planar compound than 3,4-TCB, competitively inhibit H-TCDD binding to this

cytosolic receptor; the tetrachlorobiphenylene compound is nearly as potent as TCDD and 30 time more potent than 3,4-TCB (139). They maintain that the abilities of these compounds to induce a 3-methylcholanthrene pattern of enzyme activity depends on their structural similarity to TCDD and the rigidity of planarity of the two phenyl rings. Chlorine substitution at the ortho position (number 2 position in chlorobiphenyls) results in marked nonplanarity of the rings (129), and this effect would explain the inability of 2,5-TCB, which is subsituted in the ortho position, to induce a 3-methycholanthrene pattern of enzyme activities.

Thus, there appears to be a high degree of correlation among the chlorobiphenyl isomers, chlorodibenzodioxins, and chlorodibenzofurans in toxicity and ability to bind a specific hepatic cytosolic receptor, to induce a 3-methy-cholanthrene pattern of enzyme activity and to induce characteristic lesions (116). As yet, however, there is no biochemical explanation for the development of any of the pathologic lesions, nor is there any indication that their development is causally linked to the induction of hepatic enzymes (116).

F. Objectives of this Study

Many questions concerning the development of the PCB-induced gastropathy in rhesus monkeys remain unanswered. The ones I will examine in this study are:

a. The PCB-induced gastric lesion is clearly hyperplastic and involves an alteration in the normal dynamic equilibrium of proliferation, maturation, and cell loss in the gastric epithelium which maintains the steady-state number and distribution of cell types in normal gastric mucosa. What is the mechanism by which this steady-state is disturbed? Several possibilities are:

Mechanism 1. Proliferation occurs uniformly throughout the gastric gland, that is, all cells become capable of proliferation, and cell cycle times may or may not be altered.

Mechansim 2. Gastric epithelial cell proliferation occurs only in the normal proliferative zone in the isthmus and neck, but the cell cycle time, Tc, of the cells is shortened and therefore more cells are formed than are lost.

Mechanism 3. Proliferation occurs normally in the normal generative zone, but additional proliferation occurs in other zones and cell types, such as:

a. In the surface epithelial cells

b. In immature cells which fail to differentiate and retain their proliferative capacity

c. In parietal and zymogenic cells which have lost their specialized function and acquire proliferative capacity

In this study I tried to determine which of these or other possible mechanisms operate in the gastric lesion induced by 3,4-TCB.

b. The specialized secretory cells of the stomach, the parietal and zymogenic cells, appear to be replaced by mucus-secreting cells. Do these mucous cells also secrete acid and zymogen, or is mucus their only secretory product ?

c. Hypergastrinemia increases cell proliferation in gastric epithelia, promotes the formation of parietal and zymogenic cells, and induces hyperplasia (30, 61, 120, 174, 175). Does 3,4-TCB induce abnormal gastrin production and secretion, which could then be the cause of the observed hyperplasia, or does 3,4-TCB induce a decline in gastrin levels, which could be responsible for the failure of new parietal and zymogenic cells to be formed ?

d. Does the 3,4-TCB-induced gastric lesion have features in common with other gastric lesions with disorders of prolif-

eration and differentiation, such as atrophic gastritis, chemically induced gastric carcinoma, and Menetrier's disease, all of whose pathologic mechanisms are either unknown or poorly understood ?

II. MATERIALS AND METHODS

A. 3,4,3',4'-Tetrachlorobiphenyl

Pure 3,4-TCB was purchased from Analabs, Inc., North Haven, CT. It was checked for possible contamination by the more highly toxic tetra- and penta- chlorodibenzodioxins and chlorodibenzofurans by selected ion-monitoring gas chromatography and mass spectrometry (37). The 3,4-TCB was found to be free of contamination by the tetrachloro compounds at a detection level of 1 ppm, and free of the pentachloro compounds at a detection level of 5 ppm. Therefore the 3,4-TCB was used without further purification.

B. Animals

Eight male rhesus monkeys (Macaca mulatta), 2 to 4 years of age and weighing 2.5 to 4.5 kg, were used. All except one, 7194, had no known previous exposure to any toxic substances. Monkey 7194 had been fed a commercial mixture of PCBs in a previous experiment 1 year earlier, but had been maintained on a normal diet for over 1 year and appeared completely normal and healthy. The animals were caged one per cage, in a specially constructed building with stainless-steel-lined walls and a welded aluminum floor with sewage drains. The cages were hung from the wall in two rows per wall over large troughs with drains, which removed excrement when the animals were being fed nontoxic diet

cakes. During the toxic diet regime, large stainless steel pans encased in disposable plastic garbage bags were placed under each cage to catch excrement and any uneaten food. These toxic wastes, collected by inversion of the bags, were incinerated daily in a high-temperature incinerator equipped with an afterburner. Small quantities of waste that did not fall on the pans were washed down the trough and floor drains daily. The animal technicians who disposed of wastes, cleaned the quarters, and fed the animals were trained in the handling of these and other toxic substances, and they wore disposable protective suits and gowns. Because of the low vapor pressure of the chlorobiphenyls used in this experiment, and the non-recirculating ventilation system which completely exchanged the air every 5 minutes, no respirator masks were deemed necessary for the personnel, but surgical masks were worn at all times to prevent ingestion of splashed excrement and to minimize transmission of human disease to the animals.

The animals were fed twice daily and weighed once weekly. Daily observations were made to determine the status of each animal's health.

C. Diets

Solutions of 3,4-TCB in corn oil were prepared in a hood in the laboratory over disposable countertop covers and with disposable labware. All materials were incinerated after use.

All toxic foods were prepared in the toxic substances building under my supervision. The diets consisted of moist cakes, each weighing about 40 g. The diet cakes contained 50% by weight ground Purina Monkey Chow, 37% water, 11% bananas, 0.7% vitamin mixture, and 0.4% corn oil solution containing 3,4-TCB. The final 3,4-TCB content of the diet was 3 mg / kg, or 3 ppm for the first experiment, and 1 ppm for all the other experiments. The diet ingredients were mixed until homogeneous in a large commercial food mixer used exclusively for toxic diets. The control diets were prepared separately in another building and were identical to the toxic diets except that corn oil without 3,4-TCB was used.

D. Induction of the Gastric Lesion

The animals were fed the toxic 3,4-TCB diet cakes until their clinical condition indicated they had significant gastric lesions, i.e., until they showed loss of appetite, skin lesions, weight loss and behavior changes. See Results section.

E. Labelling of Cells in the S-phase with ^{3}H-thymidine

Food was withheld from the animals overnight. Then each animal was afixed to a restraint cross and brought to the autopsy room at 09:00 a.m., each on a separate day. An indwelling catheter was inserted in the saphenous vein and the animal received a 0.5 mCi infusion of ^{3}H-thymidine (New

England Nuclear, Boston, MA 02118; or Amersham Corp., Arlington Heights, IL 60005) per kilogram of body weight. At 09:45 each animal was anesthetized with 25 mg of ketamine (Ketalar, Park-Davis & Co., Detroit, MI 48232) per kilogram of body weight, and dissection was begun as soon as the animal showed no response to forcep-pinching of the facial skin. At approximately 10:00, the stomach and adjoining esophagus and duodenum were removed. In the first two animals, 7761 and 7194, the duodenum was ligated and the entire stomach was filled with fixative containing 4% commercial formaldehyde, 1% electron microscope grade glutaraldehyde (TAAB Laboratories, Reading England 475388) in a pH 7.4 buffer containing 150 mM Na^+ and 84 mM PO_4^- (abbreviated 4F1G) (113). The esophagus was then ligated, and the entire fixative-filled stomach was placed in a large container of fixative and allowed to sit for 1 week. In the remaining animals, 9273, 8911, 9246, and 9921, the stomachs were removed as before, but they were then cut along the greater curvature, pinned out on a sheet of cardboard, and cut once more, this time along the lesser curvature, to divide the stomach into two parts, one consisting of the anterior wall of the stomach, and the other the posterior wall. The posterior wall was then placed in a jar and stored in a freezer at -20° C for subsequent assay of the pepsin content of the mucosa. The anterior wall, still pinned to the cardboard, was floated stomach-side-down in a pan of fixative for 48 hours. All procedures were carried

out over disposable plastic sheets, which, along with all other radioactive wastes, were disposed of by incineration or by a commercial radioactive waste disposal service.

F. Grain-Count-Decay Experiment

One animal on the control diet, 8553, and one animal maintained on a 1 ppm 3,4-TCB diet for 30 days, 8686, were fasted overnight and brought to the surgery suite on separate days affixed to restraint crosses. At 09:00 an indwelling catheter was placed in the saphenous vein and 0.5 mCi of ^{3}H-thymidine / kg of body weight was infused into the animals. Each animal was prepared for the operation and 45 minutes after the ^{3}H-thymidine infusion was anethetized with halothane; then a laparotomy was performed. Approximately 1 hour after the ^{3}H-thymidine infusion, an elliptic biopsy sample about 1.5 x 1.0 cm was excised from the anterior wall of the body of the stomach and was immediately pinned to a small piece of balsa wood and placed in a jar of fixative. The stomach incision was sutured, and the laparotomy site was closed in layers, and the animal returned to its cage for recovery. At intervals of 3 and 7 days after the initial injection of ^{3}H-thymidine and the first biopsy, additional biopsy specimens were taken from each animal, and a biopsy specimen was also taken from animal 8553 on day 9. Care was taken to insure that each specimen was taken at least 2 cm away from the wound of any previous biopsy site. The specimens were kept in fixative until 2 days after the

last biopsy specimen had been obtained.

G. Tissue Preparation for Light Microscopy

The fixed tissues from both the S-phase labeling experiment and the grain-count-decay experiment were prepared similarly. The stomachs or stomach halves from the S-phase labeling experiment were cut from the stomach so that adjacent samples 1.5 x 0.3 cm were obtained from the entire length of the greater curvature; the first sample included a portion of the esophagus, and the last a portion of the duodenum. Samples from the grain-count-decay experiment were simply divided and trimmed to blocks of tissue 1.5 x 0.2 cm. The tissue samples were then dehydrated through an ascending series of ethanol and water solutions (50, 70, 85, and 95%); they were in each solution for at least 15 minutes. Tissue samples were then infiltrated for 1 to 3 days at room temperature in glycol methacrylate monomer, JB-4 Solution A (Polyscience, Inc., Warrington, PA 18976) with 1% benzoyl peroxide, according to Bennett, et al. (15). Embedding was done in a 4° C cold room using JB-4 Solution A with 1% benzoyl peroxide and 1% JB-4 Solution B, a hardener. Plastic molds and aluminum chucks (DuPont-Sorvall, Newton CT 06470) were used; the chuck was placed on the surface of the embedding mixtures so that the plastic-embedded specimens would harden directly onto the microtome chucks. The specimens were allowed to harden for 4 to 6 hours, or longer before they were

transferred to a 60° C oven, where they were left overnight to completely harden.

The hardened specimens were removed from the oven, and excess plastic was trimmed while they were still warm. Sections 2 μm thick were cut on a DuPont-Sorval JB-4 microtome with glass knives made on a Dupont-Sorvall GKM knife maker. The plastic sections were collected from the knife surface with forceps during each pass of the specimen over the knife edge. The sections were floated on a water bath and picked up with glass microscope slides. The slides were placed directly onto a 80° to 90° C hot plate to dry for several minutes. The slides could then be stained without further treatment or prepared for autoradiography.

H. Autoradiography

Only glass and plastic labware, free of any exposed metal surfaces, were used in the autoradiographic procedures. The labware were washed in detergent and then in a dilute solution of sodium hypochlorite. Slides for autoradiography were placed in glass slide holders, washed in deionized water for 5 minutes and air dried. Coating and development of the slides were done in a darkroom equipped with a deep amber-red safelight. Kodak NTB2 liquid emulsion (Eastman Kodak Co., Scientific Products Division, Rochester, NY 14650) was liquified by being warmed to 45° C in a water bath; it was then diluted 1:1 with water. The slides were dipped into a container of diluted emulsion kept at 45° C

and were placed in test tube racks in a light-tight cabinet to dry for 4 hours. The slides were then placed in plastic slide boxes with desicant, sealed in light-tight boxes, and stored in a -20° C freezer for 4 weeks. The autoradiographs were developed in undiluted Kodak D-19 at 15° C for 6 minutes, which optimized the development of exposed silver grains and minimized background grains (21). The developed slides were rinsed in water for 1 minute, fixed in Kodak fixer with hardener for 10 minutes, washed for 10 minutes in water, and air-dried. The autoradiographs were then stained for 1 minute in a solution containing 0.65 M sodium phosphate buffer (pH 7.4), 25% ethanol, 0.025% methylene blue, and 0.025% basic fuchsin. The slides were washed for 5 minutes and air dried. A coverslip with conventional mounting medium was put on top of each. The frequency of background grains was low, 1.5 grains per 1000 square micrometers.

I. Transmission Electron Microscopy

Small (2-3 mm thick) blocks were cut from the wall of the body of the stomach and immediately fixed in 4F1G fixative for 24 hours. Alternatively, specimens from animals 7761 and 7194 were cut after 1 week fixation in 4F1G. After a 30-minute rinse in 0.03 M sodium phosphate buffer (pH 7.4) the specimens were postfixed in 1% OsO4 in 0.08 M sodium phosphate buffer for 2 to 3 hours at 4 C. They were then dehydrated for 10 minutes in each grade of an

ascending ethanol-in-water series (50, 70, 85, 95, 100%) and through two changes of propylene oxide. Afterwards they underwent overnight infiltration and embedding in a low-viscosity embedding medium according to the method of Spurr (157). The embedded specimens were polymerized overnight in a 60° C oven.

Thin sections were cut on a DuPont-Sorvall MT 5000 ultramicrotome with diamond knives. Sections were collected either on uncoated 200-mesh copper grids, or on formvar-coated 1 mm or 2 mm slotted copper grids. These coated grids were produced in the following manner: clean microscope slides were dipped in a solution of 0.3% formvar resin (Ted Pelco, Inc., Tustin, CA 92690) in ethylene dichloride. After the slides had been dried in an atmosphere saturated with ethylene dichloride, their edges were scored with a plastic rod. Then the slides were breathed upon and slid into a water bath at an angle to allow the formvar film to float to the surface. The grids were coated through floation on top of the floating formvar film. A piece of Parafilm was floated on top of the grids, and then lifted carefully to remove the coated grids from the water surface. After being air-dried for 1 hour, the grids were removed from the Parafilm and were ready to use.

Sections were stained for 20 minutes in a saturated aqueous solution of uranyl acetate, rinsed, and stained for 1 minute in lead citrate prepared according to Luft's version (unpublished) of Reynolds' method (136). The sect-

ions were then rinsed and dried.

The sections were examined in a Philips EM-300 electron microscope. Medium- and high-magnification micrographs were taken in a conventional manner with the double-condensor system. For low-magnification micrographs either the current in the projector lens was reduced or the microscope was used in the scan mode, i.e., the objective lens current was greatly reduced and the diffraction lens was used as an objective lens.

J. Scanning Electron Microscopy

Representative blocks of 4F1G-fixed stomach were dehydrated through a graded alcohol series. Some of the specimens were freeze-fractured perpendicularly to the surface of the gastric mucosa; rectangular strips of the tissue were placed in small tubes made of Parafilm and filled with alcohol. The tubes were sealed, immersed in liquid nitrogen, and when frozen, split on a large piece of metal in a pan of liquid nitrogen by means of a single-edged razor and a hammer. The fractured pieces were transferred to alcohol at room temperature. Tissue samples in alcohol were transferred through a graded alchohol-in-trichlorotrifluoroethane series (Genetron 113, Allied Chemical Corp., Morristown, NJ 07960). Once equilibrated with 100% trichlorotrifluoroethane, the specimens were placed in a Bomar SPC-900/EX critical point dryer (The Bomar Co., Tacoma, WA 98401), rinsed with CO_2, and taken to the

critical temperature and pressure for CO_2; the CO_2 was vented through the exhaust system slowly, and the dried specimens were removed. They were then glued to aluminum stubs with epoxy glue and sputter-coated with gold and palladium in a Hummer V sputter coater (Technics Inc., Alexandria, VA 22304).

Once coated, they were examined and photographed in an AMR model 1000 scanning electron microscope (Advanced Metal Research Corp., Burlington, MA 01803).

K. Histochemistry

The histochemical techniques described below were applied to 2-μm-thick sections of tissue embedded in glycol methacrylate.

1. Periodic acid-Schiff's reagent

A modified version of the original method of McManus (15, 110) was employed to demonstrate neutral mucosubstances. Slides were oxidized in 0.5% periodic acid for 5 minutes, rinsed, stained in Schiff's reagent for 15 minutes, washed until the stain developed a dark pink color, counterstained in hematoxylin, washed, air-dried, and mounted.

2. Alcian blue

This stain was employed to demonstrate acidic mucosubstances (101). Slides were stained in an

aqueous solution of 0.2% alcian blue 8GX (Bio/Medical Specialties, Santa Monica, CA 90406) and 3% acetic acid for 30 minutes. The slides were then washed for 10 minutes, counterstained in a solution of 0.1% nuclear fast red and 5% aluminum sulfate, washed again, and mounted.

3. High-iron diamine

The high-iron diamine method of Spicer (155) was used to distinguish sulfated from nonsulfated muco-substances. Slides were stained for 24 hours in a solution of 0.24% N,N-dimethyl-m-phenylenediamine HCl (Sigma Chemical Co., St. Louis, MO 63178), 0.04% N,N-dimethyl-p-phenylenediamine HCl (J.T. Baker Co., Phillipsburg, NJ 08865) and 10 mM Fe+++. The slides were then washed for 10 minutes, air-dried and mounted.

4. Grimelius argyrophil stain

Gastrin-containing cells (G cells) were stained by the Grimelius procedure (53). Slides were incubated in a solution of 0.03% silver nitrate in 0.02 M sodium acetate for 24 hours at 37° C. The slides were then removed, briefly drained, and immersed for 1 minute in a freshly prepared reducing solution of 1% hydroquinone and 5% sodium sulfite at 40° C. So

that staining would be intensified, the slides were incubated again in the silver nitrate solution for 15 minutes, and then immersed again in fresh, unused reducing solution for 1 minute at 40°C. They were then washed for 5 minutes, air-dried, and mounted.

L. Serum Gastrin Levels

An experiment was performed to find out if the 3,4-TCB diet would change the fasting and postprandial serum gastrin levels in the monkeys. Before toxic feeding was begun, blood was collected from four monkeys (8911, 9273, 9246, and 9921) before their morning feeding. The monkeys were then fed 75 ml of Cutter Formula 2 liquid diet via an intragastric tube inserted through their noses. Additional blood samples were collected approximately 60, 120, 180, and 240 minutes after the intragastric feeding. This sampling was done on 3 separate days to obtain baseline values. The tube feeding was considered necessary to ensure that the time and amount of feeding were constant, as they would otherwise vary, particularly when the animals became ill after ingesting the toxic food. In one additional experiment, blood was collected from the animals in the morning, before feeding, as before, but the animals were returned to their cages and presented with their standard diet cakes, and then blood was collected at hourly intervals, as above, to determine whether gastrin levels after intragastric feeding were similar to levels occurring

after normal feeding.

The blood samples were allowed to clot at 4° C for several hours and then centrifuged; the serum was removed for storage at -20° C. The effects of such storage were investigated: four fresh samples were assayed, stored for 2 months at -20° C, and reassayed. The prestorage and poststorage gastrin levels were the same in two samples, but in the other two samples the levels declined 20%. I concluded that storage for 2 or 3 weeks would not seriously affect the results.

Serum gastrin levels were determined with fresh gastrin kits (Radioassay Systems Laboratories, Inc., Carson, CA 90746). These kits use a competitive binding assay in which nonradioactive gastrin competes with ^{125}I-labeled human gastrin for binding sites on anti-human gastrin immunoglobulin. A second antibody is used to precipitate the anti-gastrin immunoglobulin. Unbound ^{125}I-labeled gastrin is aspirated out, and bound ^{125}I-gastrin remaining in the precipitate is counted in a gamma counter (Searle Model 1185).

After the baseline values had been determined, the experimental feeding was begun. Two animals, 8911 and 9273, remained on the control diet, and 9246 and 9921 were fed diet cakes containing 1 ppm of 3,4-TCB. Fasting and postprandial serum samples were collected and assayed , as above, after approximately 1, 3, 4, 6, and 10 weeks of experimental feeding, during which time the animals on the

toxic diet became clinically very ill.

M. Pepsin levels in the gastric mucosa

The posterior walls from three monkeys fed toxic 3,4-TCB diet cakes and three monkeys fed control cakes were collected at autopsy and immediately placed in a -20° C freezer until assayed. Pepsin was assayed by the method of Ryle (143), in which the rate of hydrolysis of denatured hemoglobin is measured.

1. Preparation of denatured hemoglobin

First 12.5 g of bovine hemoglobin substrate (Worthington Biochemical Corp., Freehold, NJ 07728) was dissolved in 500 ml of water and dialyzed for 3 days against 8 liters of water, which was changed several times. Then the hemoglobin solution was denatured by the addition of a 25% (by volume) 0.3 N HCl solution, divided into small lots, and frozen until use.

2. Preparation of the gastric mucosa for assay

Portions of the frozen stomach wall were cut from the body region near the greater curvature with scissors; the gastric mucosa was scraped from these portions with a razor blade. The gastric mucosa scrappings were weighed, and 10 times their weight of 0.01 N HCl were added. The tissue was macerated and then homogenized with a Potter-Elvehjem

homogenizer attached to a portable electric hand drill. Care was taken to keep the homogenate at 0 to 4° C throughout this procedure. The acidic condition of the homogenate assured that all the pepsinogen was converted to pepsin. The homogenate was centrifuged at 5000 rpm (4000 x g) for 10 minutes, and the resultant clear supernatant was serially diluted with 0.01 N HCl in the ratios of 1:3, 1:9, 1:19, 1:49, 1:99, and 1:199 of supernatant to dilute HCl. The protein concentration of each of these dilutions was determined by the method of Lowry (108).

3. Assay procedure

All solutions and reaction mixtures were kept at 0° to 4° C except during the 37°C incubation of the assay. A 0.1 ml portion of each supernatant dilution was added in quadruplicate to 10 x 75 mm disposable glass test tubes. Then 1.0 ml of denatured hemoglobin was added to each tube, and 2.5 ml of 5% trichloroacetic acid (TCA) were added to one of each series of four tubes of the same supernatant dilution; these tubes served as blanks for the others. They were immediately inverted to mix the TCA with the other solutions. The reaction started when the tubes were placed in a 37° C water bath, and continued for 10 minutes, when it was

stopped by the addition of 2.5 ml of 5% TCA to each of the tubes (except the blank, which already contained TCA). The tubes were inverted and centrifuged at 2,500 rpm (1000 x g) for 15 minutes to form a packed precipitate. After the clear supernatant had been aspirated, the absorbance at 280 nm due to the free tyrosine liberated from the hemoglobin by pepsin was measured against the corresponding blank for each enzyme dilution. The results were plotted as absorbance, (A), at 280 nm as a function of the protein concentration. Because this function proved to be linear in the range of 0 to 100 µg of protein per assay, the best fit linear regression of the data within that range was calculated and the enzyme activity was expressed as the slope of this function, that is ΔA at 280 nm per mg of protein for the 10 minutes of incubation. This value was the then multiplied by 100 to convert it to the units conventionallly used to describe pepsin activity (1000 X ΔA at 280 nm/ mg of protein/ minute of incubation). A commercial preparation of pepsin (crystallized hog stomach mucosa pepsin; Sigma Chemical Corp., St. Louis, MO 63178) evaluated by this method was found to have 92% of the activity stated by the manufacturer.

N. Morphometry

1. General instrumentation

The measurements of the distributiion of stained and ^{3}H-thymidine-labeled cells and gastric mucosal thickness were made by a microscope optically coupled to a digitizer, which was in turn coupled to a minicomputer (figure 4). Specifically, a standard light microscope was equipped with a drawing tube attachment, whose field of view encompassed a large portion of the active area of the digitizing tablet of a Zeiss MOP-3 digital measuring instrument. The cursor of this instrument was modified to include a grain of wheat light bulb attached just above the point on the cursor, which interacted with the digitizing tablet. This light bulb was connected to a variable transformer and the light was adjusted so it was comfortably visible as a bright spot superimposed over the magnified image of gastric mucosa as seen through the eyepieces. The room was darkened so that an image of the cursor, the digitizing tablet, and the operator's hand did not also appear superimposed over the image seen through the microscope. The distances between features, A and B, as seen through the microscope, were measured by movement of the cursor on the digitizing tablet so that an image of the cursor's light was superimposed over feature A. The button on the cursor was then pressed, the cursor moved to point B, and the button was pushed again. These steps generated signals in the Zeiss MOP-3, which,

when appropriately programmed, measured the distance in millimeters that the cursor had moved. This was calibrated to the corresponding distances between A and B in the microscope by measurement of known distances on a stage micrometer and determination of a conversion factor. This factor was then programmed into the Zeiss MOP-3 so that the distances would be converted directly to micrometers.

The Zeiss MOP-3 was interfaced to a Tektronics Graphic Systems 4051 minicomputer equipped with a 4051 ED1 ROM expander, a 4907 flexible disc data storage unit, and a 4662 interactive digital plotter. Distance measurements were sent from the Zeiss MOP-3 to the Tektronics computer and stored on flexible discs. A separate file was created for each set of measurements, for example, all the thickness measurements from one microscope slide. Thus, a large number of measurements could be made and stored very rapidly and extremely precisely, with as little as 1% error.

Programms were written in the BASIC language so that these data could be treated as desired. A typical program sorted all of the values of a given set of measurements by means of a binary shell sort subroutine, then the median value, and the mean, standard deviation, and other values were determined. Histograms of the distribution of measurements were constructed by the program and displayed on the cathode ray tube of the computer. These histograms could then be drawn as required on the interactive digital plotter.

2. Mucosal thickness

The distance from the muscularis mucosae to the luminal surface of the gastric epithelium was measured at random intervals along the entire length of each section. This measurement was made on each slide also being measured for other purposes. Typically, 30 to 50 measurements were made on each slide.

3. Range of cells positive for periodic acid-Schiff's reagent

Since the epithelial cells above the deepest PAS-positive cells to those on the luminal surface were all PAS-positive except the parietal and enteroendocrine cells, the range of PAS-positive cells was the region from the lowest PAS-positive cells to the surface. Therefore, the distance between the lowest PAS-positive cells and the muscularis mucosae was measured at intervals along the entire length of each section. Typically 70 to 100 measurements were made on each slide. The mucosal thickness was also determined, as above.

Histograms constructed for each stomach showed the median values of mucosal thickness and the median values for the deepest PAS-positive cells for each section taken along the length of the greater curvature.

4. Range of alcian-blue-positive cells

The range of AB-positive cells was determined identically to the PAS-positive range, since all the epithelial cells above the deepest AB-positive cells, except the parietal and enteroendocrine cells, were AB-positive.

5. Range and distribution of ^{3}H-thymidine labeled cells in the S-phase

Epithelial cells with three or more silver grains above each nucleus were considered labeled and their distances from the muscularis mucosae were measured. The distances of all the labeled cells on a section, or portion of a section, were measured; typically 100 to 300 such measurements were made per slide. Histograms showing the distribution of these distances were constructed from each section taken along the greater curvature. Mucosal thicknesses were also measured, and their median values were displayed on each histogram.

6. Relative labeling densities of ^{3}H-thymidine labeled cells in the S-phase

A grid with white lines on black paper was placed under the view of the microscope drawing tube and a bright light was shone on it so that the white grid lines were visible through the microscope superimposed over the image of the gastric mucosa. The grid was rectangular, and the width corresponded to 200 μm in the microscope field with the 20 X

objective. One of the 200-μm wide sides of the rectangle was placed in a position parallel to the muscularis mucosae; all the labeled cells within the confines of the long sides of the rectangle from the luminal surface to the muscularis mucosae were counted. The grid was then shifted to another position along the muscularis mucosae in a random manner, and the number of labeled cells in that area was counted. Ten such determinations were made for each section from each stomach, and the results were expressed as the number of cells in the S-phase per 200-μm-long length of muscularis mucosae. The results were also expressed as the number of S-phase cells per area of gastric mucosa in cross section. The area was determined through multiplication of 200 μm by the median mucosal height for the section.

7. Labeling indices

The LIs were determined in a conventional manner; labeled cells in the S-phase were counted in a particular gastric gland, and all the nonlabeled cells between the uppermost and the lowermost labeled cells were also counted. Parietal cells, which were never seen labeled, were not considered proliferative cells, and therefore were not counted with the nonlabeled cells. The LI was calculated as:

$$LI = \text{labeled cells}/(\text{labeled} + \text{unlabeled cells}) \times 100$$

Since the proliferative but unlabeled cells could also be located somewhat above and below the uppermost and lowermost labeled cells, the number of nonlabeled cells was somewhat underestimated, and thus the LI was somewhat overestimated; No correction was attempted since only a relative comparison between LIs in normal stomachs and in stomachs from animals fed 3,4-TCB was necessary. Measurements were made on 15 glands from each section, and the results were averaged. The LIs of the gastric epithelium below the muscularis mucosa in animals fed 3,4-TCB were counted separately.

III. RESULTS

A. Clinical Observations

All the monkeys appeared healthy and were gaining weight at an average rate of 75 ± 10 g per month while they were maintained on control diet cakes (figures 5 and 6). Once placed on experimental diets containing 3,4-TCB, the animals immediately began to lose weight, even though they eagerly ate the toxic diet. Initially only two animals were used: 7761, which was kept on the control diet, continued to gain weight, and 7194, which was fed a diet containing 3 ppm of 3,4-TCB, and immediately began losing weight at the rapid rate of 480 g per month. Subsequently, the experimental anmals were fed diet cakes containing only 1 ppm of 3,4-TCB so that they would not rapidly become sick and die before advanced gastric lesions could develop. At this lower level of toxicity, the animals lost weight at a rate of only 110 g per month (animal 9921) to 350 g per month (animal 9246).

Other signs of toxicity were observed: hyperkeratosis of the nail beds, chloracne, and swelling of the eyelids with loss of the eyelashes. These changes were first noted after the toxic diet cakes had been eaten for 3 weeks; they became pronounced in all the animals after 4 weeks. These pathologic changes have been described in detail in a publication by McNulty, Cory, and me (116).

The control animals remained vigorously active and demonstrated aggressive behavior at the least provocation. Subtle behavior changes, such as general quietness and timidness, were noted in the 3,4-TCB-fed animals after a few weeks of toxic feeding. Also noted was a slight jerkiness in the movements of the animals after 3 weeks; it became pronounced as their condition deteriorated rapidly after 6 or more weeks of toxic feeding. The signs of illness displayed by the monkeys were minimal at first, but rhesus monkeys, unlike their human relatives, typically do not show signs of pain and discomfort, unless severe. Animal 9921 remained very alert and active throughout the 14 weeks of experimental feeding, but then suddenly became very ill and sat nearly motionless for 1 day; he was found lying in his cage, alive but unconcious, the next morning. He was given an injection of ^{3}H-thymidine and killed 1 hour later in the autopsy room. Animals 7194 and 9246, also fed 3,4-TCB, were more alert, though somewhat lethargic, on the days they were killed. Animal 8686 never appeared very ill, even after several laparotomies.

B. Autopsy Findings

All animals, except one, were examined post mortem, and their stomachs with adjoining esophageal and duodenal segments were removed. A final full-thickness gastric biopsy specimen was taken at laparotomy from control animal 8553; this animal was then released from the project and is

still alive today. Each animal, except 8686, that was examined post mortem had received an injection of 0.5 mCi of ^{3}H-thymidine / kg of body weight 1 hour before autopsy in order to label the proliferative cells in the gastric mucosa. Animal 8686 had received the same injection 1 hour before his first gastric biopsy, 9 days earlier. Since these animals were very radioactive, only abbreviated autopsies were performed.

No abnormalities were noted at autopsy in any of the three control animals. The principal findings in the 3,4-TCB fed animals were cachexia, dry scaly skin, chloracne, thickened eyelids, loss of eyelashes, raised or absent fingernails, loss of hair throughout the body, and keratin plugs in the auditory canals; dilatation of the gallbladder was seen in animal 9246. The stomachs of animals 7194 and 9246 had somewhat reduced circumferences. No other organs were observed in these animals; however, in other experiments by McNulty et al., monkeys fed 3,4-TCB diet cakes were examined thoroughly at autopsy, and the only consistent additional finding was involution of the thymus (116).

No photographs of the stomachs from these animals were taken at autopsy since it was necessary to prepare and fix the stomachs immediately for light and electron microscopy, in order to minimize post mortem changes. However, stomachs from other toxic feeding experiments conducted for other purposes were photographed. The appearance of a normal

stomach, cut open along the greater curvature, is seen in figure 7a, while the stomach from a monkey fed diet cakes containing toxic levels of 3,4-TCB for 62 days is seen in figure 7b: The foldings of mucosa, called rugae, which are readily apparent in a normal stomach, have been replaced by a thickened, irregular mucosa. The dark areas are focal hemorrhages. Signs of hyperkeratosis of the esophagus were visible to the naked eye in animals fed 3,4-TCB diet cakes, but the cardia, fundus, and antrum appeared relatively normal. Thickened, irregular gastric mucosa was seen only in the body of the stomach, where parietal cells are normally abundant. In stomachs cut along the greater curvature and spread open, this lesion forms a butterfly pattern: the wings correspond to the anterior and posterior walls of the body region, and the body of the butterfly corresponds to the lesser curvature. Severe gastric lesions were seen in animals 7194 and 9246; 8686 had only a moderate lesion, and the stomach of 9921 showed the least thickening of all the animals fed 3,4-TCB diet cakes.

C. Light Microscopic Examination of the Gastric Mucosa and Adjoining Esophagus and Duodenum

Blocks of tissue 0.5 cm X 1.5 cm, including the entire thickness of the stomach wall, were taken along the greater curvature of each stomach beginning with a block that included a portion of the distal esophagus and ending with a block that included a portion of the duodenum, (figure 2).

Sections of tissue (2 μm thick) embedded in glycol methacrylate were cut from each block and stained with methylene blue and basic fuchsin. Figure 8 compares a section from the body of a control stomach with a section from the body of a stomach from a monkey fed a diet containing 3 ppm of 3,4-TCB for 53 days. Hyperplasia of the gastric mucosa was very obvious in the treated animal. In the control stomach (figure 8a), the mucosa occupied the upper half of the total thickness of the stomach wall, and the outermost layer of the stomach, the serosa, which was continuous with the peritoneum, occupied the bottommost layer. In the stomach with the 3,4-TCB induced lesion (figure 8b), the mucosa was twice as thick as normal, and had invaded the muscularis mucosae. The total stomach wall thickness was so great that the muscle wall lay outside the field of view.

I measured the total thickness of the gastric mucosa in each section from the cardia to the pylorus of each stomach (figure 9); in two of the monkeys fed 3,4-TCB diet cakes, 7194 and 9246, the gastric mucosa became much thicker in the body of the stomach; it was not significantly thicker in animal 9921. The stomachs of animals 7761 and 7194 were fixed by ligating the duodenum, filling the stomachs with fixative, and ligating the esophagus. The stomachs of the other animals were cut and pinned flat to cardboard and floated in fixative. Although the intact, fixative filled stomachs were distended, this did not decrease the

thicknesses of their mucosae compared to the other stomachs. Areas of the stomach proximal and distal to the body region were not any thicker in experimental monkeys than in control animals. The sections showing the increased thickness corresponded to the irregular mucosal surface seen in gross specimens (figure 7b).

The severe gastric lesion was confined to the body region of the stomach, but other less striking alterations of mucosal structure occurred in all sections from the esophagus to the duodenum. A pronounced thickening of the squamous epithelial mucosa of the esophagus was seen in the 3,4-TCB-fed animals (figure 10b). The layer of dead epithelial cells covering the surface was thickened, and the squamous cells beneath appear to be larger than normal.

In the cardia (figure 11), the mucosal thicknesses were not altered, but changes in the epithelial cell types were evident. The foveolae of control cardiac glands (figure 11a) were lined with surface epithelial cells, and the glands proper are lined with mucous neck cells in the neck region and zymogenic cells in the bases of the glands. The latter cells were clearly seen as the darker epithelial cells in the bottom third of the mucosa. In 3,4-TCB-fed animals (figure 11b), nearly all the epithelial cells were converted to mucous-secreting cells, and only a few isolated zymogenic cells can be seen in the bases of the glands. The lumen of the glands were dilated and the foveolae were somewhat more irregular than in the control stomachs.

The most severe morphological changes occurred in the body regions of the stomachs of monkeys fed 3,4-TCB diet cakes. There the gastric mucosa became hyperplastic and resulted in the formation of tall irregular glands, some of which invaded and penetrated the muscularis mucosae (figure 8b). In a less advanced lesion (shown at a higher magnification in figure 12b; note that the area of penetration of the mucosa into the submucosa is prominent in the center of the figure), the glands were abnormally dilated and irregular; however, they were of normal height. One of the dilated glands apparently formed a spherical cyst. As in the cardiac and fundic regions, all epithelial cells were converted to or replaced by mucus-secreting cells, and zymogenic and parietal cells were nearly absent.

In control stomachs, the foveolae of the antra were lined with surface epithelial cells, and the glands proper were lined principally with cells similar to the mucous neck cells of the body of the stomach (figure 13a). Enteroendocrine cells were also abundant in the antra, where they were interspersed among mucus-secreting cells. In the 3,4-TCB-fed animals, the glands were dilated (figure 13b). Enteroendocrine cells were also seen, but they appeared less abundant, and were only seen near the bases of the glands.

In each control duodenum (figure 14a), the epithelium lining the intestinal villi was composed of absorptive cells and mucus-secreting goblet cells. Intestinal glands, called crypts of Lieberkühn, branched off from the pits or foveolae

between the villi, in the same manner that gastric glands branched off from the bottom of gastric foveolae. The intestinal glands were lined by undifferentiated cells, absorptive cells, zymogenic cells, (called Paneth cells here), mucous cells and enteroendocrine cells. The submucosa was occupied by Brunner's glands. These branched and highly coiled glands secrete mucus and zymogens into the intestinal glands through short ducts penetrating the muscularis mucosae. In one of the 3,4-TCB-fed animals, these Brunner's glands appeared large and dilated and the cells contained less mucus than in the controls (figure 14b), but the villi and intestinal glands appeared unaltered. The Brunner's glands in the other two experimental animals appeared identical to the controls.

Clearly, the morphological alterations induced by 3,4-TCB diets extended throughout all the blocks of tissue from the distal esophagus to the antrum, and in one of the experimental animals, as far as the proximal duodenum. The hyperkeratosis of the distal esophagus and the greatly thickened mucosa in the body of the stomach suggest hyperplasia in these regions. A loss of specialized epithelial cells, the zymogenic and parietal cells, was especially obvious in the body region of the stomach; in control stomachs these cells were most abundant in that area. The number of parietal cells per 200-um of length of muscularis mucosae was plotted as a function of the relative positions of the sections along the greater curvature

(figure 15). In control stomachs, the number of parietal cells reaches a maximum in the body region, declined rapidly toward the antrum, and approached zero in the pylorus. In all the animals fed 3,4-TCB diet cakes, parietal cells were virtually absent: only a few were encountered in animal 7194, and in animals 9921 and 9246 only an occasional parietal cell was encountered. The peak for the maximum number of parietal cells occurred in the body region in nearly the same relative position as the peak for total mucosal thickness in the 3,4-TCB-fed animals 7194 and 9246 (figure 9).

D. Histochemical Staining for Mucosubstances

1. Periodic acid-Schiff's reagent

Sections were stained for mucosubstances with PAS, which nonspecifically stains most acidic and all neutral mucosubstances. In the control stomachs, the surface epithelial cells were uniformly strongly PAS-positive in all sections from the cardia to the pylorus (figure 16a). The only other cells that were strongly PAS-positive in the control stomachs were mucous neck cells. Mature parietal and zymogenic cells did not stain with PAS. Some cells staining relatively weaker than mucous neck cells were seen. These cells were in the lower neck region of the glands in the cardiac, fundic, and body regions of the stomachs, and were usually side by side with either brightly staining

mucous neck cells, or PAS-negative zymogenic cells. Because of their large size and their large secretory granules, these weakly PAS-positive cells resembled zymogenic cells, an indication that they were mucous neck cells undergoing differentiation to zymogenic cells. Mature zymogenic cells, found toward the bases of the glands, were always PAS-negative.

In the stomachs from the 3,4-TCB-fed animals (figure 16c), nearly all the epithelial cells of the gastric glands were PAS-positive, except for a few remaining zymogenic cells occasionally encountered deep in the glands. This change in the distribution of PAS-positive cells was quantitified through measurement of the deepest extent of PAS-positive cells within the glands of each section taken from the cardia to the pylorus from the control and the 3,4-TCB-fed monkeys (figures 17 and 18). About 100 to 150 measurements of the height above the muscularis mucosae of the deepest PAS-positive cells were made from each section, and the median height was determined. The median height of the gastric mucosa measured from the muscularis mucosae was also determined for each section. The distance between the median mucosal height and the median deepest PAS-positive cell is shown as the heavily hatched area in figures 17 and 18. This heavily hatched area represents the total extent of PAS-positive cells within the mucosa. The area below the deepest PAS-positive cells and the muscularis mucosae is lightly shaded in the histograms. This area corresponds to

the region of the glands occupied largely by zymogenic cells. In the control histograms this area represents about 16% of the total mucosal area. In the stomachs of the animals fed 3,4-TCB diet cakes (figure 18), PAS-positive cells extended deeper; they reached all the way to the bases of the glands in many more experimental sections than in control sections. In the experimentals the mean of the percent of the total areas occupied by zymogenic cells, about 4%, was significantly less (t-test, $p < 0.01$) than the mean of the percent of the total areas occupied by zymogenic cells in the controls, 16.5%. The region of the greatest change corresponded to the body of the stomach, where zymogenic and parietal cells were most numerous in control stomachs. Submucosal cysts, which occurred in the body region of the stomachs of 3,4-TCB-fed animals, were always formed by PAS-positive epithelial cells (figure 16c), although occasional cells nearly devoid of secretory granules were seen.

2. Alcian blue stain

Sections were stained for acidic mucosubstances with AB at pH 2.35. In control animal 9273, only the surface epithelial cells were AB-positive, except in the pyloric region, where the mucus-secreting glandular cells were also AB-positive. In animals 8911 and 7761, surface epithelial cells and mucous neck cells were AB-positive. By comparison, in the stomachs of the 3,4-TCB-fed animals,

nearly all the cells shown to be PAS-positive were also AB-positive, and the staining reaction was generally much stronger than in the controls. Only the cells at the very bases of the glands were AB-negative. These AB-negative cells extended somewhat higher in the pylorus in the animals fed toxic diet cakes. The epithelial cells that had invaded the submucosa and formed cysts were nearly always strongly AB-positive.

Measurements of the deepest AB-positive cells, like those of the PAS-positive cells, were plotted in histogram form (figures 19 and 20). In these histograms, the dark striped area represents the extent of AB-positive cells, and the light area beneath it represents the extent of AB-negative cells. In the control animals, these AB-negative cells were the parietal cells, some of the mucous neck cells, and zymogenic cells. In the 3,4-TCB-fed animals, these AB-negative cells were mostly mucus-secreting cells (which are PAS-positive); a few were zymogenic cells. This AB-neagtive area occupies a mean of 50% of the total area of the control histograms and a mean of only 19% of the total area of the experimental histograms. These means are significantly different by the t-Test ($p < 0.02$). These values are less than the corresponding values for PAS, since PAS-positive cells were found deeper in the glands of both control and 3,4-TCB-fed animals than were AB-positive cells.

3. High-iron diamine stain

Sections were stained for acidic mucosubstances with high-iron diamine. In both the control and 3,4-TCB-fed animals (figures 16b and 16d) the high-iron diamine pattern was indistinguishable from the alcian blue pattern. Therefore, the AB-positive areas in figures 18 and 19 also represent the extent of sulfomucin-producing cells.

4. Summary of mucosubstance staining

In control animals mucosubstances were produced by the surface epithelial and mucous neck cells. Acidic sulfomucins were produced primarily by the surface epithelial cells, but the weaker and more variable staining of the mucous neck cells suggested that their secretory granules also contain acidic sulfomucins, in a relatively smaller proportion than that in surface epithelial cells. The mucous neck cells, and probably also surface epithelial cells, also produced neutral mucosubstances since PAS-positive mucous neck cells lower in the glands were AB-negative, or stained only very weakly. Moreover, the PAS reaction was always very strong in the surface epithelial and mucous neck cells.

In the 3,4-TCB-fed animals, nearly all the cells of the gastric glands produced mucosubstances. These cells stained more intensely for AB and high-iron diamine than either the surface epithelial or mucous neck cells in control animals. This fact suggests not only that 3,4-TCB induced a

conversion of specialized cells to mucous-secreting cells, but also that their secretory granules contained relatively more acidic sulfomucins than mucus-secreting cells in control animals.

E. Pepsin Activity

Frozen samples of gastric mucosa were homogenized and assayed for pepsin activity by the method of Ryle (143) in which the release of tyrosine from hemoglobin is measured spectrophotometrically at 280 nm. Three samples of tissue were assayed from the body region of each stomach. The results are shown below.

PEPSIN ACTIVITY

Control Animals		3,4-TCB Fed Animals	
Animal	Activity *	Animal	Activity *
7994 **	3.2	8686	9.1
	4.0		3.5
	6.5		6.9
7006**	5.0	9921	0
	5.5		1.8
	7.3		2.6
9273	12.9	9246	0
	20.1		0
	10.4		1.2

* Activity is expressed as Δ A280 nm / mg protein / minute.

** Animals 7994 and 7006 were healthy young rhesus adult females killed as controls for other experiments.

The pepsin activity in animals 9921 and 9246 was considerably less than in control animals, but the activity in 8686 was within the range for controls. Considered as a group, the specimens from the 3,4-TCB-fed animals were not significantly different from the controls (Mann-Whitney U test, $p = 0.4$).

Animals 9921 and 9246 had very few remaining zymogenic cells in the tissue samples examined microscopically. Some samples from 8686 had numerous zymogenic cells, and in others all gastric epithelial cells were converted to mucus-secreting cells. The pepsin activity seen in the gastric mucosa of 8686 may have been due to the persistence of zymogenic cells in the areas that were assayed.

F. Autoradiography of Gastric Epithelial Cells in the S-Phase

1. General remarks

Animals were maintained on control diets or on 3,4-TCB diets until the animals fed toxic diet cakes began to demonstrate signs of malaise and loss of appetite. Through previous experience we knew that the animals could be expected to have significant gastric lesions when these signs appeared, but not always before they appeared. In this study, the signs appeared at between days 53 and 97. The animals were brought to the autopsy room, given injections of ^{3}H-thymidine, and killed 1 hour later. Their stomachs were removed and specimens were taken along the full length of the greater curvature. These were prepared for histology and subjected to autoradiography.

2. Description of labeled cells and their location

Nuclei with three or more overlying silver grains were considered labeled, but in general many more silver grains were present over each nucleus and the labeled nuclei were readily visible (figures 21 and 22). In the control animals, labeled nuclei occurred exclusively in the lower foveolae and in the neck regions of the gastric glands in all the sections examined, from the cardia to the pylorus.

The labeled cells were mucous neck cells in the neck region of the glands, and immature surface epithelial cells in the bases of the foveolae (figure 21). Parietal and zymogenic cells were not labeled.

All the animals fed 3,4-TCB diet cakes had gastric lesions with nearly complete conversion or replacement of specialized gastric epithelial cells with mucus-secreting cells. In these animals, labeled cells were seen throughout the gastric glands (figure 22) from below the muscularis mucosae in submucosal cysts to relatively high in the foveolae, although no surface epithelial cells on the surface lining the lumen of the stomach were labeled. A wide variety of mucus-secreting epithelial cell types were labeled. Some were tall cylindrical cells containing large numbers of secretory granules (figure 22a) and others were short cuboidal cells with few mucus granules (figure 22c). In both the control and 3,4-TCB fed animals, labeled cells did not have features that distinguished them from their unlabeled neighbors. Labeled cells were sometimes seen in clusters, an indication that their cell cycles were in synchrony, but labeled cells were just as often randomly dispersed throughout the gastric glands.

3. Frequency distribution of ^{3}H-thymidine labeled cells with respect to their positions

The shortest distance from each labeled cell to the muscularis mucosae was measured in each tissue block from

the cardia to the pylorus of the stomachs. All the labeled cells within a given area of a section were measured: usually 150 to 300 cells. These distances were measured under a microscope with a drawing tube attachment and a digitizing tablet interfaced to a computer as described in the Materials and Methods section. The data were accumulated in separate files for each section, and a program was written to construct frequency distribution histograms with a digital plotter. The results are shown in figures 23 through 25 for the control animals; and 26 through 28 for the animals fed 3,4-TCB diet cakes. The ordinate represents the distance above muscularis mucosae and the abscissa represents the relative frequency as percentage of the total.

The frequency distribution of labeled cells with respect to their distance from the muscularis mucosae closely followed a normal distribution in nearly all sections from the control animals. Few labeled cells were between 50 and 100 μm above the muscularis mucosae; none were less than 50 μm above it. In contrast, in the 3,4-TCB-fed animals, many of the frequency distributions were skewed toward the base of the glands, or were very broad (platykurtic) or narrow (leptokurtic). In addition, labeled cells were found 50 to 100 μm and only 0 to 50 μm above the muscularis mucosae in many more sections in the experimentals than in the controls (no labelled cells were found 0 to 50 μm above the muscularis mucosae in the

controls). The means of the percentage of sections with cells in these regions were significantly less in the controls than in the experimental stomachs (t-Test, $p < 0.01$ for both distance intervals).

Labeled cells were found deeper in the glands of experimental animals than in those of control animals, but the median value in each distribution was not not shifted significantly downward, as can be seen in figure 29 which shows the median distance above the muscularis mucosae for labeled cells from each tissue block for each animal. Although these median distances were not shifted downward, (the mucosal height was somewhat higher in the bodies of the stomachs from 3,4-TCB animals than those from controls; compare figures 17 and 18) the labeled cells were lower in the glands in relation to the height of the mucosa. This relationship is shown in figure 30, in which the ratio of the median height of labeled cells above the muscularis mucosae to the median mucosal height is plotted as a function of the position of the section along the greater curvature of the stomach. It can be seen that in control stomachs this ratio was somewhat constant, about 0.5 throughout the stomach, whereas in the body regions of the stomachs of 3,4-TCB-fed animals it was only 0.15 to 0.3. The mean of the ratios in the body region of the experimental stomachs was significantly less than the the mean of the ratios from the same region in the controls (t-test, $p < 0.01$).

These results indicate that although the mucosal height increased with development of the gastric lesion, the proliferative region did not maintain its same relative position within the gland (its height above the muscularis mucosa was not more than in the controls, and some labeled cells were found lower than those in the control tissue).

4. Labeling Density of ^{3}H-thymidine labeled gastric epithelial cells

To estimate whether more gastric epithelial cells were proliferating in the 3,4-TCB-fed animals than in the controls, I determined the number of H-thymidine labeled epithelial cells per 200 μm of muscularis mucosal length for all the sections taken along the greater curvature of the stomach. This value represented the labeling density per unit length of muscularis mucosae. The results shown in figure 31 indicate that the density of labeled cells in the gastric mucosa of 3,4-TCB-fed animals was no greater than that in controls. Actually, the mean of the density values just distal to the cardia was significantly less in the 3,4-TCB-fed animals than in the controls (t-test, $p < 0.05$). In two of three controls and two of three of experimental animals, the density of labeled cells was 3 to 10 fold greater in the distal body and antral regions than in the cardiac and fundic regions, but this increase did not occur in the third animal of either group.

The number of labeled cells was also determined per

square millimeter of mucosal area in cross section. This estimated the labeling density relative to the volume of gastric mucosa. As seen in figure 32, the labeling densities expressed in this manner presented very similar patterns of fluctuation along the length of the greater curvature as did the labeling densities expressed per unit of length of muscularis mucosae in figure 31.

5. Labeling indices of gastric epithelial cells

The proliferative cells of the gastric epithelium could have shortened cell cycle times in the 3,4-TCB-fed animals; if they did, this would explain the development of the hyperplastic lesion. Since the duration of the S-phase in gastric epithelial cells remains somewhat constant, even in the presence of gastric disease (63), the percentage of cells in the S-phase, referred to as the labeling index (LI), can be a measure of the relative cell cycle times. The LI would be expected to increase if the cells were proliferating more rapidly; faster proliferation would depend on a shortening of G_1 and G_2, and hence the S-phase would occupy a greater portion of the total cell cycle time.

The LIs were determined in sections from control animals and animals fed 3,4-TCB diet cakes. These LIs showed similar patterns of change from the cardia to the pylorus of each animal (figure 33), as did the corresponding labeling density determinations (figures 31 and 32). However, one notable exception was that I found no relative

increase in the LI in the pylorus of animal 9921, in which a marked increase in labeling density was seen. The reason for this phenomenon is that, although there were more cells in the S-phase in this section, they were spread out throughout the deep pyloric glands; hence the percentage of labeled cells, the LI, was small. Nevertheless, the LIs of 3,4-TCB-fed animals clearly were not greater than those in corresponding sections from controls; moreover, the mean of the LIs distal to the cardia was significantly less (t-test, $p < 0.01$) in the 3,4-TCB-fed animals than in the controls. I therefore think it unlikely that the 3,4-TCB induced hyperplasia was due to a decrease in cell cycle times, and hence an increase in the rate of cell proliferation. However, the possibility remains that the S-phase time might also have been shortened proportionately, in which case the LIs would have remained unaltered, even if the total cell cycle time had shortened. I don't consider this possibility likely since alterations in cell cycle times are usually due to changes in the "resting" periods of the cell cycle, G_1 or G_2, and the time it takes for the genome to be replicated, the S-phase, usually remains constant.

The mean of the LIs within the submucosal glands in the body region of the stomachs of the animals fed 3,4-TCB was only 7.9 ± 1.2 (s.e.m.), significantly less (t-test, $p < 0.01$), than the mean of the LIs in the primary proliferative zone above the muscularis mucosae in the same animals; there the mean of the LIs was 18.1 ± 3.6 (s.e.m.). It was

also significantly less ($p < 0.05$) than in the corresponding sections from the controls, for whom the mean of the LIs was 16.1 ± 1.4 (s.e.m.).

6. Grain-count-decay experiment

The grain-count-decay method more directly indicates the rate of cell proliferation than the LI method. The mean grain counts of ^{3}H-thymidine-labeled cells remaining within the proliferative compartment were determined and plotted semilogarithmically as a function of the time elapsed since the cells had been labeled initially. A least-squares, best-fit linear regression line was constructed; its slope approximated the rate of decay of labeling in the cells as the cells divided. From this line, the time it took for the mean grain count to become half of the original value was estimated. This time approximately corresponded to the cell cycle time, since with each division the amount of labeled DNA remaining in the daughter cells was halved. In figure 34 are shown the results of one such experiment, in which control animal 8553 and 3,4-TCB-fed animal 8686 received injections of ^{3}H-thymidine; 1 hour later biopsy specimens were removed at laparotomy, and again on days 3 and 7, and also on day 9 for animal 8686. Sections from all the biopsy specimens were uniformly examined by autoradiography and the mean grain counts of cells remaining within the proliferative region were determined. Although the slopes of the regression lines were not significantly different by

analysis of covariance ($0.2 < p < 0.4$), the results suggested half-times of about 1.6 days for the control animal and 3.0 days for the animal maintained on the 3,4-TCB diet. The biopsy specimens from the control animal all appeared normal; those from the 3,4-TCB fed animal showed development of the characteristic hyperplastic, cystic glands seen in 3,4-TCB poisoning.

These results suggested a longer cell cycle time for the 3,4-TCB-fed animal than for the control, the opposite of what would be expected if the observed hyperplasia had resulted from an increase in the rate of proliferation of the gastric epithelial cells.

Because the cell cycle times could only be imprecisely estimated by this method, and because the results did not suggest that the 3,4-TCB-induced hyperplasia resulted from a shortening of the cell cycle time, the experiment was not repeated.

G. Electron Microscopic Examination of the Gastric Mucosa

1. Scanning electron microscopy: Changes on the surface of the gastric mucosa

Representative blocks of tissue were taken from all regions of the stomachs of the animals fed control diet cakes and the animals fed 3,4-TCB diet cakes. Changes were seen in the surface architecture of the gastric mucosa from 3,4-TCB-fed animals that had not been readily apparent in

cross-sectioned, embedded tissue examined under a light microscope. The changes included irregularities in the openings of the foveolae to the surface and outward extrusions or bulges of individual and groups of surface epithelial cells. These changes were seen in all regions of the stomach, but were most pronounced in the cardiac, fundic, and body regions.

In the cardia, the most prominent change was a bulging of surface epithelial cells above the surface. In control animals (figure 35a), the surface epithelium formed a smooth contour of hills and deep valleys; the valleys were the openings to the foveolae. In the 3,4-TCB-fed animals (figure 35b), many surface epithelial cells protruded above their neighboring cells, to make the surface very uneven; many of these cells had discharged their apical secretory granules.

Only in the 3,4-TCB-fed animals did the entire surface epithelium in the body region of the stomach seem to bulge out around each foveola (figures 36b and 36c); individual surface epithelial cells were also seen bulging outward. In 3,4-TCB animal 8686, the surface epithelium was particularly irregular (figure 36c).

The foveolae (seen at a higher magnification in figure 37) presented only narrow slit-like openings to the surface in the specimens from the control stomachs, but in the 3,4-TCB-fed animals, these openings were much larger.

In the antral and pyloric regions of the stomach, the

changes were less severe, and were limited primarily to protrusion of the surface epithelial cells above the surface in 3,4-TCB-fed animals (figure 38b).

These phenomena, protrusion of cells above the surface and an irregular surface contour, can be more clearly seen at higher magnifications in figure 40. Control surface epithelial cells from the body region (figure 39) presented a uniformly smooth surface, much like a well-constructed cobblestone road. However, in the 3,4-TCB-fed animals (figure 40), the surface epithelial cells seemed to have lost their cohesiveness to one another or to the basement membrane, or were somehow forced upward. In any case, they presented highly irregular patterns of surface contours, and many of the cells clearly bulged above the surface. The apical surfaces of individual epithelial cells from 3,4-TCB-fed animals (seen at higher maginification in figure 40) were often quite similar to those from control animals (figure 39). However, cells with portions of their apices discharged, or completely missing, were also seen in the toxic fed animals, and they were rare in the controls (figures 36b and 40b).

2. Scanning electron microscopy: Cystic gastric glands in animals fed 3,4,3',4'-tetrachlorobiphenyl

Freeze-fractured and cut surfaces of critical-point-dried gastric mucosa from normal and 3,4-TCB-fed animals were examined by scanning electron microscopy. In specimens of control gastric mucosa the lumen of the glands were very narrow, and little cellular detail was visible that could not be better seen by light and transmission electron microscopy in cross-sectioned, plastic-embedded specimens. However, in specimens from the 3,4-TCB-fed animals, the cystic nature of the gastric glands was very prominent (figures 41 and 42). Masses of material, almost certainly mucus secreted by the cells lining the glands, were seen in the dilated lumen (figure 42a). This mucus may have obstructed the lumen, restricted the outlow of mucus, and thereby caused the glands to be swollen and cystic.

The luminal surface of the cells lining the cystic glands was covered by numerous small blebs, probably microvilli (figure 42b).

3. Transmission electron microscopy: Gastric mucosa from control and 3,4,3',4'-tetrachlorobiphenyl-fed animals

Samples of gastric mucosa were obtained at autopsy from the body regions of stomachs from animals sacrificed at autopsy. The samples were fixed immediately; embedded; and prepared for electron microscopy by conventional methods. Since the structure of the gastric epithelial cells in the animals fed 3,4-TCB diet cakes undergoes profound changes, it was important to examine the normal structure of these cells to establish a baseline. In control gastric mucosa the diversity of cell types and the structural diversity of this tissue were evident in low-magnification micrographs (figure 43). Surface epithelial cells (SEC) lining the lumen of the stomach were clearly seen (figure 43a). They are the tall, cylindrical, mucus-secreting epithelial cells whose prominent dark apical regions are filled with secretory granules. The downward indentations of epithelium, the gastric foveolae or pits, were also lined with surface epithelial cells. Cells deeper in the foveolae were somewhat shorter and had fewer secretory granules. These were immature surface epithelial cells that were formed lower in the isthmus region of the glands and had migrated upward, to eventually replace surface epithelial cells lost at the luminal surface of the stomach. The lamina propria (LP) (loose connective tissue that serves as a barrier to infection and provides structural support and nourishment to the cells of the

structural support and nourishment to the cells of the gastric epitelium) contained fibrocytes, the endothelial cells of capillaries and lymphatics, macrophages, lymphocytes, mast cells, eosinophils and others. The neck region, which began beneath the foveolae, was lined with mucous neck cells (MNC) and parietal cells (P) (figures 43b and 43c) These MNCs and immature SECs are the proliferative cells of the gastric epithelium. MNCs, like SECs, secrete mucus. The MNCs were more cuboidal than SECs, and their secretory granules appeared rounder and sometimes less electron-dense.

The uppermost parietal cell marked the upper limit of the isthmus region of the gastric gland. More parietal cells (whose function is to secrete HCl) were seen deeper in the glands (figure 43c). The uppermost and the lowermost MNCs marked the boundaries of the neck region of gastric glands. A gradual transition of structure was seen from the MNCs to zymogenic cells (Z) (figure 43c).

Deeper in the glands (figure 43d), zymogenic cells predominated, but occasional enteroendocrine cells were also seen (arrows). The muscularis mucosae (composed of smooth muscle cells) lay at the bases of the glands.

The apical regions of the mature SECs were filled with polygonal electron-dense secretory granules (figure 44a). A few microvilli were visible on the luminal surface. These were probably identical to the small surface blebs seen by scanning electron microscopy. The middle region of these

cells were filled with endoplasmic reticulum, ribosomes, and small secretory granules. A few of these smaller granules below the larger apical masses of granules appeared to be moving upward to fuse with each other and the large granules. Less mature SECs were seen toward the bases of the foveolae above the isthmus of the glands (figures 44c and 44d). Cytoplasmic details were more distinct in these cells. As in mature SECs, smaller electron-dense vesicles appeared to migrate toward the apices of the cells, where they fused and formed larger secretory granules. The smaller secretory granules were less dense than the larger granules near the luminal surface. In the perinuclear regions of these cells horseshoe-shaped Golgi apparati and numerous mitochondria were seen. Their cytoplasm appeared to be specialized for the production of mucus.

Mucous neck cells (figure 45) were shorter than SECs and usually contained fewer secretory granules, which tended to be round, unlike the polygonal granules seen in mature SECs (figure 44a). Interdigitations of the plasmalemma with neighboring cells, common features of all gastric epithelial cells, were especially evident in mucous neck cells (figure 45b).

Mucous neck cells are proliferative cells that differentiate to become other mature gastric epithelial cell types. Those moving upward become SECs, and those moving downward become zymogenic cells; some MNCs differentiate within the neck region to become parietal cells. Evidence

for the differentiation of MNCs to parietal cells is seen in figure 46. Mucous neck cells with only a few secretory granules and numerous clear vesicles were seen between neighboring, young parietal cells (Figure 46a). These small vesicles were similar to those of the tubulovesicular system in resting parietal cells (figure 47). Mitochondria, very numerous in parietal cells (figure 47), were also numerous in MNCs; their presence in large numbers in the MNCs was further evidence that these cells were differentiating into parietal cells. Canaliculi, numerous mitochondria with closely packed cristae, and many electron-lucent tubulovesicles were clearly seen in mature parietal cells (figure 47).

Mature zymogenic cells were found in the base regions of gastric glands (figure 48). They contained an extensive, well-developed system of rough endoplasmic reticulum. Large secretory granules filled most of the cytoplasm, especially in the apical regions of the cells. These granules were more electron-lucent than the mucous granules of MNCs and SECs. Enteroendocrine cells, (figure 48b) were most abundant in the bases of the gastric glands. These cells, whose origin is uncertain, were located above the basement membrane, and hence were within the gastric glands, as were the other gastric epithelial cells. Mast cells (figures 48a and 48b) were located beneath the basement membrane in the lamina propria.

As already shown by light microscopy, the gastric

glands of normal gastric mucosa were converted to cystic, hyperplastic glands in animals fed 3,4-TCB diet cakes. Histochemical and pepsin assays of the tissue demonstrated that the specialized epithelial cell types of normal gastric mucosa were replaced by mucus-secreting cells. The structural details of these altered epithelial cells were more clearly seen by transmission electron microscopy. The changes from normal gastric mucosa were very marked (figure 49). The foveola of a dilated gland is seen in figure 49a. The cells lining the dilated glands were all mucus-secreting, but their structure was unlike the normal SECs seen at this level in control gastric glands. Many of the cells appeared to have discharged all their mucous granules into the lumen in an apocrine manner, i.e. the entire apical portions of the cells were discharged. All cells had irregular apical surfaces, and the lumens of the glands appeared to be distended with mucus. The lamina propria was very attenuated, unlike that in the upper portion of control gastric mucosa (figure 43a)

Dilated glands also occurred deeper in the mucosa (figure 49b). The lamina propria was very thin and flattened here, as elsewhere, possibly owing to to the dilation of the glands. The apical surfaces of the mucus-secreting epithelial cells were very irregular (figures 49a to 49d). Frequently the mucus granules had fused together, broken through the plasmalemma, and left the cell without any membrane facing the lumen of the gland

(figures 49 and 50c).

Animal 9921 had the least severe gastric changes of all the animals in this study. Presumably the lesion in this animal had not progressed as far as those as in other animals. Electron microscopic examination showed that although nearly all the cells were mucus-secreting, they lacked severe signs of cell injury seen in the other animals, and more closely resembled the MNCs of the normal control animals. Their apical surfaces were, however, frequently very irregular (figure 49c).

Perhaps the most impressive feature of the mucus-secreting epithelial cells was the great diversity of their structures. In 3,4-TCB animal 9921 rather normal appearing mucus-secreting cells were seen (figures 50a and 50b). They contained some mucous granules in their apices, and intact plasmalemma with numerous microvilli on the luminal, apical, surface. Unremarkable mitochondria were also numerous in the cytoplasm, and a few electron-lucent vesicles were seen. These vesicles were also found in control MNCs that appeared to be differentiating into parietal cells, but there they were more numerous. Other cell structures such as junctional complexes and elaborate interdigitations of the plasmalemma with neighboring epithelial cells were seen frequently (figures 50a and 50b). Yet no cells undergoing differentiation to parietal cells, nor mature parietal or zymogenic cells were seen. Occasionally a few remaining zymogenic cells were seen by

light microscopy in the bases of isolated glands, although none were encountered in any of the sections prepared for electron microscopy.

In contrast to the relatively normal cells seen in the animal 9921 were the epithelial cells in 3,4-TCB animal 9246 (figure 49b and 49d) and at higher magnification in figure 51c); these showed striking changes. The mucous granules had fused and broken through the apical plasmalemma into the lumen of the gland. Furthermore, the remaining cytoplasm was disorganized, and the nucleus was flattened and has an irregular outline. Cells in the lamina propria also appeared disorganized.

In 3,4-TCB animal 7194 (figure 50d), a quite different type of epithelial cell was seen. These tall cylindrical epithelial cells from a submucosal cyst did not appear to contain mucus-laden secretory granules, a not unexpected finding since light microscopic examination of PAS-stained sections had revealed occasional groups of epithelial cells without appreciable numbers of PAS-positive granules in gastric mucosa from 3,4-TCB animals.

Although the SECs were frequently quite normal in the mucosa from 3,4-TCB-fed animals, areas of surface mucosa with greatly altered cells were also seen (figure 51a). In these cells, the apical regions were not filled with masses of secretory granules as in control SECs (compare with figure 44a). The cytoplasm appeared disorganized and contained numerous vacuoles and irregularly shaped secretory

granules.

Irregularities in the cytoplasm of all the epithelial cells in the gastric mucosa of animals fed 3,4-TCB were a common finding, although the cytoplasmic irregularities varied greatly from cell to cell. Long fibrillar structures (figure 51b) were never seen in the gastric mucosa of control monkeys. These structures resembled the fibrils seen in fibrillovesicular cells in canine (21) and human (31) gastric mucosa.

Alterations in membrane structures were also commonly seen. Severely dilated endoplasmic reticulum (figure 51c) was a common finding. The cell-to-cell interdigitations of the plasmalemma seen in control gastric mucosa were also regularly seen 3,4-TCB mucosa, but in the 3,4-TCB-fed animals these interdigitations frequently appeared exaggerated and more extensive than normal (figure 51d). The saccules of Golgi apparati frequently were abnormally depleted and packed closely together (figures 51d and 52b). Autophagic vacuoles, seen only occasionally in control mucosa, were commonly encountered in the mucosa of 3,4-TCB-fed animals (figure 52). In the 3,4-TCB-fed animals, the autophagic vacuoles were much larger than those seen in the control animals, and they frequently were packed with many layers of membranes.

H. Serum Gastrin Levels

Serum gastrin levels were measured to determine if any change had occurred after 3,4-TCB feeding. An elevation in serum gastrin levels could have been responsible for the observed hyperplasia, or a decrease in gastrin levels could have kept the gastric epithelial cells from differentiating. Serum gastrin levels were determined by radioimmunoassay. In the first experiment, blood samples were taken at 08:30 from the animals after an overnight fast; then the animals were returned to their cages, in which control diet cakes had been placed. Additional blood samples were taken at intervals until 11:30 a.m.. The results (figure 53) showed that the serum gastrin levels rose, presumably in response to the food they had eaten. Animals 9921, 9273, and 8911 showed similar fasting levels and postprandial rises; animal 9246 had a fasting level three times that of the others, and his postprandial levels were proportionately higher.

In order to minimize variations in the postprandial responses of the four animals that might be due to differences in eating habits, I altered the procedure. After their overnight fast, the animals were removed from their cages and affixed to restraint crosses; a blood sample was taken from each at 08:30. Nasogastric tubes were then inserted and each animal was fed 75 ml of Cutters Formula 2 liquid diet. Additional blood samples were then taken about 75, 130, 180 and 240 minutes after the feeding.

This regime was repeated on 3 separate days for the four animals. The fasting and postprandial gastrin levels (figures 54, 55, 56, and 57) were very similar to those of the previous experiment. Animal 9246 continued to have high gastrin levels. These values were considered baseline.

Animals 9246 and 9921 were placed on diets containing 1 ppm of 3,4-TCB, and animals 8911 and 9273 were left on control diets. Fasting and postprandial serum gastrin levels were monitored throughout the experimental feeding (figures 54, 55, 56, and 57), and no significant changes were observed in animals 9273 and 8911 (control diets) or in animal 9921 (3,4-TCB diet). The very high gastrin levels in animal 9246, seen in all four of the determinations made before the experimental feeding had begun, persisted only in the determination performed after 8 days of 3,4-TCB feeding. After 22 days of 3,4-TCB feeding, the gastrin levels were much lower and were similar to those seen in the other animals, except that no postprandial rise occurred.

In animals 9921 and 9246 significant gastric lesions developed and the specialized gastric epithelial cells were replaced with mucus-secreting cells. Since the fasting and postprandial gastrin levels appeared unchanged throughout the experimental feeding of animal 9921, I concluded that alterations in gastrin levels were not necessary for the development of the 3,4-TCB-induced gastropathy.

The stomach contents of all four of these animals were aspirated through the nasogastric tube before the

introduction of food throughout the experiment. In all animals the contents were consistently of a neutral pH before and after the experimental feeding. Correct placement of the stomach tube was confirmed in one instance by X-ray examination; and in all other instances by introducion of 10 ml of water and subsequent recovery of the water through the nasogastric tube. Animal 9246 had very high fasting and postprandial gastrin levels and appeared entirely normal before experimental feeding, but his fasting stomach contents were never acidic.

One hypothesis for the decline in serum gastrin levels in animal 9246 is that the production of abnormal amounts of gastrin occurred in overactive or overabundant G cells in his stomach: after prolonged feeding of 3,4-TCB diet cakes to this animal, the gastric epithelial cells, including the G cells in the stomach, but not those in the pylorus, were converted to mucus-secreting cells. Thus, the only remaining gastrin production would have been in the gastrin-secreting G cells in the pylorus.

The gastrin levels of animal 9921 did not change. A possible explanation, persistence of G cells in the duodenum, is consistent with the histological observations of sections stained by the Grimelius argyrophilic reaction, which specifically stains gastrin-containing G cells. Only occasional G cells were seen in the body regions of stomachs from control animals (figure 58a), but many more were found in the antrum and duodenum. Although Grimelius-positive

cells were absent from the body regions of animals 9921 and 9246, they were still present in areas of the antrum and were abundant in the pylorus (figure 58b). Thus the abundant G cells remaining in the pylorus of the 3,4-TCB-fed animals may have sustained the gastrin levels in animal 9921 and provided the remaining gastrin seen in animal 9246.

IV. DISCUSSION

In previous studies my colleagues and I (13) and others (2, 7, 14) have clearly established that commercial mixtures of PCBs induce pronounced morphological changes in the gastric mucosa of rhesus monkeys when fed at dietary levels as low as 10 ppm and at levels as low as 0.3 to 3.0 ppm of 3,4-TCB (116). These changes include the development of hyperplastic, cystic, gastric glands that extend beneath the muscularis mucosae to form submucosal cysts (2, 7, 14, 13, 116). To investigate the manner in which this lesion develops, my colleagues and I fed monkeys diet cakes containing 0, 3, 10, 30 or 100 ppm of a commercial mixture of PCBs, Aroclor 1242 (13). Serial biopsy specimens were taken from the animals at monthly intervals for as long as 6 months. The PCBs caused an apparent failure of the proliferative cells in the mucous neck region to differentiate to zymogenic and parietal cells. Mature parietal and zymogenic cells were seen, but only in the bases of the gastric glands, where normally the oldest gastric epithelial cells are found. Other evidence (McNulty, unpublished data) suggests that PCBs and their related compounds may also be capable of converting mature zymogenic and parietal cells into mucus-secreting cells. When a rhesus monkey was fed a diet containing 20 parts per billion of TCDD, it became ill after only 5 days, and died

after 12 days of the TCDD regimen. In this animal virtually all the cells of the gastric epithelium were mucus-secreting cells. If the mucosa was normal before the TCDD feeding, the epithelial cells must have somehow been converted to or replaced by mucus-secreting cells. But since this occurred more rapidly than could be explained by the normal turnover of zymogenic and parietal cell populations, I believe that the mature, specialized cells were converted directly to mucus-secreting cells.

Regardless of whether or not mature zymogenic cells can be converted to mucus-secreting cells, or only replaced as they die by younger mucus-secreting cells which have failed to differentiate, these previous studies did not explain the mechanism of gastric epithelial hyperplasia and resultant mucosal thickening and extension of the gastric glands below the muscularis mucosae. Clearly, there is an alteration in the steady-state dynamic equilibrium of cell loss and replacement. As postulated in the Introduction, the hyperplastic changes could be caused by any one or combination of different mechanisms, including those discussed below.

Mechanism 1. Proliferation occurs uniformly throughout the gastric gland, that is, all cells become capable of proliferation, and cell cycle times may or may not be altered.

Mechanism 2. Gastric epithelial cell proliferation occurs only in the normal proliferative zones in the isthmus and the neck, but the cell cycle times are shortened, and therefore more cells are formed than are lost.

Mechanism 3. Proliferation may occur normally in the normal proliferative zone, and additional proliferation occurs in other zones and cell types, such as:

a. In the surface epithelial cells
b. In immature cells that retain their proliferative capacity and fail to differentiate
c. In parietal and zymogenic cells that have lost their specialized function and have acquired proliferative capacity

In this study, three control monkeys and three monkeys fed a highly toxic polychlorinated biphenyl, 3,4,3',4'-tetrachlorobiphenyl (3,4-TCB), received injections of ^{3}H-thymidine and were sacrificed one hour later. Autoradiographs were prepared of sections from blocks of tissue taken along the greater curvature from the esophagogastric junction to the pylorus. The positions of ^{3}H-thymidine-labeled gastric epithelial cells were measured in relation to the muscularis mucosae, and frequency distribution histograms were constructed of these positions.

In control animals (figures 23, 24, and 25), the pattern of distribution approximated a normal distribution in nearly all the sections, and the median position was about midway from the muscularis mucosae to the surface of the gastric mucosa. Almost no labeled cells were encountered in the bottom of the glands, less than 100 μm from the muscularis mucosae, and none were seen less than 50 μm from the muscularis mucosae.

In sharp contrast to the control animals, the animals fed 3,4-TCB had quite varied distributions of labeled cells (figures 26, 27, and 28). In some sections the distribution was very narrow (leptokurtic) and was located near the bases of the glands; in other sections the distribution was very broad (platykurtic) and ranged from the bases of the glands to near the surface; while in many other sections the distribution was more normal. Most importantly, however, labeled cells were seen in the bases of the glands, less than 50 μm from the muscularis mucosae, in the majority of the sections of two of the animals, and in all of the sections of one animal. The percentage of the labeled cells in this region was always less than 10% and was usually only 1 or 2% of the total number of labeled cells. These few labeled cells in the base regions may be very important, as I will explain.

In the normal gastric mucosa, the majority of all newly formed epithelial cells migrate upward to the surface, where they become the surface epithelial cells (74, 118, 165) and

are eventually either extruded into the lumen of the stomach, or degenerate in situ (62). Only a small number of the newly formed cells migrate downward (65, 81, 172) to replace the older zymogenic and parietal cells, which either are extruded, in this case into the glandular lumen, or degenerate in situ. The number of cells that migrate downwards must exactly balance the number lost in order to maintain the population of cells in a steady-state. Since no labeled cells were seen in the base regions of control animals, I have concluded that cell proliferation does not normally occur there.

Therefore the presence of even a few labeled cells in the base region of the gastric glands of 3,4-TCB-fed monkeys represents an additional source of new epithelial cells for this region. Without a corresponding increase in cell loss, which was not observed, the increase in the number of cells being added to the base region above that required to balance normal loss must surely cause the total population of cells in the base region to increase.

The labeled cells in the bases of the glands and elsewhere in the 3,4-TCB-fed monkeys were indistinguishable from their neighbors; thus, it may be that all the cells in the bases of these glands are in various stages of the proliferative cycle. It is quite possible they are since no cells were observed differentiating into mature specialized cells; therefore cell aging and death might not occur. The cell population would then be expanding exponentially,

limited in growth only by the availability of an adequate blood supply.

In mechanism 1, postulated above, all the epithelial cells in the gastric mucosa would uniformly become capable of proliferation. The results shown in figures 26, 27, and 28 indicate that this mechanism is very unlikely; labeled cells did not occur with a uniform frequency throughout the glands, but rather were more frequent in a zone, usually centered in the middle of the gastric mucosa. Cells were less frequently labeled, in general, the further away they were from this zone; and no labeled cells were seen at the surface.

In mechanism 2, above, cell proliferation would occur only in the same population of proliferative cells as in normal animals, except that the cell cycle times would be shortened. Cell formation would exceed cell loss and hyperplasia would result. However, two independent observations indicate that this mechanism is also unlikely. First, in the grain-count-decay experiment (figure 34), the grain-count-decay rate in the 3,4-TCB-fed animal was not greater, and even appeared less than that in the control animal, an indication that the cell cycle time may even be somewhat longer in 3,4-TCB-fed animals than in controls. Secondly, the relative labeling densities were determined throughout the stomachs of the animals (figures 31 and 32), and the results indicated that regardless of whether the labeling density was expressed in relation to a unit length

of muscularis mucosae or in relation to the area of mucosa in cross-section, the relative numbers of cells in the S-phase in 3,4-TCB-fed animals were not measurably greater than those in controls. The labeling density was even less near the cardiac region in the 3,4-TCB-fed animals than in the controls. Similarly, comparison of the labeling indices in the proliferative zone in the 3,4-TCB-fed animals with the controls also failed to show any increase (figure 33), and the labeling index was actually less in the same region near the cardia, as was the labeling density.

Use of relative measurements of the number of cells in the S-phase, such as the labeling index and the labeling density as indicators of the rates of proliferation of cell populations has as its principal limitation the fact that changes in the S-phase duration could increase or decrease the labeling index or density without any real change in the number of proliferating cells or their total cell cycle times. Lacking knowledge of the duration of the S-phase in the gastric mucosa of these animals, I cannot exclude the possibility that there may be differences in the proliferation rates in the 3,4-TCB-fed animals that are masked by changes in the S-phase duration.

The estimation of cell cycle time by the grain-count-decay method was limited by its imprecision. Despite the limitations of the methods used in this study, I found no evidence of a more rapid rate of cell proliferation due either to a shorter cell cycle or a larger proliferative

cell population in the gastric mucosa of the 3,4-TCB-fed animals.

Therefore I believe that mechanism 3 is more likely, i.e., additional proliferation occurs in cells that failed to differentiate, and possibly also in zymogenic and parietal cells which loose their specialized functions. The downward growth of the gastric glands may be explained by the presence of proliferating cells in the bases of these glands, where proliferation does not normally occur. If this abnormal proliferation results in excess numbers of cells in the bases of the glands that cannot expand upward, these cells would be forced to expand downward through weak points in the muscularis mucosae. This would form submucosal glands and submucosal cysts would result from the continued proliferation of the cells lining these glands and by the secretion and accumulation of viscous mucous material.

Although a plausible explanation for the development of submucosal cysts has been presented, the increased height of the gastric mucosa and the irregular configurations of surface epithelial cells seen by scanning electron microscopy cannot be so easily explained. If the middle and upper regions of the gastric gland are simply forced upwards as the base region increases in mass due to the abnormal occurence of proliferation in the base, the major zone of proliferation should also be forced upward. But this major zone of proliferation seems to remain at a nearly constant

height. Figure 29 shows the median heights of labeled cells above the muscularis mucosae. The data clearly indicate that the proliferative zone has not shifted upward, and may even be shifted downward somewhat.

In any case, Hattori (64) has demonstrated that the proliferative zone in the gastric mucosa of hamsters is firmly anchored by a stromal sheath of fibrocytes and collagen fibrils which are in contact with the basement membrane of the proliferative cells. Hattori believes that the tight stromal sheath plays an important role in maintaining the proliferative capacity of the cells it surrounds; and once newly formed cells leave the confines of the sheath, they lose their proliferative capacity. Rhesus gastric glands do not appear to be as rigorously ordered as those of the hamster, and I could not clearly identify a stromal sheath as described by Hattori. Further morphological studies are needed to determine whether the proliferative region is as firmly anchored in monkeys as it appears to be in hamsters.

If the proliferative region is somehow anchored in rhesus monkeys, and remains so after 3,4-TCB feeding, the following hypothetical mechanism for the development of the 3,4-TCB induced gastric lesion would be reasonable: In normal animals a stromal sheath maintains the position of the proliferative zone. Most of the newly formed cells migrate upward and differentiate to surface epithelial cells, and some of the newly formed cells begin to

differentiate into parietal cells and continue this differentiation as they migrate downward (figure 59). The newly formed parietal cells must in some way, presumably mechanical, be prevented from migrating up very far, since they are never encountered above the isthmus regions of the glands. Some newly formed undifferentiated cells, as well as young parietal cells, migrate downward, but only when cell loss from the base regions of the glands creates vacancies. Such vacancies would release the pressure of the cells on their neighbors; when this cell-to-cell pressure in the base of the glands becomes less than the cell-to-cell pressure in the proliferative zone, cells would migrate downward from the region of greatest pressure, in the proliferative region, to the region of least pressure, in the bases of the glands. Cells other than parietal cells that migrated downward would become zymogenic cells. This differentiation might be determined by environmental factors in the base regions of the glands, and not by the actual downward migration itself.

Next, consider the effects of feeding 3,4-TCB to rhesus monkeys. My proposed model for the altered proliferation and migration of gastric epithelial cells is shown in figure 60. According to this model, the cells which migrate downward fail to respond to environmental cues to differentiate. They continue to proliferate after migrating downward and their number exceeds the number of vacancies created. The extra cells cause increased cell-to-cell

pressure within the glands and where possible, the glands are forced downward through weak points in the muscularis mucosae, e.g., where the blood vessels from below penetrate. These become submucosal glands, and ultimately cysts. Where the glands cannot penetrate the muscularis mucosae, the cell-to-cell pressure increases until it becomes impossible for cells to migrate downward from the principal zone of proliferation in the isthmus and neck regions. Continued proliferation in these regions forces newly formed cells to migrate in the only direction remaining: up. There may even be a net migration of cells from the base region upward through the neck and isthmus regions to the surface. Cells normally migrate upward to fill vacancies created by loss of surface epithelial cells by extrusion into the lumen of the stomach and by in situ degeneration. The upward redirection of newly formed cells that would normally migrate downward, plus a possible upward migration of cells from the base region, could create a greater number of cells migrating to the surface than is required to fill the vacancies caused by normal cell loss at the surface. This surfeit of cells arriving at the surface could account for the apparent foveolar hyperplasia and abnormal outward bulging of surface epithelial cells seen in the 3,4-TCB-fed animals.

The mechanism just described still requires that there be a net production of new cells that is greater than cell loss, in order that the glands become hyperplastic and increase in height. Yet, as just discussed, I have no

evidence even suggestive of a greater production of new epithelial cells. The missing factor may be a decrease in cell loss from the base regions of the glands rather than an increase in cell production. Indeed, such a decrease in cell loss is quite likely since it appears that cell division continues and differentiation is halted in the base regions of glands in 3,4-TCB induced lesions. As these cells continue to divide, they may escape aging, and the cessation of normal cell loss in their bases may be sufficient to result in the accumulation of excess cell numbers in the gastric mucosa. Considering that it usually takes weeks to months for the hyperplastic changes to develop, even though conversion of specialized cells to mucus-secreting cells may occur in less time, this may be a reasonable explanation for the development of this hyperplasia.

The altered functional and structural characteristics of the epithelial cells in the 3,4-TCB-induced gastric lesion were examined by a variety of methods. Histochemical reactions clearly established that the specialized zymogenic, parietal, and enteroendocrine cells had been replaced by mucus-secreting cells. The mucous material was shown by the high-iron diamine reaction to contain acidic sulfomucins. Recent work with human gastric mucosa has shown that the production of sulfomucins may be used as a marker of precancerous changes in humans (78, 152). However, the occurrence of sulfomucins in the 3,4-TCB

induced lesions of monkeys may not have the same significance, because sulfomucins were also observed in the mucous neck cells and to a lesser extent in the surface epithelial cells, whereas in humans sulfomucins are not normally seen in the gastric mucosa (78, 150).

The conversion or replacement of cells to mucus-secreting cells was also accompanied by a loss of pepsin activity in two of the three animals fed 3,4-TCB. In addition, parietal cells were absent, and in one animal, the pentagastrin-stimulated production of gastric acid steadily decreased when the animal was placed on a 3,4-TCB diet, but this phenomenon was not studied in the other animals owing to their inconsistent response to pentagastrin before toxic feeding began. But since no cells with structures resembling the tubulo-vesicular system of parietal cells were seen in the experimental stomachs, it is unlikely that these stomachs could produce acid.

Examination of the gastric mucosa by transmission electron microscopy established the fine structure of the normal gastric epithelium in rhesus monkeys and provided control data against which the epithelial cells in the 3,4-TCB-induced lesion could be compared. Perhaps the most striking feature of the epithelial cells in this lesion was their diversity of structure. Some cells were tall and cylindrical with few secretory granules; others in neighboring areas were short and filled with secretory granules in their apical regions. The epithelial cells in

this lesion showed many of the specialized structures seen in normal cells, such as junctional complexes, plasmalemma interdigitations with neighboring cells, well-developed endoplasmic reticulum and Golgi bodies, and numerous microvilli. Not surprisingly, however, these cells also showed many of the same morphological changes that my colleagues and I previously noted in the earlier stages of minimally developed PCB-induced gastric lesions (13). These included such changes as dilated rough endoplasmic reticulum, an increase in the number and size of autophagic vacuoles, and irregular apical surfaces facing the lumen of the glands. In the advanced lesions described here, many of the specialized membrane structures appeared abnormal. For example, the Golgi apparati appeared depleted and their cisternae were closely packed together. The plasmalemma interdigitations appeared excessively elaborate, and many of the secretory granules were fused together. In some instances, the entire apical region appeared to have been discharged into the lumen. Other abnormalities were irregularly shaped nuclei, suggestive of pyknosis, and disorganization of the entire cytoplasm in some cells. Although many of these changes were suggestive of cell injury, or even death, there was no corresponding inflammatory reaction or other signs indicative of cellular necrosis. Even the most irregular appearing cells were occasionally labeled with ^{3}H-thymidine, an indication that despite the profound morphological changes, cellular

proliferation continued.

In the first report of this PCB-induced lesion, Allen and Norback in 1973 (7) described stratified arrangements of proliferating epithelial cells that they believed penetrated the basement membrane in serial sections of the submucosal cysts examined by light microscopy. I, however, could find no evidence for such aggressive and malignant behavior. Rather I found that the epithelial cells throughout this lesion, including those in submucosal cysts, always remained arranged in a single layer of columnar or cuboidal epithelium bounded by an intact basement membrane.

Examination of the surface of the gastric epithelium by scanning electron microscopy revealed changes not readily apparent by transmission electron microscopy or light microscopy. These changes included foveolar hyperplasia with dilated foveolae, irregular protrusions of the surface epithelial cells from the surface and clusters of cells bulging from the surface. These changes were not confined to the body region of the stomach, where the pronounced mucosal thickening and invasion of the submuosa occurred, but were seen throughout the stomach from the cardiac to the antral regions.

Many of the other changes were also seen throughout the stomach. These included conversion of specialized epithelial cells to mucus-secreting cells; an increase in the extent and intensity of alcian blue staining of acidic mucosubstances; a similar increase in high-iron diamine

staining of sulfomucins; and the abnormal occurrence of proliferating epithelial cells in the bases of the gastric glands. Yet the most advanced lesion developed only in the the body region of the stomach, where parietal cells would otherwise be abundant. It may be that the body region is somehow more susceptible to the toxic effects of 3,4-TCB, that the lesion begins sooner here, and that if the animals could have lived longer on these toxic diet regimens, the pronounced gastric lesion would have developed in the other stomach regions as well. The peculiar vulnerability of the body region brings to mind the possibility that the mucosa in this area simply is exposed to 3,4-TCB in the food longer and in closer contact to the mucosa, while the food sits in the stomach and is churned around by contractions of the stomach wall before it is passed on to the duodenum. However, an experiment by McNulty (unpublished data) has indicated that direct exposure to 3,4-TCB in food is not necessary for the development of the characteristic stomach lesion. In this experiment a monkey received multiple intraperitoneal injections of 1.75 mg of 3,4-TCB three times a week for 55 days, when it died. This animal had the full spectrum of pathologic changes in the skin, the stomach, and elsewhere seen in animals fed equivalent amounts of the toxic compound.

The toxic effects also extended beyond the stomach. Increased thickness of the squamous epithelium lining the esophagus is evident in figure 10, and dilatation of

Brunner's glands in the duodenum is seen in figure 14. No pathologic changes were noted elsewhere in the gastrointestinal tract distal to the duodenum, but recently McNulty has noted metaplastic changes in the salivary glands of the tongue and in esophageal glands and hyperplasia in the bile duct (unpublished data). Therefore, these tissues may have some factor in common that is not shared by other tissues in the body. The factor could be a regulatory mechanism that develops in these tissues of similar embryonic origin, with which these chlorinated biphenyl compounds interact. It must certainly be a specific structural site of a macromolecule since 3,4-TCB and structurally related compounds are very toxic, and their toxicity depends on certain structural features of the molecules.

The mechanism of toxicity of the chlorobiphenyls and related compounds is as yet unknown (132). However, a biochemical response to these compounds has been found and extensively studied by Poland and Glover (131). They reported high affinity, stereospecifc binding of 2,3,7,8-tetrachlorodibenzodioxin (TCDD) by mouse liver cytosol. They studied numerous congeners of TCDD, chloro-biphenyls, azo and azoxybenzene, and chlorobiphenylenes (131, 132) and found that compounds with the highest affinities for mouse liver cytosol also most actively induced aryl hydrocarbon hydroxylase; moreover, these compounds all produce a similar toxic syndrome. The most

toxic compounds are all approximate stereoisomers. Their molecular structures can fit into a rectangle 30 X 100 nm, with the chlorine atoms occupying the corners (132). This biochemical induction of AHH by these compounds correlates well with their known toxicities (132), but it does not account for any of the pathologic changes seen. Even in the liver the morphological changes do not seem severe enough to cause death. However, Poland and Glover (130) have recently shown that the presence of the cytosolic TCDD binding receptor segregates with the Ah locus in mice; the toxic effect of thymic atrophy and the teratogenic effect of cleft palate formation also segregate with this locus. They maintain that since the Ah locus controls the induction of numerous enzymes besides AHH, TCDD and related compounds may induce the expression, or possibly the repression, of any number of genes, one or more of which results in the toxic effects on the animals, and the induction of AHH activity itself is not necessarily responsible for the toxicity (130).

Attempts to elucidate the biochemical basis of the toxicity of these compounds have been frustrated by the failure to find a suitable, susceptible cell line for studies on these compounds in an isolated tissue culture system. Knutson and Poland (90) tested 23 cell types for possible in vitro toxicity to TCDD. All the cell types, even those that responded to TCDD by inducing AHH activity, failed to show signs of toxicity. It may be that the

pathologic changes can only be produced in whole animals, i.e., in an environment in which different cell types interact with each other. The pathologic changes might be mediated through hormonal changes. The loss of differentiated function and the hyperplasia observed in the gastric mucosa of monkeys fed these toxic compounds suggested to me that the gastrointestinal hormone, gastrin, which is known to be important in the proliferation of and differentiation of immature gastric epithelial cells into mature parietal and zymogenic cells (30, 61, 120, 173, 174), might somehow be involved in mediating the pathologic changes seen in the stomach. However, neither the fasting nor the postprandial serum gastrin levels were altered in one of the animals in whom an advanced gastric lesion developed, and so the involvement of this hormone seems unlikely.

The possibility that other hormones, either known or yet to be discovered, might be involved in the development of this gastropathy cannot be excluded. Epidermal growth factor, a small polypeptide hormone isolated from the mouse submandibular gland has been shown to stimulate DNA synthesis in mouse tongue, esophagus and stomach (146). This hormone, which is structurally similar to human urogastrone and appears to have identical biological activities, is an example of a growth regulating hormone such as could possibly be involved in the development of the gastropathy induced by 3,4-TCB and related compounds.

However, my observations that the cell cycle time does not shorten and that the labeling index and labeling density do not increase in the gastric mucosa of monkeys fed 3,4-TCB, seem to argue against hormonal stimulation of proliferation.

It may be some time before the molecular basis for the development of the peculiar lesions induced by 3,4-TCB and related compounds is understood. We still do not know why the animals die. The morphological changes seen at autopsy do not by themselves seem sufficient. The severity of the gastric lesion does not always correlate well with the general health of the animal, but may very well contribute to the loss of appetite and subsequent weight loss. It has been suggested that malabsorption of nutrients might occur, a possible explanation for wasting seen in this syndrome. However, no impairment has been found in absorption from the intestine, or in transfer to the cells, of carbohydrates, fatty acids, and amino acids in rats fed TCDD (122).

To determine whether the wasting seen in TCDD poisoning causes death, Gasciewicz et al. (49) fed rats intravenously a total parenteral nutrition fluid on a continuous basis. When 100 μg of TCDD / kg of body weight were injected into the rats, parenteral nutrition protected the animals against weight loss, and they even gained weight. They died, nevertheless, within 13 to 17 days after treatment, and had severely damaged livers. Thus, although weight loss is a constant feature of 3,4-TCB- and TCDD-induced toxicity, it does not appear to be the cause of death. It is useful to

compare the 3,4-TCB-induced gastropathy in rhesus monkeys with other lesions of known or unknown causes, in order to see what features they may have in common. Such knowledge might help us understand the mechanisms by which these lesions develop.

The lesion in Menetrier's disease resembles advanced gastric lesions induced by 3,4-TCB, TCDD, and related compounds. The disease is characterized by deep elongated rugae, interstitial round cell inflammation, hyperplastic proliferation of gastric epithelial cells, cystic dilation of the basilar portion of the gastric glands, occasional penetration of the muscularis mucosae by the gastric glands, submucosal edema, and protein loss resulting in hypoproteinemia and peripheral edema (16, 22, 27, 135, 145). However, Menetrier's disease differs from the lesion seen in 3,4-TCB poisoning in that mature parietal and zymogenic cells frequently persist and sometimes increase in numbers, although in some areas they are totally replaced by mucus-secreting cells. Furthermore, the elongated rugae form a more regular surface pattern than the disorganized surface seen in 3,4-TCB poisoning. Also, the consistent infiltration of the lamina propria with inflammatory cells is an additional feature of Menetrier's disease not seen in 3,4-TCB poisoning. Hansen et al. (60) studied several patients with Menetrier's disease. They determined by immunofluorescence microscopy that only the IgM-containing cells, and not the IgA and IgG cells, increased in number in

the gastric mucosa. They also found that the H-thymidine labeling index of the gastric epithelial cells was elevated, but not consistently in all the patients. Menetrier's disease has also been noted in a rhesus monkey (167).

There appear to be sufficient differences between Menetrier's disease and the 3,4-TCB induced gastropathy to make a common pathologic basis unlikely. The pathologic mechanism of Mentrier's disease is unknown, but a short-lived variant, seen in children, may result from infection by cytomegalovirus (80).

Loss of parietal and zymogenic cells is also seen in atrophic gastritis and pernicious anemia (32, 43). In addition, there is an alteration in the distribution of ^{3}H-thymidine-labeled cells (40). In mild atrophic gastritis, labeled cells occur at the uppermost luminal surface of otherwise normal appearing gastric foveolae. In patients with partially intestinalized gastric mucosa, occasional labeled cells were also seen at the uppermost luminal surface of normal appearing foveolae; but in those glands with more advanced intestinal metaplasia, ^{3}H-thymidine labeled cells were located exclusively at the bases of the intestinalized glands. However, this intestinalization of gastric mucosa (replacement of normal gastric cell types by mucus-secreting cells similar to those seen in the intestine) is quite different from the increase in number and extent of distribution of cells resembling mucous neck cells seen in 3,4-TCB-induced lesions. A

further difference is that in 3,4-TCB induced lesions, ^{3}H-thymidine labeling never shifts exclusively to the base, as in intestinalized glands of atrophic gastritis, nor do ^{3}H-thymidine labeled cells occur at the surface of the gastric epithelium.

N-methyl-N'-nitro-N-nitrosoguanidine (MNNG) is a potent gastric carcinogen widely used as an experimental model for chemically induced cancer of the stomach in dogs and rats (151). In rats, MNNG induces well-differentiated and poorly differentiated types of adenocarcinomas and signet-ring cell carcinomas (160). Kohli et al. (92) found a significant difference between the labeling indices of the antra of normal rats, in the antra of MNNG-treated rats, and of cancerous lesions in the antra of MNNG-treated rats. However, they found that both the DNA-synthesizing phase (S-phase) and the total cell cycle time were longer for cancerous lesions than for normal antral tissue. Deschner et al. (39) determined the spatial distribution of ^{3}H-thymidine labeled cells in the pyloric glands of rats treated with MNNG for 10 and 15 weeks and of control rats. They found a significant shift of labeled cells downward toward the muscularis mucosae in the MNNG treated rats. The labeling indices of atypical appearing pyloric foveolae in the treated rats were 1.5 to 5.5 times those of normal appearing foveolae in the same animals. The proliferative zone in some of these atypical foveolae extended further downward, and in others further upward, than in the normal

appearing foveolae. A shift in the distribution of gastric proliferative cells was also noted in a study on MNNG-treated mice (151). Deschner at al. (39) examined the labeling indices of various regions of MNNG-induced pyloric adenocarcinomas; they found that the labeling indices of neoplasms were significantly higher than those of adjacent normal mucosa. This result is in contrast to those of Kohli et al. (92), possibly because of the higher dose of MNNG used by Deschner et al.

This chemically induced carcinoma shares some properties with the 3,4-TCB-induced gastropathy, in that both lesions demonstrate a downward shift in the proliferative zone, and in both the gastric epithelium penetrates the muscularis mucosae and invades the submucosa (92). However, the MNNG-induced carcinoma has been shown to metastasize (151, 160), unlike the gastric epithelium in the 3,4-TCB induced lesion, which was never seen to penetrate the basement membrane. Furthermore, the MNNG-induced changes are frequently focal, i.e., atypical glands occur next to normal appearing glands (39, 92), whereas in the 3,4-TCB induced lesion, all glands are altered, and those in the body region of the stomach are most severely affected.

The surface of the gastric mucosa in 3,4-TCB poisoning in monkeys resembles that seen in both acute and chronic gastritis in humans (44, 165). In acute gastritis, the gastric foveolae are dilated and the surface is irregular, owing to bulging of the epithelial cells above the surface.

In nonflorid chronic gastritis, foveolar hyperplasia with irregular, wide foveolar openings, is seen. In florid chronic gastritis, hyperplasia with outward bulging epithelial cells is also seen, but the openings of the foveolae are covered by the hyperplastic folds of surface epithelium (44). Variations in these surface changes are also seen in monkeys fed 3,4-TCB. Moreover, the apical erosion and extensive extrusion of surface epithelial cells that are commonly seen in 3,4-TCB-fed animals are also seen in rats subjected to behavioral and acetlysalicylic acid stress (62), an indication that the surface changes seen in the stomachs of monkeys fed 3,4-TCB may represent a common pattern of reaction to stress and injury.

Thus, the downward shift in the proliferative zone seen in 3,4-TCB-fed rhesus monkeys resembles the changes seen in MNNG-treated rats; the conversion of specialized gastric epithelial cells to less differentiated cell types resembles changes seen in atrophic gastritis, MNNG-induced carcinoma, and Menetrier's disease; the surface changes resemble those seen in acute and chronic gastritis; and the alterations in membranes structures resemble those seen in chemically induced cell injury. However, the complete spectrum of changes I have described in this study on the 3,4-TCB-induced gastropathy in rhesus monkeys appears to be unique.

This study has presented evidence of the failure of newly formed gastric epithelial cells to differentiate, and

thereby lose their proliferative capacity. The implication is that 3,4-TCB and its related compounds interact in some highly specific manner with the regulatory mechanisms of susceptible epithelial cells. Whether 3,4-TCB interacts directly with gastric epithelial cells, or indirectly by interacting first with other cells or tissues that produce a chemical messenger, such as a hormone, that modifies the behavior of gastric epithelial cells, cannot be ascertained from the evidence accumulated in this study. However, gastric epithelial cells show a number of signs of cell injury, such as the formation of autophagic vacuoles, and autophagocytosis is a common reaction pattern of sublethally damaged cells (11, 12, 45, 47). Therefore it seems that these toxic compounds may act directly upon these cells. Failure of tissue culture cells to respond to a closely related and more toxic compound, TCDD (90), suggests that an interaction of several cell types is necessary, or that these compounds must first be metabolized by another organ to their active metabolites, or possibly both, in order for the toxic effects to become evident. The elucidation of the biochemical mechanism of induction of the gastric lesion described in this study probably must await the development of a suitable in vitro experimental model.

V. SUMMARY AND CONCLUSIONS

Rhesus monkeys were fed diet cakes containing 1 to 3 mg / kg of the toxic polychlorinated biphenyl, 3,4,3',4'-tetrachlorobiphenyl. Characteristic skin and stomach lesions developed in these animals and the stomach lesion was examined in detail by light microscopy, scanning and transmission electron microscopy. The gastric mucosa thickened and appeared hyperplastic and the gastric glands were dilated and cystic. Some glands were seen penetrating the muscularis mucosa and forming submucosal cysts. The specialized gastric epithelial cells, the zymogenic and parietal cells, were replaced with mucus-secreting cells with a wide range of morphologic characteristics. Many showed signs of cell injury such as autophagocytosis and irregular apical membranes. All the gastric epitheial cells were shown to react strongly with alcian blue and the high-iron diamine stains, which stain respectively acidic mucosubstances and sulphomucins. In contrast, in control animals the staining reaction was much weaker and was confined mainly to the surface epithelial cells.

Examination of autoradiographs of ^{3}H-thymidine pulse-labelled gastric mucosa revealed that in control animals the proliferative cells were located exclusively in the isthmus and the neck region of the gastric glands. In the experimental-fed animals, proliferative cells were also seen in the bases of the gastric glands where the mature and

nonproliferative cells, the parietal and zymogenic cells, were found in the controls. Consequently the pattern of distribution of proliferating cells was frequently extended downward, and in some cases further upward in the glands than in the controls, however, no increase was seen in the relative numbers of proliferating cells in the experimental animals. These data suggest that the hyperlasia seen in this lesion may result from the proliferation and accumulation of cells in the base region of the glands. Scanning electron microscopic examination of the surface of the gastric epithelium showed changes suggestive of hyperplasia in this region as well.

Therefore this compound appears to alter the normal pattern of differentiation of gastric epithelial cells. Cells continue to proliferate after they leave the normal proliferative zone and hyperplastic changes result.

VI. REFERENCES

1. Allen, A., & Garner, A. Progress report. Mucus and bicarbonate secretion in the stomach and their possible role in mucosal protection. Gut, 1980. 21, 249-262.

2. Allen, J.R. Response of the nonhuman primate to polychlorinated biphenyl exposure. Fed. Proc., 1975. 34, 1675-1679.

3. Allen, J.R., Abrahamson, L.J., & Norback, D.H. Biological effects of polychlorinated biphenyls and triphenyls on the subhuman primate. Environ. Res., 1973. 6, 344-354.

4. Allen, J.R., Barsotti, D.A., Van Miller, J.P., Abrahamson, L.J., & Lalich, J.J. Morphological changes in monkeys consuming a diet containing low levels of 2,3,7,8-tetrachlorodibenzo-p-dioxin. Food Cosmet. Toxicol., 1977. 15, 401-410.

5. Allen, J.R., & Carstens, L.A. Light and electron microscopic observations in Macaca mulatta monkeys fed toxic fat. Am. J. Vet. Res., 1967. 28, 1513-1526.

6. Allen, J.R., Carstens, L.A., Abrahamson, L.J., & Marlar, R.J. Responses of rats and nonhuman primates to 2,5,2',5'tetrachlorobiphenyl. Environ. Res., 1975. 9, 265-273.

7. Allen, J.R., & Norback, D.H. Polychlorinated biphenyl- and triphenyl-induced gastric mucosal hyperplasia in primates. Science, 1973. 179, 498-499.

8. Altman, N.H., New, A.E., McConnell, E.E., & Ferrell, T.L. A spontaneous outbreak of polychlorinated biphenyl toxicity in rhesus monkeys (Macaca mulatta): clinical observations. Lab. Animal Sci., 1979. 29, 661-665.

9. Alumets, J., Ekelund, M., El Munshid, H.A., Hakanson, R., Loren, I., & Sundler, F. Topography of somatostatin cells in the stomach of the rat: Possible functional significance. Cell Tiss. Res., 1979. 202, 177-188.

10. Alvares, A.P., Bickers, D.R., & Kappas, A. Polychlorinated biphenyls: a new type of inducer of cytochrome P-448 in the liver. Proc. Natl. Acad. Sci., U.S.A., 1973. 70, 1321-1325.

11. Arstila, A. U., Jauregui, H.O., Chang, J., & Trump, B.F. Studies on cellular autophagocytosis. Relationship between heterophagy and autophagy in HeLa cells. Lab. Invest., 1971. 24, 162-174.

12. Arstila, A.U., & Trump, B.F. Studies on cellular autophagocytosis. The formation of autophagic vacuoles in the liver after glucagon administration. Am J. Pathol., 1968. 53, 687-733.

13. Becker, G.M., McNulty, W.P., & Bell, M. Polychlorinated biphenyl-induced morphologic changes in the gastric mucosa of the rhesus monkey. Lab. Invest., 1979. 40, 373-383.

14. Bell, M. Ultrastructural features of gastric mucosa and sebaceous glands after ingestion of Aroclor 1242 by rhesus monkeys. In J.L. Buckley (Ed.) National conference on polychlorinated biphenyls. Washington, D.C.: Environmental Protection Agency, 1976. (pages 350-358)

15. Bennett, H.S., Wyrick, A.D., Lee, S.W., & McNeil, J.H. Science and art in preparing tissues embedded in plastic for light microscopy, with special reference to glycol methacrylate, glass knives and simple stains. Stain Technol., 1976. 51, 71-97.

16. Berenson, M.M., Sannella, J., & Freston, J.W. Menetrier's disease. Serial morphological, secretory and serological observations. Gastroenterology, 1976. 70, 257-263.

17. Berringer, O.M., Browning, F.M., & Schroeder, C.R. An atlas and dissection manual of rhesus monkey anatomy. Tallahassee: Anatomy Laboratory Aids, 1968. (page 61)

18. Bickers, D.R., Harber, L.C., Kappas, A., & Alvares, A.P. Polychlorinated biphenyls: comparative effects of high and low chlorine containing Aroclors on hepatic mixed function oxidases. Res. Commun. Chem. Pathol. Pharmacol., 1972. 3, 505-512.

19. Biocca, M., Moore, J.A., Gupta, B.N., & McKinney, J.D. Toxicology of selected symmetrical hexachlorobiphenyl isomers. I. Biological responses in chicks and mice. In J.L. Buckley (Ed.) National conference on polychlorinated biphenyls. Washington, D.C.: Environmental Protection Agency, 1976. (pages 67-72)

20. Bonne, C., & Sandground, J.H. On the production of gastric tumors, bordering on malignancy, in Javanese monkeys through the agency of Nochtia nochti, a parasitic nematode. Am. J. Cancer, 1939. 37, 173-185.

21. Boren, H.G., Wright, E.C., & Harris, C.C. Quantitative light microscopic autoradiography. Methods Cell Biol., 1974. 8, 277-288.

22. Brdlik, O.B. Giant hypertrophy of the gastric mucosa (Menetrier's disease): A survey of the literature and a report of a case. J. Am. Osteopath. Assoc., 1976. 76, 198-203.

23. Bruckner, J.V., Khanna, K.L., & Cornish, H.H. Polychlorinated biphenyl-induced alteration of biologic parameters in the rat. Toxicol. Appl. Pharm., 1974. 28, 189-199.

24. Bruckner, J.V., Khanna, K.L., & Cornish, H.H. Effect of prolonged ingestion of polychlorinated biphenyls on the rat. Food Cosmet. Toxicol., 1974. 12, 323-330.

25. Bullough, W.S. Stress and epidermal mitotic activity. I. The effects of the adrenal hormones. J. Endocrinol., 1952. 8, 265-274.

26. Bussolati, G. & Pearse, A.G.E. Immunofluorescent localization of the gastrin secreting cells in the pyloric antrum of the pig. Histochemie, 1970. 21, 1-4.

27. Butz, W.C. Giant hypertrophic gastritis. A report of fourteen cases. Gastroenterology, 1960. 39, 183-190.

28. Cantrell, J.S., Webb, N.C., & Mabis, A.J. The identification and crystal structure of a hydropericardium-producing factor: 1,2,3,7,8,9-hexa-chlorodibenzo-p--dioxin. Acta Cryst., 1969. 25, 150-156.

29. Carter, J.W., & Cameron, I.L. Sublethal effects of a pure polychlorobiphenyl on mice. Exp. Mol. Pathol., 1977. 26, 228-250.

30. Castrup, H.J., Fuchs, K., & Peiper, H.J. Cell renewal of gastric mucosa in Zollinger-Ellison syndrome. Acta Hepato-Gastroenterology, 1973. 22, 40-43.

31. Chen, K.Y., & Withers, H.R. Proliferative capability of parietal and zymogen cells. J. Anat., 1975. 120, 421-432.

32. Chiao, S.F., & Weisberg, H. Ultrastructure of the gastric mucosa in patients with atrophic gastritis and pernicious anemia. Gastroenterology, 1970. 59, 36-45.

33. Clarkson, B., Ohkita, T., Ota, K., & Fried, J. Studies of cellular proliferation in human leukemia. J. Clin. Invest., 1967. 46, 506-529.

34. Cleaver, J.E. Thymidine metabolism and cell kinetics. New York: American Elsevier Publ. Co., 1967.

35. Cordle, F., Corneliussen, P., Jelinek, C., Hackley, B., Lehman, R., McLaughlin, J., Rhoden, R., & Shapiro, R. Human exposure to polychlorinated biphenyls and polybrominated biphenyls. 1978. Environ. Health Perspect., 1978. 24, 157-172.

36. Corpron, R.E. The ultrastructure of the gastric mucosa in normal and hypophysectomized rats. Am. J. Anat., 1966. 118, 53-90.

37. Cory, H.T., Isabelle, L.M., Smith, R.G., McNulty W.P., & Daves, G.D. Metabolism of 3,4,3',4'- and 2,5,2',5'-tetrachlorobiphenyls in rhesus monkeys. Submitted for publication.

38. Creamer, B., Shorter, R.G., & Bamforth, J. The turnover and shedding of epithelial cells. Part I. The turnover in the gastro-intestinal tract. Gut, 1961. 2, 110-118.

39. Deschner, E.E., Tamura, K., & Bralow, S.P. Sequential histopathology and cell kinetic changes in rat pyloric mucosa during gastric carcinogenesis induced by N-methyl-N'-nitro-N-nitrosoguanidine. J. Nat. Cancer Inst., 1979. 63, 171-179.

40. Deschner, E.E., Winawer, S.J., & Lipkin, M. Patterns of nucleic acid and protein synthesis in normal human gastric mucosa and atrophic gastritis. J. Natl. Cancer Inst., 1972. 48, 1567-1573.

41. DiBona, D.R., Ito, S., Berglindh, T., & Sachs, G. Cellular site of gastric acid secretion. Proc. Natl. Acad. Sci. U.S.A., 1979. 76, 6689-6693.

42. Elias, H., Pauly, J.E., & Burns, E.R. Histology and human anatomy. New York: John Wiley & Sons, 1978. (page 304)

43. Elliott, R.L., & Guillen, R. Gastric biopsies. An ultrastructural study with special refernce to pernicious anemia. Arch. Pathol., 1964. 77, 258-267.

44. Fallah, E., Schuman, B.M., Watson, J.H.L., & Goodwin, J. Scanning electron microscopy of gastric biopsies. Gastrointest. Endoscop., 1976. 22, 137-144.

45. Fedorko, M.E., Hirsch, J.G., Cohn, Z.A. Autophagic vacuoles produced in vitro. I. Studies on cultured macrophages exposed to chloroquine. J. Cell Biol., 1968. 38, 377-391.

46. Fishbein, L. Toxicity of chlorinated biphenyls. Ann. Rev. Pharmacol. Toxicol., 1974. 14, 139-156.

47. Frank, A.L., & Christensen, A.K. Localization of acid phosphatase in lipofuchsin granules and possible autophagic vacuoles in interstitial cells of the guinea pig testis. J. Cell Biol., 1968. 36, 1-13.

48. Frexinos, J., Carballido, M., Louis, A., & Ribet, A. Effects of pentagastrin stimulation on human parietal cells. An electron microscopic study with quatitative evaluation of cytoplasmic structures. Am. J. Dig. Dis., 1971. 16, 1065-1074.

49. Gasiewicz, T.A., Holscher, M.A., and Neal, R.A. The effect of total parenteral nutrition on the toxicity of 2,3,7,8-tetrachlorodibenzo-p-dioxin in the rat. Toxicol. Appl. Pharm., 1980. 54, 469-488.

50. Gerard, A., Regeneration cellulaire dans la muquese gastrique du chien sous l' effet de divers stimulants et de diverses droques ulcerigenes. Biol. Gastroenterol., 1969. 1, 5-14.

51. Goldstein, J.A., Hickman, P., Bergman, H., McKinney, J.D., & Walker, M.P. Separation of pure polychlorinated biphenyl isomers into two types of inducers on the basis of induction of cytochrome P-450 or P-448. Chem. Biol. Interact., 1977. 17, 69-87.

52. Grant, J.C.B. An atlas of anatomy. Baltimore: Williams & Wilkins Co., 1972. (figure 128)

53. Grimelius, L. A silver stain for the α_2 cells in human pancreatic islets. Acta Societatis Medicorum Upsaliensis, 1968. 73, 243-270.

54. Grube, D., & Forssmann, W.G. Morphology and function of the entero-endocrine cells. Horm. Metab. Res., 1979. 11, 589-606.

55. Hacking, M.A., Budd, J., & Hodson, K. The ultrastructure of the liver of the rainbow trout: normal structure and modifications after chronic administration of a polychlorinated biphenyl, Aroclor 1254. Can. J. Zool., 1978. 56, 477-491.

56. Hakanson, R., Owman, C.H., Sjoberg, N.O., & Sporrong, B. Amine mechanisms in enterochromaffin and enterochromaffin-like cells of the gastric mucosa of various mammals. Histochemie, 1970. 21, 189-200.

57. Hammond, J.B., & LaDeur, L. Fibrillovesicular cells in the fundic glands of the canine stomach: evidence for a new cell type. Anat. Rec., 1968. 161, 393-412.

58. Hansen, L.G., Beamer, P.D., Wilson, D.W., & Metcalf, R.L. Effects of feeding polychlorinated biphenyls to broiler cockerals in three dietary regimes. Poult. Sci., 1976. 55, 1084-1088.

59. Hansen, L.G., Wilson, D.W., & Byerly, C.S. Effects on growing swine and sheep of two polychlorinated biphenyls. Am. J. Vet. Res., 1976. 37, 1021-1024.

60. Hansen, O.H., Jensen, K.B., Larsen, J.K., & Soltoft, J. Gastric mucosal cell proliferation and immunoglobulin-containing cells in Menetrier's disease. Digestion, 1977. 16, 293-298.

61. Hansen, O.H., Pederson, T., Larsen, J.K., & Rehfeld, J.F. Effect of gastrin on gastric mucosal cell proliferation in man. Gut, 1976. 17, 536-541.

62. Harding, R.K., & Morris, G.P. Cell loss from normal and stressed gastric mucosae of the rat. An ultrastructural analysis. Gastroenterology, 1977. 72, 857-863.

63. Hart-Hansen, O., Johansen, A.A., Larsen, J.K., & Svendsen, L.B. Cell proliferation in normal and diseased gastric mucosa. Autoradiography after in vitro continuous labelling with tritiated thymidine. Acta Pathol. Microbiol. Scand. Sect. A. 1979. 87, 217-222.

64. Hattori, T. On cell proliferation and differentiation of the fundic mucosa of the golden hamster. Fractographic study combined with microscopy and H-thymidine autoradiography. Cell Tiss. Res., 1974. 148, 213-226.

65. Hattori, T., & Fujita, S. Tritiated thymidine autoradiographic study on cellular migration in the gastric gland of the golden hamster. Cell Tiss. Res., 1976. 172, 171-184.

66. Hattori T, & Fujita S. Tritiated thymidine autoradiographic study of cell migration and renewal in the pyloric mucosa of golden hamsters. Cell Tiss. Res., 1976. 175, 49-57.

67. Helander, H.F. Ultrastructure of the fundus glands of the mouse gastric mucosa. J. Ultrastruct. Res. Suppl. 4, 1962. 1-123.

68. Helander, H., & Ekholm, R. Ultrastructure of epithelial cells in the fundus glands of the mouse gastric mucosa. J. Ultrastruct. Res., 1959. 3, 74-83.

69. Higuchi, K. Outline. In K. Higuchi (Ed.) PCB poisoning and pollution. New York: Academic Press, 1976. (pages 3-7)

70. Hinton, D.E., Glaumann, H., & Trump, B.F. Studies on the cellular toxicity of polychlorinated biphenyls (PCBs). I. Effect of PCBs on microsomal enzymes and on the synthesis and turnover of microsomal and cytoplasmic lipids of rat liver - a morphological and biochemical study. Virchows Arch. B Cell Pathol., 1978. 27, 279-306.

71. Hirschowitz, B.I., & Gibson, R.G. Effect of cimetidine on stimulated gastric secretion and serum gastrin in the dog. Am. J. Gastroenterol., 1978. 70, 437-447.

72. Hirst, B.H., Reed, J.D., Lund, P.K., & Sanders, D.J. Sensitivity of parietal cells to gastrin in the cat: Comparison with man and dog. Digestion, 1980. 20, 300-306.

73. Howard, A., & Pelc, S.R. Synthesis of deoxyribonucleic acid in normal and irradiated cells and its relation to chromosome breakage. Heridity, 1953. 6, 261-273.

74. Hunt, T.E., & Hunt, E.A. Radioautographic study of the proliferation in the stomach of the rat using thymidine-H3 and compound 48/80. Anat. Rec., 1962. 142, 505-517.

75. Hutzinger, O., Safe, S., & Zitko, V. The chemistry of the PCB's. Cleveland: CRC Press, 1974. (pages 1-39)

76. Ito, N., Nagasaki, H., Arai, M., Makiura, S., Sugihara, S., & Hirao, K. Histopathologic studies on liver tumorigenesis induced in mice by technical polychlorinated biphenyls and its promoting effect on liver tumors induced by benzene hexachloride. J. Natl. Cancer Inst., 1973. 51, 1637-1646.

77. Ito, S., & Winchester, R.J. The fine structure of the gastric mucosa in the bat. J. Cell Biol., 1963. 16, 541-577.

78. Jass, J.R., & Filipe, M.I. Sulphomucins and precancerous lesions of the human stomach. Histopathology, 1980. 4, 271-279.

79. Johnson, F.R., & Young, B.A. Undifferentiated cells in the gastric mucosa. J. Anat., 1968. 102, 541-551.

80. Kadlec, G., Goodwin, R., Fellows, R., & Andrews, B. Menetrier's disease in children. South. Med. J., 1979. 72, 33-36.

81. Kaku, H. Dynamic analysis of the stomach epithelium. H-thymidine autoradiographic study. Arch. Histol. Jap., 1966. 27, 223-246.

82. Kasza, L., Weinberger, M.A., Carter, C., Hinton, D.E., Trump, B.F., & Brouwer, E.A. Acute, subacute, and residual effects of polychlorinated biphenyl (PCB) in rats. II. Pathology and electron microscopy of liver and serum enzyme study. J. Toxicol. Environ. Health, 1976. 1, 689-704.

83. Kataoka, K. Electron microscopic observations on cell proliferation and differentiation in the gastric mucosa of the mouse. Arch. Histol. Jap., 1970. 32, 251-273.

84. Kent, T.H. Staphylococcal enterotoxin gastroenteritis in rhesus monkeys. Am. J. Path., 1966. 48, 397-407.

85. Kikuchi, M., & Masuda, Y. The pathology of yusho. In. K. Higuchi (Ed.) PCB poisoning and pollution. New York: Academic Press, 1976. (pages 69-86)

86. Kimbrough, R.D. The toxicity of polychlorinated polycyclic compounds and related chemicals. CRC Crit. Rev. Toxicol., 1974. 2, 445-498.

87. Kimbrough, R., Buckley, J., Fishbein, L., Flamm, G., Kasza, L., Marcus, W., Shibko, S., & Teske, R. Animal toxicology. Environ. Health Perspect., 1978. 24, 173-184.

88. Kimbrough, R.D., & Linder, R.E. Induction of adenofibrosis and heptaomas of the liver in BALB/cJ mice by polychlorinated biphenyls (Aroclor 1254). J. Natl. Cancer Inst., 1974. 53, 547-551.

89. Klaunig, J.E., Lipsky, M.M., Trump, B.F., & Hinton, D.E. Biochemical and ultrastructural changes in teleost liver following subacute exposure to PCB. J. Environ. Pathol. Toxicol., 1979. 2, 953-963.

90. Knutson, J.C., & Poland, A. 2,3,7,8-tetrachloro-dibenzo-p-dioxin: failure to demonstrate toxicity in twenty-three cultured cell types. Toxicol. Appl. Pharmacol., 1980. 54, 377-383.

91. Kohli, K.K., Gupta, B.N., Albro, P.W., Mukhtar, H., & McKinney, J.D. Biochemical effects of pure isomers of hexachlorobiphenyl: fatty livers and cell structure. Chem. Biol. Interact., 1979. 25, 139-156.

92. Kohli, Y., Hashimoto, Y., Takeda, S., & Kawai, K. Cell kinetics of gastric carcinoma and other gastric lesions in rats by N-methyl-N'-nitro-N-nitrosoguanidine with or without Tween 60. Gann, 1975. 66, 133-140.

93. Kolbye, A.C. Food exposures to polychlorinated biphenyls. Environ. Health Perspect., 1972. 1, 85-88.

94. Koller, L.D., & Zinkl, J.G. Pathology of polychlorinated biphenyls in rabbits. Am. J. Pathol., 1973. 70, 363-378.

95. Krause, W.J., Ivey, K.J., Baskin, W.N., & Mackercher, P.A. Morphological observations on the normal human cardiac glands. Anat. Rec., 1978. 192, 59-72.

96. Kuratsune, M. Epidemiologic studies on yusho. In K. Higuchi (Ed.) PCB poisoning and pollution. New York: Academic Press, 1976. (pages 9-23)

97. Kusumoto, Y., Iwanaga, T., Ito, S., & Fujita, T. Juxtaposition of somatostatin cell and parietal cell in the dog stomach. Arch. Histol. Jap., 1979. 42, 459-465.

98. Larsson, L.I. Pathology of the gastrointestinal endocrine cells. Scand. J. Gastroenterol. (Suppl.), 1979. 14, 1-8.

99. Larsson, L.I., Sundler, F., Hakanson, R., Grimelius, L., Rehfeld, J.F., & Stadil, F. Histochemical properties of the antral gastrin cell. J. Histochem. Cytochem., 1974. 22, 419-427.

100. Lennartz, K.J., & Mauer W. Autoradiographische Bestimmung der Dauer der DNS-Verdopplung und der Generationszeit beim Ehrlich-Ascitestumor der Maus durch Doppelmarkierung mit C- und H-Thymidin. Z. Zellforsch., 1964. 63, 478-495.

101. Lev, R., & Spicer, S.S. Specific staining of sulphate groups with alcian blue at low pH. J. Histochem. Cytochem., 1964. 12, 309.

102. Levine, J.S., Nakane, P.K., & Allen, R.H. Immunocytochemical localization of human intrinsic factor: The nonstimulated stomach. Gastroenterology, 1980. 79, 493-502.

103. Liebman, W.M., & Samloff, I.M. Immunochemical characterization and cellular localization of pepsinogens in cat and dog. J. Histochem. Cytochem., 1978. 26, 1115-1120.

104. Lillibridge, C.B. The fine structure of normal human gastric mucosa. Gastroenterology, 1964. 47, 269-290.

105. Lipkin, M. Proliferation and differentiation of gastrointestinal cells. Physiol. rev., 1973. 53, 891-915.

106. Lipkin, M., Sherlock, P., & Bell, B. Cell proliferation kinetics in human gastrointestinal mucosa. II. Cell renewal in stomach, ileum, colon and rectum. Gastroenterology, 1963. 45, 721-729.

107. Litterst, C.L., Farber, T.M., Baker, A.M., & Van Loon, E.J. Effects of polychlorinated biphenyls on hepatic microsomal enzymes in the rat. Toxicol. Appl. Pharmacol., 1972. 23, 112-122.

108. Lowry, O.H., Rosebrough, N.J., Farr, A.L., & Randall, R.J. Protein measurement with the Folin phenol reagent. J. Biol. Chem., 1951. 193, 265-275.

109. Luciano, L., Reale, E., & Engelhardt, W.V. The fine structure of the stomach mucosa of the llama (Llama guanacoe) II. The fundic region of the hind stomach. Cell Tiss. Res., 1980, 208, 207-228.

110. Luna, L.G. (Ed.) Manual of histologic staining methods of the Armed Forces Institute of Pathology (3rd Ed.). New York: McGraw-Hill Book Co., 1968. (pages 158-160)

111. Lushbaugh, C.C. Experimental hyperplastic gastritis and gastric polyposis in monkeys. J. Natl. Cancer Inst., 1947. 7, 313-320.

112. McConnell, E.E., Hass, J.R., Altman, N., & Moore, J.A. A spontaneous outbreak of polychlorinated biphenyl (PCB) toxicity in rhesus monkeys (Macaca mulatta): Toxicopathology. Lab. Anim. Sci., 1979. 29, 666-673.

113. McDowell, E.M. & Trump, B.F. Histologic fixatives suitable for diagnostic light and electron microscopy. Arch. Pathol. Lab. Med., 1976. 100, 405-414.

114. McKinney, J.D., Chae, K., Gupta, B.N., Moore, J.A., & Goldstein, J.A. Toxicological assessment of hexachlorobiphenyl isomers and 2,3,7,8-tetrachlorodibenzofuran in chicks. I. Relationship of chemical parameters. Toxic. Appl. Pharmacol., 1976. 36, 65-80.

115. McNulty, W.P. PCB toxicity in rhesus monkeys. In J.L. Buckley (Ed.) National conference on polychlorinated biphenyls. Washington, D.C.: Environmental Protection Agency, 1976. (pages 347-350)

116. McNulty, W.P., Becker, G.M., & Cory, H.T. Chronic toxicity of 3,4,3',4'- and 2,5,2',5'-tetrachlorobiphenyls in rhesus macaques. Toxicol. Appl. Pharmacol., 1980. 56, 182-190.

117. Meigs, J.W., Albom, J.J. & Kartin, B.L. Chloracne from an unusual exposure to Aroclor. J. Am. Med. Assoc., 1954. 154, 1417-1418.

118. Messier, B., Leblond, C.P. Cell proliferation and migration as revealed by autradiography after injection of thymidine-H3 into male rats and mice. Am. J. Anat., 1960. 106, 247-285.

119. Meyer, J.S. & Bauer, W.C. In vitro determination of tritiated thymidine labelling index (LI). Evaluation of a method utilizing hyperbaric oxygen and observation on the LI of human mammary carcinoma. Cancer, 1975. 36, 1374-1380.

120. Miller, L.R., Jacobson, E.D., & Johnson, L.R. Effect of pentagastrin on gastric mucosal cells grown in tissue culture. Gastroenterology, 1973. 64, 254-267.

121. Myrhe, E. Regeneration of the fundic mucosa in rats. V. An autoradiographic study on the effect of cortisone. Arch. Pathol., 1960. 70, 476-485.

122. Neal, R.A., Beatty, P.W., & Gasiewicz, T.A. Studies on the mechanisms of toxicity of 2,3,7,8-tetrachlorodibenzo-p-dioxin (TCDD). Ann. N.Y. Acad. Sci., 1979. 320, 204-213.

123. Nielsen-Smith, K.A. 2,5,2',5'-tetrachlorobiphenyl and 3,4,3',4'-tetrachlorobiphenyl as inducers of hepatic microsomal enzymes in rhesus monkeys. Unpublished master's thesis, Ore. Grad. Ctr., Beaverton, OR., 1980.

124. Nishizumi, M. Light and electron microscope study of chlorobiphenyl poisoning in mouse and monkey liver. Arch. Environ. Health, 1970. 21, 620-632.

125. Norback, D.H., & Allen, J.R. Chlorinated aromatic hydrocarbon induced modifications of the hepatic endoplasmic reticulum: concentric membrane arrays. Environ. Health Perspect., 1972. 1, 137-143.

126. Palade, G.E. A study of fixation for electron microscopy. J. Exp. Med., 1952. 95, 285-298.

127. Pictet, R.L., Rall, L.B., Phelps, P., & Rutter, W.J. The neural crest and the origin of the insulin-producing and other gastrointestinal hormone producing cells. Science, 1976. 191, 191-192.

128. Poland, A., & Glover, E. Comparison of 2,3,7,8-tetrachlorodibenzo-p-dioxin, a potent inducer of aryl hyrdocarbon hydroxylase, with 3-methylcholanthrene. Mol. Pharmacol., 1974. 10, 349-359.

129. Poland, A., & Glover, E. Chlorinated biphenyl induction of aryl hydrocarbon hydroxylase activity: a study of the structure activity relationship. Mol. Pharmacol., 1977. 13, 924-938.

130. Poland, A., & Glover, E. 2,3,7,8-tetrachlorodibenzo-p-dioxin: segregation of toxicity with the Ah locus. Mol. Pharmacol., 1980. 17, 86-94.

131. Poland, A., Glover, E., & Kende, A.S. Stereospecific, high affinity binding of 2,3,7,8-tetrachlorodibenzo-p-dioxin by hepatic cytosol. J. Biol. Chem., 1976. 251, 4936-4946.

132. Poland, A., Greenlee, W.F., & Kende, A.S. Studies on the mechanism of action of the chlorinated dibenzo-p-dioxins and related compounds. Ann. N.Y.

Acad. Sci., 1979. 320, 214-230.

133. Quastler, H., & Sherman, F.G. Cell population kinetics in the intestinal epithelium of the mouse. Exp. Cell Res., 1959. 17, 420-438.

134. Ragins, H., Wincze, F., Liu, S.M., & Dittbrenner, M. The origin and survival of gastric parietal cells in the mouse. Anat. Rec., 1968. 162, 99-110.

135. Reese, D.F., Hodgson, J.R., Dockerty, M.B. Giant hypertrophy of the gastric mucosa (Menetrier's disease): A correlation of the roentgenographic, pathologic and clinical findings. Am. J. Roent. Rad. Ther. Nucl. Med., 1962. 88, 619-626.

136. Reynolds, E.S. The use of lead citrate at high pH as an electron-opaque stain in electron microscopy. J. Cell Biol., 1963. 17, 208-212.

137. Rhodin, J.A.G. Histology. A text and atlas. New York: Oxford Univ. Press, 1974. (pages 538-540)

138. Risebrough, R.W., & de Lappe, B. Accumulation of polychlorinated biphenyls in ecosystems. Environ. Health. Perspect., 1972. 1, 39-45.

139. Rosa, F. Ultrastructure of the parietal cell of the human gastric mucosa in the resting state and after stimulation with histalog. Gastroenterology, 1963. 45, 354-363.

140. Rosato, E.F. Mayer, L.J., Arenschield, S., Rosato, F.E., & Brooks, F.P. Acid secretory responses to histamine and pentagastrin in concious monkeys. Am. J. Dig. Dis., 1974. 19, 1111-1115.

141. Rubin, W., Ross, L.L., Sleisenger, M.H., & Jeffries, G.H. The normal human gastric epithelia. A fine structural study. Lab. Invest., 1968. 19, 598-626.

142. Ryabchikova, E.I., & Vinogradova, M.S. Parietal cell ultrastructure in relation to location along the fundic gland. Byull. Eksp. Biol. Med., 1979. 88, 226-229.

143. Ryle, A.P. The porcine pepsin and pepsinogens. In G.E. Perlmann & L. Lorand (Eds.) Methods of enzymology, Vol. XIX. New York: Academic Press, 1970. (pages 316-336)

144. Samloff, I.M. Pepsinogens, pepsins, and pepsin inhibitors. Gastroenterology, 1971. 60, 586-604.

145. Scharschmidt, B.F. Tha natural history of hypertrophic gastropathy (Menetrier's disease). Report of a case with 16 year follow-up and review of 120 cases from the literature. Am. J. Med., 1977. 63, 644-652.

146. Scheving, L.A., Yeh, Y.C., Tsai, T.H., & Scheving, L.E. Circadian phase-dependent stimulatory effects of epidermal growth factor on deoxyribonucleic acid synthesis in the tongue, esophagus, and stomach of the adult male mouse. Endocrinology, 1979. 105, 1475-1480.

147. Schusdziarra, V. The role of somatostatin during the gastric phase of a meal. Hepatogastroenterology, 1980. 27, 240-246.

148. Sedar, A.W. The fine structure of the oxyntic cell in relation to functional activity of the stomach. Ann. N.Y. Acad. Sci., 1962. 99, 9-29.

149. Sedar, A.W., & Friedman, M.H.F. Correlation of the fine structure of the gastric parietal cell (dog) with the functional activity of the stomach. J. Biophys. Biochem. Cytol., 1961. 7, 349-363.

150. Sheahan, D.G., & Jervis, H.R. Comparative histochemistry of gastrointestinal mucosubstances. Am. J. Anat., 1976. 146, 103-132.

151. Sigaran, M.F., Con-Wong, R. Production of proliferative lesions in gastric mucosa of albino mice by oral administration of N-methyl-N'-nitro-N-nitrosoguanidine. Gann, 1979. 70, 343-352.

152. Sipponen, P., Seppala, K., Varis, K., Hjelt, L., Ihamaki, T., Kekki, M., & Siurala, M. Intestinal metaplasia with colonic-type sulphomucins in the

gastric mucosa; its association with gastric carcinoma. Acta Pathol. Microbiol. Scand. Sect. A. 1980. 88, 217-224.

153. Snell, R.S. Clinical anatomy for medical students. Boston: Little, Brown & Co., 1973. (pages 186-189)

154. Solcia, E., Capella, C., Vassallo, G., & Buffa, R. Endocrine cells of the gastric mucosa. Int. Rev. Cytol., 1975. 42, 223-286.

155. Spicer, S.S. Diamine methods for differentiating mucosubstances histochemically. J. Histochem. Cytochem., 1965. 13, 211-234.

156. Spicer, S.S., Katsuyama, T., & Sannes, P.L. Ultrastructural carbohydrate cytochemistry of gastric epithelium. Histochem. J., 1978. 10, 309-331.

157. Spurr, A.R. A low-viscosity epoxy resin embedding medium for electron microscopy. J. Ultrastruct. Res., 1969. 26, 31-43.

158. Stephens, R.J., & Pfeiffer, C.J. Ultrastructure of the gastric mucosa of normal laboratory ferrets. J. Ultrstruct. Res., 1968. 22, 45-62.

159. Stevens, C.E., & Leblond, C.P. Renewal of the mucous cells in the gastric mucosa of the rat. Anat Rec., 1953. 115, 231-245.

160. Sugimura, T., & Kawachi, T. Experimental stomach cancer. Methods Cancer Res., 1973. 7, 245-308.

161. Szelenyi, I. Calcium, histamine, and pentagastrin: Speculations about the regulation of gastric acid secretion at the cellular level. Agents Actions, 1980. 10, 187-190.

162. Tatsukawa, R. PCB pollution of the Japanese environment. In K. Higuchi (Ed.) PCB poisoning and pollution. New York: Academic Press, 1976. (pages 147-179)

163. Teir, H., & Rasanen, T. A study of mitotic rate in renewal zones of nondiseased portions of gastric mucosa in cases of peptic ulcer and gastric cancer, with observations on differentiation and so-called "intestinalization" of gastric mucosa. J. Natl. Cancer Inst., 1961. 27, 949-971.

164. Tokii, S., & Tsukamoto, A. The distribution of parietal cells in the stomach in monkeys. Okajimas Folia Anat. Jap., 1953. 25, 27-36.

165. Trötschler, H., Koch, H.K., & Oehlert, W. Changes in morphology and cellular replacement of surface epithelia in human gastric mucosa affected by different pathological changes. A scanning electron microscopical study of human gastric biopsy material. Pathol. Res. Pract., 1980. 169, 58-71.

166. Turner, J.C., & Green, R.S. The effect of a polychlorinated biphenyl (Aroclor 1254) on liver microsomal enzymes in the male rat. Bull. Environ. Contam. Toxicol., 1974. 12, 669-671.

167. Uemura, E., Houser, W.D., & Cupp, C.J. Menetrier's disease in a rhesus monkey (Macaca mulatta). J. Med. Primatol., 1979. 8, 252-256.

168. Vainio, H. Enhancement of microsomal drug oxidation and glucuronidation in rat liver by an environmental chemical, polychlorinated biphenyl. Chem. Biol. Interact., 1974. 9, 379-387.

169. Vos, J.G., & Koeman, J.H. Comparative toxicologic study with polychlorinated biphenyls in chickens with special reference to porphyria, edema formation, liver necrosis, and tissue residues. Toxicol. Appl. Pharmacol., 1970. 17, 656-668.

170. Vos, J.G., & Notenboom-Ram, E. Comparative toxicity study of 2,4,5,2',4',5'-hexachlorobiphenyl and a polychlorinated biphenyl mixture in rabbits. Toxicol. Appl. Pharmacol., 1972. 23, 563-78.

171. Wattel, W., Geuze, J.J., & de Rooij, D.G. Ultrastructural and carbohydrate histochemical studies on the differentiation and renewal of mucous cells in

the rat gastric fundus. Cell Tiss. Res., 1977. 176, 445-462.

172. Willems, G., Galand, P., Vansteenkiste, Y., Zeithoun P. Cell population kinetics of zymogen and parietal cells in the stomach of mice. Z. Zellforsch. Mikrosk. Anat., 1972. 134, 505-518.

173. Willems, G., Gepts, W. & Bremer, A. Endogenous hypergastrinemia and cell proliferation in the fundic mucosa of dogs. Am. J. Digest. Dis., 1977. 22, 419-423.

174. Willems, G., & Lehy, T. Radioautographic and quantitative studies on parietal and peptic cell kinetics in the mouse. A selective effect of gastrin on parietal cell proliferation. Gastroenterology, 1975. 69, 416-426.

175. Willems, G., Vansteenkiste, Y., & Limbosch, J.M. Stimulating effect of gastrin on cell proliferation kinetics in canine fundic mucosa. Gastroenterology, 1972. 62, 583-589.

176. Yoshimura, H., Ozawa, N., & Saeki, S. Inductive effect of polychlorinated biphenyls mixture and individual isomers on the hepatic microsomal enzymes. Chem. Pharmacol. Bull., 1978. 26, 1215-1221.

177. Yoshimura, H., Yoshihara, S., Ozawa, N., & Miki, M. Possible correlation between induction modes of hepatic enzymes by PCBs and their toxicity in rats. Ann. N.Y. Acad. Sci., 1979. 320, 179-192.

178. Zalewsky, C.A., & Moody, F.G. Stereological analysis of the parietal cell during acid secretion and inhibition. Gastroenterology, 1977. 73, 66-74.

VII. FIGURES

Figure 1. Structures of biphenyl, 3,4,3′,4′-tetrachloro-biphenyl and related isosteric, toxic compounds. The four toxic tetrachloro- compounds shown all have in common two phenyl rings which are approximately coplanar and four chlorine atoms occupying the four corners. These compounds all form rectangles approximately 30 nm X 100 nm (132). 2,3,7,8-tetrachlorodibenzofuran and 2,3,7,8-tetrachloro-dibenzodioxin are respectively approximately 100 and 1000 times more toxic than 3,4,3′,4′-tetrachlorobiphenyl for rhesus monkeys (McNulty, unpublished). It appears that the toxicities of these approximately isosteric compounds correlate with the rigidity of planarity of the two biphenyl rings.

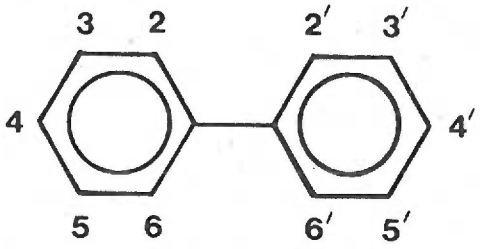

Biphenyl

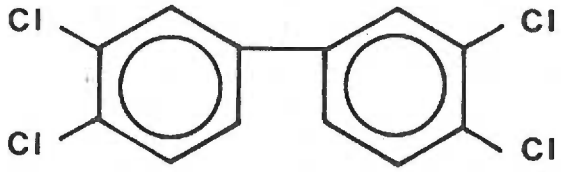

3,4-3′,4′- Tetrachlorobiphenyl

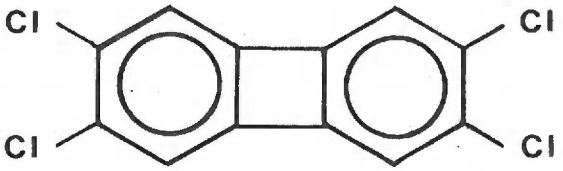

2,3,6,7- Tetrachlorobiphenylene

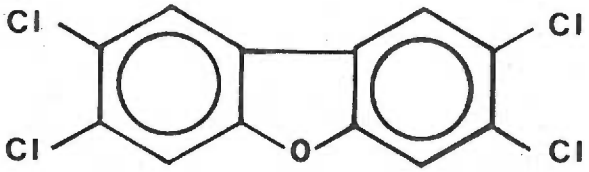

2,3,7,8- Tetrachlorodibenzofuran

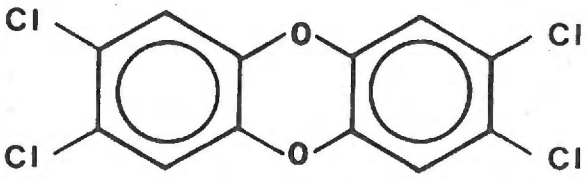

2,3,7,8- Tetrachlorodibenzodioxin

Figure 2. The stomach of the rhesus monkey. The approximate locations of the regions of the stomach are shown. Contiguous blocks of tissue 0.5 X 1.5 cm were cut from along the greater curvature, marked by X's in the diagram, beginning at the esophagogastric junction and ending in the pylorus.

Figure 3. Phases of the cell cycle. Located in the Introduction. (page 23)

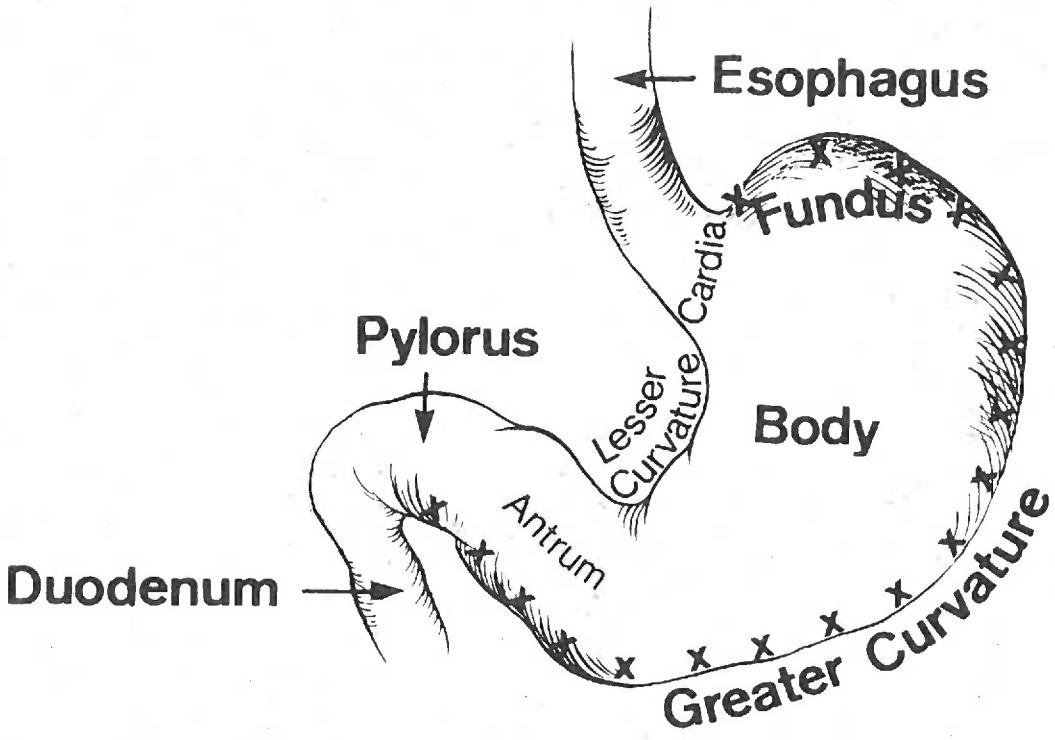
Esophagus
Fundus
Cardia
Pylorus
Lesser Curvature
Body
Antrum
Duodenum
Greater Curvature

Figure 4. Instrumentation used in morphometry. Slides of gastric tissue were viewed through a microscope equipped with a drawing tube attachment. An image of the light on the cursor, located on the digitizing tablet near B in the diagram, could be seen through the microscope superimposed over the image of the specimen. The cursor was moved so that the light appears over feature A, the cursor button pushed, the light moved to feature B, and the button pushed again. This generated a signal which could be programmed to measure the distance between features A and B in the specimen. These measurements were accumulated by the computer and stored on flexible discs. By appropriate programming, the data was recalled and analyzed as required, and graphs constructed on the digital plotter. Drawing by J. Ito.

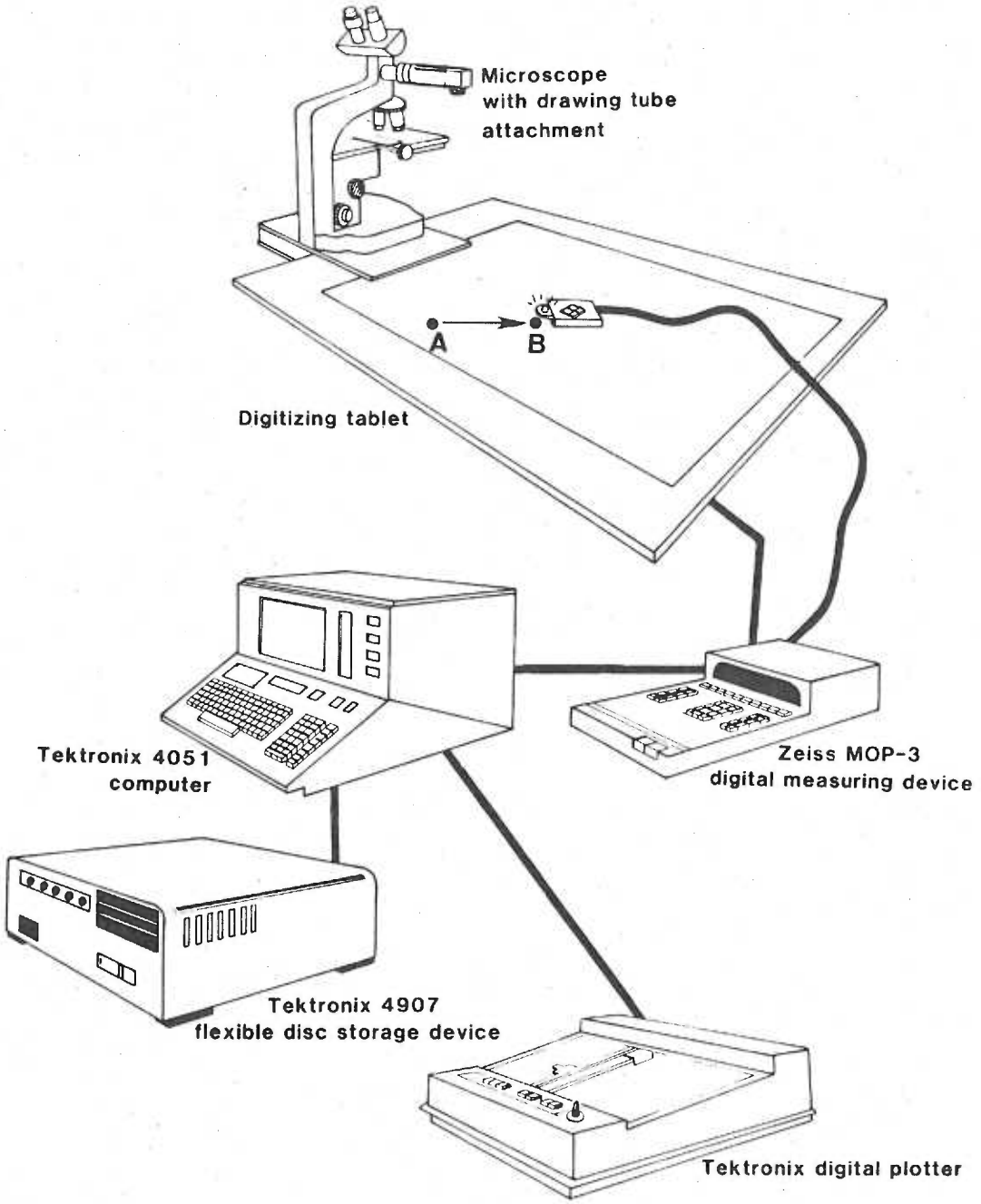
Microscope
with drawing tube
attachment
A
B
Digitizing tablet
Tektronix 4051
computer
Zeiss MOP-3
digital measuring device
Tektronix 4907
flexible disc storage device
Tektronix digital plotter

Figure 5. Body weights of rhesus monkeys as a function of their ages: control animals. Ages are in days. The animals gained weight at the rate of 70 g ± 17 (s.e.m.) per month. At the date indicated by Experiment Begun, these animals remained on control diets, while the other animals, whose weights are shown in figure 6, were placed on 3,4-TCB diets. The first three animals received injections of ^{3}H-thymidine 1 hour before sacrifice at autopsy on the date of their last weighing. Full-thickness gastric biopsies were taken at laparotomy from control animal 8553. He had received an injection of ^{3}H-thymidine 1 hour before the first biopsy. After the last biopsy he was transferred to another project.

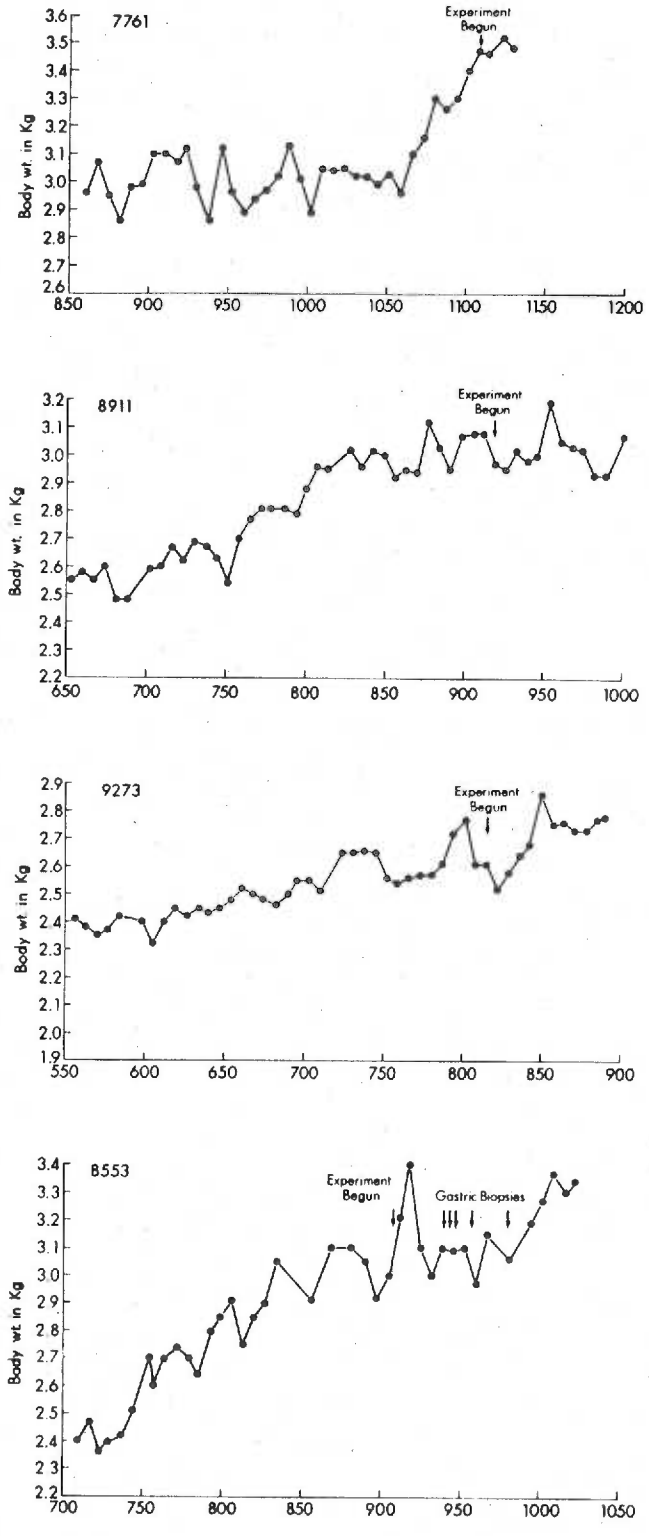
7761
Experiment Begun
Body wt. in Kg
8911
Experiment Begun
Body wt. in Kg
9273
Experiment Begun
Body wt in Kg
8553
Experiment Begun
Gastric Biopsies
Body wt in Kg
Age in days

Figure 6. Body weights of rhesus monkeys as a function of their ages: 3,4-TCB-fed animals. Ages are in days. The animals gained weight at the rate of 80 g ± 12 g (s.e.m.) per month before being placed on the 3,4-TCB diets. Animal 7194 was fed a diet containing 3 ppm of 3,4-TCB, while the other animals were fed the same compound at a level of 1 ppm. Although the animals eagerly ate the 3,4-TCB diets, they rapidly lost weight at rates of 110 g per month (animal 9921) to 480 g per month (animal 7194). The first three animals received injections of ^{3}H-thymidine 1 hour before sacrifice at autopsy of the date of their last weighing. Animal 8686 also received an injection of ^{3}H-thymidine, but had a full-thickness gastric biopsy taken at laparotomy. Additional specimens were taken at laparotomy and he was then sacrificed at autopsy on the date of his last weighing. Animal 8686 was maintained on the 3,4-TCB diet for 39 days before sacrifice, animal 7194 for 48 days, animal 9246 for 55 days, and animal 9921 for 97 days.

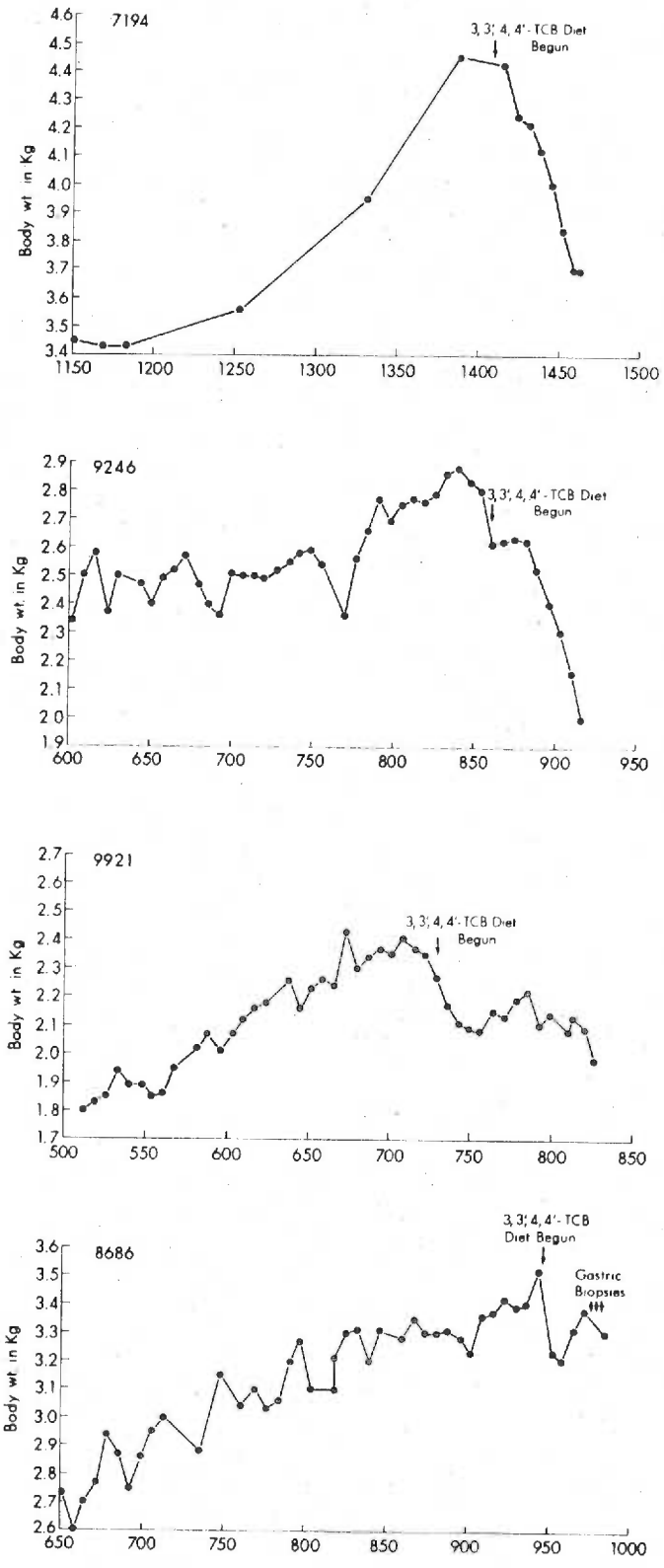
7194
3,3',4,4'-TCB Diet Begun
Body wt in Kg
4.6
4.5
4.4
4.3
4.2
4.1
4.0
3.9
3.8
3.7
3.6
3.5
3.4
1150
1200
1250
1300
1350
1400
1450
1500
9246
3,3',4,4'-TCB Diet Begun
Body wt. in Kg
2.9
2.8
2.7
2.6
2.5
2.4
2.3
2.2
2.1
2.0
1.9
600
650
700
750
800
850
900
950
9921
3,3',4,4'-TCB Diet Begun
Body wt in Kg
2.7
2.6
2.5
2.4
2.3
2.2
2.1
2.0
1.9
1.8
1.7
500
550
600
650
700
750
800
850
8686
3,3',4,4'-TCB Diet Begun
Gastric Biopsies
Body wt. in Kg
3.6
3.5
3.4
3.3
3.2
3.1
3.0
2.9
2.8
2.7
2.6
650
700
750
800
850
900
950
1000
Age in days

Figure 7. Control rhesus monkey stomach and a stomach from a 3,4-TCB-fed monkey. The stomachs were cut along the greater curvature and then spread out flat. A portion of the distal esophagus is seen at the top, and a portion of duodenum is seen at the bottom of each stomach.

Figure 76a (top). Foldings of the gastric mucosa, called rugae, are prominent throughout this control stomach.

Figure 7b (bottom). Stomach from an animal fed 3 ppm of 3,4-TCB for 26 days, then an average of 1 ppm for 24 days, then 0.3 ppm of 3,4-TCB for 12 days when he was moribund and was sacrificed. The rugae have been replaced by a thickened and irregular gastric mucosa, which is confined to the body of the stomach. The dark areas are focal hemorrhages. The cardia adjacent to the esophagus and the antrum beneath the body, both appear relatively uninvolved.

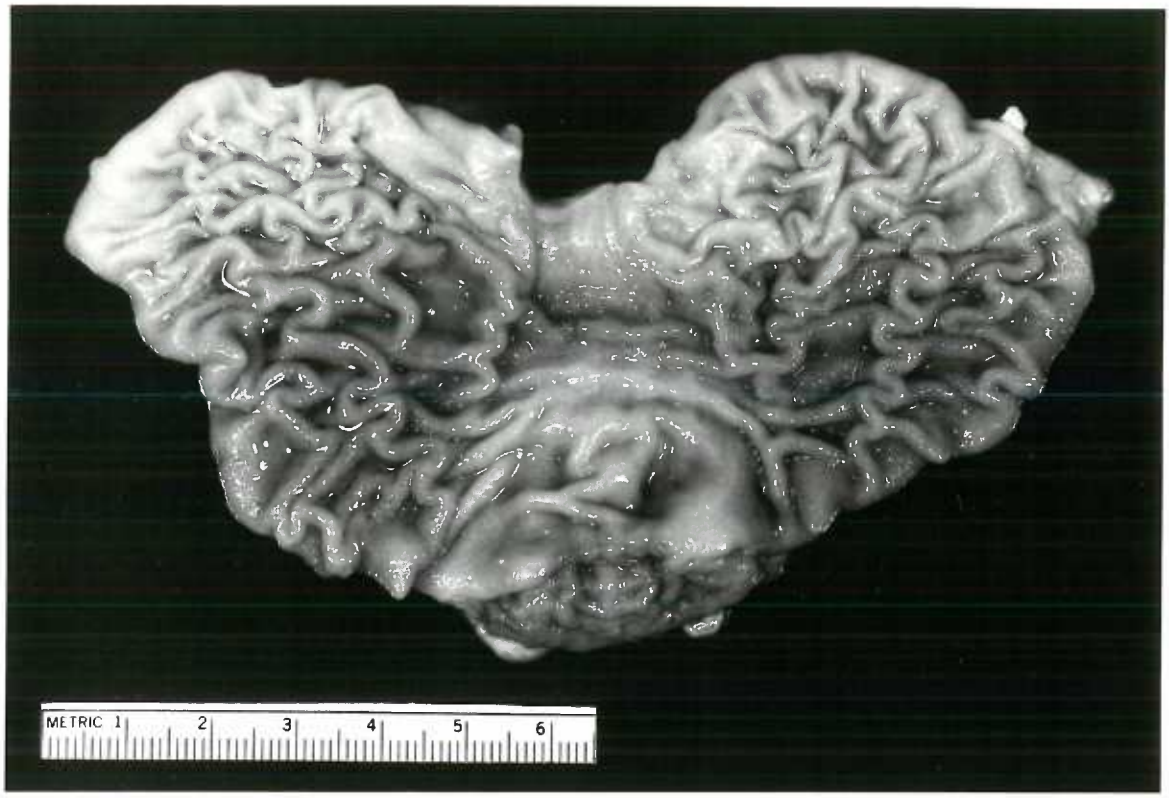
METRIC 1 2 3 4 5 6


METRIC 1 SYSTEM 2 3 4 5 6

Figure 8. Gastric mucosa from the body region of a control stomach and a stomach from a 3,4-TCB-fed animal.

Figure 8a (top). The entire thickness of the stomach wall can be seen in this control animal.

Figure 8b (bottom). The stomach wall from this monkey fed 3 ppm of 3,4-TCB for 53 days extended beyond the field of view, even at this low magnification (35 X). The gastric mucosa is clearly hyperplastic and has penetrated the muscularis mucosae.

2 µm thick glycol methacrylate sections; stained with methylene blue and basic fuchsin. (X 35)

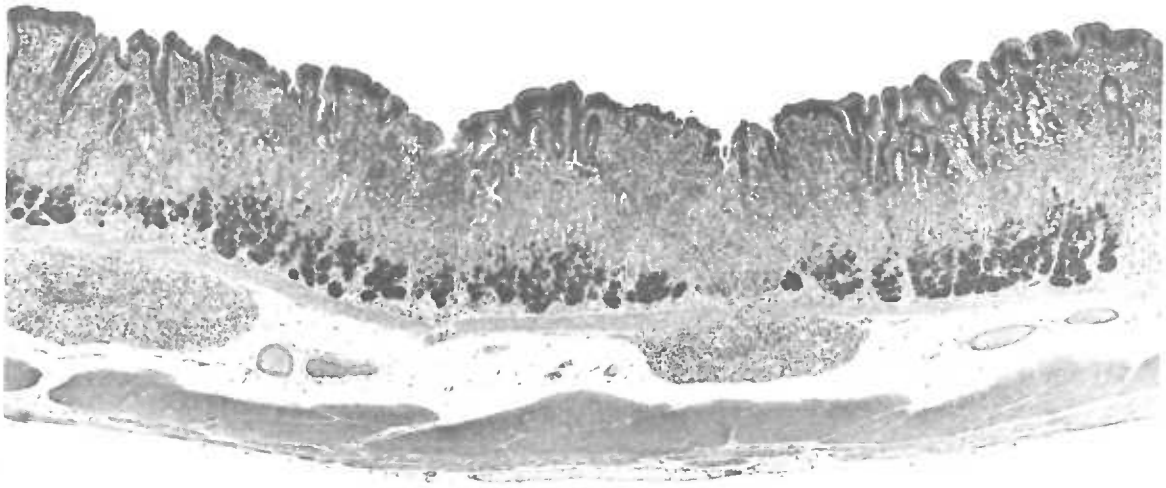

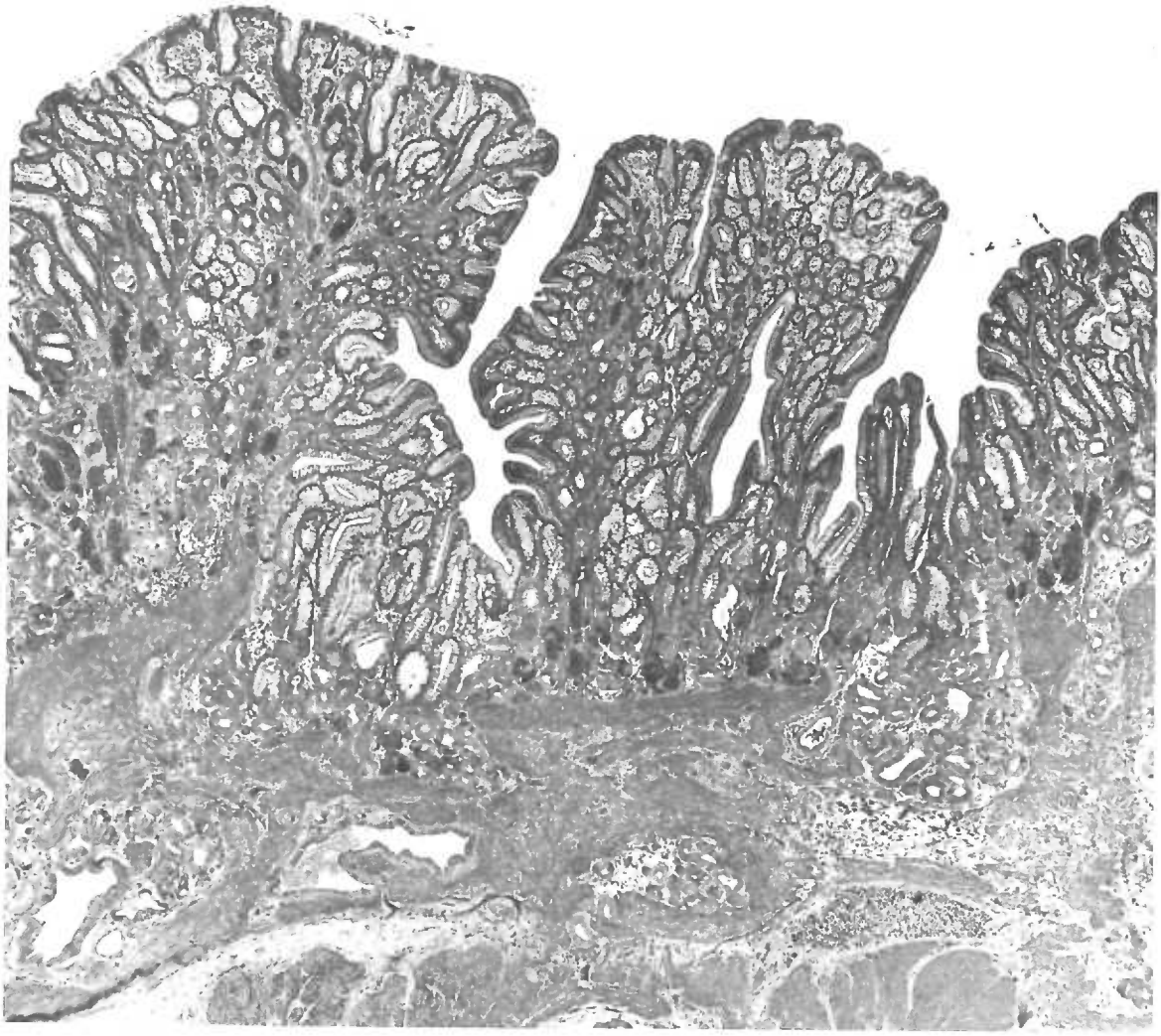

Figure 9. Comparison of gastric mucosal thickness in control monkeys and monkeys fed 3,4-TCB diets. The ordinate represents thickness in microns and the abcissa represents the relative position along the greater curvature. The mucosal thicknesses of all the control animals (top) were relatively constant from the cardia to the pylorus. The mucosal thickness of animal 8911 was consistently greater than that of animals 7761 and 9273, which were nearly the same. In contrast, the mucosal thickness of two of the 3,4-TCB-fed animals, 7194 and 9246, showed a marked increase in total mucosal thickness, as measured from the deepest invasions of the mucosa into the submucosa to the luminal surface. This increased thickness corresponded to the gastric lesion as seen in the gross specimen in figure 7b.

○ 7761 control animal

△ 8911 control animal

□ 9273 control animal

● 7194 3,4-TCB-fed animal

▲ 9921 3,4-TCB-fed animal

■ 9246 3,4-TCB-fed animal

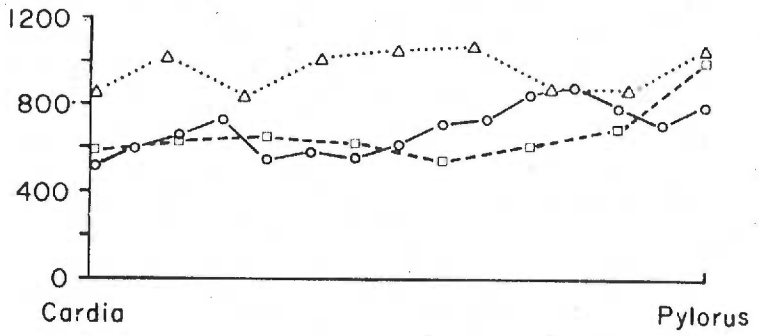
1200
800
400
0
Cardia
Pylorus

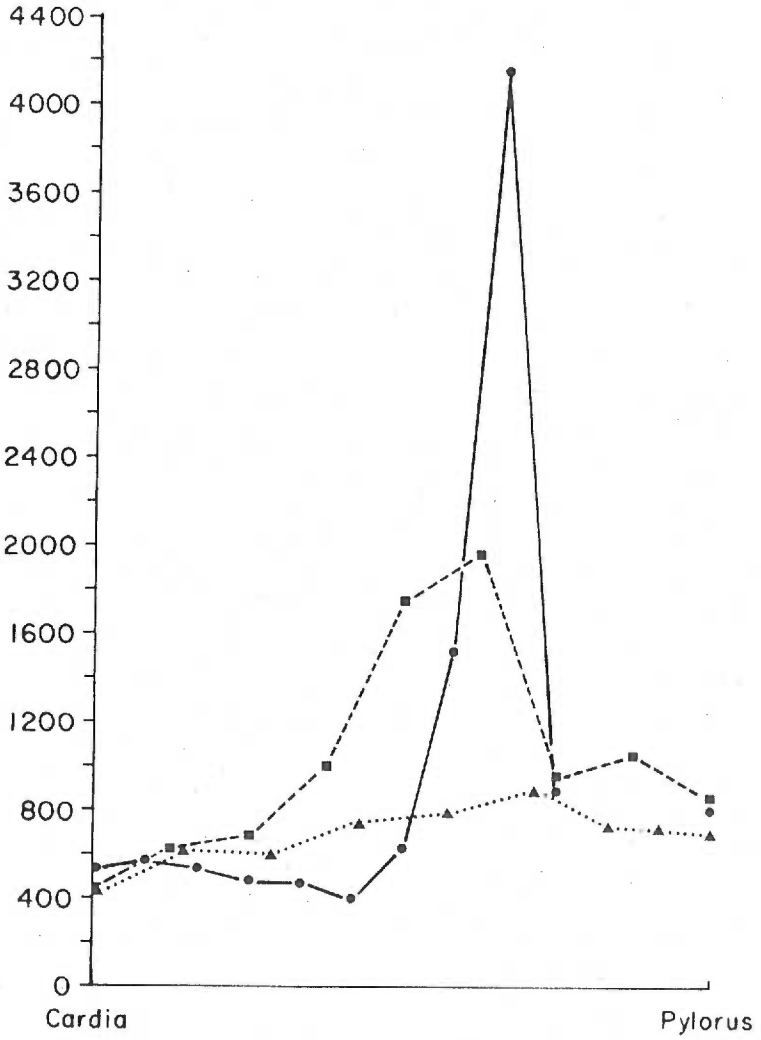
4400
4000
3600
3200
2800
2400
2000
1600
1200
800
400
0
Cardia
Pylorus

Figure 10. Distal esophagus near the esophagogastric junction of a control monkey and a 3,4-TCB-fed-monkey.

Figure 10a (top). Control monkey. The esophagus is covered by a thin layer of dead squamous epithelial cells.

Figure 10b (bottom). This same layer is markedly thicker in this 3,4-TCB-fed animal. The underlying squamous epithelial cells appear larger and the entire mucosa is considerably thicker than normal.

2 μm thick glycol methacrylate sections; stained with methylene blue and basic fuchsin. (X 70)

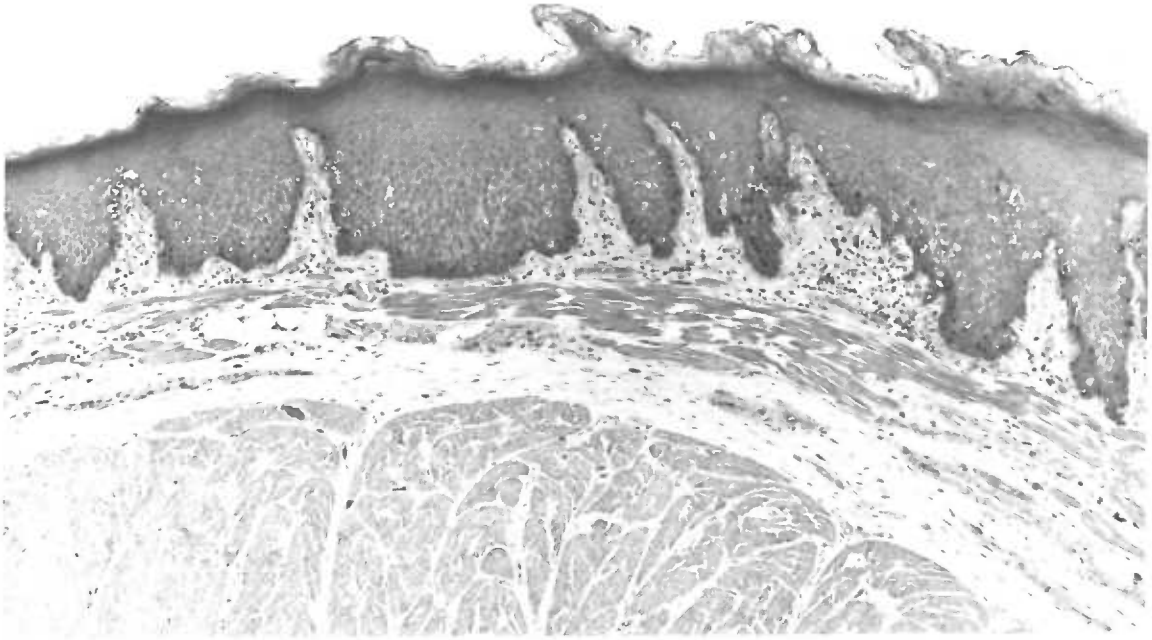

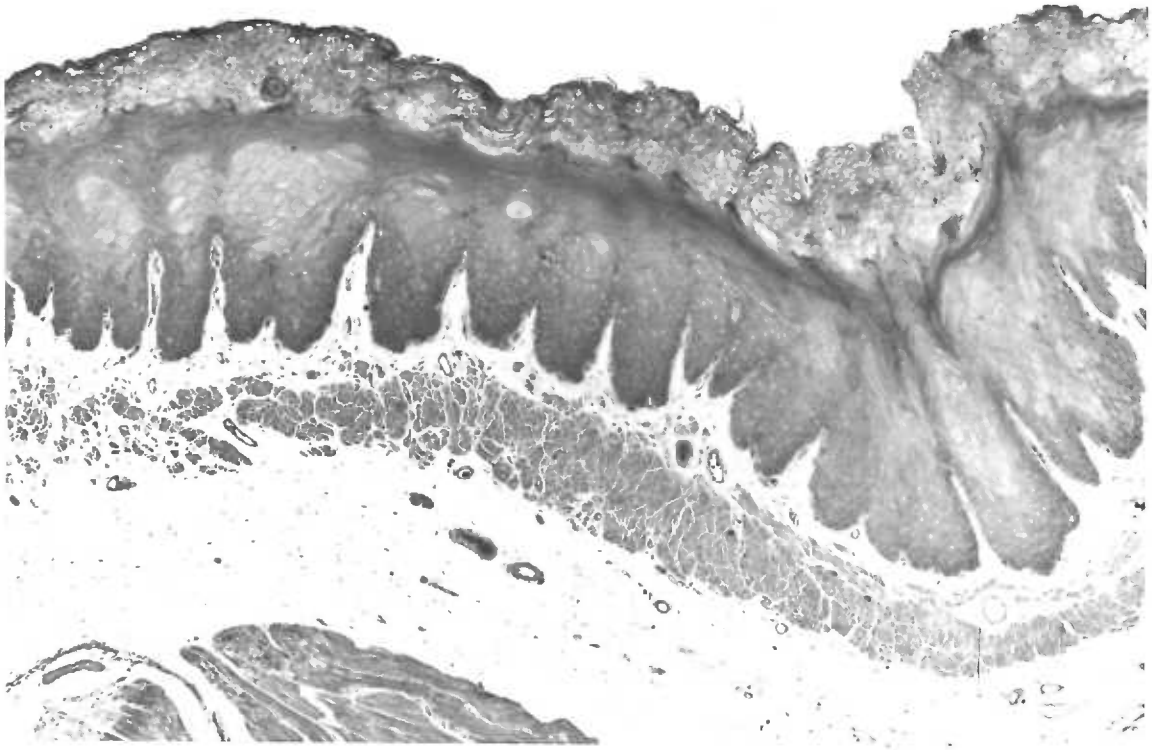

Figure 11. Gastric mucosa from the cardias of a control stomach and a stomach from a 3,4-TCB-fed monkey.

Figure 11a (top). In this control animal the gastric foveolae are lined with surface epithelial cells and the glands proper are lined with mucous neck cells in the neck region and zymogenic cells in the base region. The zymogenic cells are clearly seen as the dark staining epithelial cells in the bases of the glands.

Figure 11b (bottom). In this 3,4-TCB-fed animal the zymogenic and parietal cells have nearly all been replaced by mucus-secreting cells. The lumen of the glands are markedly dilated. The material above the mucosa in the lumen of the stomach is a mat of long gram positive filiform bacteria and mucus.

2 μm thick glycol methacrylate sections; stained with methyelene blue and basic fuchsin. (X 70)

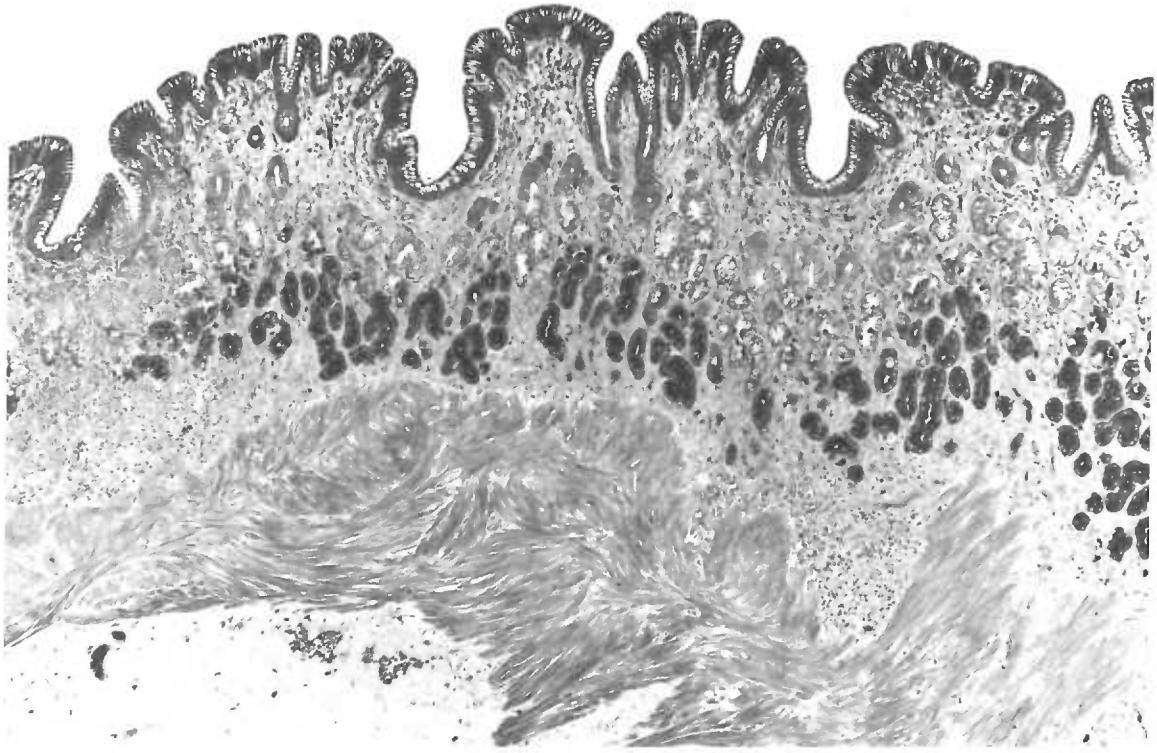

Figure 12. Gastric mucosa from the body region of a control stomach and of a stomach from a 3,4-TCB-fed monkey.

Figure 12a (top). As in the cardia of control stomachs, the gastric foveolae are lined with surface epithelial cells. However, in the body region of control stomachs the gastric glands proper contain parietal cells as well as mucous neck cells in the neck region. Parietal cells are also seen adjacent to zymogenic cells in the bases of the glands. The parietal cells are the pale cells prominent in the middle third of the normal gastric mucosa, and the zymogenic cells are the dark staining cells at the bases of the glands.

Figure 12b (bottom). In this 3,4-TCB-fed monkey, the parietal and zymogenic cells have been converted to or replaced with mucus-secreting cells. The glands are dilated and irregular, and have invaded the submucosa. One gland has formed a large spherical cyst. The surface of the epithelium facing the lumen of the stomach also appears irregular.

2 μm thick glycol methacrylate sections; stained with methylene blue and basic fuchsin. (X 70)

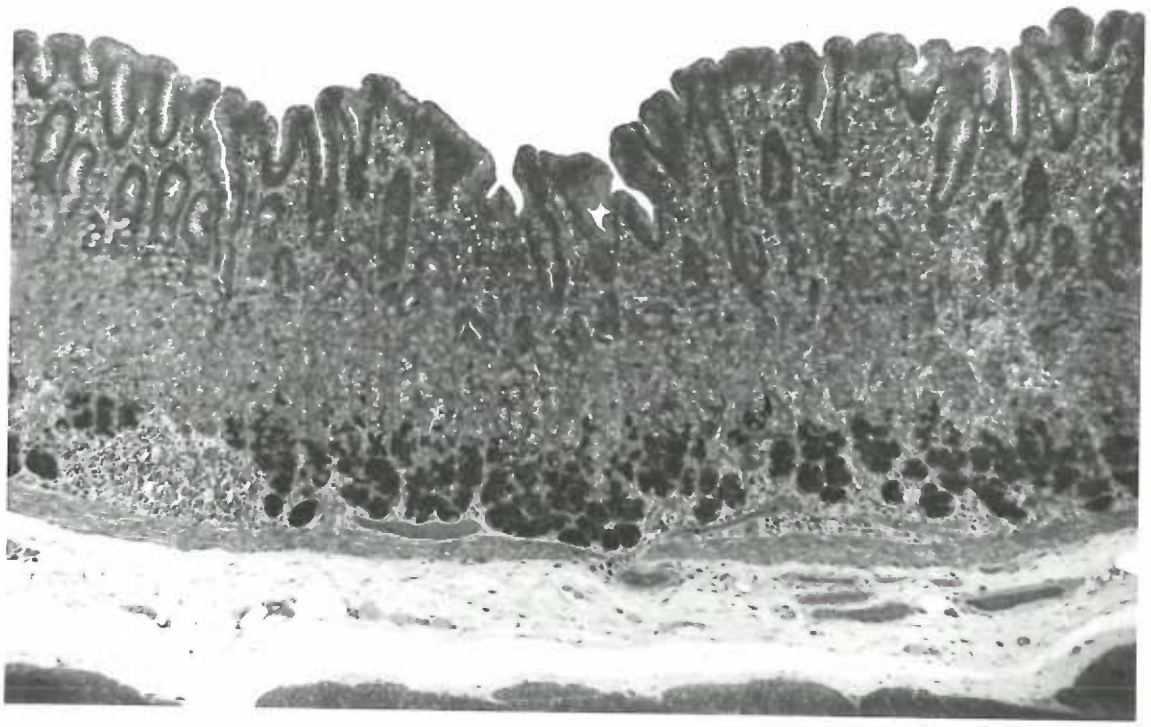

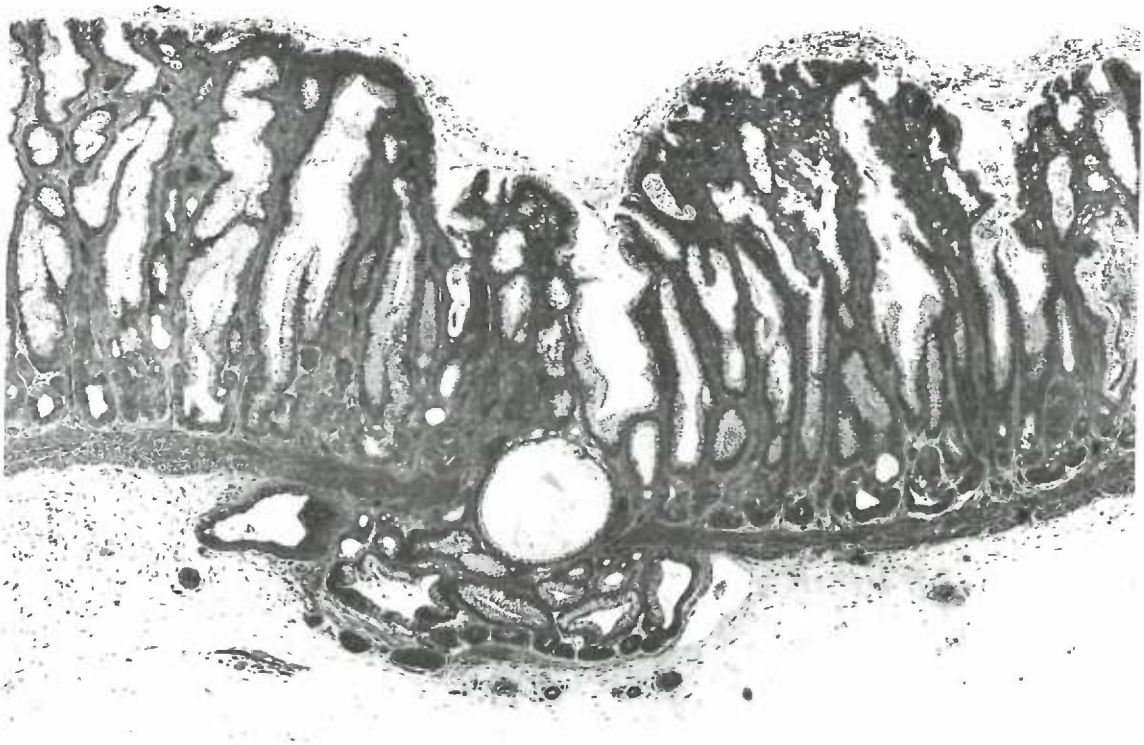

Figure 13. Gastric mucosa from the antra of a control monkey and from a 3,4-TCB-fed monkey.

Figure 13a (top). In this control monkey the gastric glands are lined principally with mucus-secreting cells identical to those of the mucous neck region of glands in the body of the stomach. Enteroendocrine cells are also abundant, but cannot be distinguished at this low magnification.

Figure 13b (bottom). In the antrum of this 3,4-TCB-fed monkey, the glands are markedly dilated and the surface appears less uniform than in the control animals.

2 μm thick glycol methacrylate sections; stained with methylene blue and basic fuchsin. (X 70)

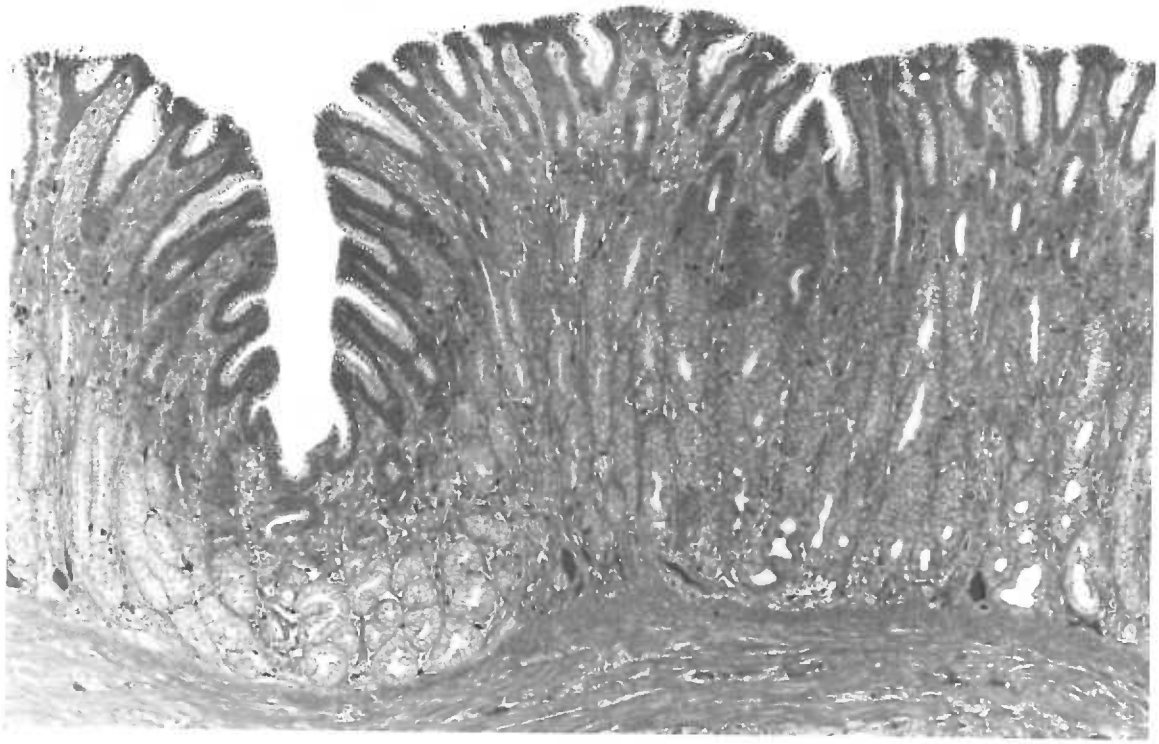

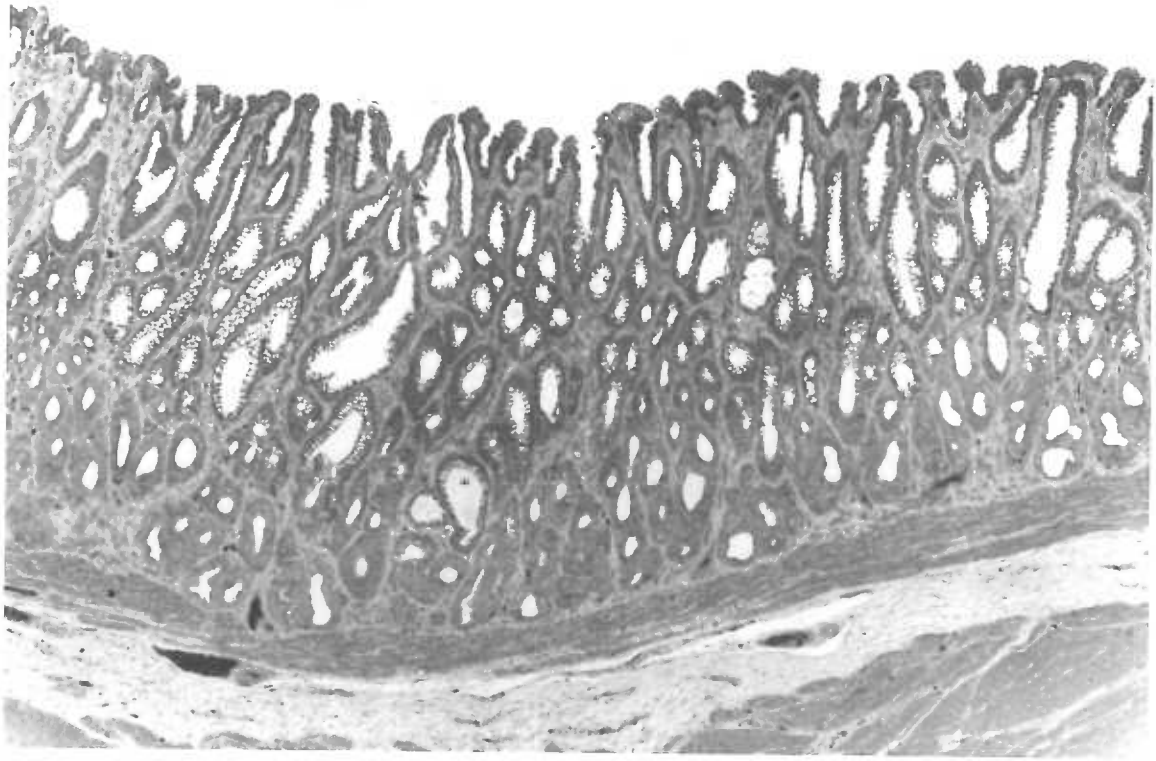

Figure 14. Proximal duodena from a control monkey and a 3,4-TCB-fed monkey.

Figure 14a (top). In the duodenum of this control monkey, the villi are lined with absorptive epithelial cells (darker staining cells) interspersed with mucus-secreting goblet cells (the apices of these cells are clear and round). The spaces between the villi form pits into which the underlying intestinal glands secrete mucus and zymogens. The submucosa is filled with mucus- and zymogen-secreting Brunner's glands. These glands are clearly seen as the very lightly staining glandular structures beneath the muscularis mucosae.

Figure 14b (bottom). In this 3,4-TCB-fed animal the villi and intestinal glands appear normal; the submucosal layer of Brunner's glands is considerably thicker and the glands themselves appear dilated.

2 µm thick glycol methacrylate sections; stained with methylene blue and basic fuchsin. (X 70)

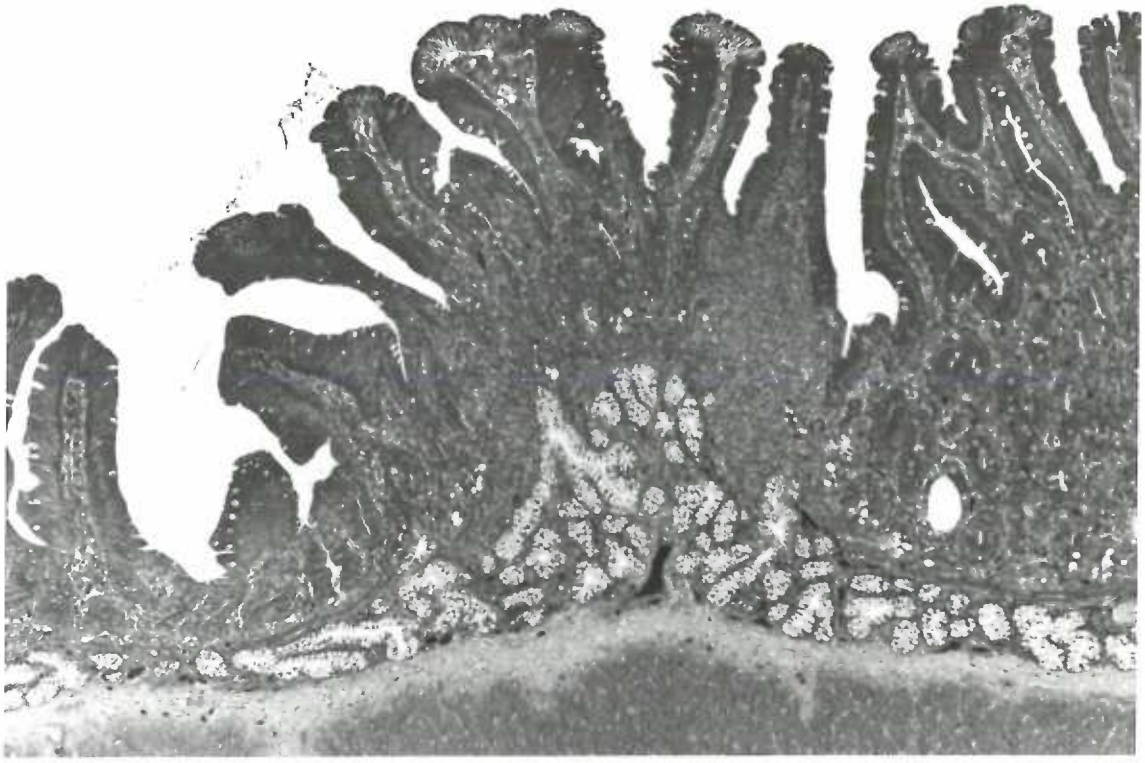

Figure 15. Number of parietal cells per 200 μm length of muscularis mucosae. Each point represents the mean of 10 measurements. Standard errors of the means were usually between 10 and 20% of the values shown. No parietal cells were seen in animal 9921 fed 1 ppm 3,4-TCB for 97 days and only occasional parietal cells were seen in animal 9246 fed 1 ppm 3,4-TCB for 55 days. Parietal cells were somewhat more numerous in animal 7194 fed 3 ppm 3,4-TCB for 53 days, but the numbers were very much lower than in the control animals.

○ 7761 fed control diet

△ 8911 fed control diet

□ 9273 fed control diet

● 7194 fed a 3 ppm 3,4-TCB diet for 53 days

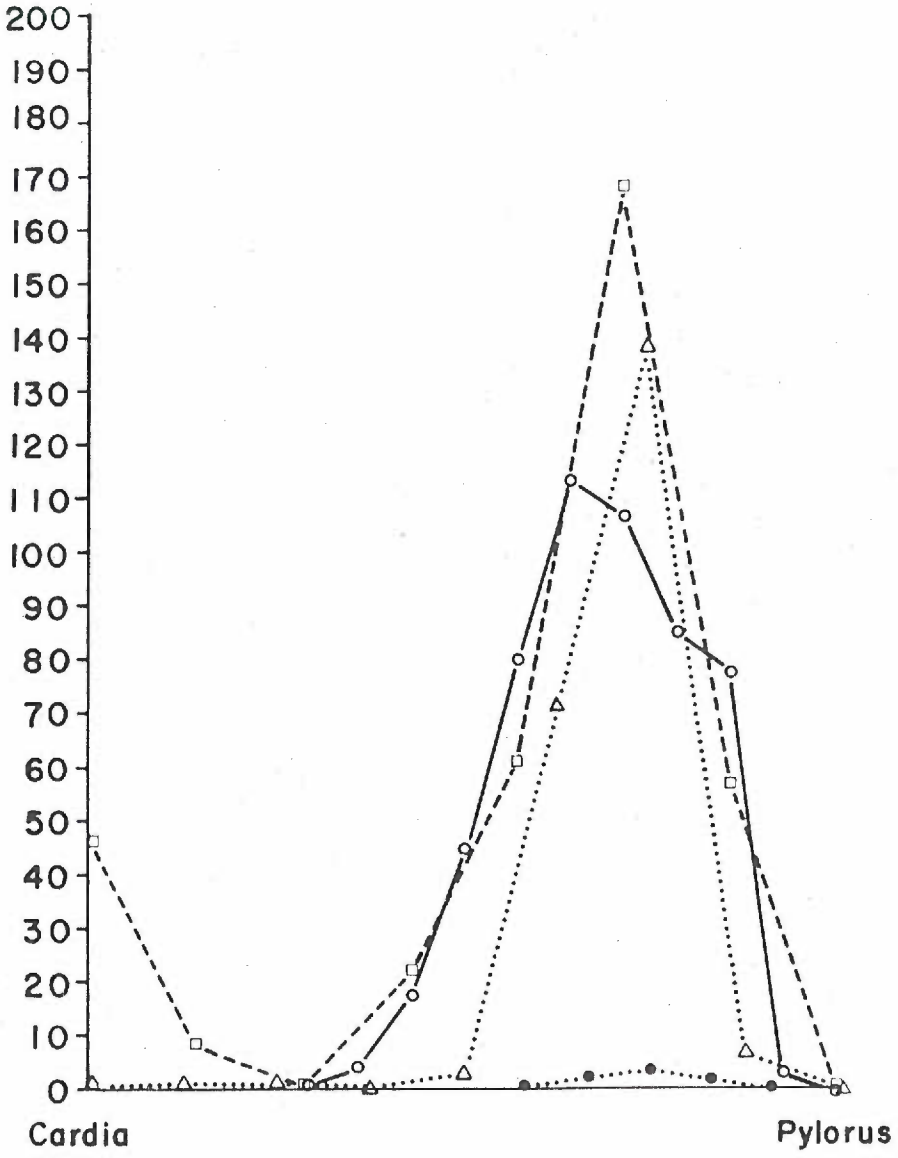
200
190
180
170
160
150
140
130
120
110
100
90
80
70
60
50
40
30
20
10
0
Cardia
Pylorus

Figure 16. Light micrographs of gastric mucosa stained for mucosubstances with the periodic acid-Schiff and the high-iron diamine reactions. All micrographs are from sections taken from the body regions of the stomachs.

Figure 16a (top left). This control micrograph shows normal gastric mucosa stained by the PAS reaction. The surface epithelial cells and the mucous neck cells are strongly positive. The large, pale, ovoid cells above and interspersed with the mucous neck cells are parietal cells. The PAS-negative cells beneath the mucous neck cells are zymogenic cells.

Figure 16b (top right). A similar section of control gastric mucosa stained by the high-iron diamine reaction. The surface epithelial cells and the mucous neck cells show a positive reaction indicating that these cells probably produce acidic sulfomucins.

Figure 16c (bottom left). Gastric mucosa from an animal fed 3,4-TCB; stained with the PAS reaction. Nearly all the cells are PAS-positive. Those few which are not probably were not sectioned through the apical regions, where secretory granules accumulate. Note the prominent penetration of the gastric glands through the muscularis mucosae.

Figure 16d (bottom right). A similar area as in figure 16c stained by the high-iron diamine reaction. Nearly all the epithelial cells show a positive reaction, indicating that these cells probably produce sulfomucins. The alcian blue stain for acidic mucosubstances (not shown) gave very similar results to the high-iron diamine reaction.

2 μm thick glycol methacrylate sections. (X 70)

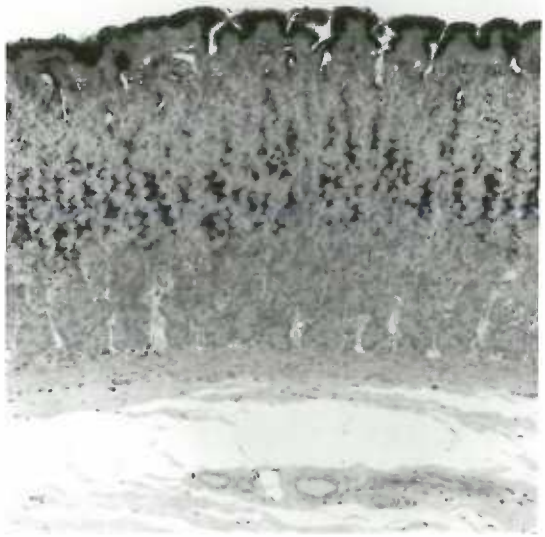

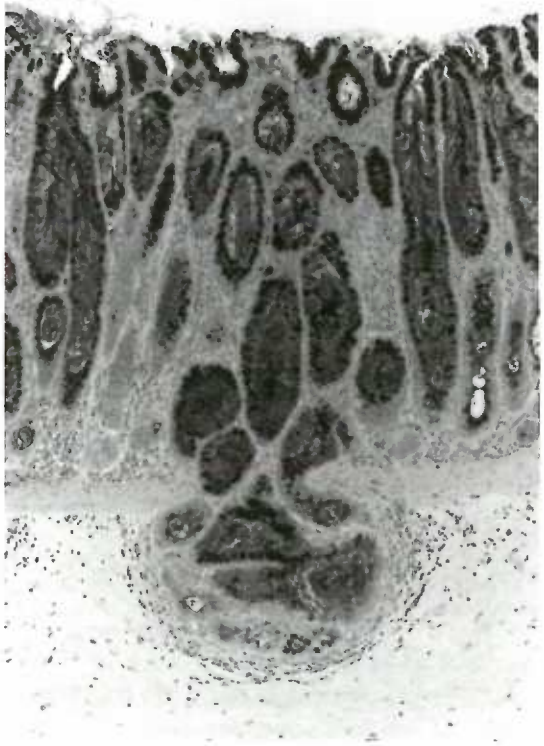

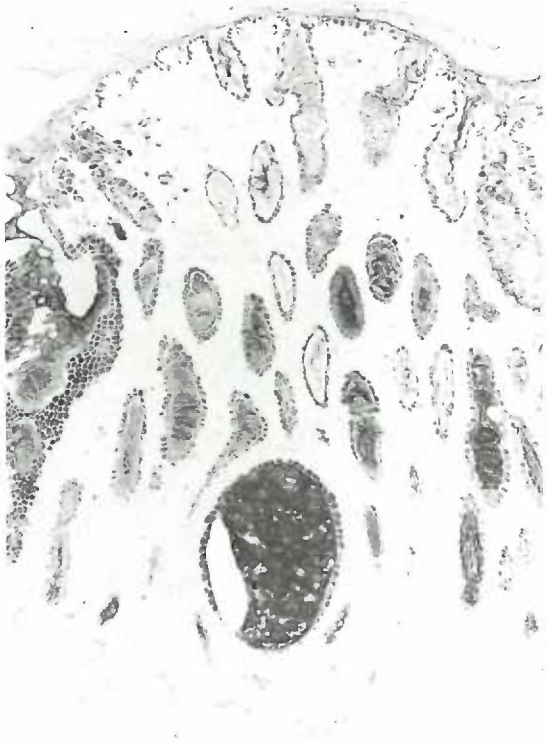

Figure 17. The range of periodic acid-Schiff-positive cells in control gastric mucosa. The ordinate represents the distance in μm from the muscularis mucosae and the abscissa represents the contiguous series of blocks of tissue taken from the cardia to the pylorus. The uppermost boundary represents the median value (30 to 50 measurements) of mucosal height above the muscularis mucosae for each section, while the lowermost boundary of the darkly hatched area is the median value (100 to 150 measurements) of the distances of the lowermost PAS-positive cells above the muscularis mucosae. Therefore the range of PAS-positive cells is represented by the area darkened by the heavy hatching, while the area beneath, only lightly hatched, represents the area occupied by PAS-negative cells. In control animals, this lightly hatched area is occupied principally by zymogenic cells. The total PAS-positive and -negative areas were measured by a digital measuring device to determine the percent of the total area occupied by PAS-negative cells. This was 18.6% for animal 9273; 17.5% for animal 8911; and 13.3% for animal 7761. The mean was 16.5 ± 1.6% (s.e.m.).

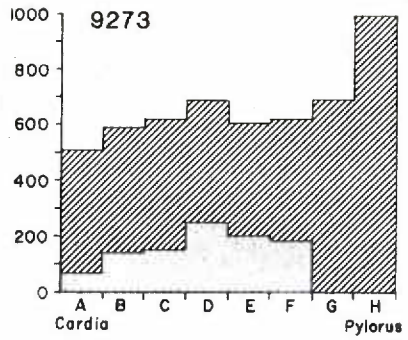
9273
1000
800
600
400
200
0
A
B
C
D
E
F
G
H
Cardia
Pylorus

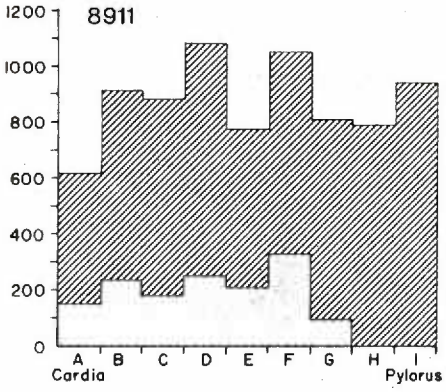
8911
1200
1000
800
600
400
200
0
A
B
C
D
E
F
G
H
I
Cardia
Pylorus

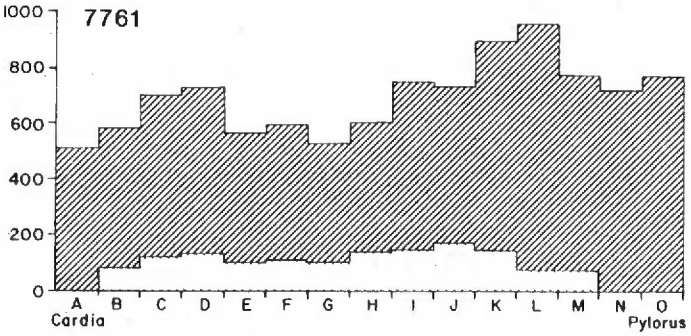
7761
1000
800
600
400
200
0
A
B
C
D
E
F
G
H
I
J
K
L
M
N
O
Cardia
Pylorus

Figure 18. The range of periodic acid-Schiff-positive cells in the gastric mucosa of 3,4-TCB-fed animals. The ordinate represents the distance in μm from the muscularis mucosae and the abscissa represents the contiguous series of blocks of tissue taken from the cardia to the pylorus. The uppermost boundary represents the median value (30 to 50 measurements) of mucosal height above the muscularis mucosae for each section and the lowermost boundary of the darkly hatched area is the median value (100 to 150 measurements) of the distance of the lowermost PAS-positive cells above the muscularis mucosae. Therefore the range of the PAS-positive cells is represented by the darkly hatched area, while the area beneath, only very lightly hatched, represents the area occupied by the PAS-negative cells. In these 3,4-TCB-fed animals this light area is occupied by the remaining zymogenic cells. The total PAS-positive and -negative areas were measured with a digital measuring device to determine the percent of the total area occupied by PAS-negative cells. This was 5.1% for animal 9921; 3.18% for 9246; and 4.1% for 7194. The mean was 4.2 $\pm$ 0.6% (s.e.m.). This mean value was significantly less (t-test, $p < 0.01$) than the value obtained in the control animals; 16.5 $\pm$ 1.6 % (s.e.m.).

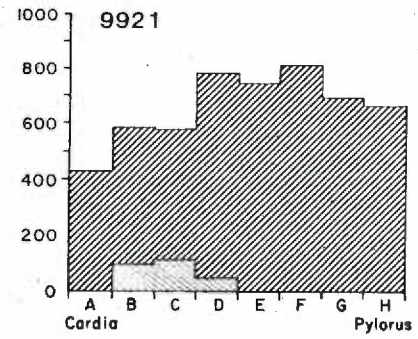
9921
1000
800
600
400
200
0
A
B
C
D
E
F
G
H
Cardia
Pylorus

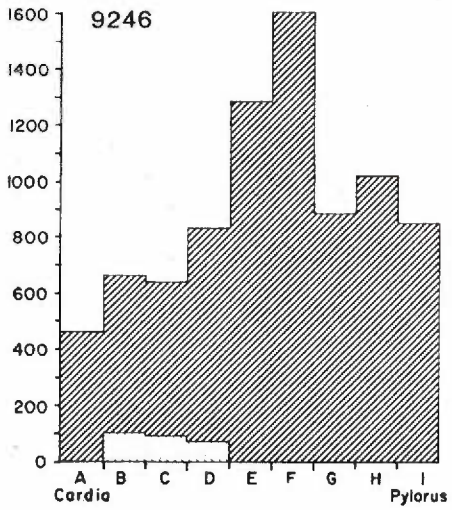
9246
1600
1400
1200
1000
800
600
400
200
0
A
B
C
D
E
F
G
H
I
Cardia
Pylorus

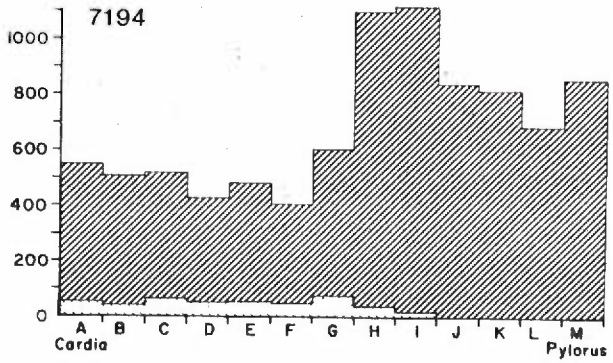
7194
1000
800
600
400
200
0
A
B
C
D
E
F
G
H
I
J
K
L
M
Cardia
Pylorus

Figure 19. The range of the alcian blue-positive cells in control gastric mucosa. The ordinate represents the distance in μm from the muscularis mucosae and the abscissa represents the contiguous series of blocks of tissue taken from the cardia to the pylorus. The uppermost boundary represents the median value (30 to 50 measurements) of mucosal height above the muscularis mucosae for each section, while the lowermost boundary of the striped darkened area is the median value (100 to 150 measurements) of the distances of the lowermost alcian blue-positive cells above the muscularis mucosae. Therefore the median range of AB-positive cells is represented by the striped darkened area, while the area beneath, lightly stippled with dots, represents the area occupied by AB-negative cells. In these control animals, this light area is occupied by those mucous neck cells which are AB-negative, by parietal cells and zymogenic cells. The total AB-positive and -negative areas were measured with a digital measuring device to determine the percent of the total area occupied by AB-negative cells. This was 59.0% for animal 9273; 48.3% for 8911; and 42.5% for 7761. The mean was 50.8% $\pm$ 4.2% (s.e.m.).

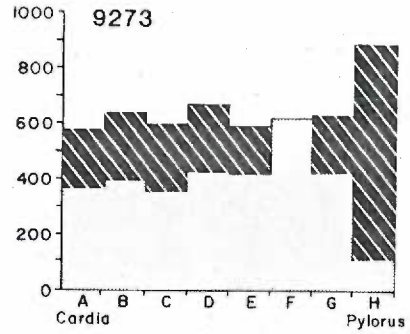
9273
1000
800
600
400
200
0
A
B
C
D
E
F
G
H
Cardia
Pylorus

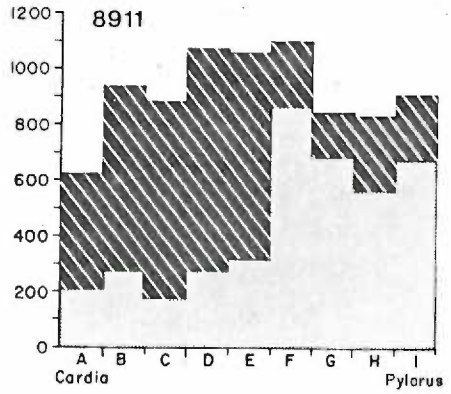
8911
1200
1000
800
600
400
200
0
A
B
C
D
E
F
G
H
I
Cardia
Pylorus

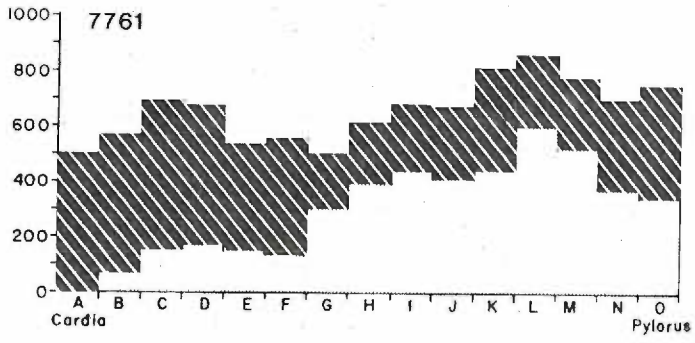
7761
1000
800
600
400
200
0
A
B
C
D
E
F
G
H
I
J
K
L
M
N
O
Cardia
Pylorus

Figure 20. The range of the alcian blue-positive cells in the gastric mucosa of 3,4-TCB-fed animals. The ordinate represents the distance in μm from the muscularis mucosae and the abcissa represents the contiguous series of blocks of tissue taken from the cardia to the pylorus. The uppermost boundary represents the median value (30 to 50 measurements) of mucosal height above the muscularis mucosae for each section; the lowermost boundary of the striped darkened area is the median value (100 to 150 measurements) of the distances of the lowermost AB-positive cells above the muscularis mucosae. Therefore the median range of AB-positive cells is represented by the darkened area and the lightly stippled area beneath represents the area occupied by AB-negative cells. In these 3,4-TCB-fed animals, this light area is occupied by mucus-secreting PAS-positive cells which are AB-negative, and the few remaining zymogenic cells. The total AB-positive and -negative areas were measured with a digital measuring device to determine the percent of the total area occupied by AB-negative cells. This was 25.1% for animal 9921, 16.0% for 9246, and 15.9% for 7194. The mean was 19.0 $\pm$ 3.0% (s.e.m.). This mean value was significantly less (t-Test, $p < 0.02$) than the mean value obtained in the control animals: 50.8 $\pm$ 4.2% (s.e.m.).

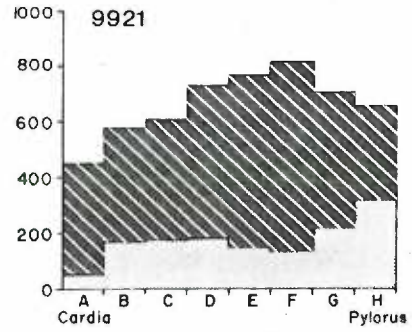
9921
1000
800
600
400
200
0
A
B
C
D
E
F
G
H
Cardia
Pylorus

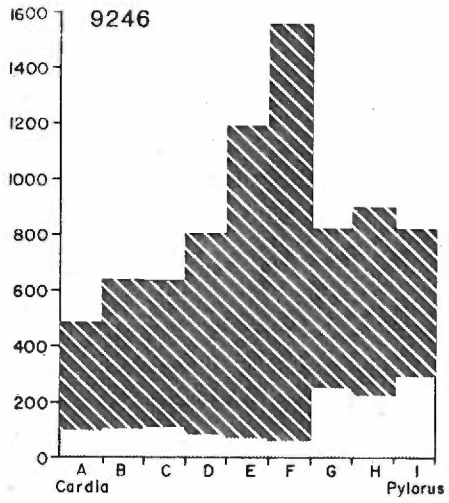
9246
1600
1400
1200
1000
800
600
400
200
0
A
B
C
D
E
F
G
H
I
Cardia
Pylorus

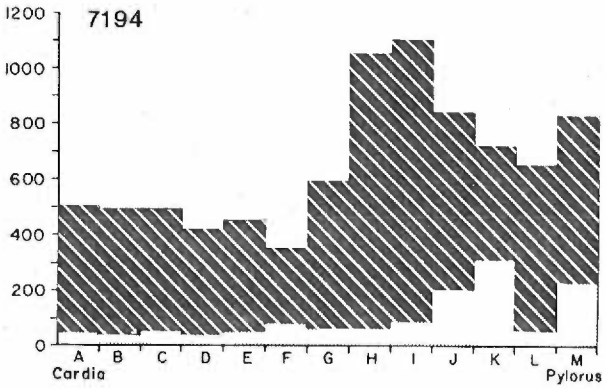
7194
1200
1000
800
600
400
200
0
A
B
C
D
E
F
G
H
I
J
K
L
M
Cardia
Pylorus

Figure 21. Autoradiographs of gastric mucosa from the body region of control stomachs. The animals received injections of ^{3}H-thymidine 1 hour before sacrifice. Silver grains can be seen overlying nuclei in S-phase which had incorporated ^{3}H-thymidine into DNA during the hour between injection and sacrifice.

Figure 21a (left). In this autoradiograph, immature surface epithelial cells are labeled in the isthmus of a gastric foveola.

Figure 21b (right). In this autoradiograph, labeled mucous neck cells are seen in the neck region of gastric glands. The large pale ovoid cells are parietal cells, which were never labeled.

2 μm thick glycol methacrylate sections; coated with liquid photographic emulsion and exposed for 1 month before development. Stained with methylene blue and basic fuchsin. (X 630)

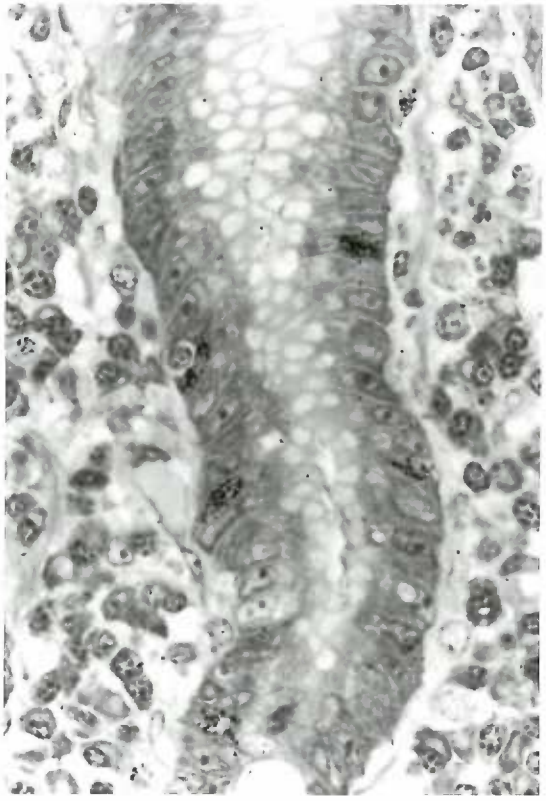

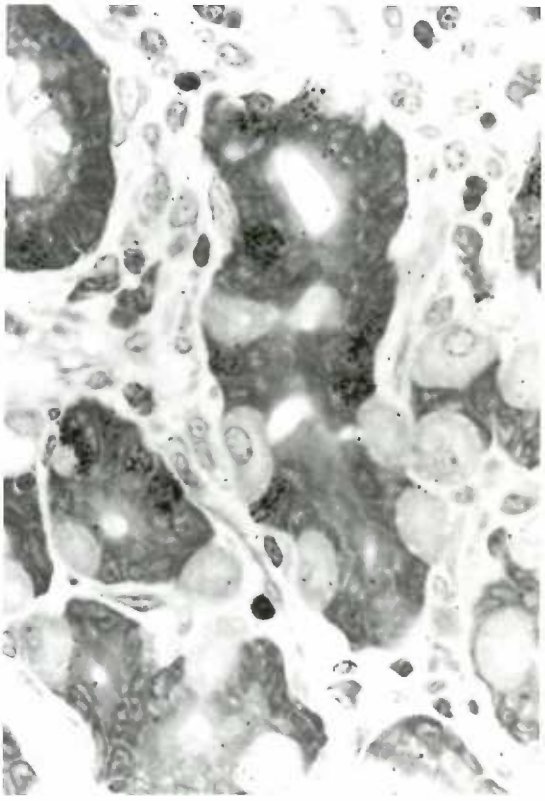

Figure 22. Autoradiographs of gastric mucosa from the body regions of stomachs from 3,4-TCB-fed animals. The animals received injections of ^{3}H-thymidine 1 hour before sacrifice. Silver grains can be seen overlying nuclei in the S-phase which had incorporated ^{3}H-thymidine into DNA during the hour between injection and sacrifice.

Figure 22a (top left). Labeled mucus-secreting cells are seen high in a cystic gland near the surface. These cells all have large accumulations of mucus-containing secretory granules in their apices, which appear colorless with this stain.

Figure 22b (top right). Labeled cells are seen in the upper portion of a gland.

Figure 22c (bottom left). Labeled cells are seen lining the middle portion of dilated, cystic glands.

Figure 22d (bottom right). Labeled cells can be seen in glands which have penetrated the muscularis mucosae (MM) and formed a submucosal cyst (SC).

2 µm thick glycol methacrylate sections; coated with liquid photographic emulsion and exposed for 1 month before development. Stained with methylene blue and basic fuchsin. (X 630)

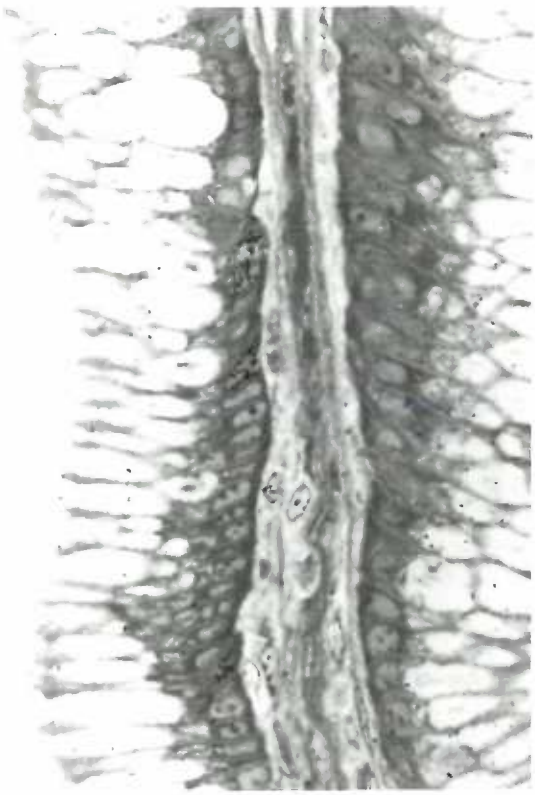

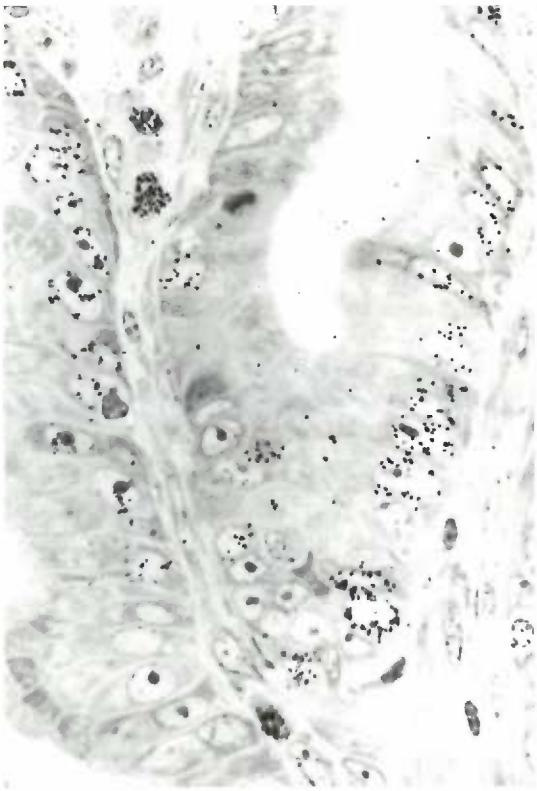

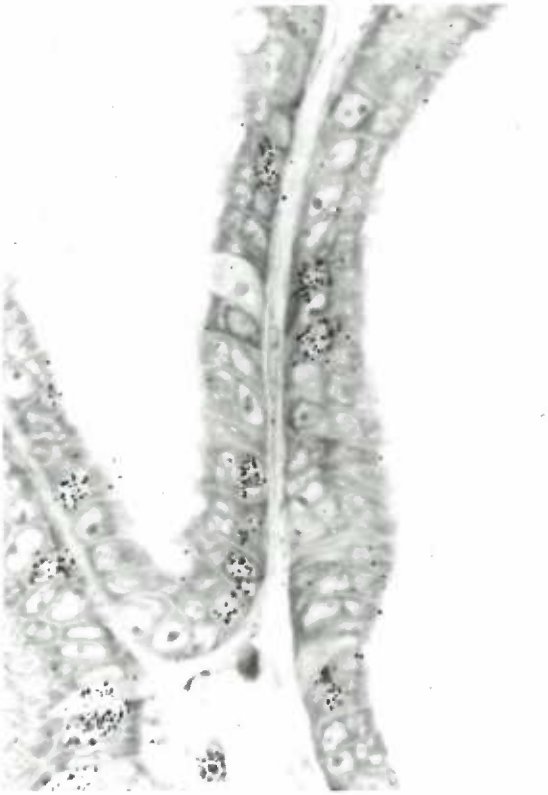

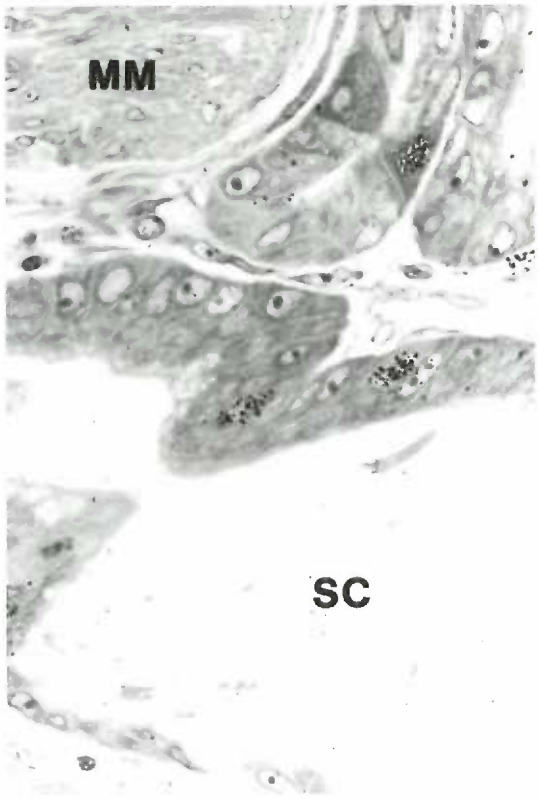
MM
SC

Figure 23. Frequency distribution histograms of the distances above the muscularis mucosae of ^{3}H-thymidine labeled gastric epithelial cells in control animal 7761. Section A begins at the esophagogastric junction and section O ends at the pyloroduodenal junction. The ordinates are the distance above the muscularis mucosae in μm and the abcissas are the relative frequency in percent of the total. The distances of between 150 and 300 labeled cells were measured from each section to compile each histogram. Each dotted line indicates the median mucosal height (20 to 40 measurements) over the region in which the labeled cells were measured. Only section B, in the cardiac-fundic region has labeled cells as close as 50 to 100 μm above the muscularis mucosae, and no labeled cells were less than 50 μm above. The distances appeared to be normally distributed in all the sections except A.

7761

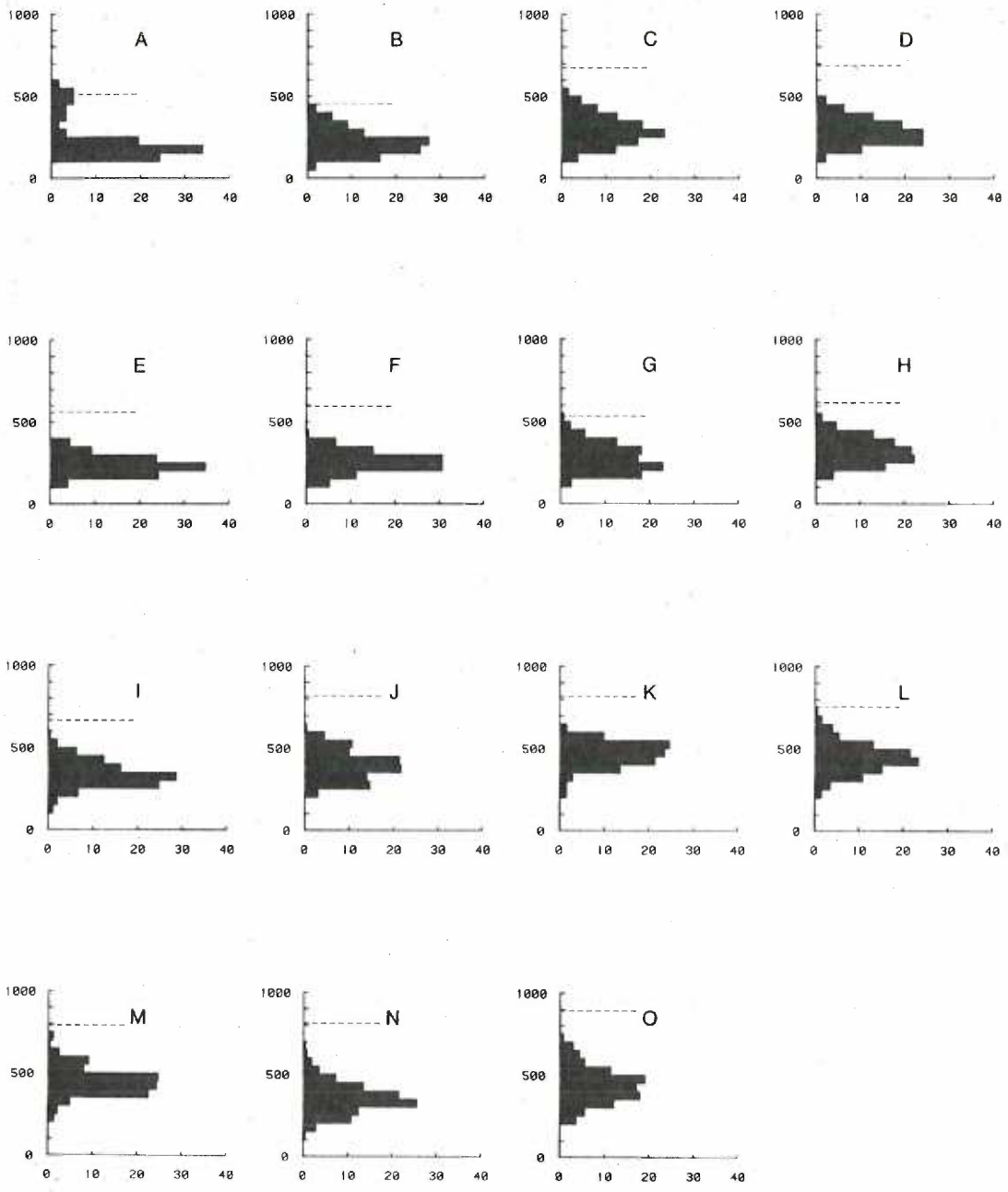

Figure 24. Frequency distribution histograms of the distances above the muscularis mucosae of ^{3}H-thymidine labeled gastric epithelial cells in control animal 8911. Section A begins at the esophagogastric junction and section I ends at the pyloroduodenal junction. The ordinates are the distance above the muscularis mucosae in μm and the abscissas are the relative frequency in percent of the total. The distances of 150 to 300 labeled cells were measured from each section to compile each histogram. Each dotted line indicates the median mucosal height (20 to 40 measurements) over the region in which the labeled cells were measured. The lowest labeled cells were at least 150 μm above the muscularis mucosae in every section. The distances appeared to be normally distributed in all the sections.

8911

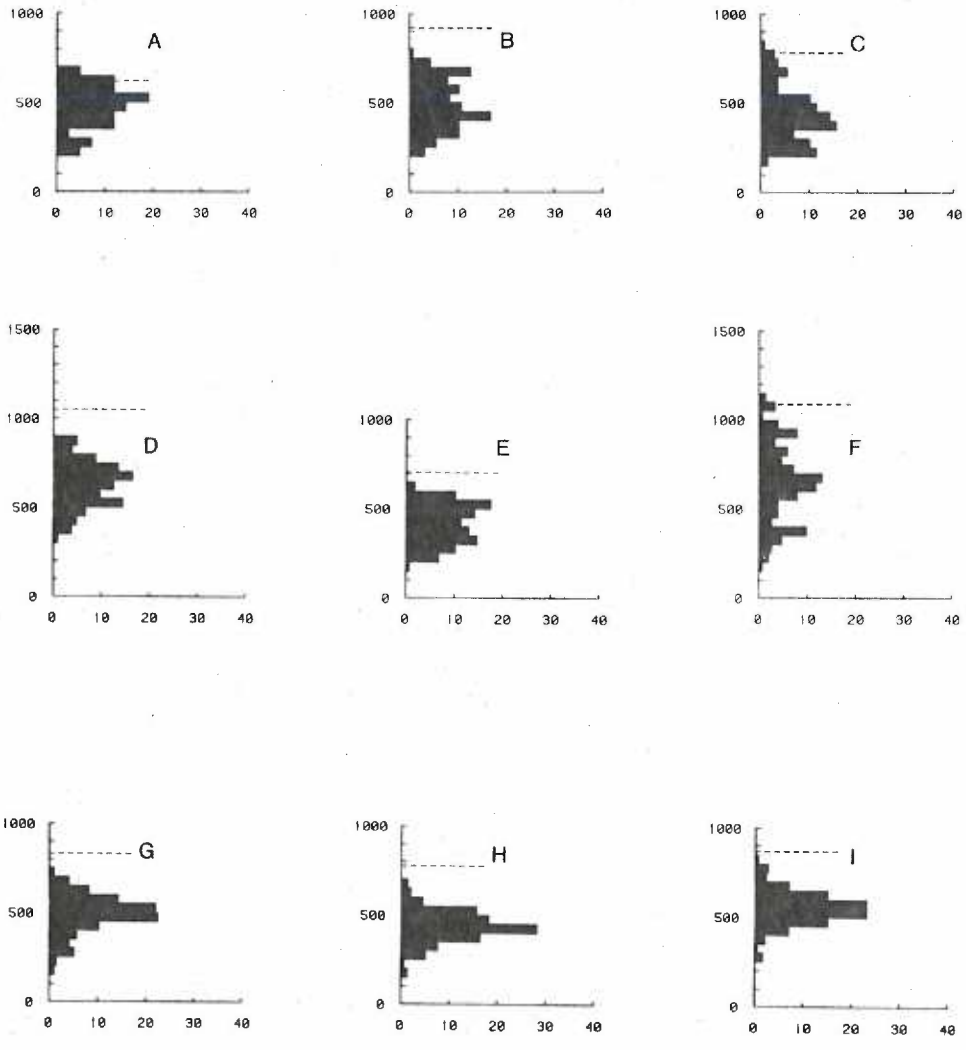

Figure 25. Frequency distribution histograms of the distances above the muscularis mucosae of ^{3}H-thymidine labeled gastric epithelial cells in control animal 9273. Section A begins at the esophagogastric junction and section H ends at the pyloroduodenal junction. The ordinates are the distance above the muscularis mucosae in μm and the abcissas are the relative frequency in percent of the total. The distances of 150 to 300 labeled cells were measured from each section to compile each histogram. Each dotted line indicates the median mucosal height over the region in which the labeled cells were measured. Only section G, in the antrum, had labeled cells as close as 50 to 100 μm above the muscularis mucosae and no labeled cells were less than 50 μm above. The distances appear to be normally distributed, except in sections G and H, where the distributions are somewhat irregular.

9273

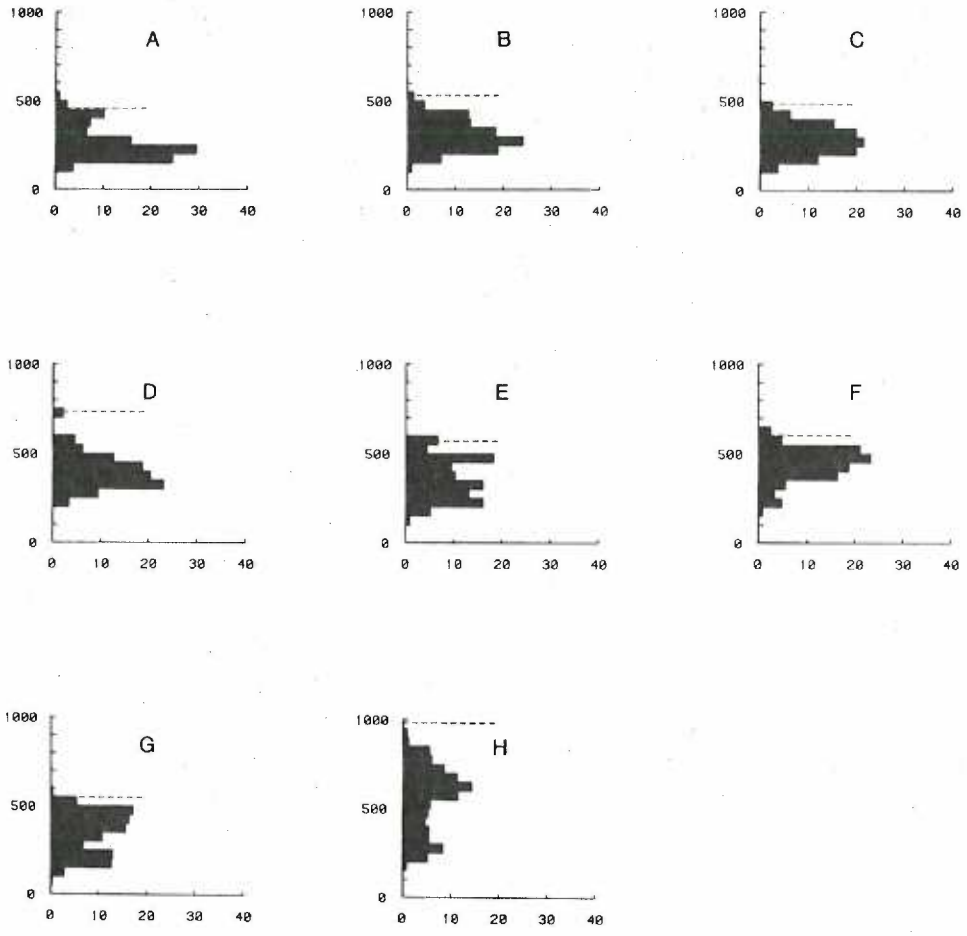

Figure 26. Frequency distribution histograms of the distances above the muscularis mucosae of ^{3}H-thymidine labeled gastric epithelial cells in the 3,4-TCB-fed animal 7194. Section A begins at the esophagogastric junction and section M ends at the pyloroduodenal junction. The ordinates are the distance above the muscularis mucosae in μm and the abscissas are the relative frequency in percent of the total. The distances of 150 to 300 labeled cells were measured from each section to compile each histogram. Each dotted line indicates the median mucosal height over the region in which the labeled cells were measured. 69% of the sections had labeled cells as a close as 50 to 100 μm above the muscularis mucosae and 46% as close as 0 to 50 μm above. The frequency distributions in sections E, F, and G are markedly leptokurtic, while I is platykurtic and H is skewed toward the base of the glands. Labeled cells which occurred beneath the muscularis mucosae in submucosal glands and cysts are not shown in these histograms.

7194

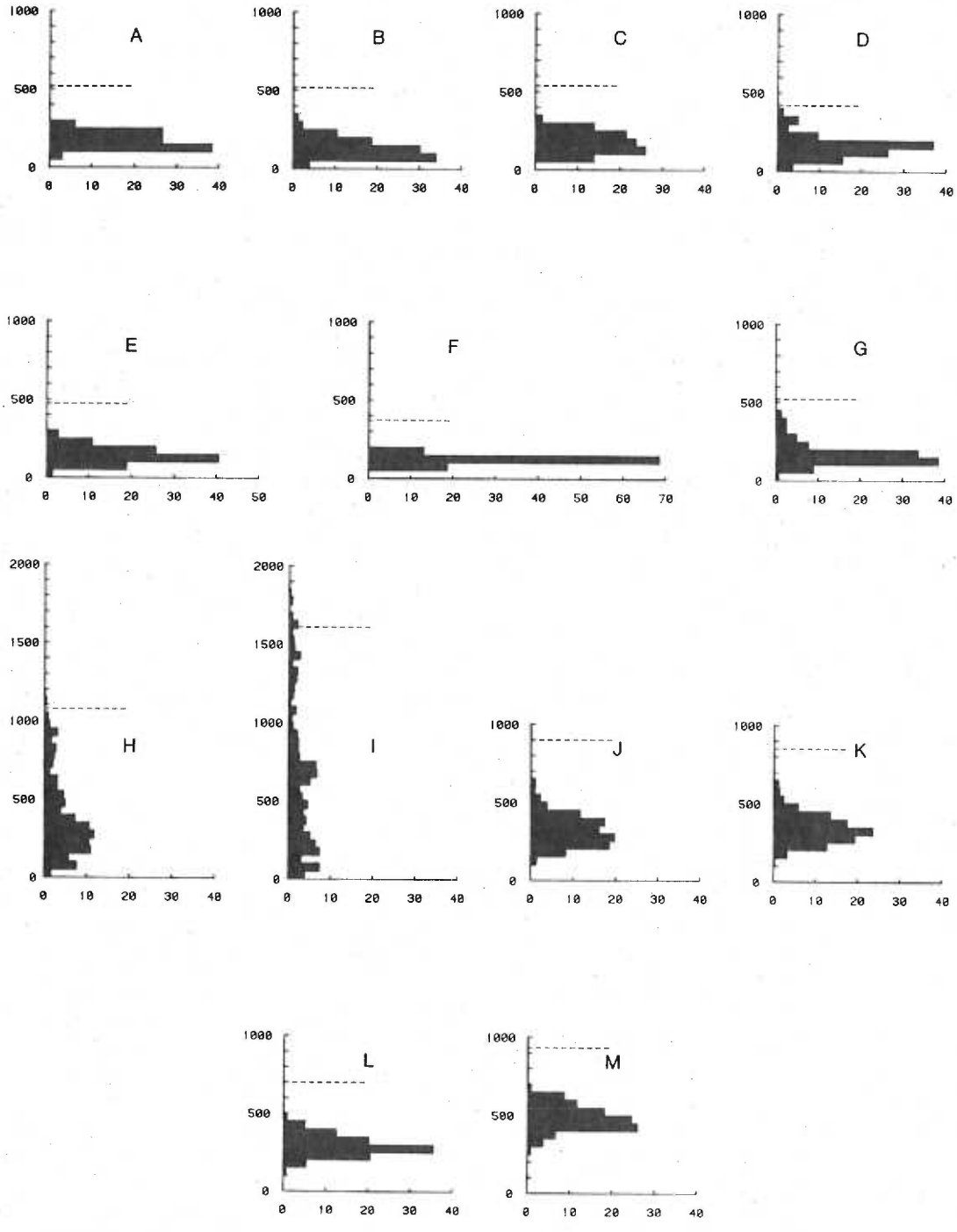

Figure 27. Frequency distribution histograms of the distances above the muscularis mucosae of ^{3}H-thymidine labeled gastric epithelial cells in the 3,4-TCB-fed animal 9246. Section A begins at the esophagogastric junction and section I ends at the pyloroduodenal junction. The ordinates are the distance in μm above the muscularis mucosae and the abcissas are the relative frequency in percent of the total. The distances of 150 to 300 labeled cells were measured from each section to compile each histogram. Each dotted line indicates the median mucosal height (20 to 40 measurements) over the region in which the labeled cells were measured. All sections had labeled cells as close as 0 to 50 μm above the muscularis mucosae. The frequency distributions of sections E and F are markedly skewed toward the muscularis mucosae, while the shapes of the others approximated normal distributions. Labeled cells beneath the muscularis mucosae in submucosal glands and cysts are not shown in these histograms.

9246

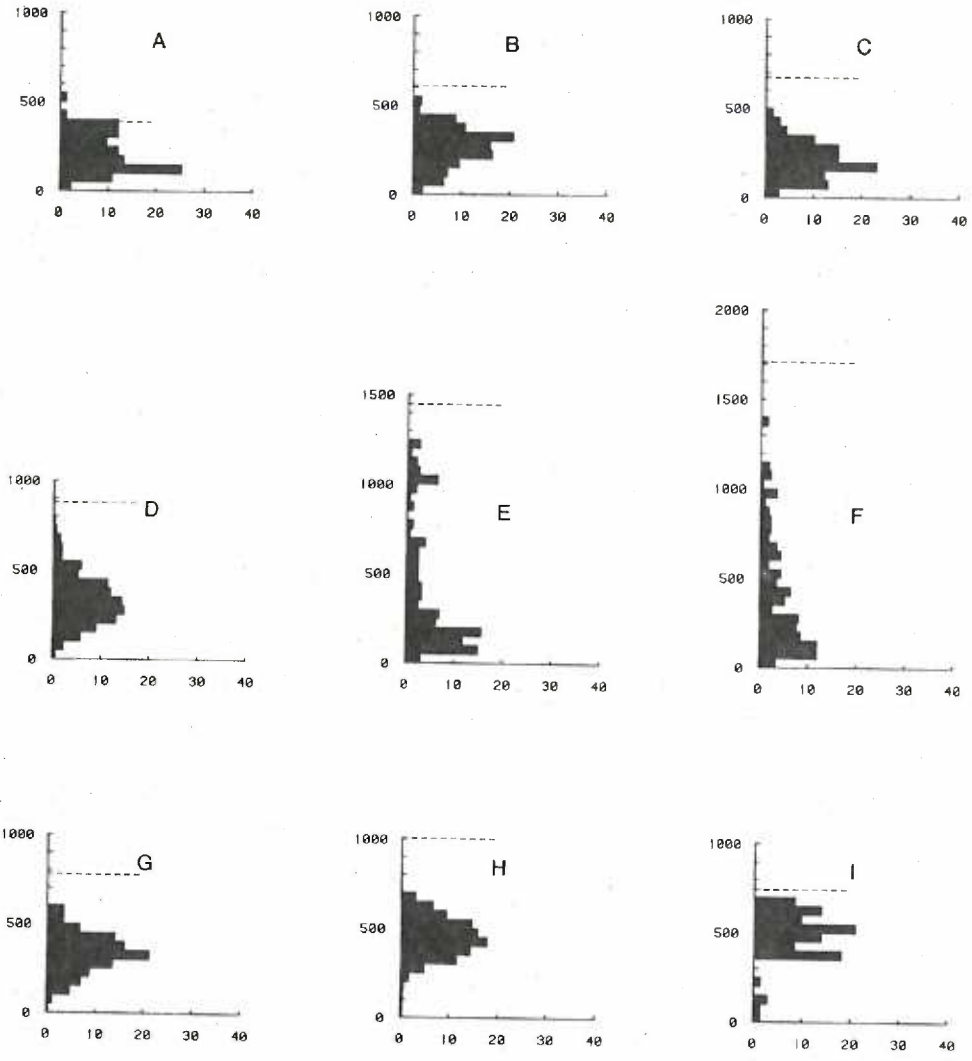

Figure 28. Frequency distribution histograms of the distances above the muscularis mucosae of ^{3}H-thymidine labeled gastric epithelial cells in the 3,4-TCB-fed animal 9921. Section A begins at the esophagogastric junction and section H ends at the pyloroduodenal junction. The ordinates are the distance in μm above the muscularis mucosae and the abcissas are the relative frequency in percent of the total. The distances of 150 to 300 labeled cells were measured from each section to compile each histogram. Each dotted line indicates the median height (20 to 40 measurements) over the region in which the labeled cells were measured. All sections except C had labeled cells as close as 0 to 50 μm above the muscularis mucosae. The distances appeared to follow normal distributions. Labeled cells beneath the muscularis mucosae in submucosal glands and cysts are not shown in these histograms.

9921

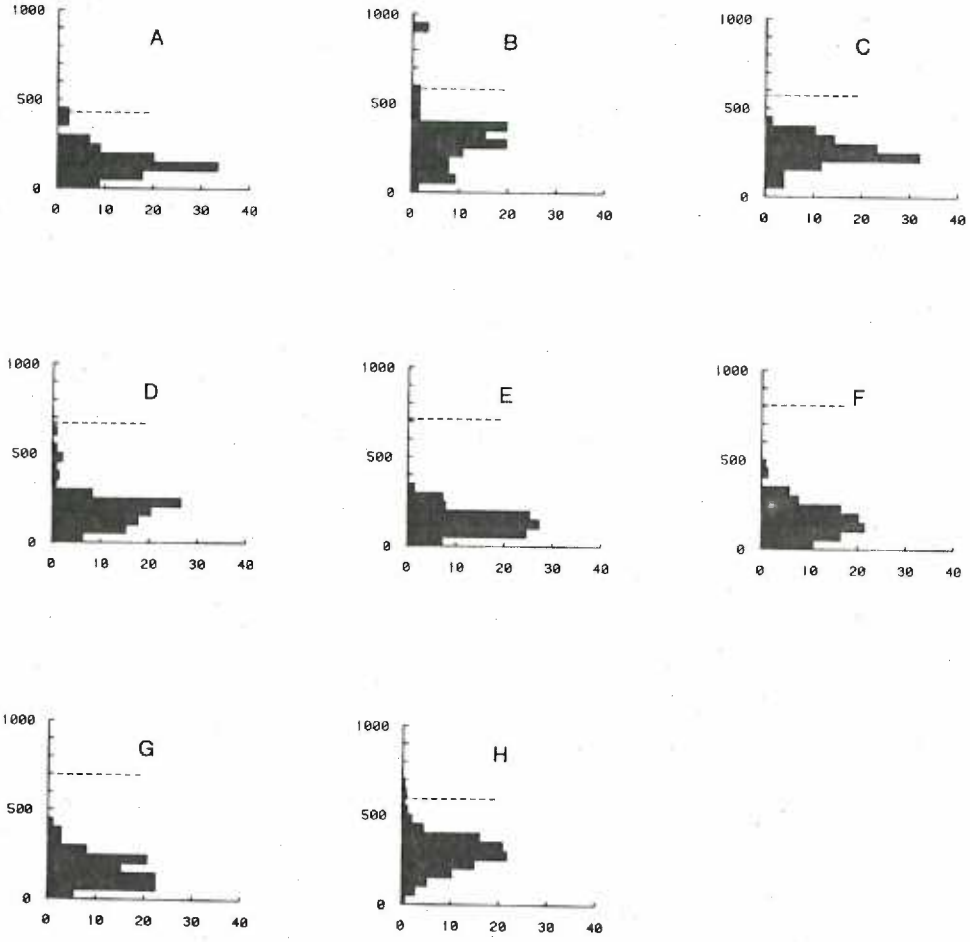

Figure 29. Median height above the muscularis mucosae of ^{3}H-thymidine labeled gastric epithelial cells. The ordinates represent the median height (150 to 300 measurements) in μm. The abcissas represent the relative position along the greater curvature. The top graph shows the data for the control animals and the bottom graph shows the data for the 3,4-TCB-fed animals. The two groups are not significantly different. In two of the controls and two of the toxic fed animals, the median value increases from the cardia to the pylorus.

○ 7761 control animal

△ 8911 control animal

□ 9273 control animal

● 7194 fed a 3 ppm 3,4-TCB diet for 53 days

■ 9246 fed a 1 ppm 3,4-TCB diet for 55 days

▲ 9921 fed a 1 ppm 3,4-TCB diet for 97 days

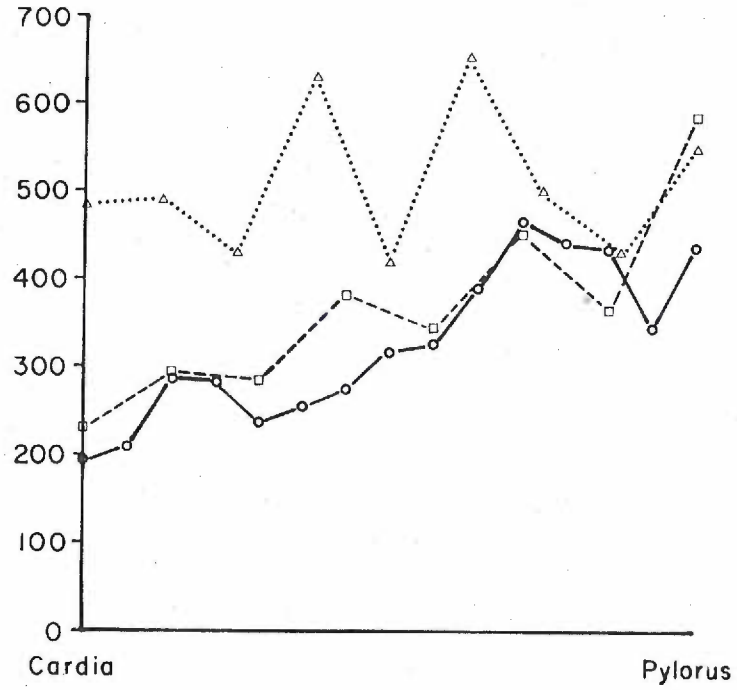
700
600
500
400
300
200
100
0
Cardia
Pylorus

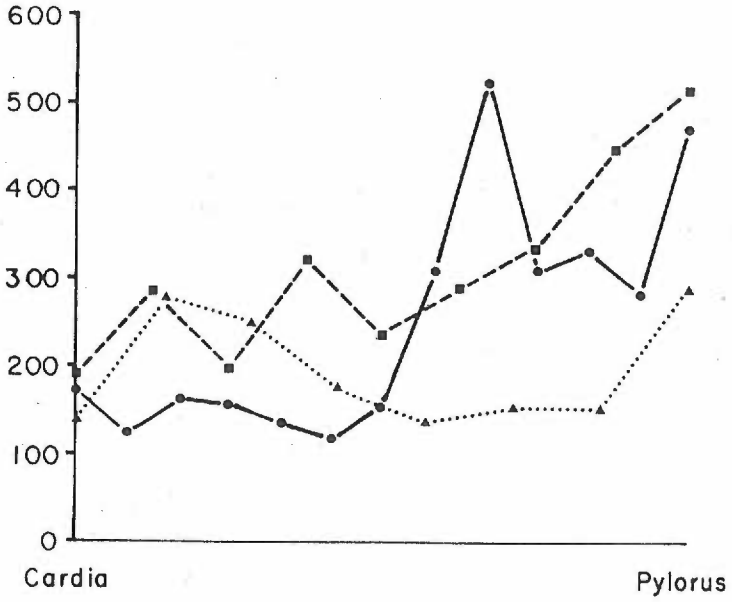
600
500
400
300
200
100
0
Cardia
Pylorus

Figure 30. Ratio of the median height of ^{3}H-thymidine labeled gastric epithelial cells to the median gastic mucosal height. The ordinate represents the ratio and the abcissa represents the relative position along the greater curvature. The top graph depicts the ratios obtained in the sections from the control animals while the bottom graph depicts the ratios obtained in the 3,4-TCB-fed animals. The ratios in the controls are somewhat constant between 0.5 and 0.6, whereas the ratios in the toxic fed animals were 0.15 to 0.3 in the body of the stomach, where the gastric lesion was most severe. The means of these ratios in the body regions were significantly different from the controls (t-test, $p < 0.01$). This indicates that while the mucosal height increased in the body of the stomach of the toxic fed animals, the zone of proliferation did not also increase to maintain the same relative position within the glands.

○ 7761 fed control diet

△ 8911 fed control diet

□ 9273 fed control diet

● 7194 fed 3,4-TCB

■ 9246 fed 3,4-TCB

▲ 9921 fed 3,4-TCB

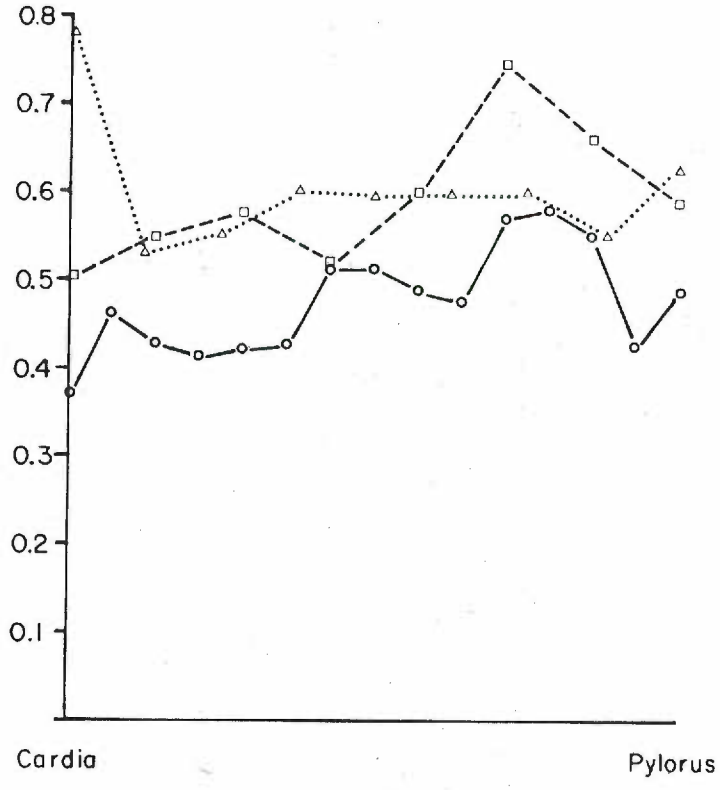
0.8
0.7
0.6
0.5
0.4
0.3
0.2
0.1
Cardia
Pylorus

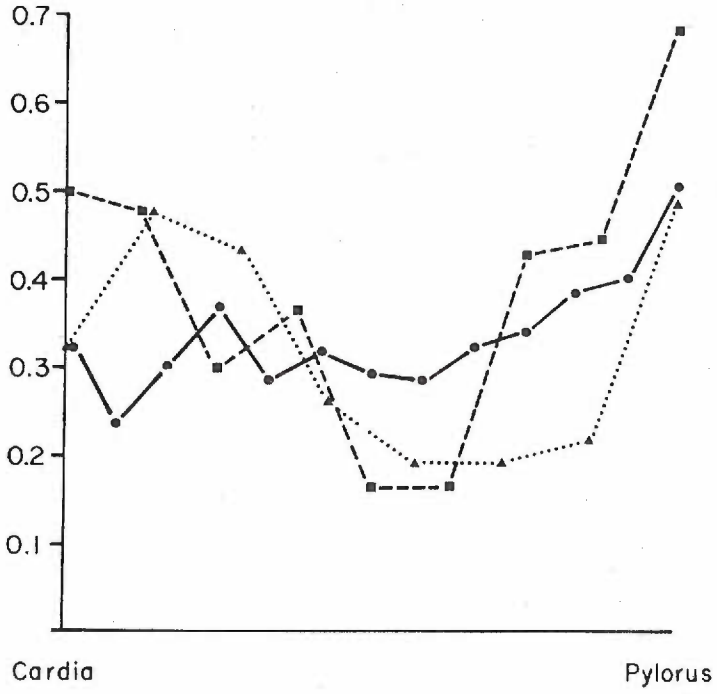
0.7
0.6
0.5
0.4
0.3
0.2
0.1
Cardia
Pylorus

Figure 31. Labeling density of ^{3}H-thymidine labeled gastric epithelial cells per 200 μm length of muscularis mucosae. The ordinate represents the number of labeled cells per 200 um length of muscularis mucosae and the abcissa represents the relative position of the sections along the greater curvature of the stomach. Each point is the mean of 10 determinations. The standard error of the mean typically was 10 to 20% of the value of the mean. The top graph depicts the results from the control animals and the bottom graph depicts the results of the 3,4-TCB-fed animals. The mean of the densities just distal to the cardia of the 3,4-TCB fed animals was significantly lower (t-Test, $p < 0.05$) than the mean for the corresponding region in the control animals. Notice that the labeling indices increased 3 to 10 fold progressing distally from the cardia to the pylorus in all the animals, and in 2 of 3 of the control animals and 2 of 3 of the toxic fed animals, the densities increased sharply in the body region.

○ 7761 fed control diet

△ 8911 fed control diet

□ 9273 fed control diet

● 7194 fed 3,4-TCB

■ 9246 fed 3,4-TCB

▲ 9921 fed 3,4-TCB

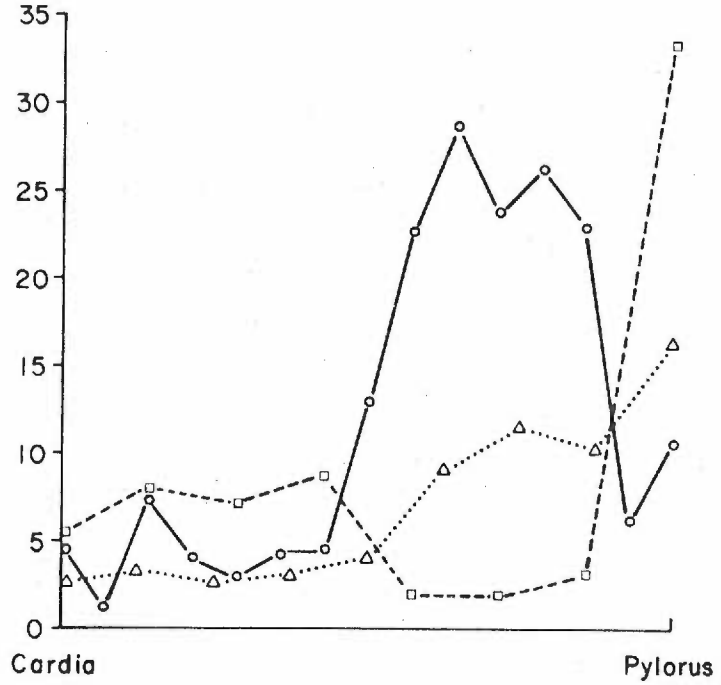
35
30
25
20
15
10
5
0
Cardia
Pylorus

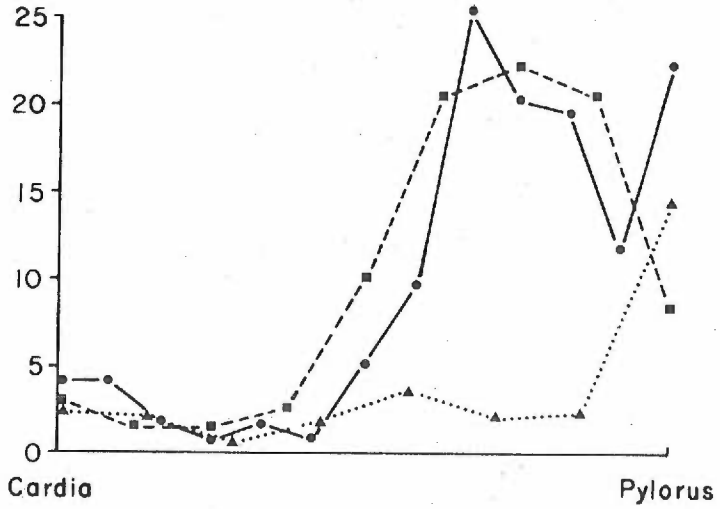
25
20
15
10
5
0
Cardia
Pylorus

Figure 32. Labeling density of ^{3}H-thymidine labeled gastric epithelial cells per square millimeter of gastric mucosa in cross section. The ordinates represent the number of labeled epithelial cells per square millimeter of mucosa and the abcissas represent the relative position of the sections along the greater curvature of the stomach. Each point is the mean of 10 determinations and the standard error of the mean was typically 10 to 20% of the value of the mean. The top graph depicts the results from the control animals and the bottom graph the results from the 3,4-TCB-fed animals. The labeling densities show the same relative changes as seen in figure 31, where the labeling density per 200 um of muscularis mucosae is shown.

○ 7761 fed control diet

△ 8911 fed control diet

□ 9273 fed control diet

● 7194 fed 3,4-TCB

■ 9246 fed 3,4-TCB

▲ 9921 fed 3,4-TCB

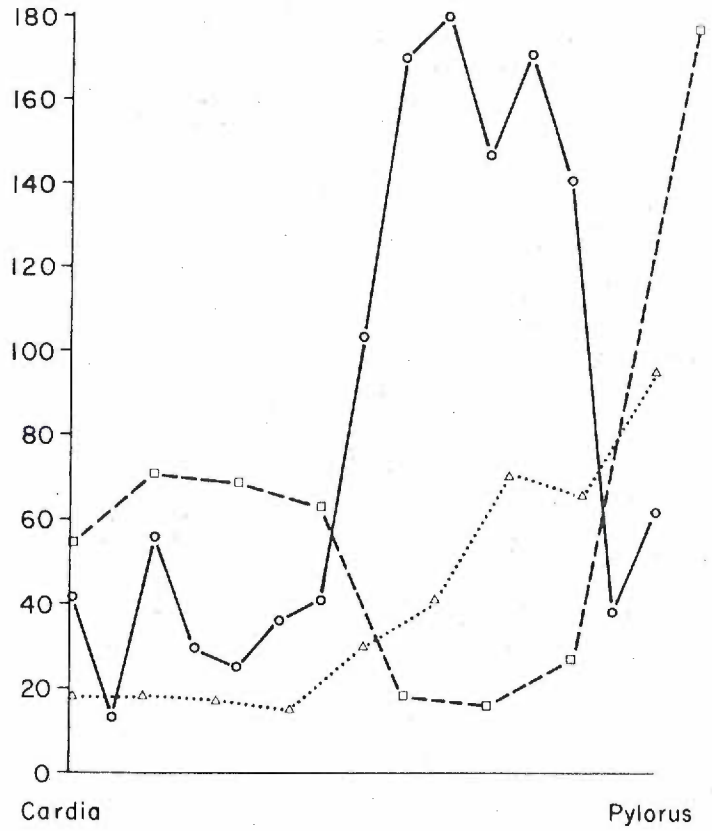
180
160
140
120
100
80
60
40
20
0
Cardia
Pylorus

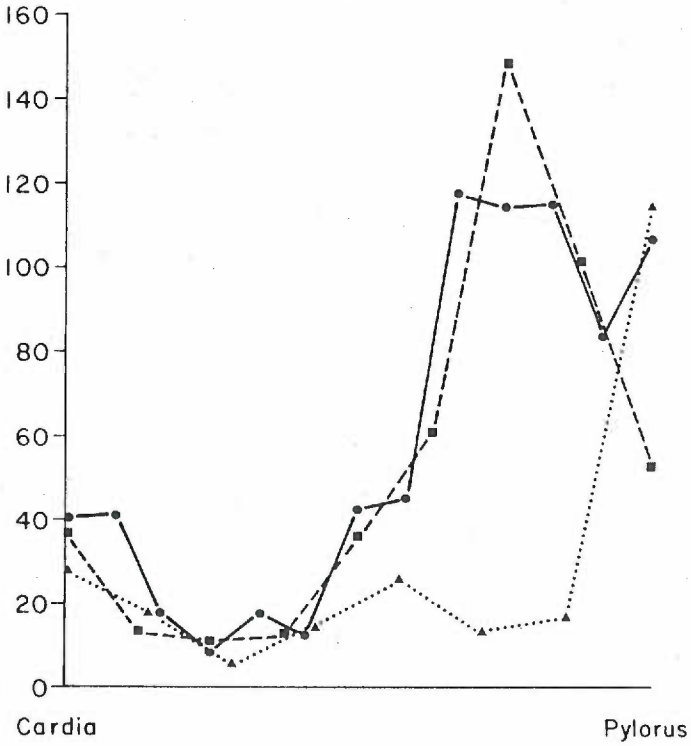
160
140
120
100
80
60
40
20
0
Cardia
Pylorus

Figure 33. Labelling indices in the gastric mucosa of control animals and 3,4-TCB-fed animals. The ordinates represent the percent of the gastric epithelial cells within the proliferative zone which were labeled with ^{3}H-thymidine and the abcissas are the relative positions of the sections along the greater curvature. The proliferative zone was estimated as the region between the uppermost and the lowermost labeled cells within a given gastric gland or segment of a gland. Zymogenic and parietal cells, which were never labeled, were not considered to be part of the proliferative cell population and were therefore not included in the determination of the labeling indices. Each point represents the mean of 15 determinations. The standard error of the mean was typically 10 to 25% of the mean. The labeling indices showed similar patterns of change from the cardia to the pylorus of each animal as do the corresponding labeling density determinations, shown previously in figure 31 and 32. One exception is the labeling index in the pylorus of 9921, which is relatively less than the labeling density of the same section. The labeling indices of the 3,4-TCB-fed animals are not greater than the controls and the region just distal to the cardia in the 3,4-TCB fed animals is significantly less (t-Test, $p < 0.01$) than the corresponding region in the controls.

○ 7761 fed control diet

△ 8911 fed control diet

□ 9273 fed control diet

● 7194 fed 3,4-TCB

■ 9246 fed 3,4-TCB

▲ 9921 fed 3,4-TCB

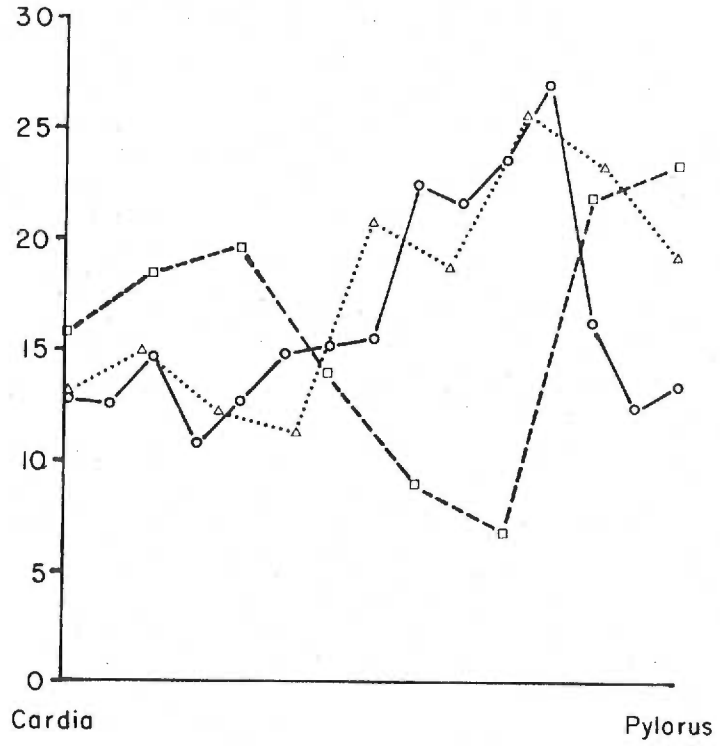
30
25
20
15
10
5
0
Cardia
Pylorus

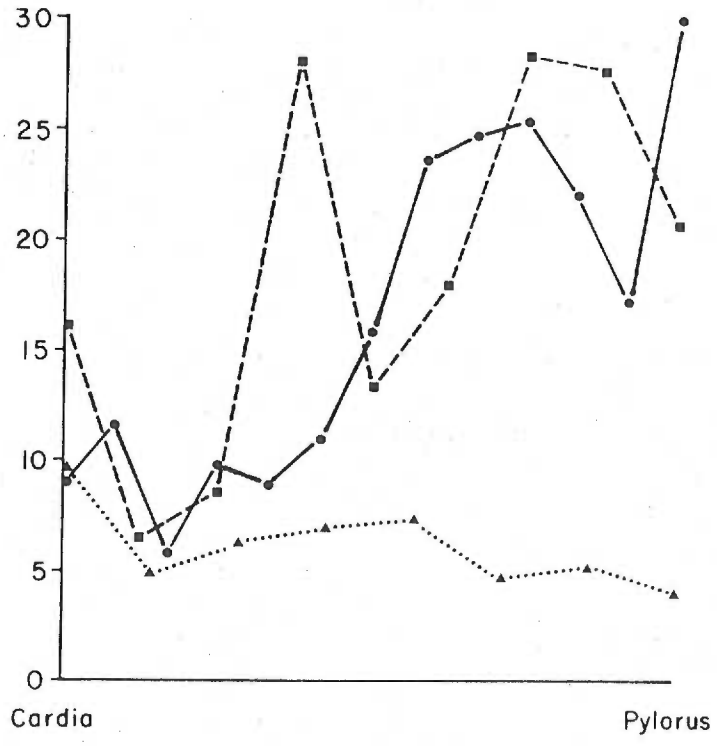
30
25
20
15
10
5
0
Cardia
Pylorus

Figure 34. Grain-count-decay experiment. The ordinate is the natural logarithm of the mean number of grains, expressed as a percent of the original value, obtained from the first biopsy specimen, taken 1 hour after injection with ^{3}H-thymidine. The abcissa represents the number of days after the initial labeling. Full-thickness biopsy specimens were taken at laparotomy from the anterior wall of the stomach. Autoradiographs of each specimen were uniformly prepared and silver grains overlying labeled gastric epithelial cells remaining in the proliferative zone were counted. The open circles are the values from the control animal, 8553 and the dark triangles are the values from animal 8686, which was fed a 1 ppm 3,4-TCB diet for for 30 days before the first biopsy. All biopsy specimens from the control animal showed normal gastric mucosa; those from the 3,4-TCB-fed animal had hyperplastic and cystic glands lacking zymogenic and parietal cells.

The dashed line is the least squares best fit linear regression for the normal animal and the dotted line is the regression line for the 3,4-TCB-fed animal. The cell cycle time is approximated by finding the time it takes for the mean grain count to halve, and hence become 50% of the original mean grain count determined in the first biopsy specimen from day 0. The natural logarithm of 50 is 3.91, therefore the estimated cell cycle times are 1.6 for the control animal, and 3.0 for the toxic fed animal.

The slopes of the lines are not significantly different (analysis of covariance, $0.2 < p < 0.4$), an indication that the cell cycle time in 3,4-TCB-fed animals may not be shorter than in control animals.

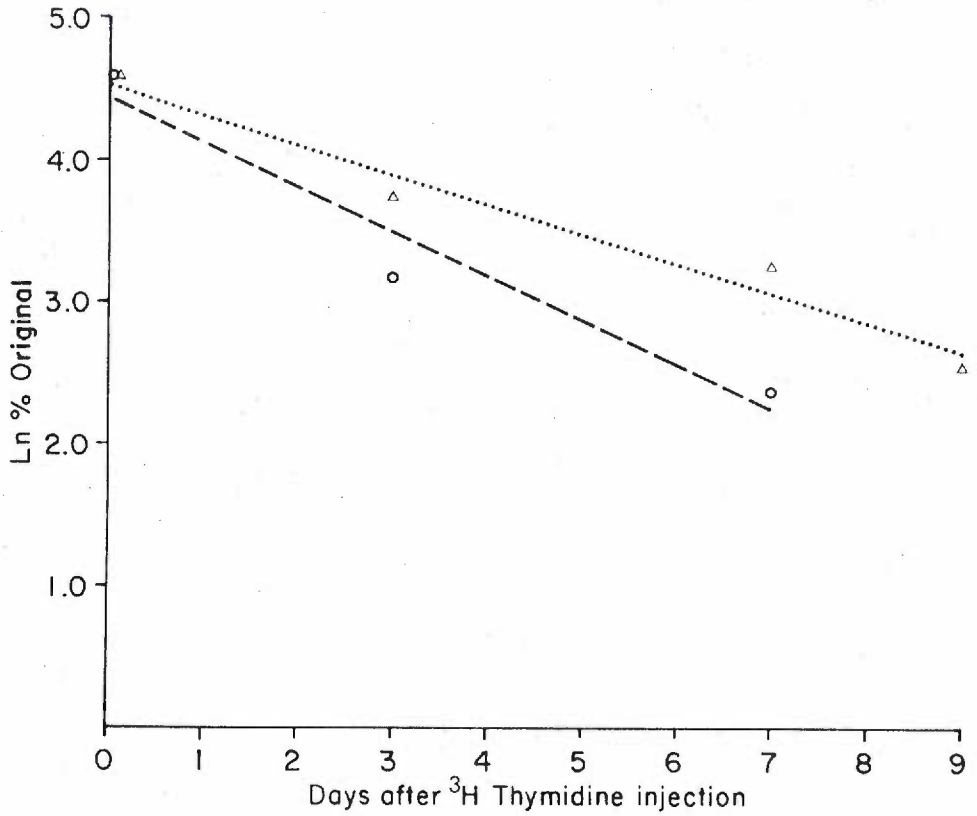
5.0
4.0
3.0
2.0
1.0
Ln % Original
0
1
2
3
4
5
6
7
8
9
Days after ^{3}H Thymidine injection

Figure 35. Scanning electron micrographs of the surface of the gastric mucosa from the cardias of a control and a 3,4-TCB-fed animal.

Figure 35a (top). The surface of this control gastric mucosa forms smooth and regular hills and valleys. The valleys are the openings of the foveolae to the surface. (X 270)

Figure 35b (bottom). The surface of the epithelium from this 3,4-TCB-fed animal (9921) is very irregular owing to the protrusion of surface epithelial cells. Many of these cells appear indented, with surrounding halos. These cells have probably just discharged the secretory granules stored in their apices. (X 360)

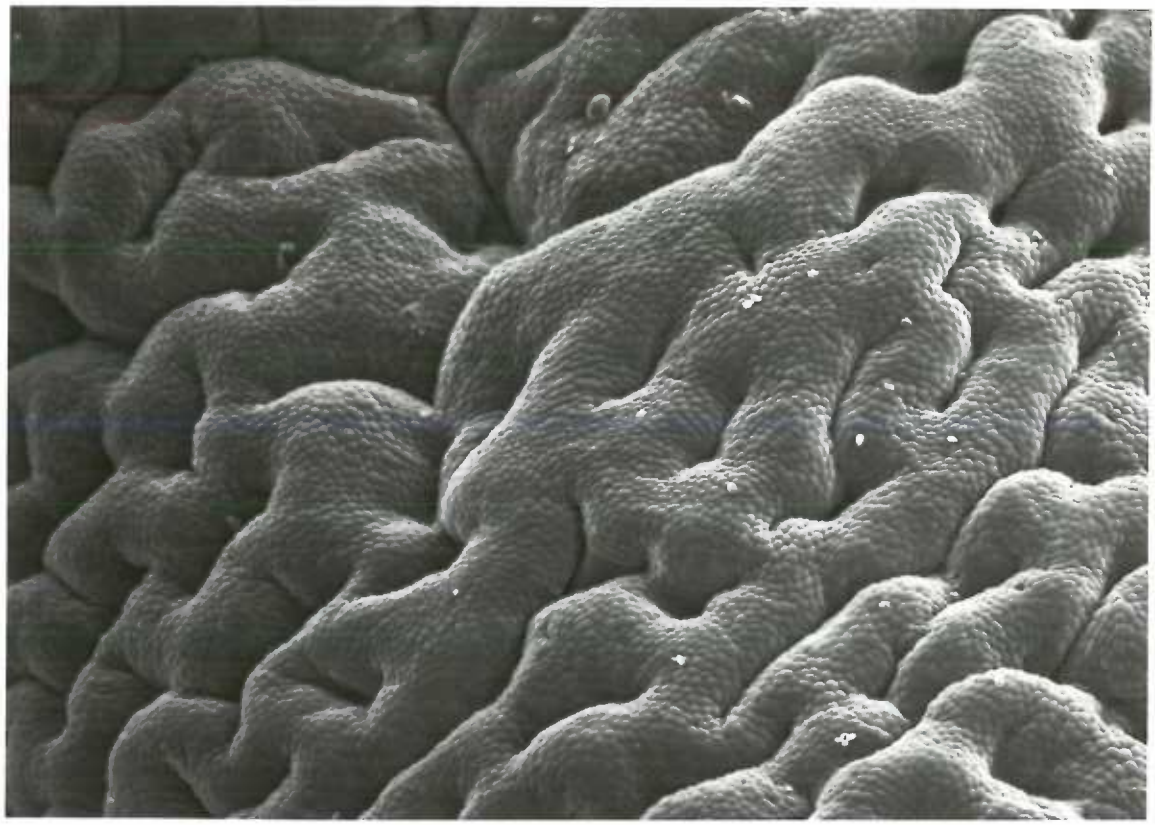

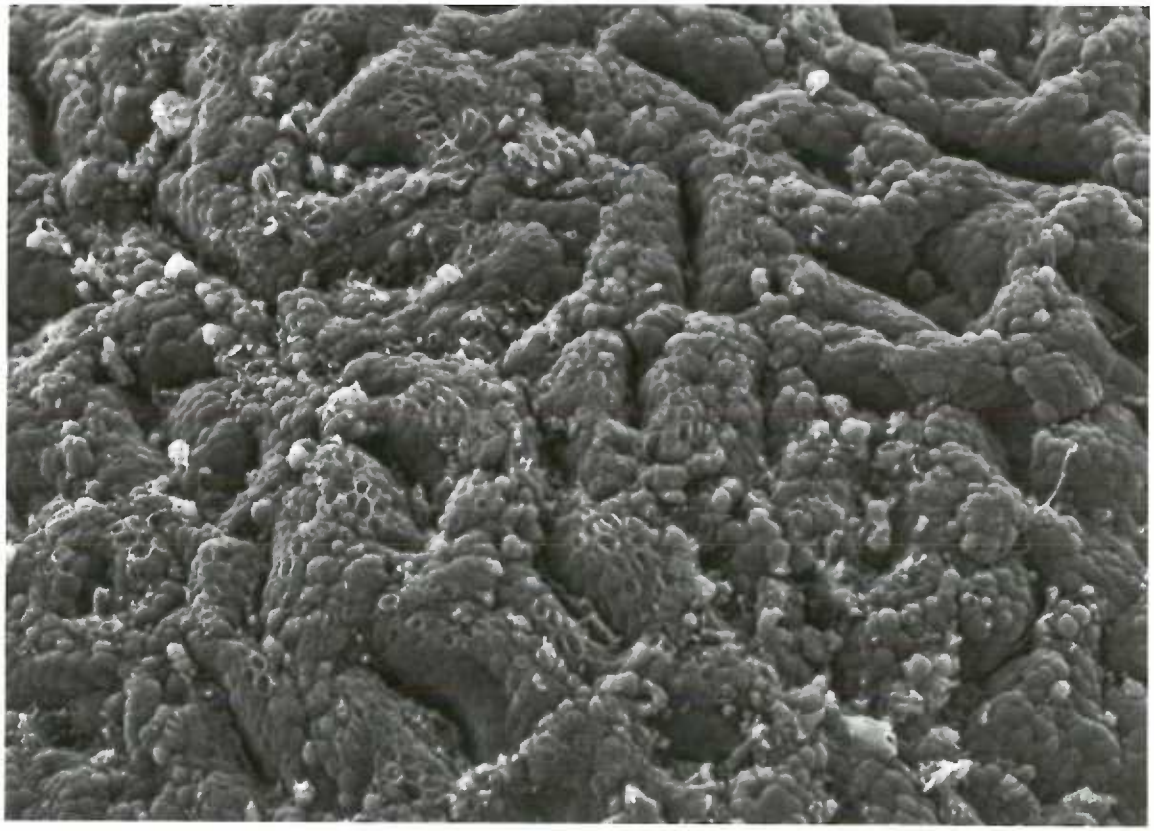

Figure 36. Scanning electron micrographs of the surface of the gastric mucosa from the body regions of control and 3,4-TCB-fed animals.

Figure 36a (top). The surface of this control mucosa is smooth and regular. Notice that the openings to the foveolae appear as narrow slits. (X 215)

Figure 36b (middle). The surface of the gastric mucosa from the body region of this 3,4-TCB-fed animal (9921) is quite irregular. The epithelium surrounding each foveola is bulging outward and gives the appearance of doughnut rings. The cells which appear indented have probably discharged the secretory granules stored in their apices. (X 215)

Figure 36c (bottom). In this 3,4-TCB-fed animal (8686), the epithelium is even more disorganized and many individual cells appear to be bulging outward. (X 215)

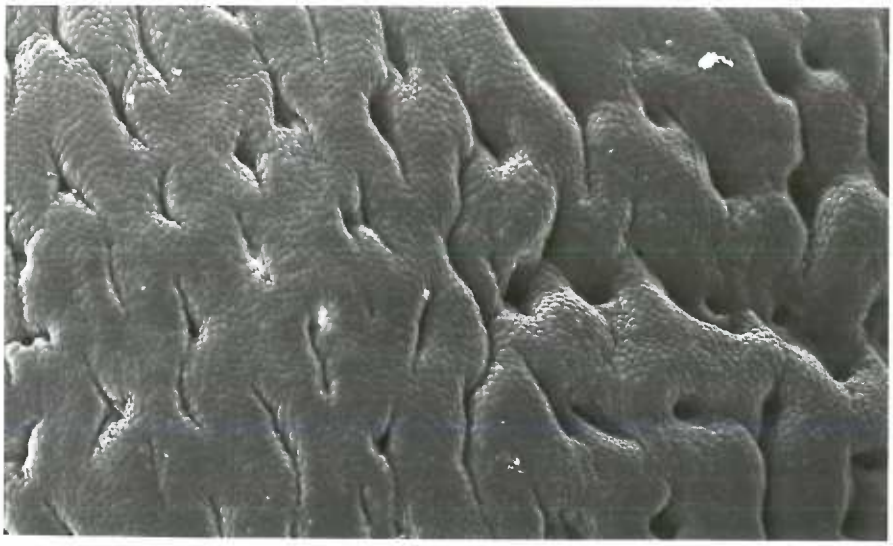

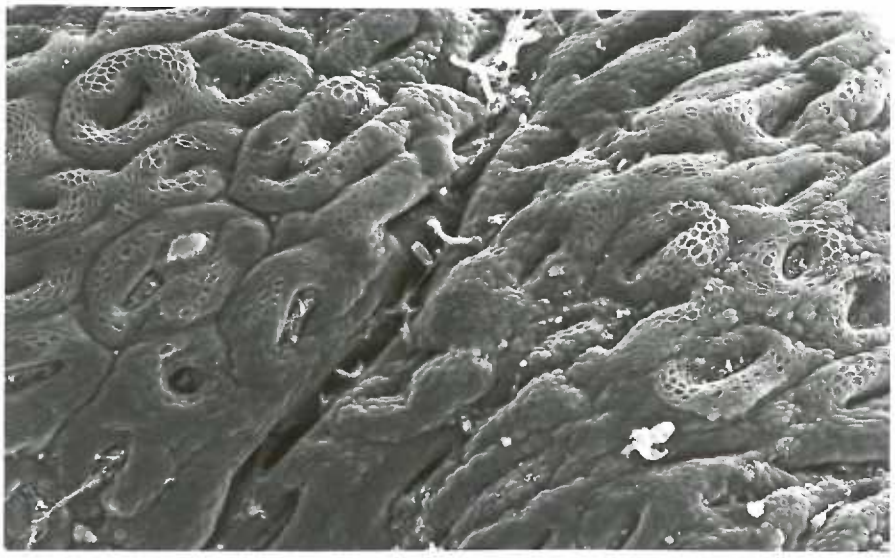

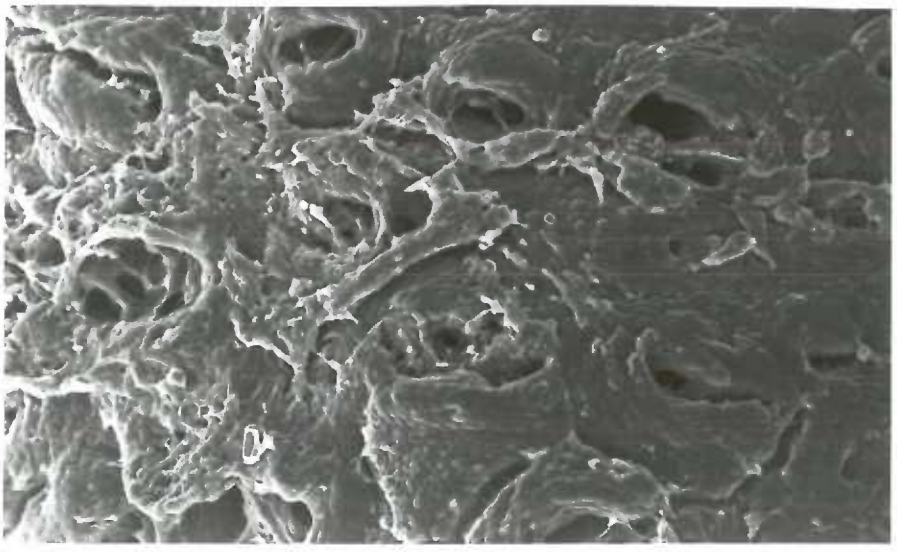

Figure 37. Scanning electron micrographs of the surface of the gastric mucosa from the body regions of a control and a 3,4-TCB-fed animal.

Figure 37a (top). This control mucosa has smooth and regular contours. The individual cells give the surface a regular cobblestone appearance. The narrow slit-like indentations are the entrances to the foveolae. (X 665)

Figure 37b (bottom). In the mucosa from this 3,4-TCB-fed animal (7194), the entrances to the foveolae are markedly dilated. The small droplets on many of the epithelial cells are probably mucus. (X 665)

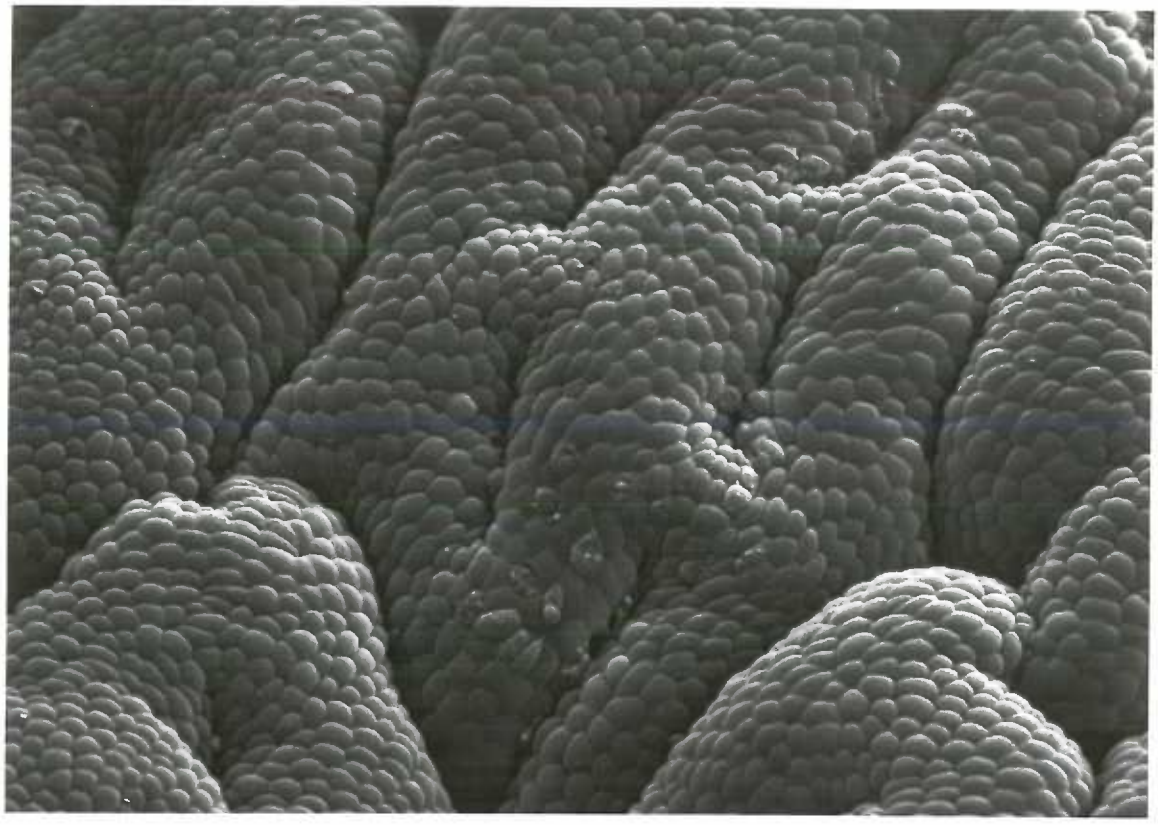

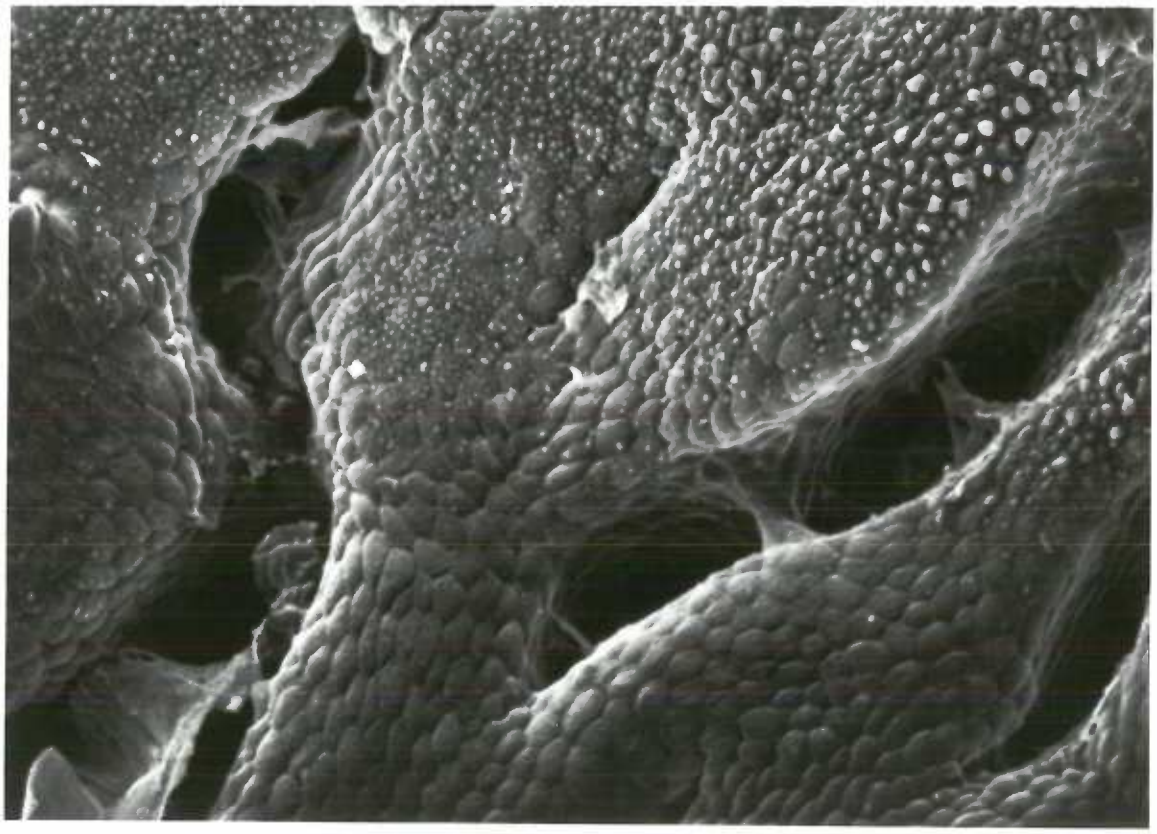

Figure 38. Scanning electron micrographs of the surface of antral gastric mucosa in a control and a 3,4-TCB-fed animal.

Figure 38a (top). The surface of normal antral mucosa is smooth and regular. (X 1000)

Figure 38b (bottom). Many of the cells on the surface of the antral mucosa in this 3,4-TCB-fed animal (7194) protruded above the surface. (X 1000)

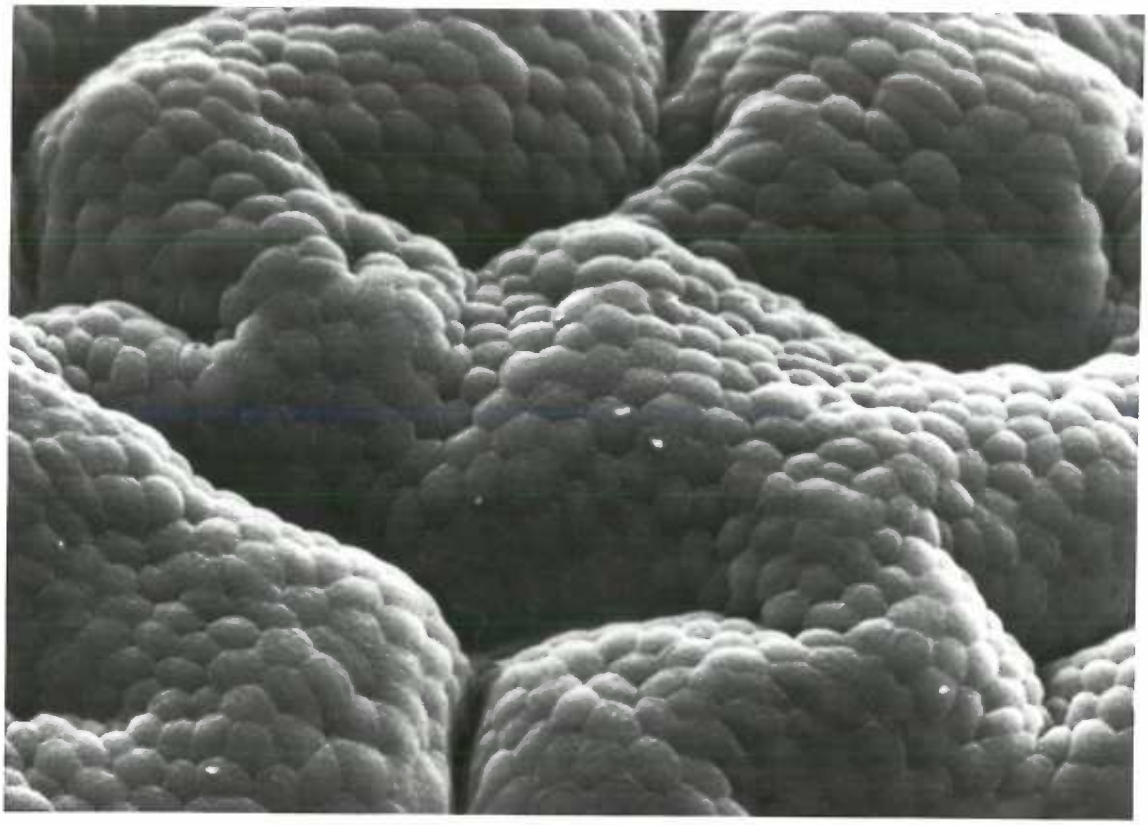

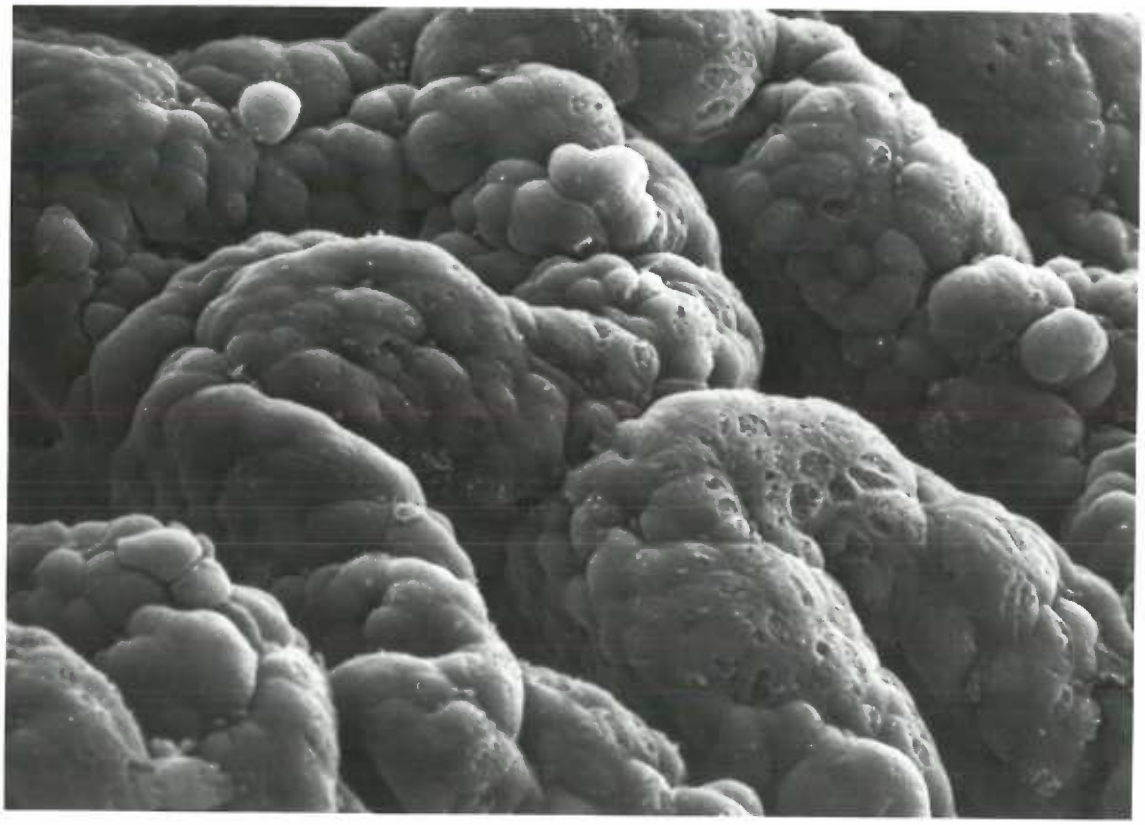

Figure 39. Detail of the surface epithelium from the body regions of control stomachs.

Figure 39a (top). This is a micrograph of the surface epithelium surrounding a foveola. It has a regular cobblestone appearance and indents into a narrow slit-like opening of a foveola. (X 1000)

Figure 39b (middle). This is a higher magnification micrograph (X 5,400) of surface epithelial cells. Note that none of these cells protrude above any of their neighbors.

Figure 39c (bottom). A higher magnification (X 11,000) micrograph of surface epithelial cells. These cells appear to be covered with mucus except in the narrow area where adjacent cells meet. Note the small blebs which can be seen in this small area between cells. They are probably the same structures as the microvilli seen in transmission electron micrographs.

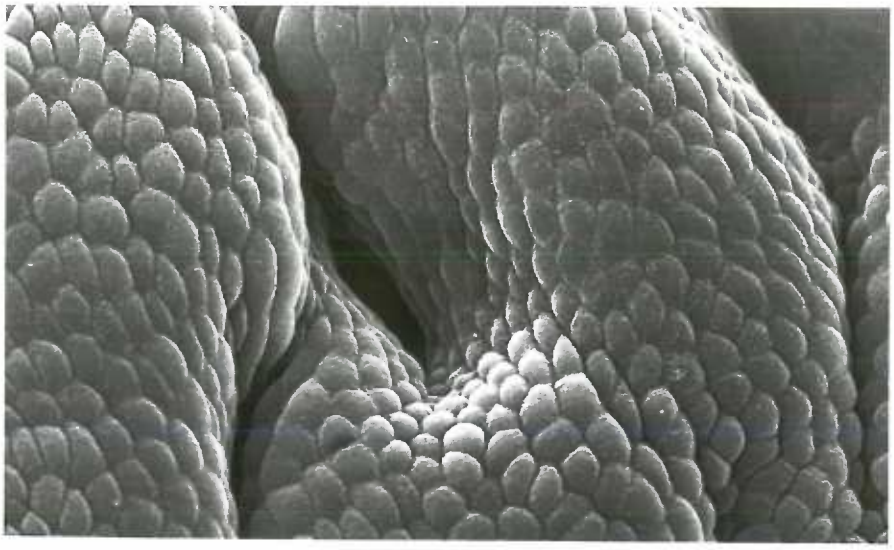

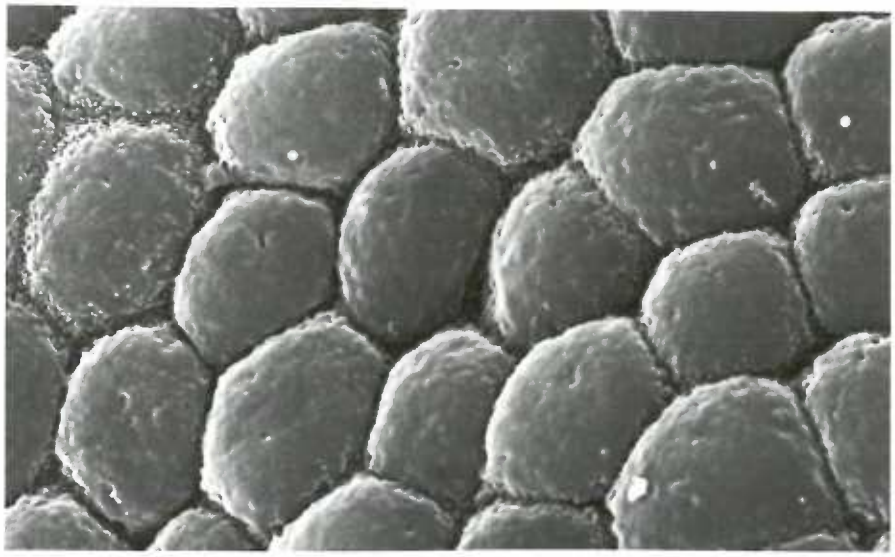

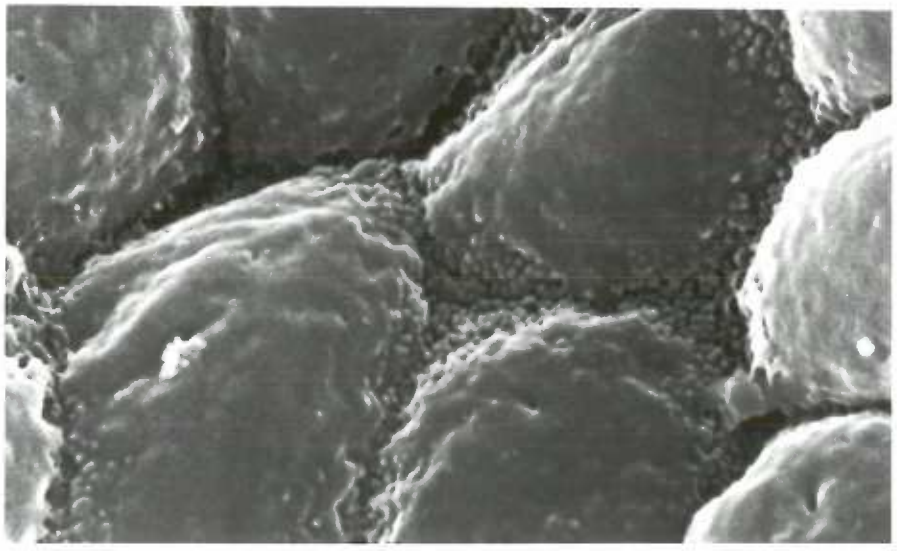

Figure 40. Detail of the surface epithelium from the body regions of stomachs from 3,4-TCB-fed animals.

Figure 40a (top). The irregular contour of the surface epithelium (from animal 9246) is readily apparent in this micrograph. Note that groups of epithelial cells seem to be elevated and folded over other surface epithelial cells. (X 1,000)

Figure 40b (middle). Surface epithelial cells seem to be protruding outward in a cluster. (animal 9921, X 2,000)

Figure 40c (bottom). This is a high-magnification view (X 11,000) of the area between several surface epithelial cells. Small blebs, which are probably microvilli, are seen here, as in the control animals. The remainder of the surface of these cells appears to be covered with mucus. The larger bumps are probably secretory granules about to rupture through the surface. (From animal 9246)

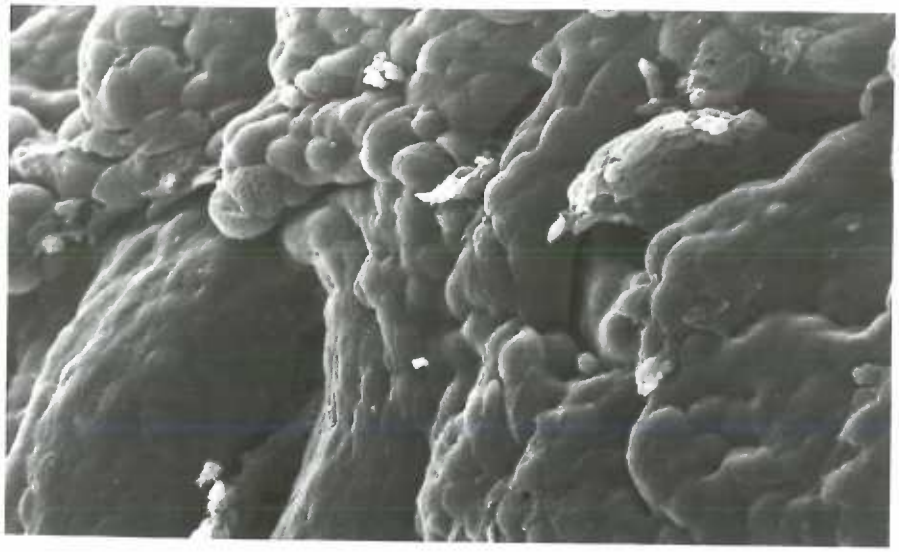

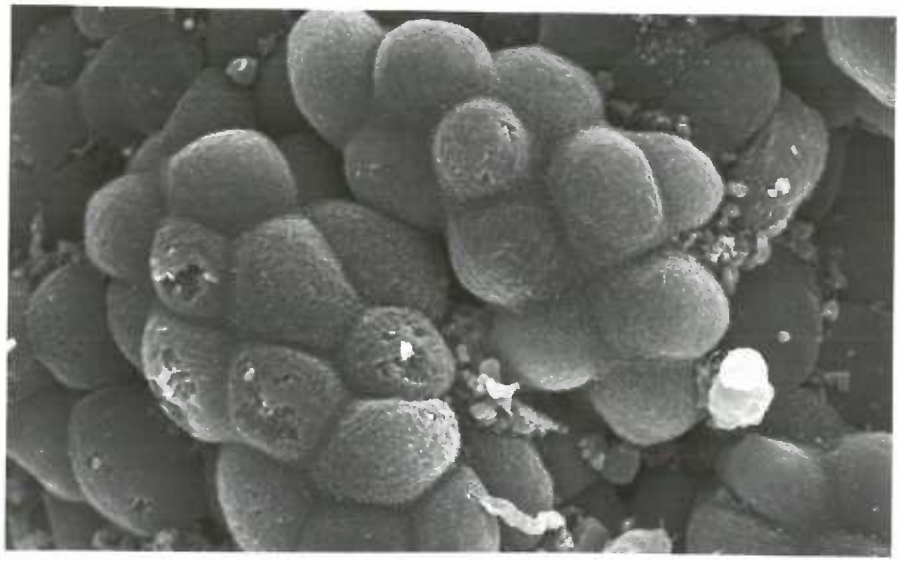

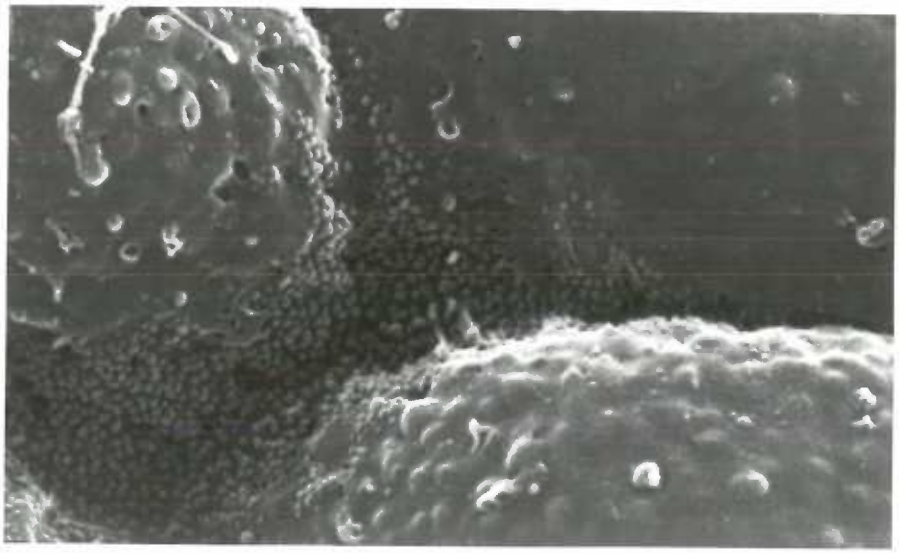

Figure 41. Scanning electron micrographs of cystic glands in a 3,4-TCB-fed animal.

Figure 41a (top). This is a low-magnification view of both the luminal surface of the gastric epithelium, and a surface cut perpendicular to it by a razor. On the cut surface, a number of large cystic glands are prominent, some of which appear to contain masses of mucous material. (animal 7194, X 90)

Figure 41b (bottom). A higher magnification view of a cystic gland like those above. A mass of mucous material is seen in the lumen. Mucus produced by the epithelial cells lining the cystic glands may accumulate and plug the lumen, and thereby cause the glands to swell. (X 2,800)

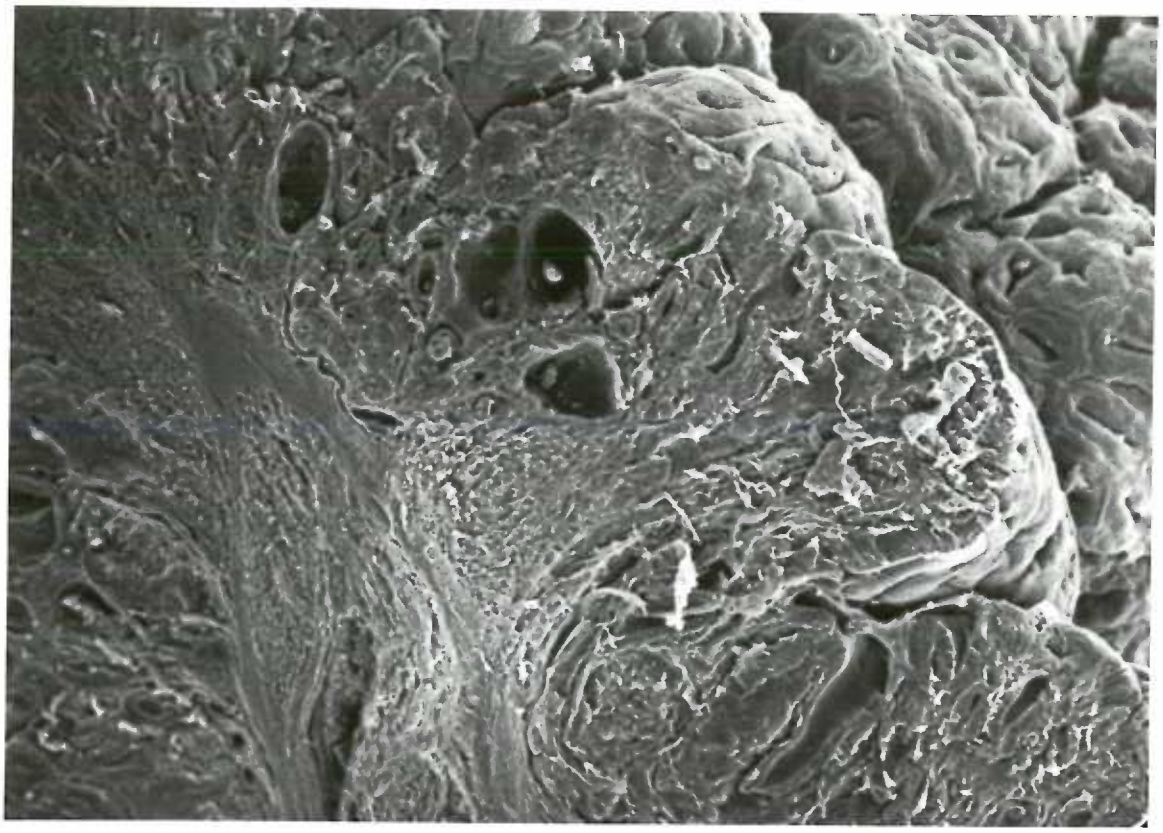

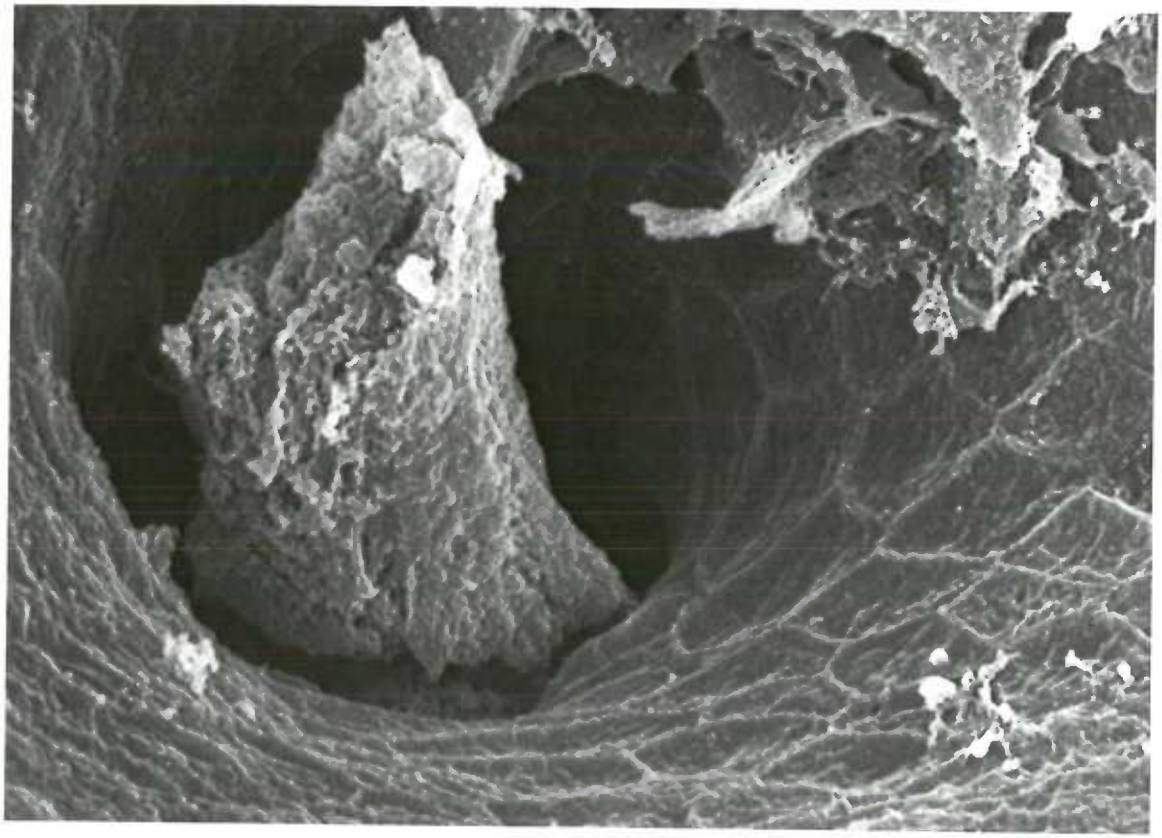

Figure 42. Scanning electron micrographs of cystic gastric glands in 3,4-TCB-fed animals.

Figure 42a (top). Freeze-fractured surface of cystic glands. The glands appear to be filled with mucous material. Before critical-point drying, this mucus might have completely filled the lumens of these glands. (animal 9246, X 550)

Figure 42b (bottom). The luminal surface of epithelial cells lining a cystic duct can be seen in this micrograph from animal 7194. Note that the cells are covered with small blebs, which may be microvilli. (X 5,500)

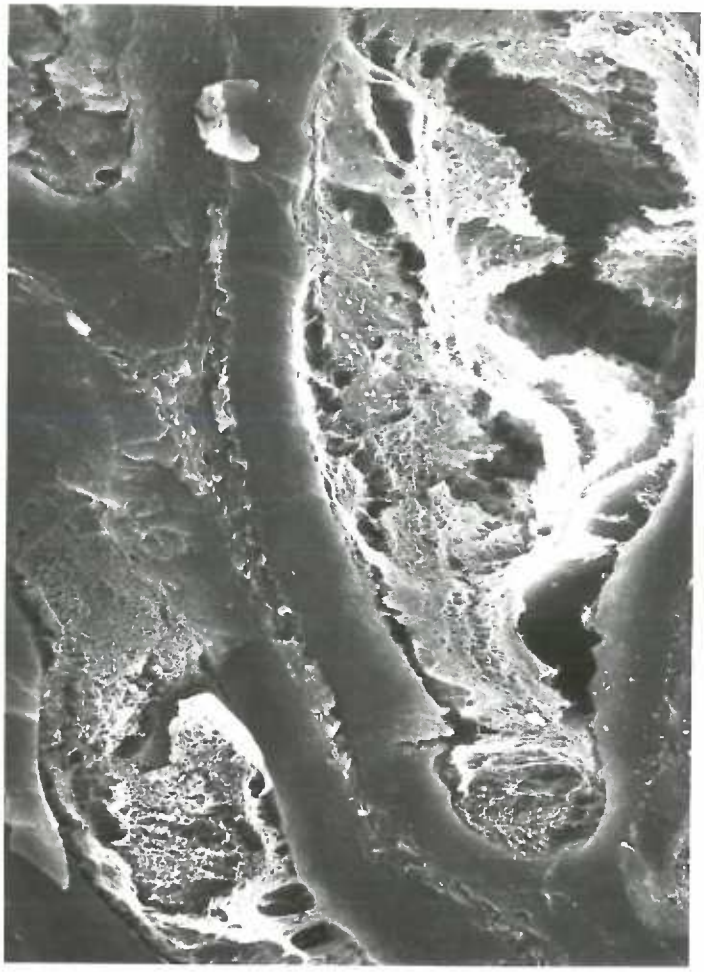

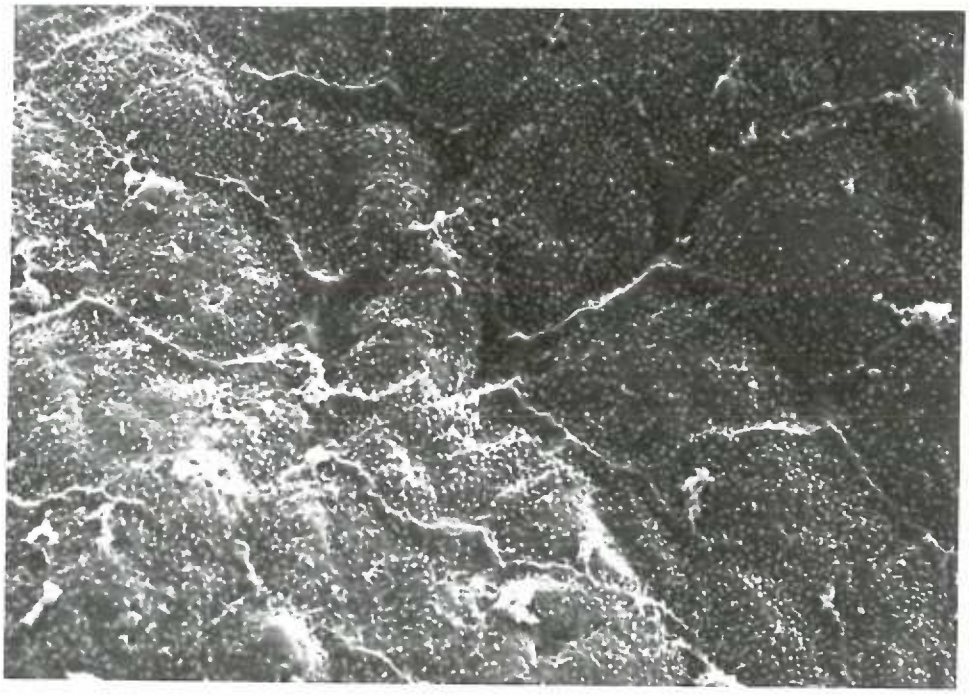

Figure 43. Low-magnification electron micrographs of control gastric mucosa. These micrographs from the body regions of a control stomach show the basic structure of the gastric mucosa and the locations of the various specialized cell types.

Figure 43a (top left). Mucus-secreting surface epithelial cells (SEC) are seen. These cells line the lumen of the stomach and the gastric foveolae, which extend beneath the surface. The lamina propria (LP) is the loose connective tissue which surrounds the epithelial cells of the glands and provides structural support, as well as nourishment to the glands. It contains capillaries, lymphatics, lymphocytes, eosinophils, macrophages, fibrocytes and other cell types. (X 525)

Figure 43b (top right). In this micrograph a portion of a foveola is seen. It is lined with immature surface epithelial cells. Beneath the foveola begins the neck region, lined with mucous neck cells (MNC) and parietal cells (P). (X 750)

Figure 43c (bottom left). A transistion from mucous neck cells to zymogenic (Z) cells is seen deeper in the gland in this micrograph. Parietal cells are numerous in this region. (X 780)

Figure 43d (bottom right). This micrograph shows the base of a gastric gland. Here zymogenic cells predominate, but enteroendocrine cells (arrows) are also numerous. The muscularis mucosae (MM), composed of smooth muscle cells, lies beneath the bases of the gastric glands. (X 650)

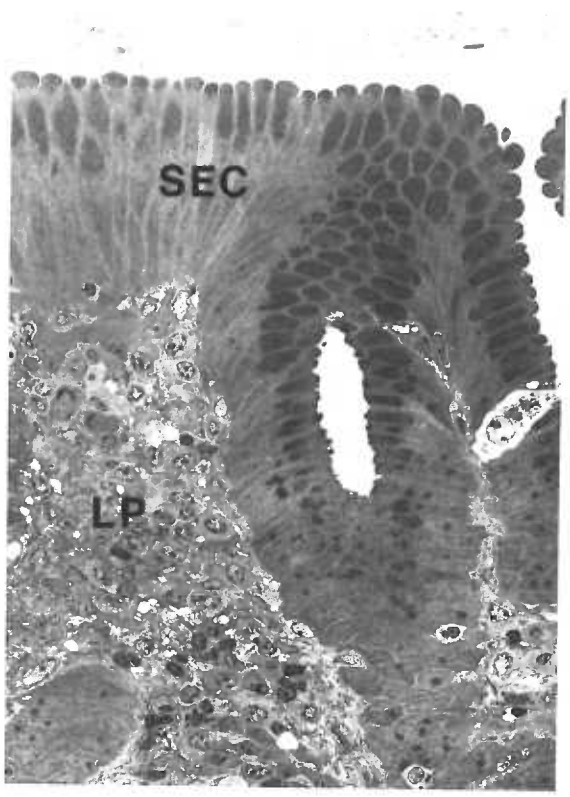
SEC
LP

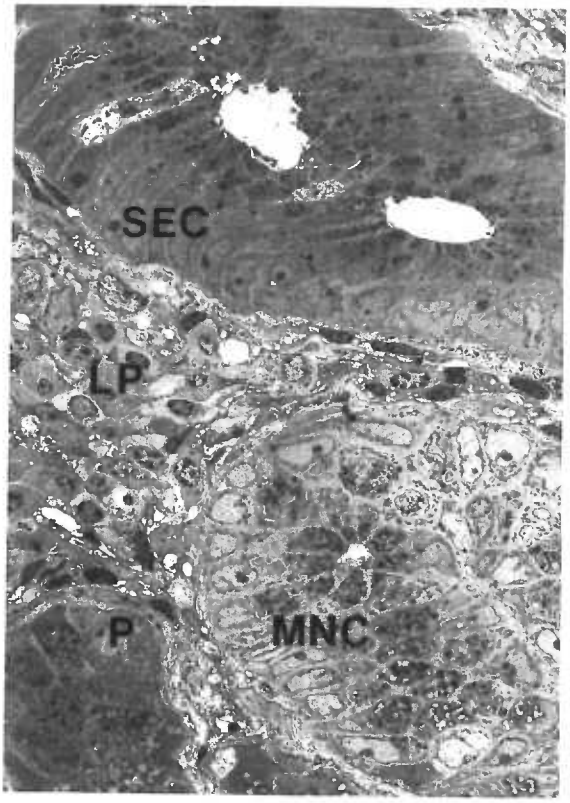
SEC
LP
P
MNC

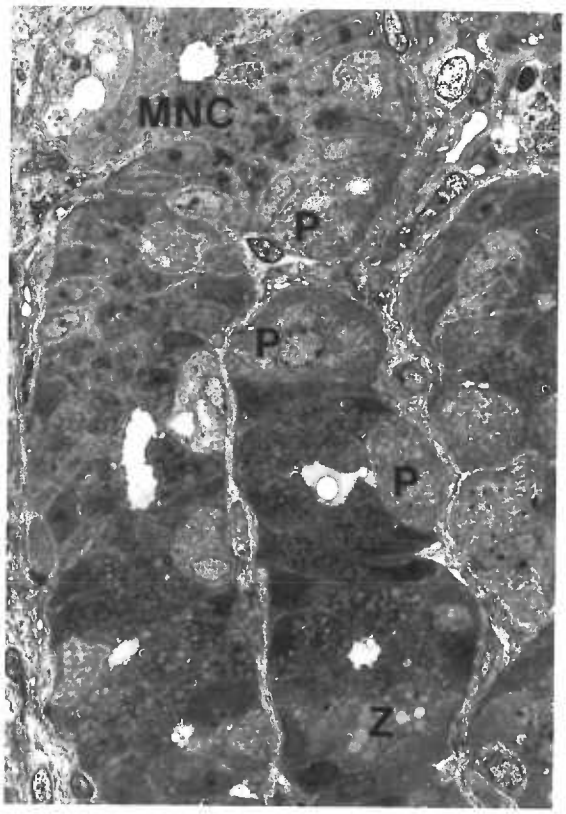
MNC
P
P
P
Z

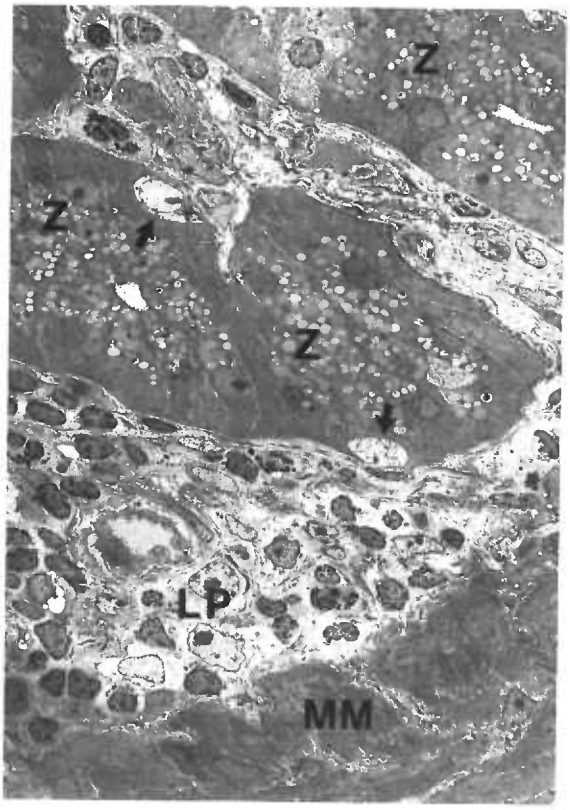
Z
Z
Z
LP
MM

Figure 44. Electron micrographs of surface epithelial cells from control animals.

Figure 44a (top left). Apical region of mature surface epithelial cells showing masses of polygonal electrondense secretory granules. A few microvilli can be seen at the luminal surface. (X 65,000)

Figure 44b (top right). Middle region of mature surface epithelial cells. The dense and somewhat indistinct cytoplasm is filled with endoplasmic reticulum, mitochondria, free ribosomes and small secretory vesicles which appear to be migrating upward to fuse with the larger granules in the apices of the cells. (X 5,700)

Figure 44c (bottom left). Immature surface epithelial cells from near the base of a gastric foveola. The cytoplasm is less dense and its fine-structure is more distinct than in mature cells. Mitochondria are readily visible and Golgi apparati can be seen above the nuclei. As in mature cells, small secretory granules can be seen, but in these immature cells they are more numerous. These granules also appear to be migrating toward the apices to fuse together and form larger granules. (X 8,000)

Figure 44d (bottom right). A higher magnification view of the perinuclear region of the same cells seen in the adjacent micrograph at the bottom left. A horsehoeshaped Golgi apparatus, and numerous mitochondria and secretory granules are seen. (X 18,000)

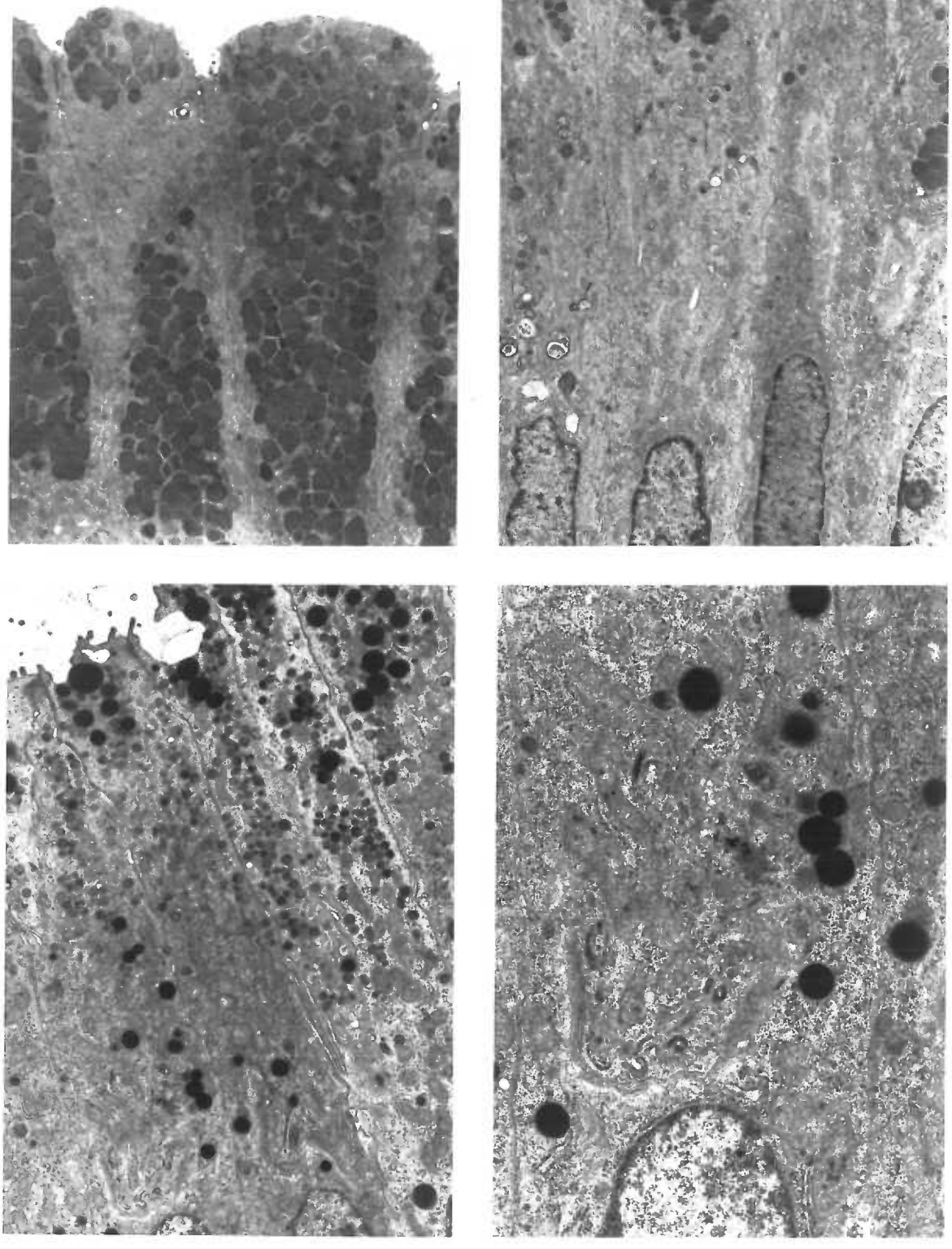

Figure 45. Electron micrographs of mucous neck cells from the neck regions of gastric glands from a control animal.

Figure 45a (top). Apical region of a mucous neck cell. Note the smaller vesicles which appear to be fusing with other vesicles to form larger secretory granules. The lumen of the gland is seen at the upper right corner of the micrograph. The apical regions of these cells contain relatively fewer secretory granules than mature surface epithelial cells. (X 27,000)

Figure 45b (bottom). Base of a mucous neck cell. Interdigitations of the plasmalemma of one cell with that of its neighbor are seen in all gastric epithelial cells; they are especially well developed in mucous neck cells, such as this one. (X 27,000)

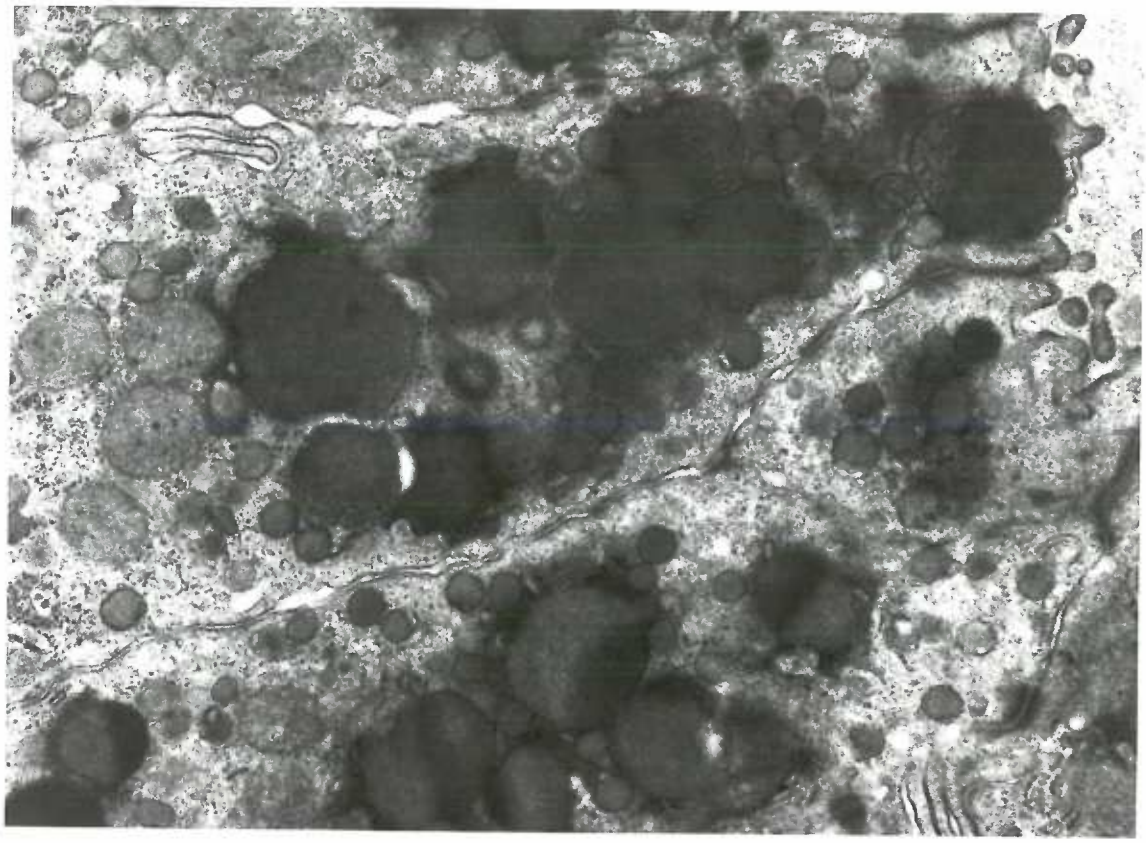

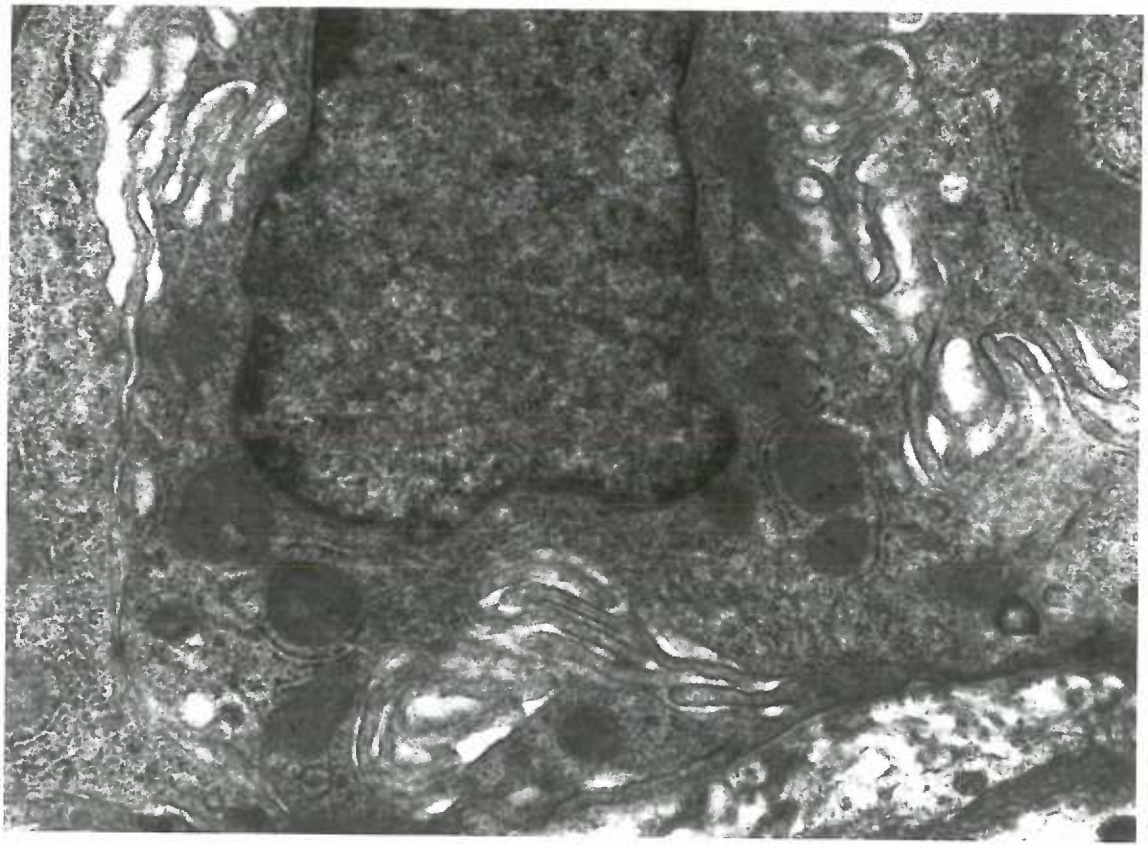

Figure 46. Mucous neck cells apparently undergoing differentiation into parietal cells in control animals.

Figure 46a (top). Mucous neck cells containing relatively few dark, electron-dense secretory granules can be seen (the darker, electron-dense cells). Many of these cells also contain numerous mitochondria and electron-lucent vesicles, as do the neighboring parietal cells. The parietal cells are easily distinguished as the lighter, more electron-lucent cells which are packed with mitochondria, tubulovesicles and canaliculi. The area within the black lines is seen at higher magnification below. (X 5,300)

Figure 46b (bottom). Higher magnification electron micrograph of the same area seen within the black lines above. The lighter, less electron-dense cytoplasm of a parietal cell is seen to the left of the darker, more electron-dense cytoplasm of a mucous neck cell apparently undergoing differentiation to a parietal cell. The principal evidence for differentiation is the presence of electron-lucent tubulovesicles in the apex of the cell. These tubulovesicles resemble those of the neighboring parietal cells, and are not normally seen in other mature gastric epithelial cells. (X 27,000)

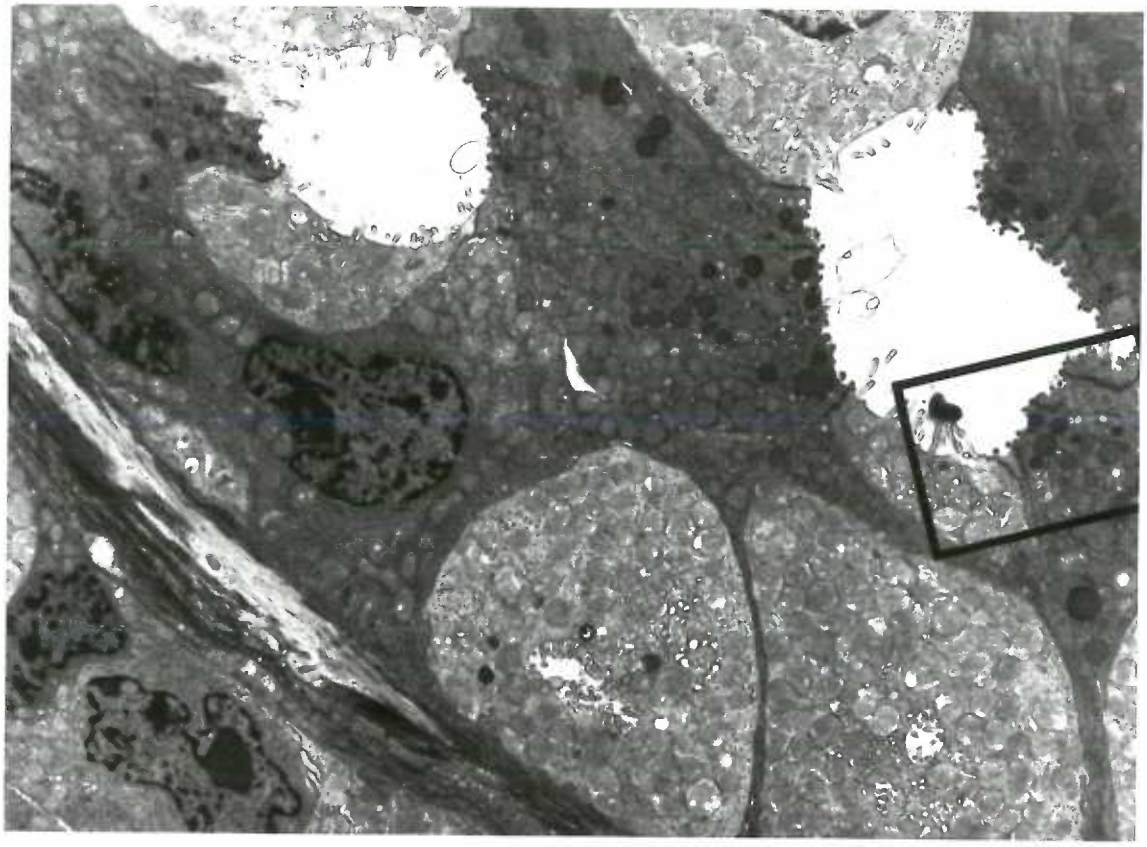

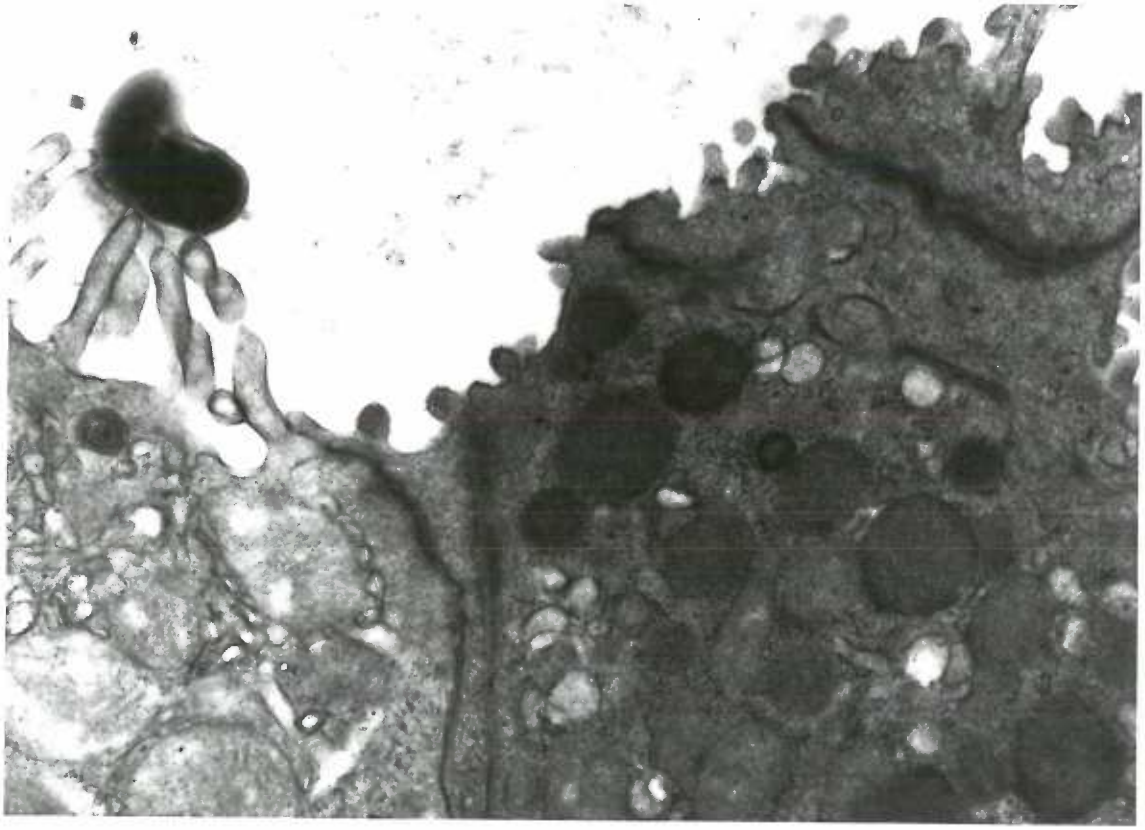

Figure 47 . Mature parietal cells in control animals.

Figure 47a (top). Mature parietal cells are large and pyramidal shaped. Their apices face the lumen of the gastric glands. In this micrograph, the lumen is just visible in the center of the top margin. The bases of parietal cells rest on a basement membrane, as do all gastric epithelial cells. The basement membrane under this parietal cell seems to be shared with another parietal cell from a neighboring gland. The cytoplasm is packed with mitochondria and with numerous electron-lucent tubulovesicles in the center of this cell. This is the usual appearance of parietal cells in fasting animals. In the stimulated state the tubulovesicles fuse to form an extensive canalicular system which is continuous with the lumen of the gastric gland. Such canaliculi are lined with microvilli, as seen in the one canaliculus visible in the top center of this cell. Portions of microvilli can also be seen on the plasmalemma facing the lumen of the gland at the top margin. (X 7,700)

Figure 47b (bottom). Parietal cell cytoplasmic details. Several canaliculi can be seen near the center, at the top margin. Long microvilli project into the lumen of the canaliculi. Electron-lucent tubulovesicles and mitochondria are numerous. The mitochondria are packed with flat cristae, a characteristic of mitochondria undergoing high rates of oxidative phosphorylation. (X 22,000)

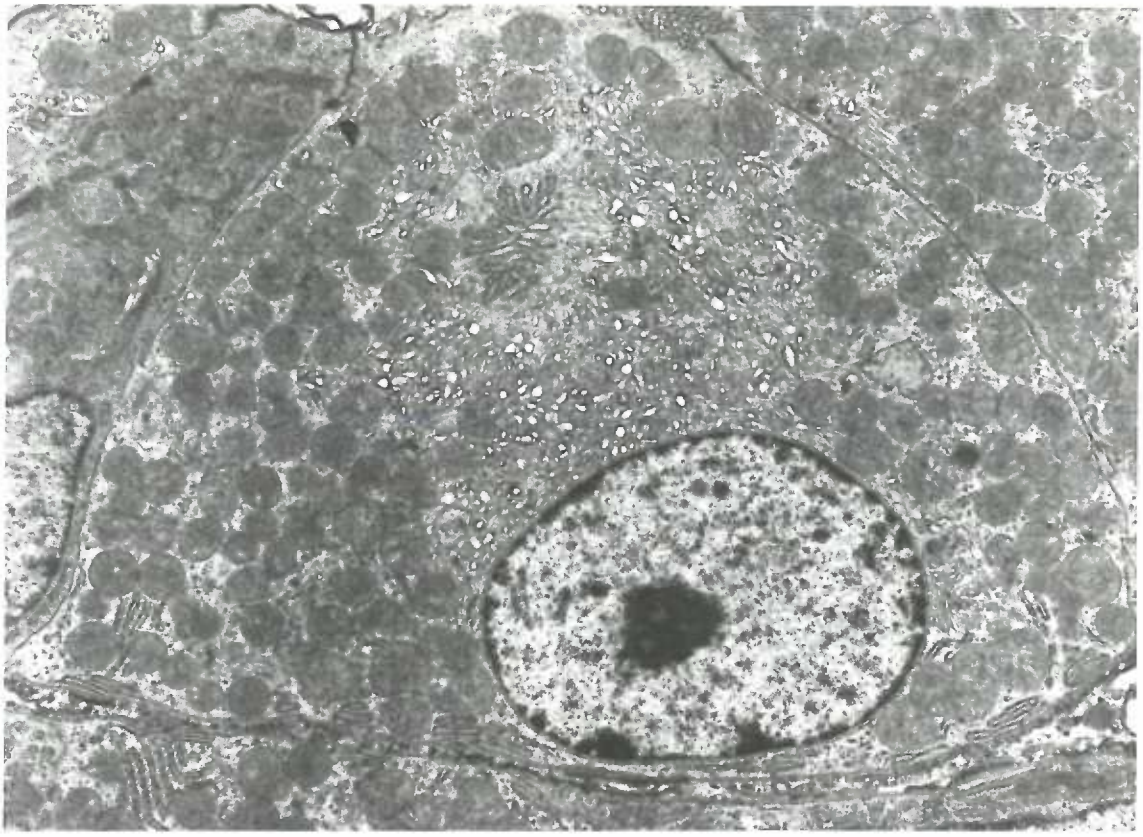

Figure 48. Zymogenic cells in control animals.

Figure 48a (top). Zymogenic cells in the bases of gastric glands. A narrow band of lamina propria runs diagonally across the view from the upper-left corner to the lower right. Several zymogenic cells face the lumen of a gland in the upper-right corner. They contain large secretory vesicles of light to moderate electron-density and a well developed system of endoplasmic reticulum. A mast cell with large electron-dense granules is prominent in the lamina propria in the center of this micrograph. To the left are two enteroendocrine cells (E), one of which contains numerous small, electron-dense granules. The other is probably the same type of cell, whose granules are not visible in this plane of section. Portions of two parietal cells can be distinguished by their numerous mitochondria. One parietal cell is prominent in the lower-right corner. (X 4,300)

Figure 48b (bottom). The bases of several zymogenic cells can be seen abutting the basement membrane and a small area of lamina propria is also visible. The bases of these zymogenic cells are filled with rough endoplasmic reticulum. Large electron-lucent secretory granules are also seen. Note the interdigitations of the plasmalemma between neighboring zymogenic cells. A mast cell is seen within the lamina propria. (X 11,400)

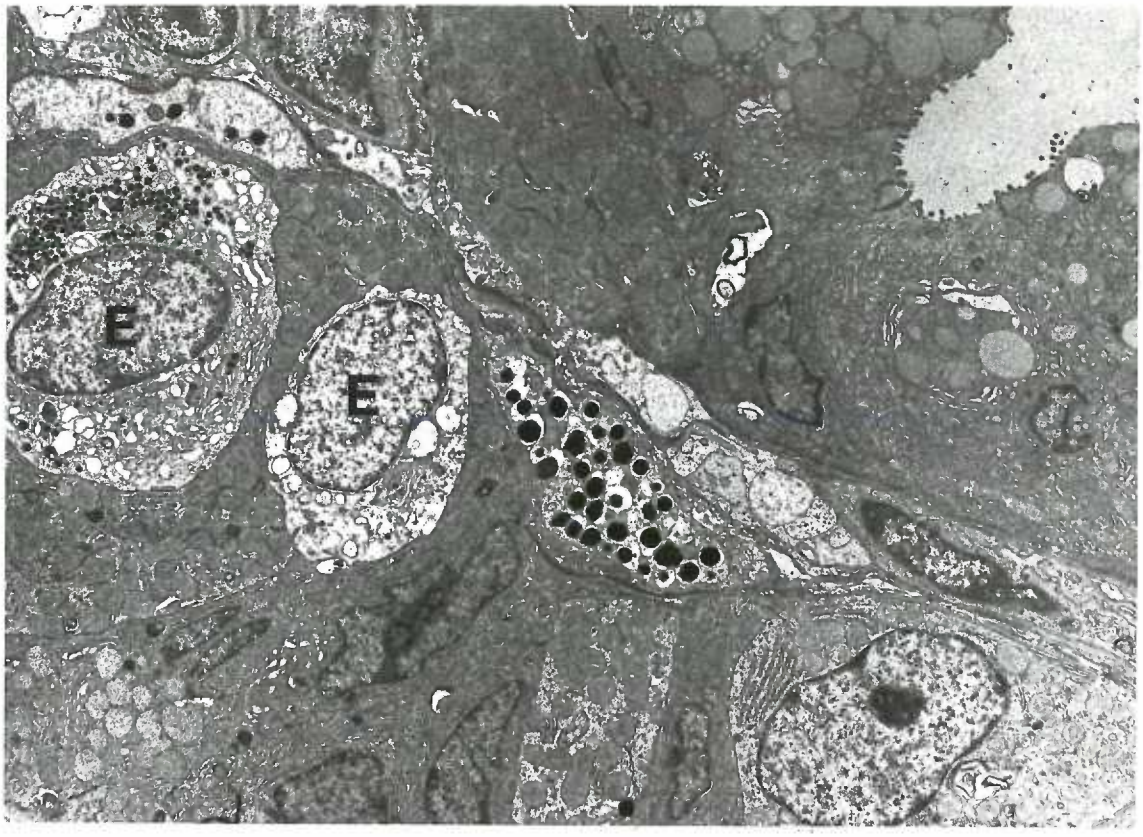
E
E

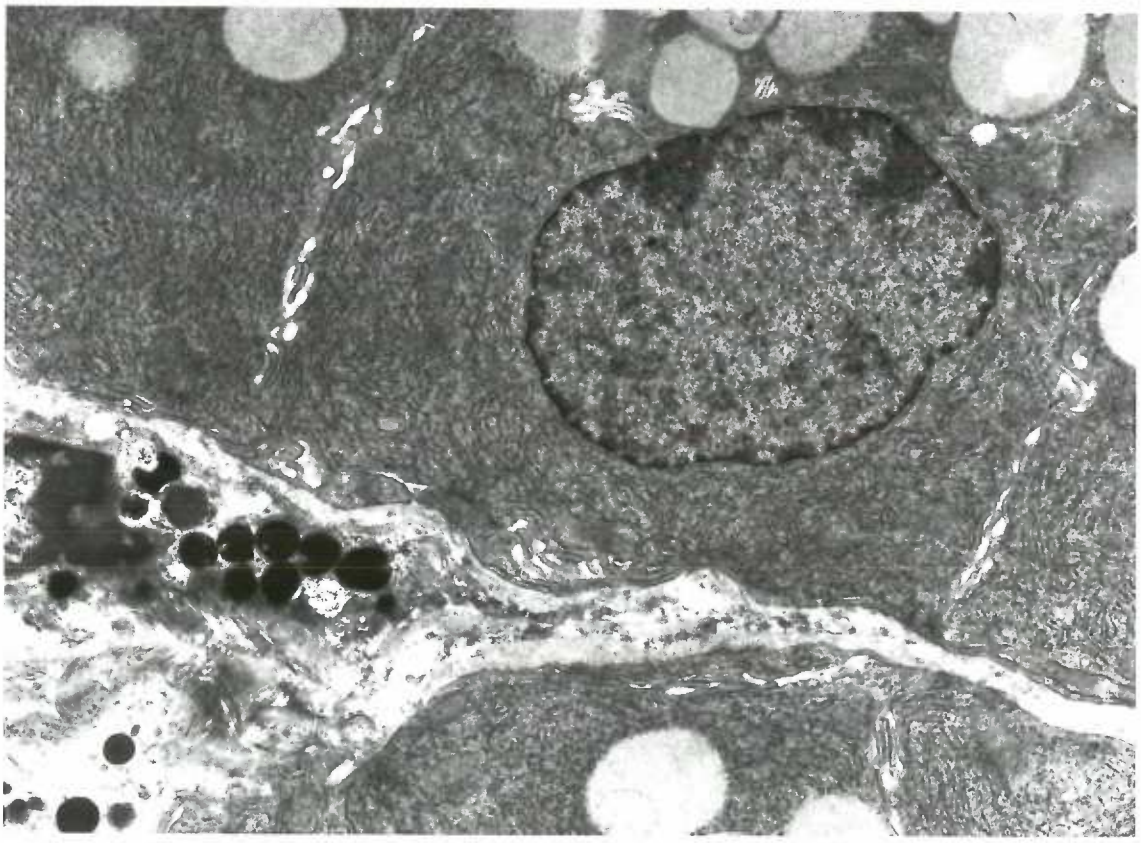

Figure 49. Low-magnification electron micrographs of the gastric mucosa in 3,4-TCB-fed animals. All normal specialized epithelial cell types have been replaced or converted to mucus-secreting cells and the lumen of the glands are markedly dilated. The apical surfaces of the cells are irregular, and in many cells the mucous granules have apparently fused and broken through the plasmalemma into the lumen, which appears filled with mucus.

Figure 49a (top left). Dilated glands just below the surface of the gastric mucosa. Notice that many of the cells have discharged their mucous granules. From animal 9921 fed 1 ppm 3,4-TCB for 97 days. (X 650)

Figure 49b (top right). Dilated glands from the middle region of the gastric mucosa. The lamina propria is flattened between the glands. Note that many of the cells have large accumulations of secretory granules. Animal 9246 fed 1 ppm 3,4-TCB for 55 days. (X 700).

Figure 49c (bottom left). Less severely involved gastric glands. These cells appear somewhat less severely altered than in the previous micrographs. They resemble mucous neck cells, except that their apices are very irregular. Animal 9921. (X 2,800)

Figure 49d (bottom right). A cystic gland. The secretory granules of all the cells in this region appear to have fused together and been discharged into the lumen of this cystic gland. Animal 9246. (X 1,200)

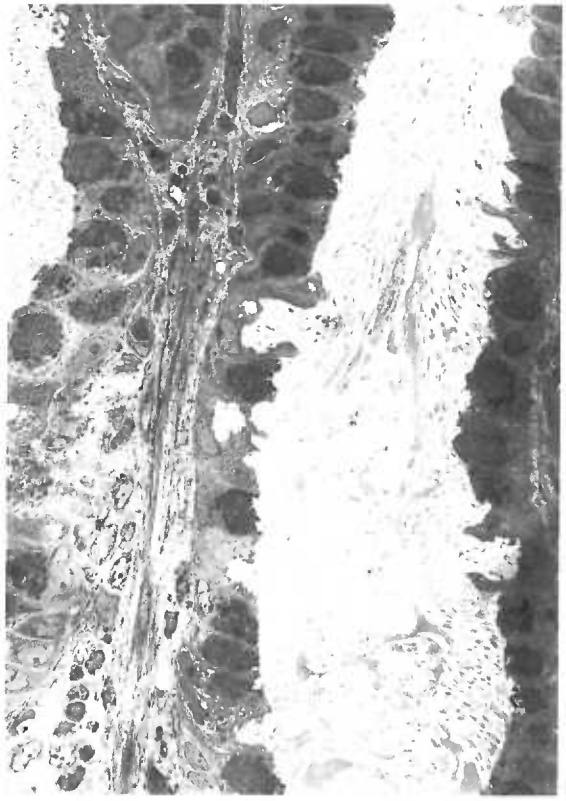

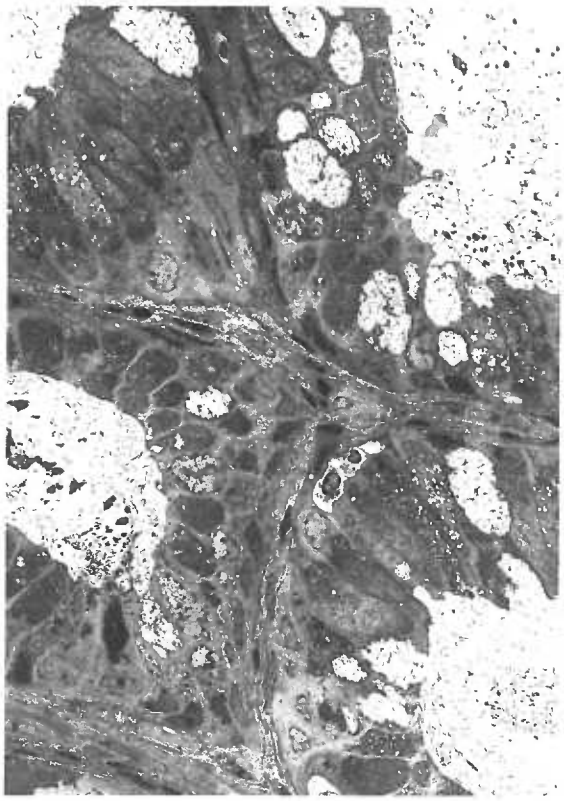

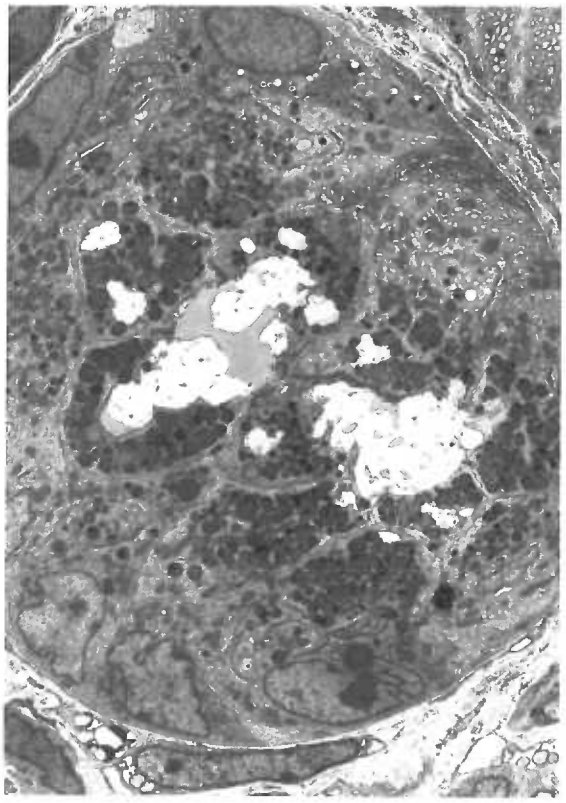

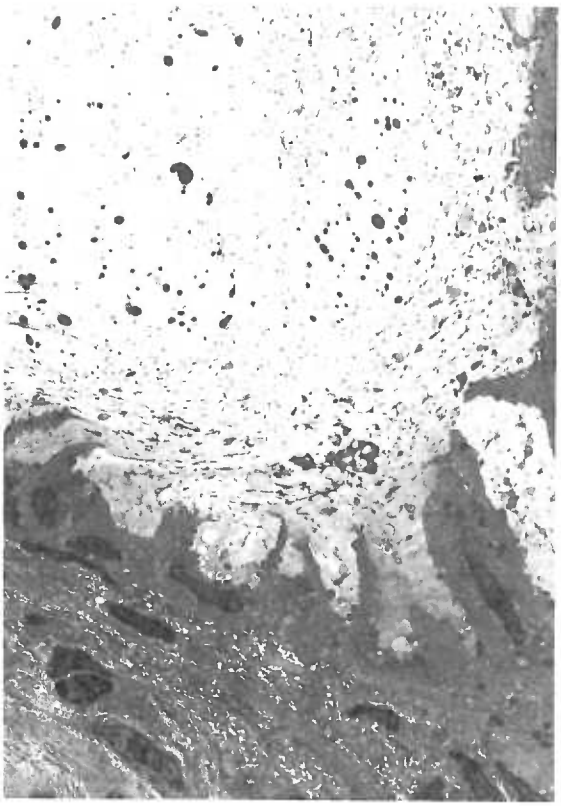

Figure 50. Variations in structure of epithelial cells from the gastric mucosa of animals fed 3,4-TCB diets.

Figure 50a (top left). These cells appear similar to control mucous neck cells. They contain numerous apical secretory granules, numerous mitochondria, microvilli and interdigitations of the plasmalemma with neighboring cells. Junctional complexes and a few electron-lucent vesicles are seen in the apical region of these cells. Animal 9921. (X 11,500).

Figure 50b (top right). Cells similar to those in the previous micrograph, but these contain fewer mitochondria and more secretory granules. Note the extensive interdigitation of the plasmalemma with the neighboring cells. Animal 9921. (X 6,600).

Figure 50c (bottom left). A higher magnification view of cells similar to those seen in figure 49d. The secretory granules appear to have fused together and broken open to the lumen of this cystic gland. The cytoplasm of these cells and those of the lamina propria appear disorganized and the nuclei have irregular outlines. Animal 9246. (X 3,600).

Figure 50d (bottom right). From a cystic gland which had penetrated the muscularis mucosae. These tall epithelial cells do not have mucous granules and the endoplasmic reticulum is disorganized. Animal 7194. (X 2,000)

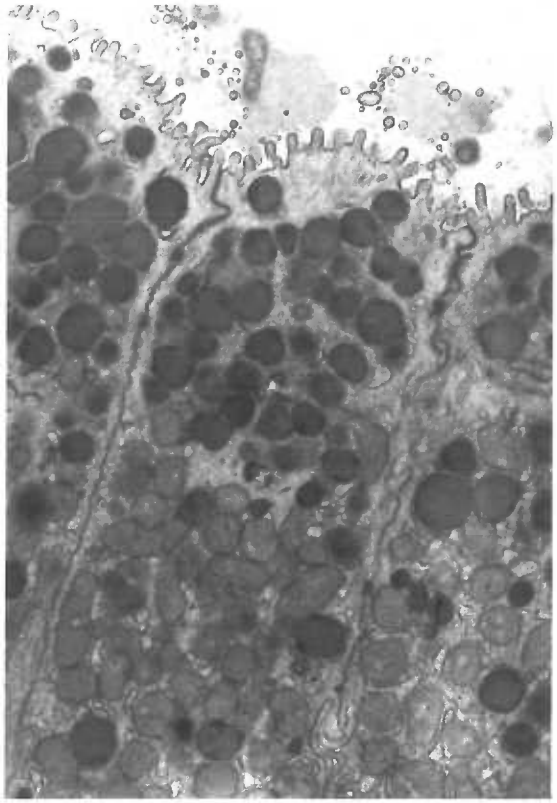

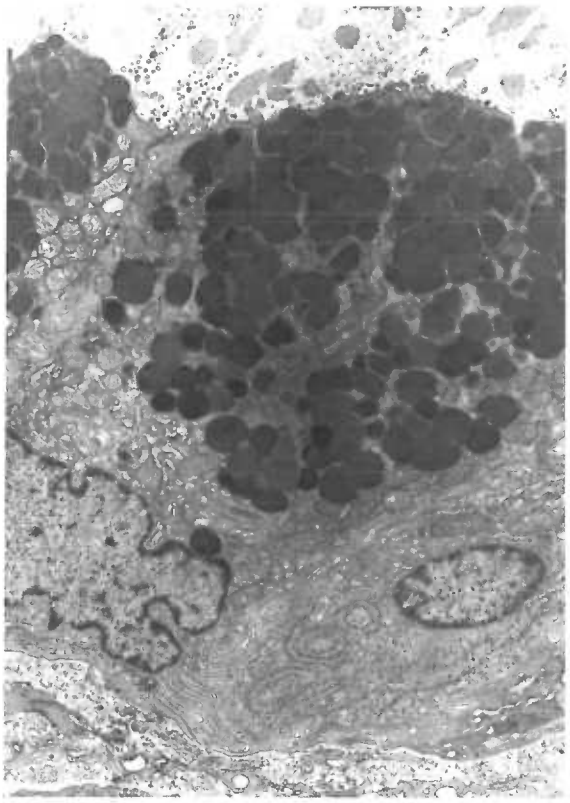

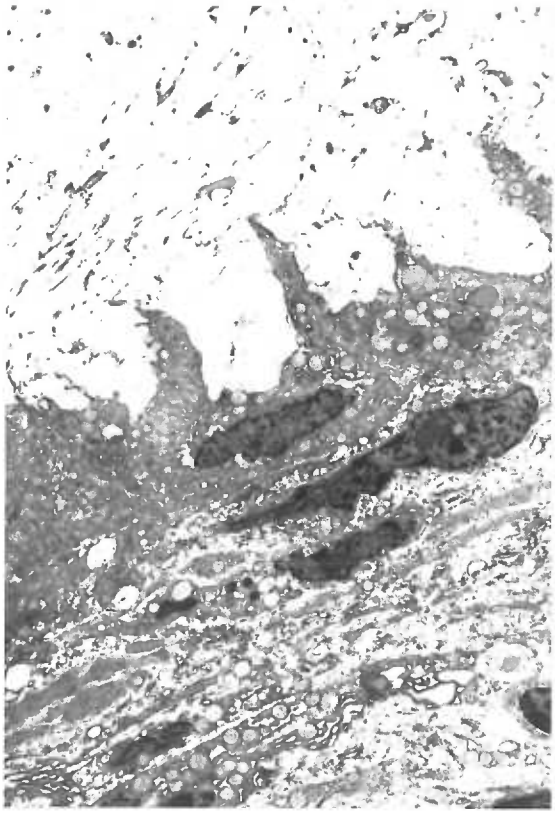

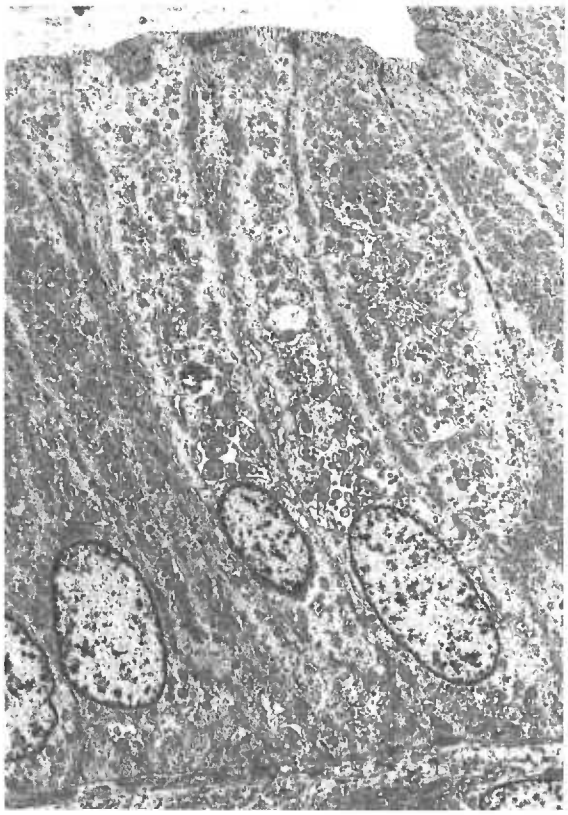

Figure 51. Cytoplasmic abnormalities in gastric epithelial cells of 3,4-TCB-fed animals.

Figure 51a (top left). Abnormal surface epithelial cells. These cells lacked the masses of tightly packed secretory granules seen in normal surface epithelial cells. The secretory granules which are present appear irregular, the cytoplasm appears disorganized and many clear vacuoles are seen. Compare with normal surface epithelial cells in figure 44a. Animal 9921. (X 4,800)

Figure 51b (top right). Fibrillar structures. This cell was lining a submucosal cyst. Cells like this were not seen in control monkey gastric mucosa, but have been reported in the gastric mucosa of dogs and humans. (X 35,000)

Figure 51c (bottom left). Dilated endoplasmic reticulum. Note that several areas of cell to cell interdigitations of the plasmalemma are present. The membranes of the secretory granules in the upper left have fused together. Animal 9921. (X 8,200)

Figure 51d (bottom right). Note the extensive cell to cell interdigitations of the plasmalemma. The saccules of the two Golgi apparati visible appear depleted and closely packed together. One Golgi apparatus is in the upper right corner and the other is the large multi-layered membrane structure to the right of center. Animal 9921. (X 18,500)

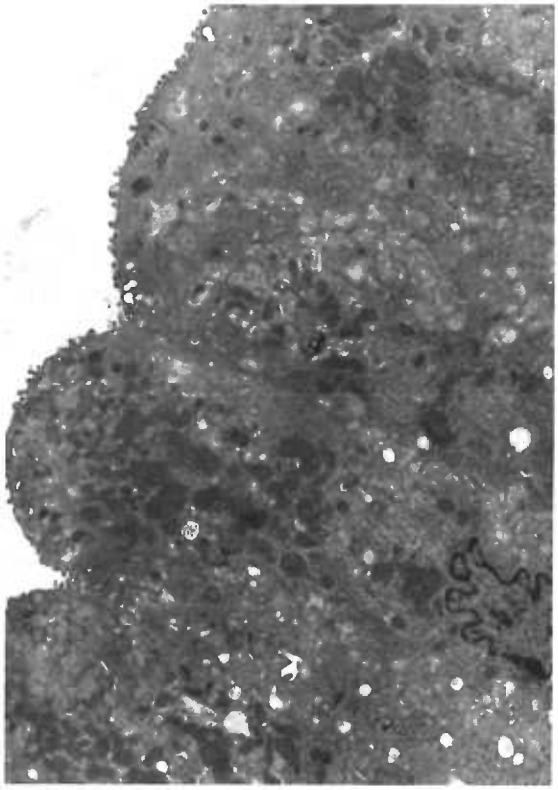

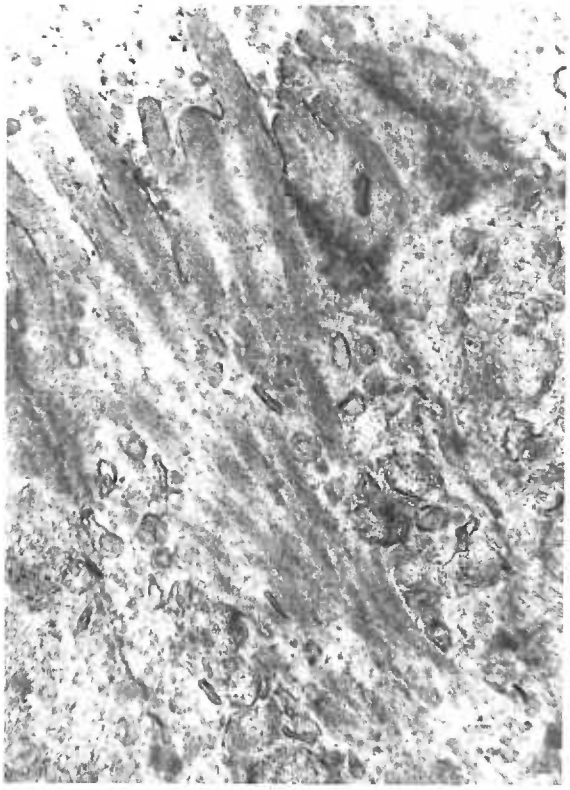

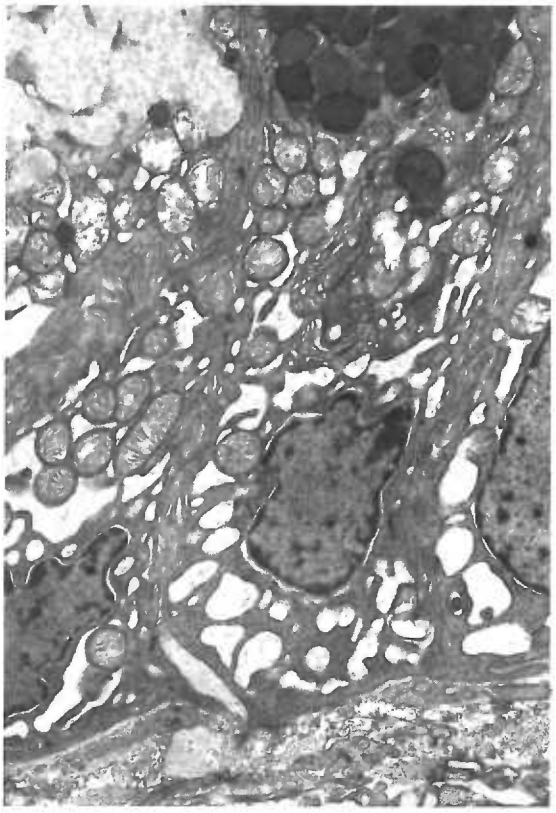

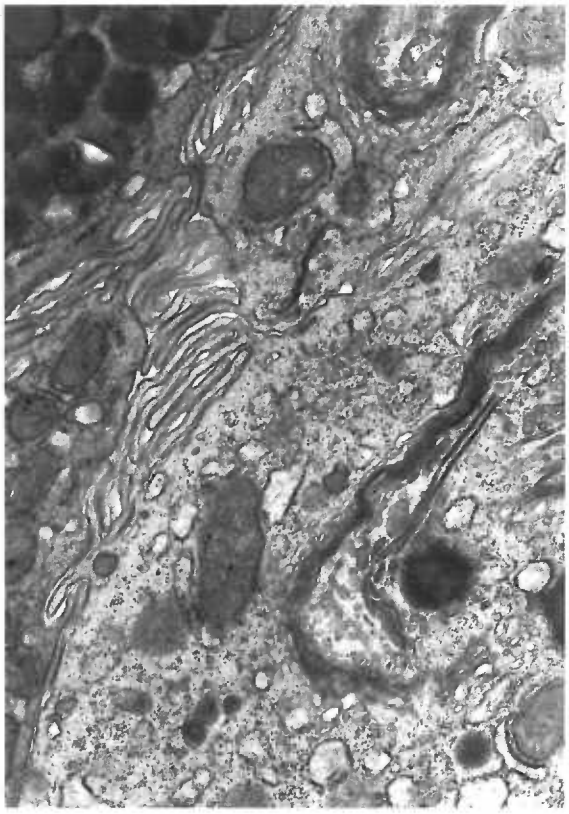

Figure 52. Autophagic vacuoles in the gastric epithelial cells of 3,4-TCB-fed animals.

Figure 52b (top). Two autophagic vacuoles filled with membranous material. Animal 9921. (X 22,000)

Figure 52a (bottom). A large autophagic vacuole is prominent in the center and a smaller vacuole is present near the left margin. Several Golgi apparati can be seen. Their saccules appear depleted and pressed together. Animal 9921. (X 22,000)

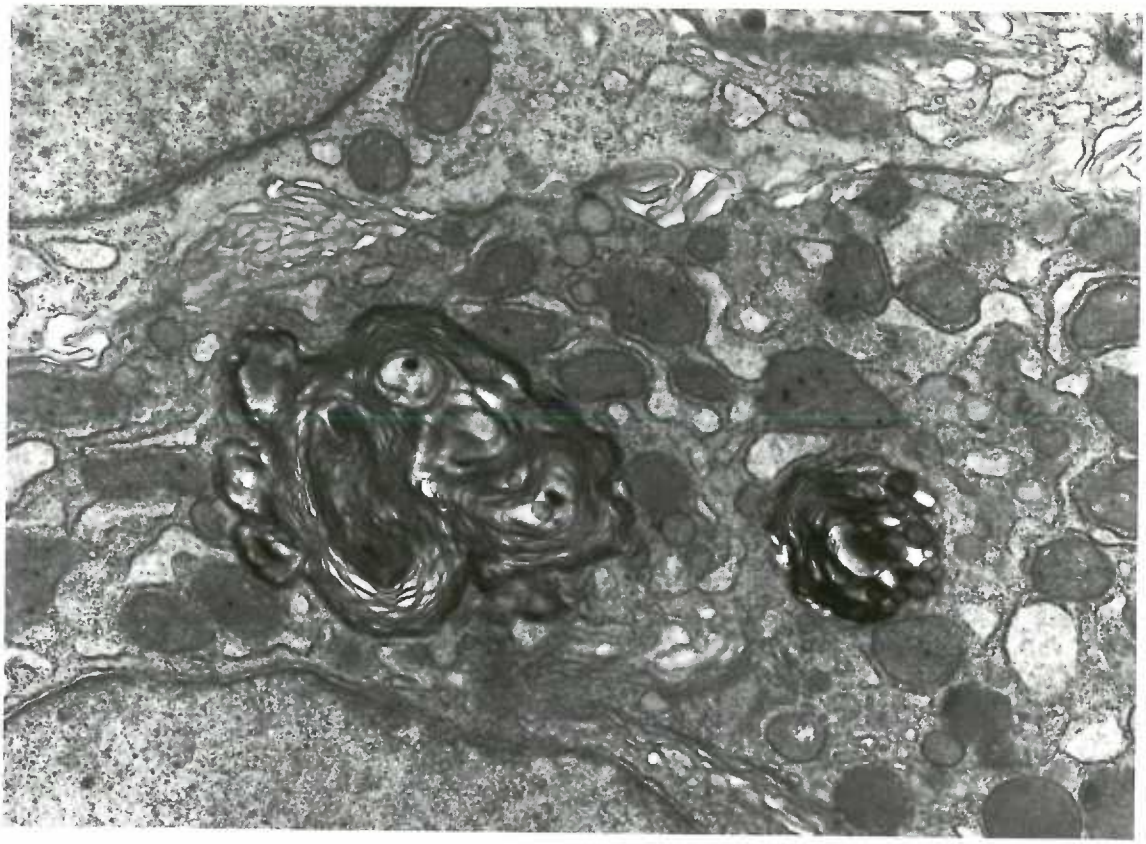

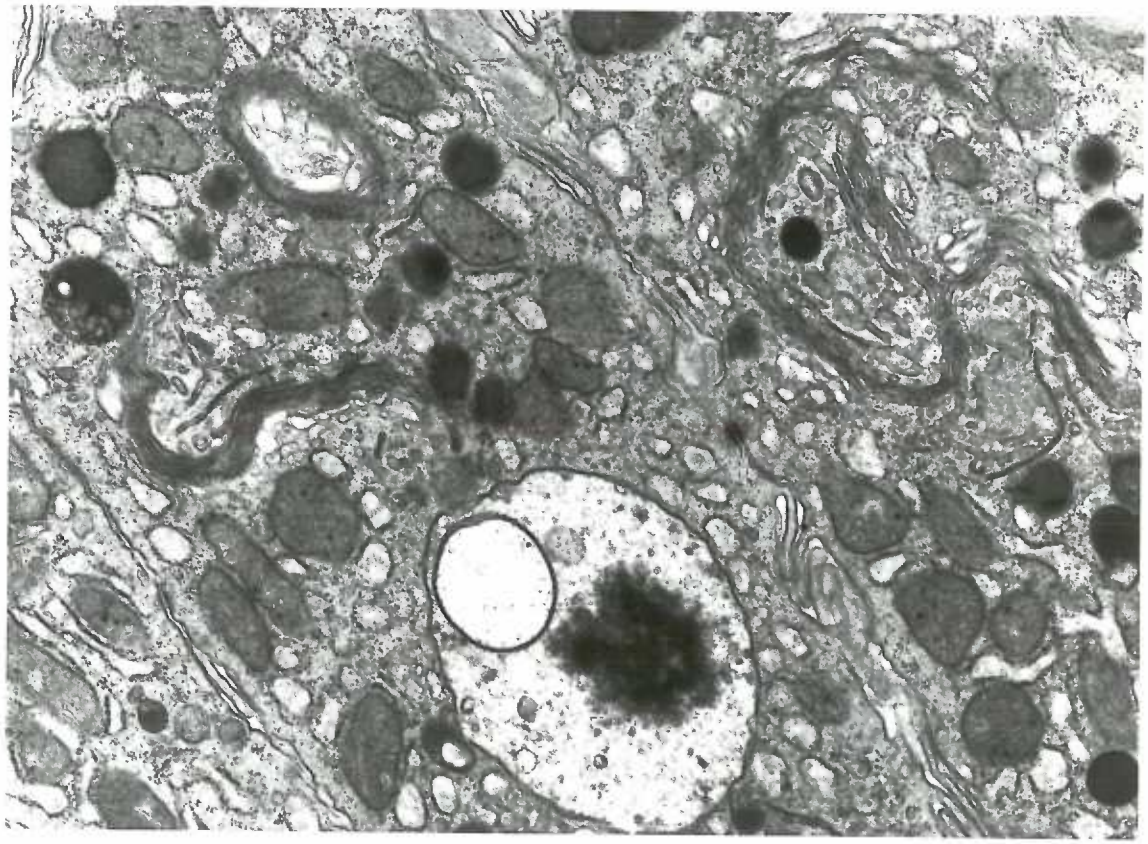

Figure 53. Fasting and postprandial serum gastrin levels. The ordinate is pg of gastrin per ml of serum. The abcissa is time in minutes after the animals were returned to their cages in which control diet cubes had been placed. Time 0 represents 08:30 when the overnight-fasted animals were removed from their cages and a sample of blood was taken by venapuncture. Additional samples of blood were taken at the times indicated. Animals 9921, 9273 and 8911 showed similar postprandial rises in serum gastrin; animal 9246 had fasting serum levels three-fold higher than the other animals, and his postprandial levels were correspondingly higher.

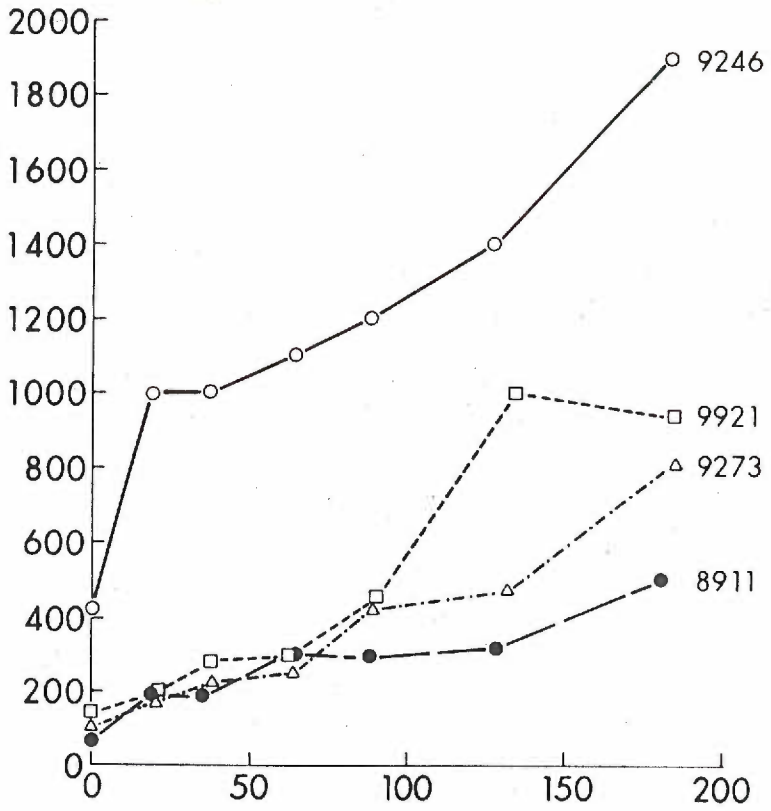
2000
1800
1600
1400
1200
1000
800
600
400
200
0
0
50
100
150
200
9246
9921
9273
8911

Minutes

Figure 54. Fasting and postprandial serum gastrin levels in control animal 9273. The ordinate is pg of gastrin per ml of serum and the abcissa is the time in minutes after feeding 75 ml of liquid diet by nasogastric tube. Overnight fasting samples, taken at 08:30, are indicated at time 0. Three determinations were made on separate days while the animal was on the control diet. These are the baseline determinations shown in the top graph. Additional measurements were made throughout the experiment (middle and bottom graphs). The numbers after the lines indicate the number of days since beginning the experimental diet, which for this animal was the control diet. Neither the fasting nor the postprandial values appeared to change in this animal throughout the experiment.

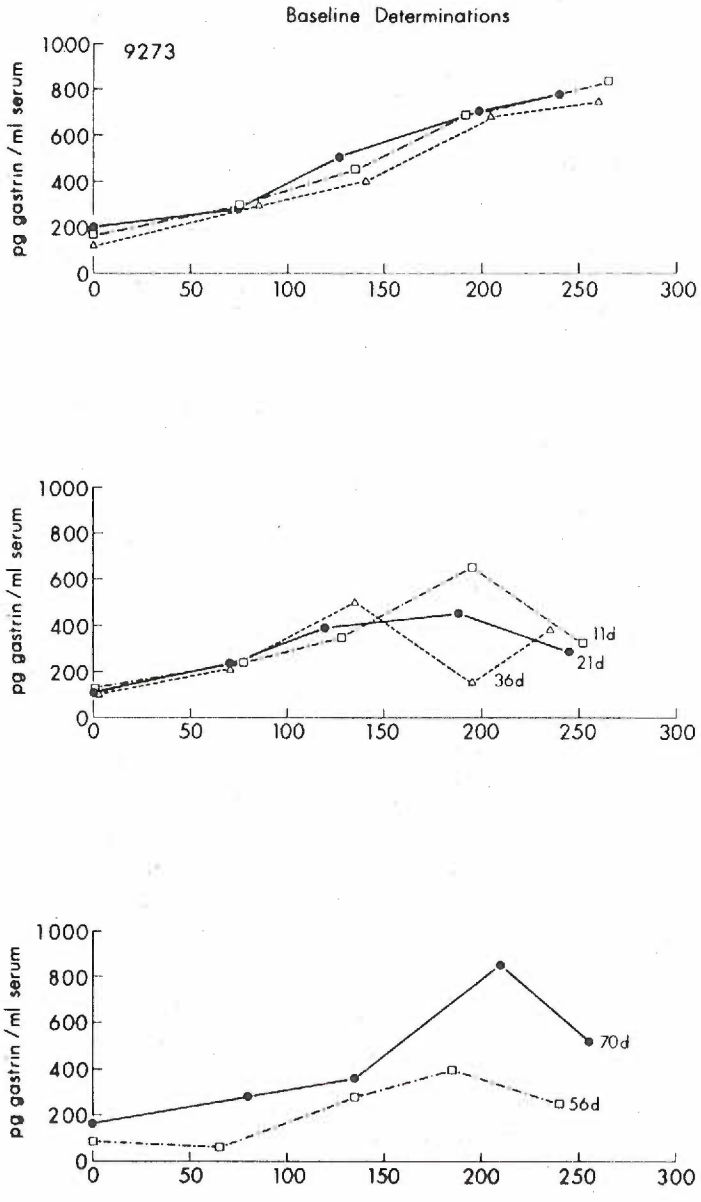
Baseline Determinations
9273
pg gastrin / ml serum
1000
800
600
400
200
0
0
50
100
150
200
250
300
11d
21d
36d
70d
56d
Minutes

Figure 55. Fasting and postprandial serum gastrin levels in control animal 8911. The ordinate is pg of gastrin per ml of serum and the abcissa is time in minutes after feeding 75 ml of liquid diet by nasogastric tube. Overnight fasting samples, taken at 08:30, are indicated at time 0. Three determinations were made on separate days while the animal was on a control diet. These are the baseline determinations shown in the top graph. Additional measurements were made throughout the experiment (middle and bottom graphs). The numbers after the lines indicate the number of days since beginning the experimental diet, which for this animal was the control diet. Note that neither the fasting nor the postprandial values appeared to change in this animal throughout the experiment.

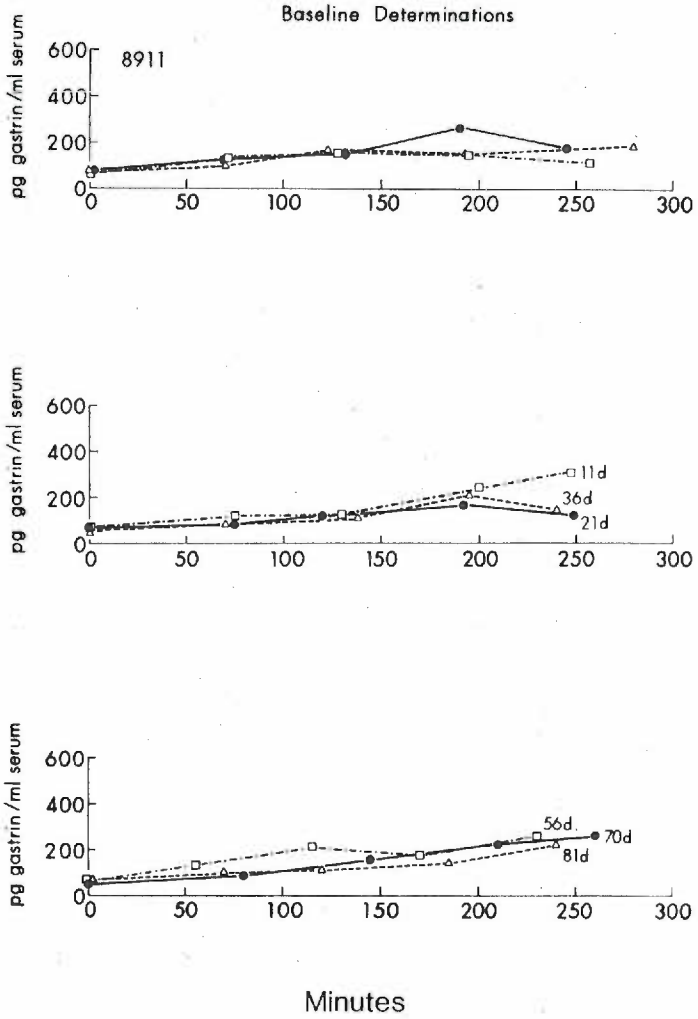
Baseline Determinations
8911
pg gastrin/ml serum
600
400
200
0
0
50
100
150
200
250
300
11d
36d
21d
56d
70d
81d
Minutes

Figure 56. Fasting and postprandial serum gastrin levels in 3,4-TCB-fed animal 9921. The ordinate is pg of gastrin per ml of serum and the abcissa is the time in minutes after feeding 75 ml of liquid diet by nasogastric tube. Overnight fasting samples, taken at 08:30, are indicated at time 0. Three determinations were made on separate days while the animal was on control diet. These are the baseline determinations shown in the top graph. Additional measurements were made throughout the experiment (middle and bottom graphs). The numbers after the lines indicate the number of days since beginning the experimental diet, which contained 1 ppm of 3,4-TCB. Note that neither the fasting nor the postprandial values changed significantly in this animal as a result of the toxic diet.

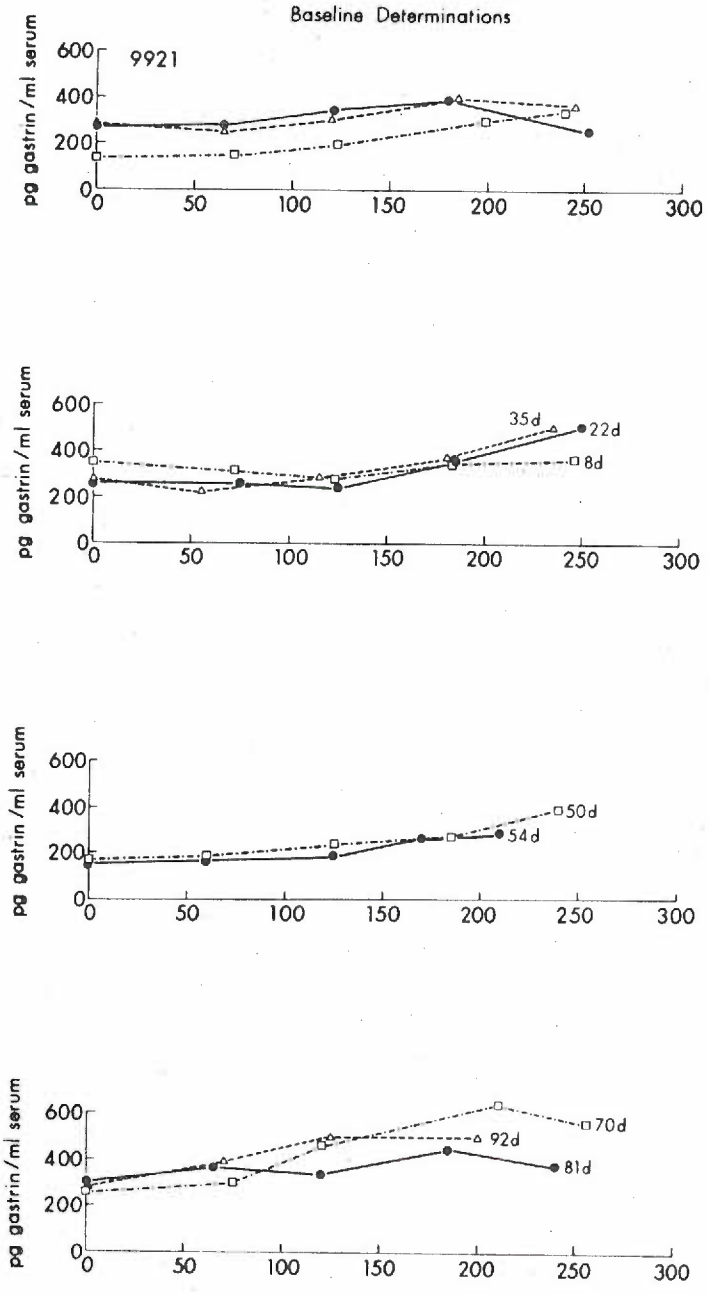
Baseline Determinations
9921
pg gastrin/ml serum
600
400
200
0
0
50
100
150
200
250
300
35d
22d
8d
50d
54d
92d
81d
70d
Minutes

Figure 57. Fasting and postprandial serum gastrin levels in 3,4-TCB-fed animal 9246. The ordinate is pg of gastrin per ml of serum and the abcissa is time in minutes after feeding 75 ml of a liquid diet by nasogastric tube. Overnight fasting samples, taken at 08:30, are indicated at time 0. Three determinations were made on separate days while the animal was on the control diet. These are the baseline determinations shown in the top graph. Additional measurements were made throughout the experiment (middle and bottom graphs). The numbers after the lines indicate the number of days since beginning the 3,4-TCB diet. Note that the baseline determinations of the fasting gastrin levels were 2 to 3 times as great as in the other three animals, and the postprandial levels were correspondingly higher. These high values persisted until 8 days of toxic feeding. However, by 22 days, and on all subsequent days, the fasting values were similar to those seen in the other animals, but no postprandial increase is seen.

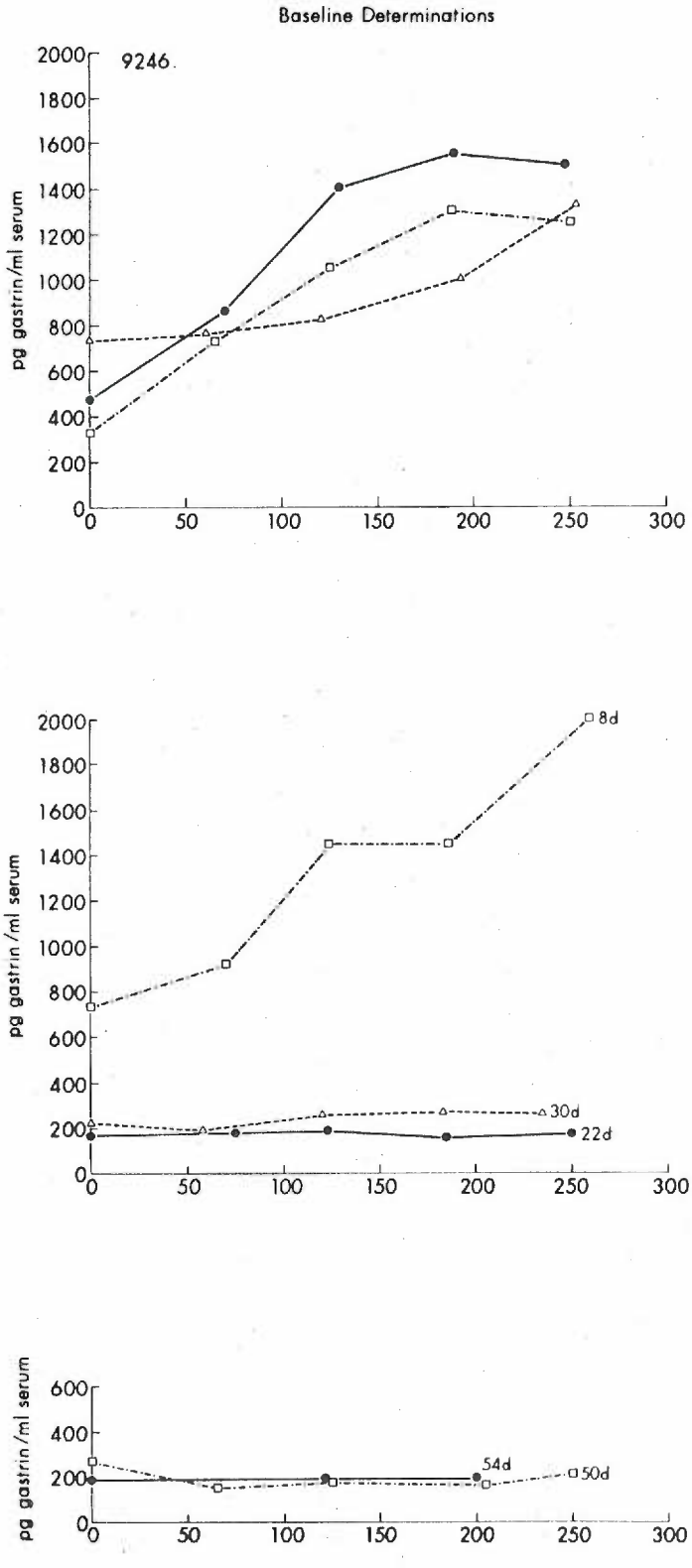
Baseline Determinations
9246
pg gastrin/ml serum
2000
1800
1600
1400
1200
1000
800
600
400
200
0
0
50
100
150
200
250
300
8d
30d
22d
54d
50d
Minutes

Figure 58. Argyrophilic epithelial cells. Sections stained with the Grimelius argyrophilic reaction specifically stain gastrin-containing G cells. These cells are most abundant in the antrum and duodenum, but a few are also seen in the body region in animals fed control diets (left). No-Grimelius positive cells were seen in the body regions of stomachs from animals fed 3,4-TCB, but they were numerous in the duodenum (right) and were also seen in the antrum of these animals.

Figure 58a (left). From the body region of the stomach of control animal 8911. Two Grimelius-positive cells can be seen opposite the arrows. (X 650)

Figure 58b (right). From the duodenum of 3,4-TCB-fed animal 9921. A number of Grimelius-positive cells can be seen opposite the arrows. (X 700)

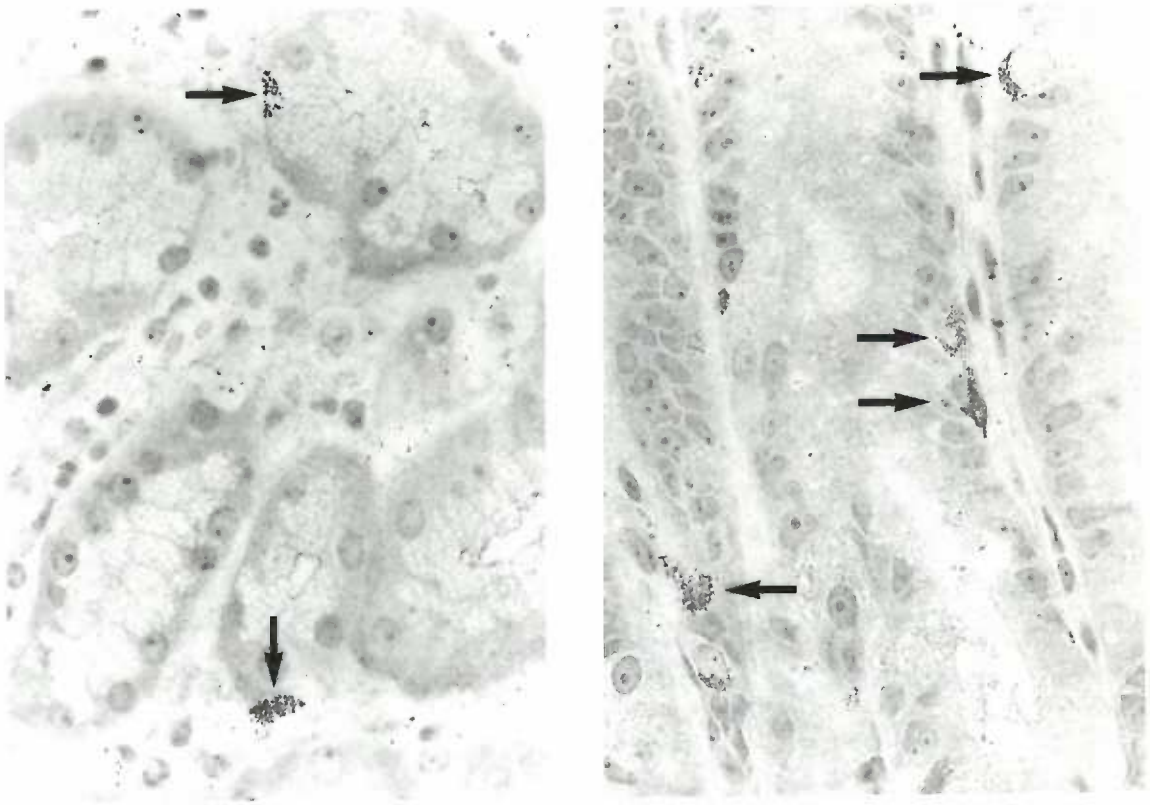

Figure 59. Model of gastric epithelial proliferation in the normal mucosa. Cellular proliferation is confined to a zone which includes the isthmus and neck regions of the glands. The majority of newly formed cells migrate upward (heavy arrow) to replace the surface epithelial cells lost by extrusion or by in situ degeneration. A few newly formed cells migrate downward (smaller arrow) to replace aged zymogenic and parietal cells which have been lost, presumably by in situ degeneration. The proliferative zone may be held in place by a network of fibrocytes and collagen, as described by Hattori in hamsters (64). A similar network may exist in monkeys. If so, this would stabilize the position of the proliferative zone. Cells would only be able to migrate downward as space became available in the bases of the glands through loss of the older cells.

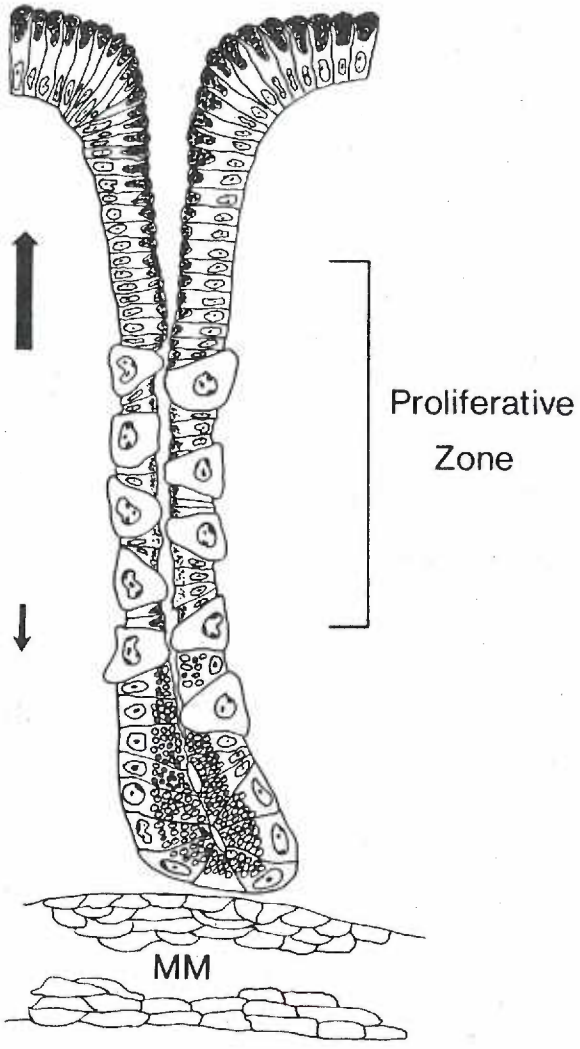
Proliferative
Zone
MM

Figure 60. Model of gastric epithelial proliferation in the mucosa of 3,4-TCB-fed animals. As in normal gastric glands (preceding figure), proliferation occurs in the isthmus and neck regions of the glands. This is the 1° proliferative zone in the diagram. However in this lesion, proliferation also takes place in the bases of the glands, and in the epithelium which penetrates the muscularis mucosae (MM) to form submucosal glands and cysts. The majority of the newly formed cells in the 1° proliferative zone migrate upward (heavy arrow) to replace surface epithelial cells lost by extrusion or in situ degeneration. The small arrows indicate where cells may migrate upward and downward, as well as laterally, in the bases of the glands. Downward migration of newly formed from cells higher in the glands, in the 1° proliferative zone, may be prevented by an excess formation of cells in the base region of the glands. The 1° proliferative zone in the 3,4-TCB-induced gastropathy may be anchored in a matrix of connective tissue, as it may be in normal gastric mucosa. If so, this would explain the failure of this 1° proliferative zone to be forced upward owing to the excess formation of cells in the bases of the glands. Instead these excess cells would tend to force the expanding gastric epithelium downward through the muscularis mucosae, forming submucosal glands and cysts.

Since cells may be prevented from migrating downward from the 1° proliferative zone, and since the base region is also producing cells which may be trying to migrate upward, the number of cells which migrate upward may exceed the number lost at the surface. This would explain the signs of apparent hyperplasia of surface epithelial cells seen by scanning electron microscopy.

The overall density of proliferative cells in this lesion does not appear to be greater than normal. However, proliferation continues in the bases of the glands, where zymogenic and parietal cells normally age and degenerate, an indication that normal cell aging and loss may not occur here. This could explain the development of hyperplasia in the absence of a shortened cell cycle time in the proliferative cells, and in the absence of increased numbers of these cells.

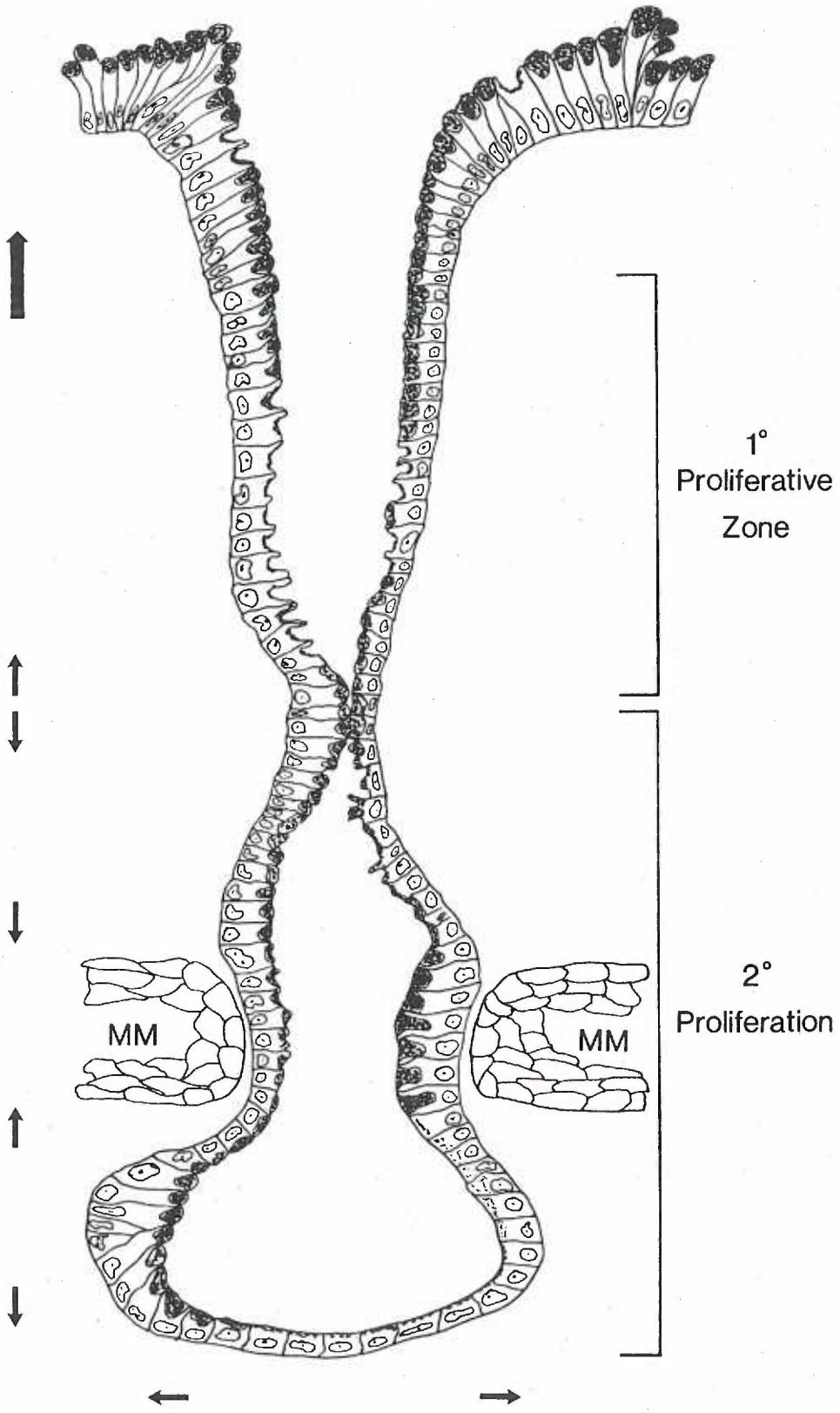
1°
Proliferative
Zone
2°
Proliferation
MM
MM